Synthesis and Reactivity of Mono- and Polycationic Phosphines and Amines

Dissertation

Zur Erlangung des akademischen Grades eines

Doktors der Naturwissenschaften

(Dr. rer. nat.)

Des Fachbereichs Chemie der Technischen Universität Dortmund

vorgelegt von

Ágnes Kozma

geboren am 26.06.1987

in Székelyudvarhely, Rumänien

Mülheim an der Ruhr, 2015

Hiermit versichere ich, dass ich die eingereichte Dissertation selbständig verfasst und keine anderen als die angegebenen Quellen und Hilfsmittel benutzt, sowie Zitate kenntlich gemacht habe.

_____ _____

(Ort, Datum) **(Unterschrift)**

Die vorliegende Arbeit entstand unter Anleitung von Herrn. Prof. Dr. Manuel Alcarazo in der Zeit von Oktober 2011 bis April 2015 am Max-Planck-Institut für Kohlenforschung in Mülheim an der Ruhr. Diese Arbeit wurde in folgenden Beiträgen veröffentlicht:

- Á. Kozma, G. Gopakumar, C. Farès, W. Thiel, M. Alcarazo, *Chem. Eur. J.* **2013**, *19*, 3542.

- Á. Kozma, T. Deden, J. Carreras, C. Wille, J. Petuškova, J. Rust, M. Alcarazo, *Chem. Eur. J.* **2014**, *20*, 2208.

- Á. Kozma, J. Rust, M. Alcarazo, *Chem. Eur. J*. **2015**, *21*, 10829.

- E. Haldón, Á. Kozma, H. Tinnermann, L. Gu, R. Goddard, M. Alcarazo, *Dalton Trans.* **2015**, DOI: 10.1039/c5dt02341f.

1. **Berichterstatter: Herr Prof. Dr. Alois Fürstner**
2. **Berichterstatter: Herr Prof. Dr. Carsten Strohmann**

Danksagung

Mein herzlichster Dank gilt Herrn Prof. Dr. Manuel Alcarazo für die Aufnahme in seinen Arbeitskreis, die Vergabe der herausfordenden Themenstellung sowie sein permanentes Interesse bezüglich meiner Arbeit. Für die hilfreichen und motivierenden Diskussionen und für seine Unterstützung bei der Durchführung dieser Doktorarbeit bin ich ebenso dankbar.

Ich danke Herrn Prof. Dr. Alois Fürstner und Herrn Prof. Dr. Carsten Strohmann für die freundliche Übernahme des Referats und Koreferats.

Allen technischen Mitarbeitern der Abteilungen Fürstner und Alcarazo - namentlich Gerlinde Mehler, Sigrid Holle und Karin Radkowski - danke ich für ihre Geduld und Hilfsbereitschaft im Labor. Frau Monika Lickfeld danke ich für ihre große und freundliche Hilfe bei allen organisatorischen Problemen. Ferner möchte ich mich allen Mitarbeitern der analytischen Abteilungen für die Messung und Auswertung zahlreicher Proben bedanken. Mein besonderer Dank gilt Herrn Dr. Goddard, Herrn Rust, Frau Schucht, Frau Dreher, Frau Dreier und Herrn Dr. Mondal für die Messung und Lösung vieler Kristallstrukturen, Frau Blumenthal, Herrn Klein und Herrn Joppek für die massenspektrometrischen Analysen, sowie Herrn Dr. Farès, Herrn Kochius und Frau Wirtz für die Aufnahme der aufwändigen NMR Spektren.

Für das sorgfältige Korrekturlesen dieser Arbeit und inspirierende Diskussionen bedanke ich mich bei Leo Nicholls, Dr. Jonathan Dube und Dr. Javier Peña. Dr. Dube danke ich auch für die Beantwortung aller meinen Fragen. Allen Mitarbeitern der Arbeitsgruppen Fürstner und Alcarazo möchte ich mich für die angenehme Atmosphäre und tolle Zusammenarbeit im Labor bedanken, besonders dankbar bin ich für meine langjährige Box- und Bürokollegen Alejandro García, Elisa Gonzalez, Lianghu Gu und Sebastian Steinberg. Weiterhin danke ich meinen ehemaligen Kollegen Dr. J. Carreras, Dr. B. Inés, Dr. J. Iglesias, Dr. S. Khan, Dr. F. Martín, Dr. I. Alonso, Dr. E. Haldón und Dr. J. Llaveria für die große Hilfe im Labor am Anfang meiner Promotion und für die schöne Zeit in Mülheim. Hendrik Tinnermann danke ich für die deutsche Übersetzung des Abstracts dieser Dissertation und für die interessanten Diskussionen über die deutsche Sprache und organische Chemie in Box 5.

Ein ganz lieber Dank geht an meinen Freunden und Kollegen auch aus anderen Arbeitsgruppen der MPI, die ich außerhalb des Labors oft getroffen habe und die während der verschiedenen Veranstaltungen und Ausflüge für viel Spaß und gute zusammenverbrachte Zeit und tolle Erinnerungen besorgt haben.

Dem Deutschen Akademischen Austauschdienst und dem Max-Planck-Institut für Kohlenforschung bin ich dankbar für die finanzielle Unterstützung meiner Promotion.

Endlich, den größten Dank verdienen meine Familie und Leo, die mich ständig auf allen Ebenen liebevoll ünterstützt haben, mein Selbstvertrauen verstärkt haben und vorzüglich bei der Anfertigung dieser Arbeit viel Geduld und Verständnis entgegengebracht haben.

Meiner Großmutter († 27.12.2013)

Zusammenfassung

Liganden mit π-Akzeptoreigenschaften sind in der Lage die Elementarschritte eines Katalysezykluses zu erleichtern, welche stark Lewis-azide Metallzentren brauchen. Leider sind die kommerziell verfügbaren π-Akzeptorliganden, wie z.B. PF_3, $P(CF_3)_3$, PCl_3, entweder sehr giftig oder sehr feuchtigkeitsempfindlich. Daher ist die Entwicklung neuer π-Akzeptorliganden nach wie vor eine Herausforderung. Im Rahmen dieser Arbeit wird das Einführen positiv geladener Substituenten als eine Möglichkeit zum Einbringen von π-Akzeptoreigenschaften auf die entsprechenden Liganden diskutiert. Des Weiteren umgeht dies die Feuchtigkeitsempfindlichkeit der oben genannten Verbindungen durch Vermeiden einer labilen P-X Bindung in der Ligandenstruktur.

Die Studien unserer Gruppe zur Struktur und Reaktivität von Cyclopropenium-basierten Phosphinen fortsetzend wurde eine zweite Generation starker π-Akzeptoren durch Einführen von polyfluorierten aromatischen Substituenten oder durch Ersetzen der Cyclopropenium-Substituenten durch die stärker elektronenaffinen Imidazolium-Reste entwickelt. Die überragende katalytische Aktivität der Platin(II)-Komplexe dieser Liganden wurde in einer Hydroarylierung sowie in der Naturstoffsynthese von Chrysotoxen und Epimedoicarisosid A gezeigt.

Die Arbeiten auf dem Gebiet der kationischen Phosphine erweiternd wurden die analogen kationischen Amine dargestellt und vollständig charakterisiert. In der Festkörperanalyse zeigt sich eine unerwartete chemische Umgebung um das zentrale Stickstoffatom. So nehmen diese Kationen, im Gegensatz zu den Phosphoranaloga, eine trigonale planare Geometrie an, auch wenn computerchemische Betrachtungen dennoch eine freies Elektronenpaar sowie eine negative Ladung am Stickstoffatom darstellen.

Um zuletzt auch die Stabilität der polykationischen Liganden zu erhöhen, wurden chelatisierende Systeme mit zwei elektronenreichen Cyclopropeniminen zur Stabilisierung der dikationischen Phosphine entwickelt. Eine Reihe verschiedener Dikationen wurde durch Transfer der –onium Substituenten in guten Ausbeuten dargestellt. Trotz ihrer hohen Ladung, können die Kationen Gold(I)- und Silber(I)zentren koordinieren und zur Phosphor(V)-Verbindung oxidiert werden.

Abstract

Ligands depicting π-acceptor properties are able to facilitate those elementary steps of a catalytic cycle that require strong Lewis acidity at the metal center. Unfortunately, commercially available π-acceptor ligands, *e.g.* PF_3, $P(CF_3)_3$, PCl_3 are either very toxic or moisture sensitive. Therefore, the design of new π-acceptor ligands is still a challenge in the field of ligand design. The approach outlined in this thesis is based on the introduction of positively charged substituents as a way to impart π-acceptor properties on the resulting ligands. In addition, it circumvents the moisture sensitivity issue avoiding any labile P-X bond in the ligand structure.

Continuing the study of the structure and reactivity of the cyclopropenium-derived phosphines developed within our group, a second generation of strong π-acceptor ligands was prepared by incorporating polyfluorinated aromatic substituents or by replacing the cyclopropenium moiety with the more electron-withdrawing dihydroimidazolium unit. The superior catalytic activity of the Pt(II) complexes derived from these ligands in a hydroarylation reaction was demonstrated as well as the application of the new catalyst in the synthesis of natural products Chrysotoxene and Epimedoicarisoside A.

As an extension of this work on cationic phosphines the analogous cationic amines were synthesized and fully characterized. The solid-state structure analyses reveal unprecedented chemical environments around the central nitrogen atom. In contrast to their phosphorus analogues, the nitrogen atom in these cations adopts a trigonal planar environment, despite the computationally calculated lone pair of electrons and negative charge at nitrogen.

Finally, in order to avoid stability issues often associated with polycationic ligands, chelating architectures, employing two electron-rich cyclopropenimines were used for the stabilization of dicationic phosphines for the first time. A series of dications were synthesized in good yields by applying the –onium substituent transfer methodology. Despite their highly charged nature, these cations were able to coordinate Au(I) and Ag(I) metal centers and could also be oxidized to the phosphorus(V) compounds.

technische universität
dortmund

Synthesis and Reactivity of Mono- and Polycationic Phosphines and Amines

Content

1. General Introduction

Phosphines, with the general formula PR_3, are arguably the most widely used ligands in organometallic chemistry, because of the easy fine-tuning of their stereoelectronic properties. Both, the steric bulk and electronic parameters of phosphines can be modified in a systematic and predictable way by attaching R substituents of different size and nature to the central phosphorus atom. Furthermore, these two characteristics can be adjusted in a relatively independent manner to achieve tailored properties for a specific catalytic transformation. In addition, the ^{31}P nucleus has a nuclear spin of ½ and is 100 % naturally abundant: in analogy to ^{1}H NMR, the ease in which phosphorus containing compounds can be structurally analyzed and monitored *in situ* – sometimes without even the need for deuterated solvents - has also likely contributed substantially to the success of phosphines as ligands.

In phosphine-metal complexes, σ-electron density donation from the phosphine to the metal takes place through the highest occupied molecular orbital (HOMO), which usually corresponds to the lone pair of electrons situated in a sp^3 hybridized orbital located at the P-atom. The lowest unoccupied molecular orbital (LUMO) of phosphines has normally the shape of a σ*(P-R) orbital, which can accept π-electron density from a filled metal d orbital (Figure 1-1). The nature of the R substituents is crucial for this interaction: π-acceptor properties can be enhanced by attaching electron withdrawing substituents, which result in a σ*(P-R) orbital of lower energy. In addition, polarization of the P-R bond causes the contribution from the phosphorus atom to the σ* orbital to become larger, resulting in a more efficient σ*(P-R) - d(M) overlap. Hence, the π-acceptor properties of phosphanes containing carbon, nitrogen, oxygen or fluorine substituents increase in that order, as expected from the relative electronegativity of these elements.[1] It is worthy to note that the π-acidity of PF_3 approaches that of the CO ligand.

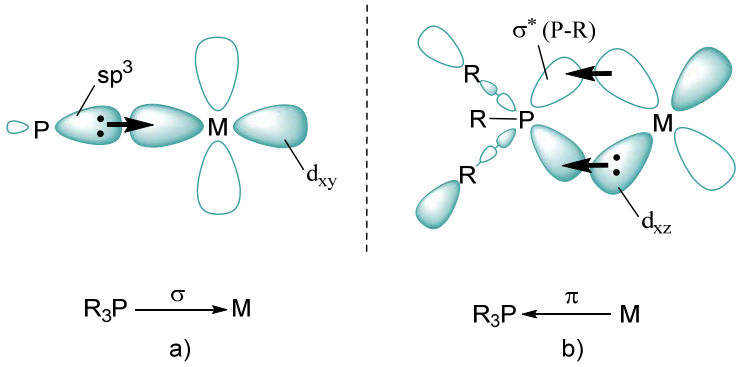

Figure 1-1. a) σ-Donation from the sp^3 orbital (HOMO) of a phosphine PR_3 into an empty d metal orbital; b) π back-donation from a filled metal d orbital into the σ*(P-R) orbital (LUMO) of phosphine PR_3.

The electronic parameters of phosphines are traditionally evaluated by the infrared (IR) stretching frequencies ($\tilde{\nu}$) of the corresponding phosphine-transition metal carbonyl complexes. This method was introduced by Tolman,[2] who described measurements of different $[Ni(CO)_3PR_3]$ complexes, obtained through the stoichiometric combination of the monodentate phosphine with nickel tetracarbonyl. Due to the high volatility and acute toxicity of nickel tetracarbonyl, the evaluation of donor properties by the measurement of rhodium carbonyl complexes has become more popular than the original Tolman method.

Carbonyl ligands have an empty, low lying π* orbital that is able to accept electron density from a filled metal d orbital. If the phosphine coordinated to the same metal is a good σ-donor, the metal has more electron density to back-donate into the carbonyl π* orbital. The consequence of this situation is a weakening of the carbonyl triple bond, resulting in a decreased wavenumber for the stretching frequency measured by infrared spectroscopy (Figure 1-2).[1]

This method is experimentally quite simple, however possesses several intrinsic limitations. Firstly, it is necessary to consider the steric properties of the ligand, as a bulky phosphine can impede the ideal orbital overlap between the metal and the carbonyl ligand. Therefore, direct comparison of electronic properties can only be made among phosphines with similar steric parameters.[3] Furthermore, analysis of carbonyl stretching frequency values does not allow the separation of the simultaneous σ-donor and π-acceptor properties of the phosphine; only the net result of both parameters can be deduced.

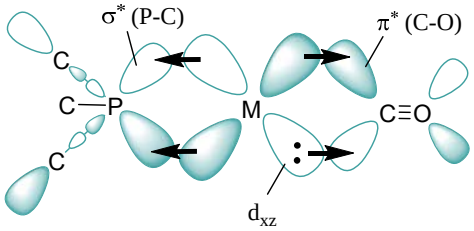

Figure 1-2. Schematic diagram of orbital overlap between a filled metal d orbital, an empty CO π* orbital and an empty σ* (P-C) orbital. Note that in the rhodium complexes prepared in this thesis, the arrangement of the phosphine and CO ligands around the metal center is *cis*.

The steric parameters of phosphines were also measured by Tolman[2] using the cone angle, θ. He defined θ as the apex angle of a cone centered at 2.28 Å from the phosphorus atom, where the cone just touches the outermost atoms of the substituents (Figure 1-3). In the case of unsymmetrical phosphines, θ can be calculated using the three half angles, $\theta_i/2$. The variable steric size of the ligands often governs how many of them will fit around the metal center. For instance, even six of the small CO ligands or PMe_3 can coordinate a metal to achieve the 18 electron complexes, *e.g.* $Cr(CO)_6$ and $W(PMe_3)_6$. In contrast, the usual maximum number of bulky phosphines such as PCy_3 or $P(iPr)_3$ that can simultaneously bind to a metal is two, *e.g.* $Pt(PCy_3)_2$, therefore they favor the formation of low-coordinate metals.[4]

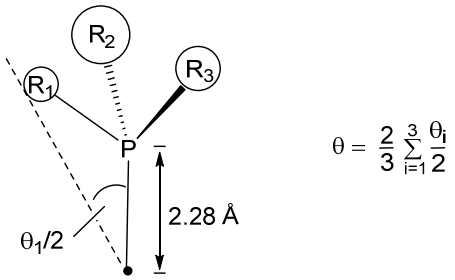

Figure 1-3. Schematic diagram and calculation of the cone angle (θ) for unsymmetrical phosphines.[2]

Combining the electronic and steric properties, Tolman presented a stereoelectronic map of phosphines, depicting the infrared stretching frequency ($\tilde{\nu}$) versus cone angle (θ) plot (Figure 1-4).[2] The map shows that many electron rich phosphines with different steric requirements are available (trialkyl and triaryl phosphines); these ligands are particularly useful to facilitate the oxidative addition step, for example, in transition metal mediated cross-couplings.[5] If good π-acceptor phosphines are necessary for a particular elementary

step of a catalytic cycle, phosphites and polyhalogenated aromatic phosphines are the ligands of choice. However, for catalytic processes requiring even higher π-acidity at the metal center only polyhalogenated phosphines, such as PF_3, $P(CF_3)_3$, PCl_3 can be considered. Unfortunately, these compounds suffer from high toxicity and sensitivity to air and water. They are thus, difficult to handle, making the availability of their metal complexes very limited.[6]

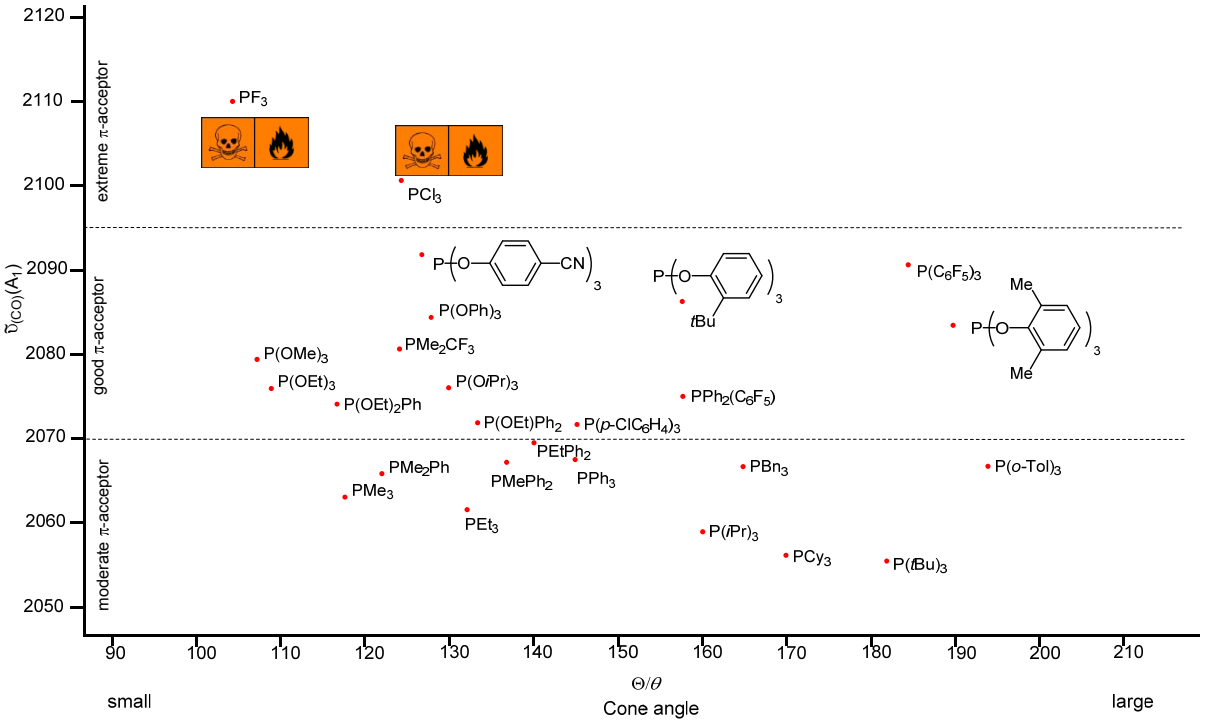

Figure 1-4. Tolman stereoelectronic map for neutral phosphines containing experimental values referring to $[Ni(CO)_3PR_3]$ complexes.

In those cases where PF_3 or $P(CF_3)_3$ would be appropriate ligands, but their use is limited by their intrinsic reactivity, the use of positively charged R groups emerges as an alternative. Since cationic moieties are by definition strongly electron-withdrawing substituents, they are expected to lower the energy of σ*(P-R) orbitals. This should lead to ligands depicting stronger π-acceptor properties.[7] For this reason, an overview of known cationic phosphines will be presented in the next section, which will be followed by the scope of this thesis.

1.1. Cationic Phosphines

Two main groups of cationic phosphines can be distinguished based on the position of the charged substituent: i) phosphines with the cationic charge placed remote to the phosphorus atom; ii) phosphines with the cationic charge attached directly (α-position) to the phosphorus atom. In the first group the positive charge is introduced to solubilize the respective phosphine ligand in water and thus achieve easily separable catalysts for homogeneous catalysis. The second approach, much more interesting for our work, attempts to adjust the electronic properties of phosphines according to the specific requirements of a certain transformation by the use of these charges.

After a general description of these two main types of cationic phosphines, the cyclopropenium-substituted phosphines - developed earlier by our group as a subclass of α-cationic phosphines - will be discussed in more detail, since these constituted the starting point of this thesis.

1.1.1. Cationic Charge Attached Remote to the Phosphorus Atom

One of the biggest challenges in homogeneous catalysis is the separation and recovery of the catalyst from the product phase, since often both have similar solubility characteristics. For this reason, despite the many attractive properties of homogeneous catalysis, such as high selectivities, industrial processes often prefer heterogeneous catalysis instead. To address this separation issue, two main approaches have been developed.[8] The first one heterogenizes the homogeneous catalyst by attaching it to a solid support (inorganic oxides or polymers) and involves separation by filtration. The second process involves the design of a catalyst that can be solubilized in a phase which is immiscible with the reaction product phase. In these biphasic reaction systems the substrate and catalyst are brought into contact by vigorous stirring; upon completion of the reaction, a simple phase separation allows for isolation of the products and recovery of the catalyst. Among several other organic immiscible phases that have been explored, such as fluorous solvents,[9] supercritical CO_2[10] and ionic liquids,[11] water[12] constitutes the most well-known example of this approach.

A large number of positively charged, hydrophilic phosphines are known in the literature, where the most commonly used cationic functionality is the ammonium ion, followed by phosphonium and guanidinium moieties (*e.g.* **1.1** and **1.2**, Scheme 1-1, a).[13] The ammonium-substituted Amphos **1.5** was prepared by Baird *et al.* through quaternization of the amine moiety in **1.3** with methyl iodide and subsequent reduction of the phosphine oxide **1.4** with trichlorosilane (Scheme 1-1, b).[14] Oxidation of the phosphorus center is necessary prior to quaternization, since the methylation of the corresponding free phosphinoethyl dimethylamine gives exclusively phosphorous-methylated product. The hexacationic phosphine **1.8** can be prepared by a similar strategy: *N*-alkylation of the triarylphosphine sulfide **1.6** yields salt **1.7**, which after removal of the sulfide protecting group is transformed into the desired water-soluble phosphine **1.8** (Scheme 1-1, c). The sterically more demanding water-soluble alkylphosphine **1.13** was prepared by Grubbs *et al.* via formation of the borane adduct **1.10**, followed by alkylation with 4-(*N*-methylpiperidyl)tosylate. Subsequent quaternization of the N-atom in **1.11** with methyl iodide and deprotection of phosphine **1.12** with morpholine afforded the desired cationic phosphine **1.13** (Scheme 1-1, d).[15]

As mentioned earlier, the advantage of charged phosphines lies in their solubility characteristics, which may lead to easily separable and recyclable catalysts of industrial interest. The hydrophilicity of these phosphines primarily depends on the ratio between the number of the solubilizing functionalities and the size of the molecule, thus, introduction of multiple charges enhances the water-solubility.

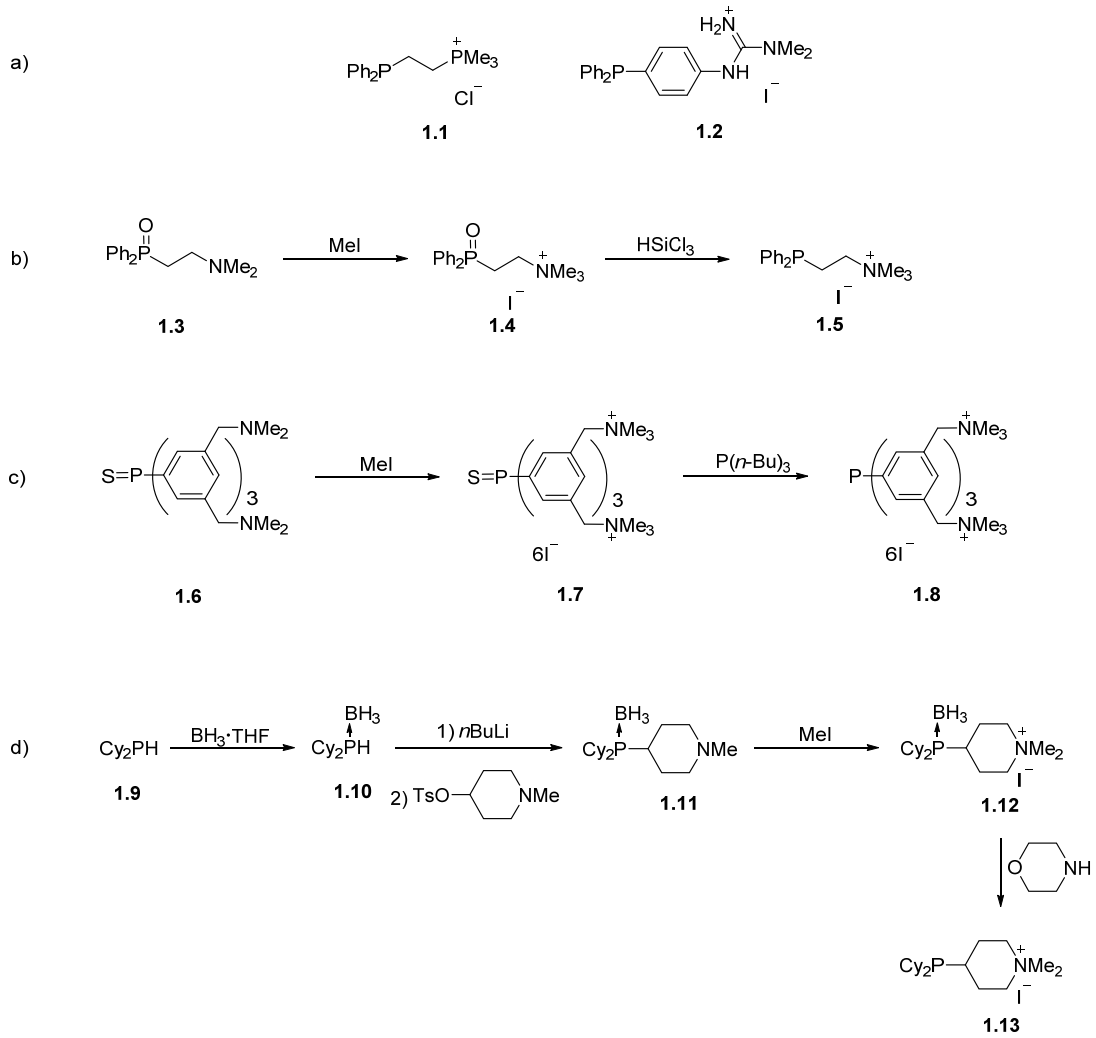

Scheme 1-1. a) Phosphonium- and guanidinium-substituted phosphines **1.1** and **1.2**. b) Synthesis of Amphos **1.5** c) Synthesis of hexacationic phosphine **1.8.** d) Synthesis of sterically hindered phosphine **1.13**.

As examples of metal complexes derived from hydrophilic cationic phosphines that have found application in catalysis,[13,16] I would like to highlight the work of Lemaire *et al.*[17] This study has shown that the ruthenium complex of the ammonium-substituted BINAP (2,2'-bis(diphenylphosphino)-1,1'-binaphtyl) **1.16** catalyzes the asymmetric hydrogenation of ethyl acetoacetate **1.14** to the desired alcohol **1.15**, using only 0.1 mol% catalyst in a biphasic mixture (water/ethyl acetoacetate) (Scheme 1-2). After completion of the reaction, alcohol **1.15** was extracted with pentane, leaving behind the catalyst in the aqueous phase, which could be reused for further six cycles with excellent enantiomeric excess (98 % ee). When the unsubstituted BINAP ruthenium complex was employed in ethanol in the same transformation, comparable catalytic activity and selectivity was obtained; however, in the case of the biphasic system the catalyst could be recycled and reused.

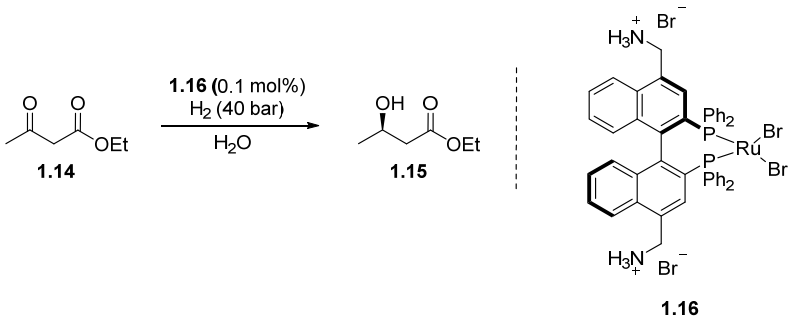

Scheme 1-2. Asymmetric catalytic hydrogenation of β-ketoester **1.14**.

Sterically demanding trialkylphosphines, such as P(*t*Bu)$_3$ are known to provide active catalysts for a range of palladium-catalyzed coupling reactions in organic solvents. The ammonium-substituted phosphine **1.20** was developed as water-soluble steric and electronic analog of P(*t*Bu)$_3$. **1.20**, in combination with palladium acetate served as an efficient catalyst for the Suzuki-coupling of 4-bromotoluene **1.17** with phenylboronic acid **1.18** in water/acetonitrile biphasic mixture (Scheme 1-3).[18] This transformation, affording the cross-coupling product in quantitative yield at room temperature, is the first application of a sterically demanding, water-soluble ligand in a biphasic Suzuki-coupling reaction. Upon completion of the reaction, the biphenyl product could be extracted with ether. The same **1.20**/Pd catalyst system could also be applied to Heck and Sonogashira couplings of aryl bromides with good activities.[19]

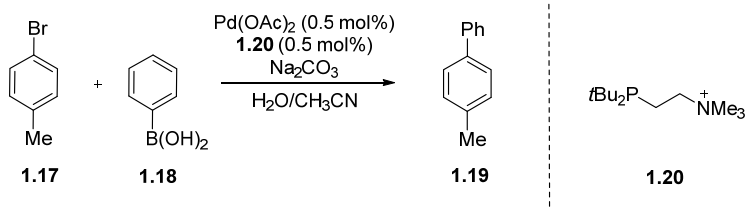

Scheme 1-3. Suzuki-coupling of 4-bromotoluene **1.17** with phenylboronic acid **1.18** catalyzed by **1.20.**

1.1.2. Cationic Charge Attached Directly (α-position) to the Phosphorus Atom

While the water-solubility of phosphines is not directly affected by the position of the positively charged functionalities, their electronic properties can dramatically change if these are attached adjacent (α-position) to the donor phosphorus atom.[7] As already mentioned, the positive charge lowers the energy of the orbitals in the molecule, most importantly the

valence orbitals responsible for σ-donor and π-acceptor properties.[20] As a consequence of their lower HOMO and LUMO, the resulting α-cationic phosphines are expected to show weaker σ-donor but stronger π-acceptor character than their neutral counterparts. Furthermore, this strategy yields more stable phosphines, due to the presence of robust P-C bonds instead of labile P-halogen bonds in the case of halogenated phosphines.

However, the choice of the cationic moiety is crucial, since these groups can contain empty low-lying π* orbitals, which are able to constructively overlap with the HOMO of the phosphine. This interaction can stabilize the σ-donating orbital at phosphorus and thus additionally weaken the σ-component of phosphine-metal bonds, to a point that can even prevent the coordination. Cationic substituents with higher energy LUMOs will then be the least prone to accept electron density from the central phosphorus atom, reducing this secondary interaction.[7] Figure 1-5 depicts the LUMO of several cationic moieties for comparitive purposes: 1,2-bis(diisopropylamino)cyclopropenium, 1,3-dimethylimidazolium, 1,4-dimethyl-1,2,4-triazolium, 1-methylpyridinium and tropylium at the B3LYP/6-31G* level. In all cases the LUMO has π-type symmetry and comparable shape, but it lies at the highest in the case of the bis(dialkylamino)cyclopropenium cation, followed by a slightly lower value for the imidazolium moiety. Hence, cyclopropenium-substituted phosphines are expected to behave more similar to neutral phosphines, therefore they depict richer coordination chemistry and stability. Phosphines containing tropylium-type substituents are expected to exhibit the weakest donor properties among the series. In fact these compounds have never been isolated, probably due to their high reactivity.

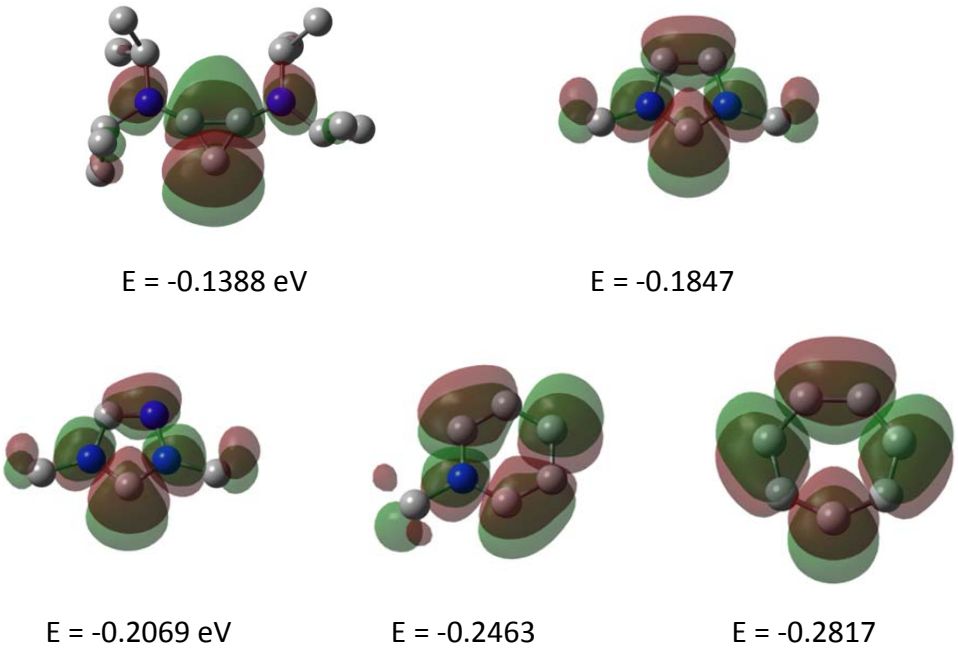

Figure 1-5. Comparison between the LUMOs of 1,2-bis(diisopropylamino)cyclopropenium (up, left), 1,3-dimethylimidazolium (up, right), 1,4-dimethyl-1,2,4-triazolium (down, left), 1-methylpyridinium (down, middle) and tropylium (down, right) at the B3LYP/6-31G* level. For the tropylium cation the LUMO+1 is depicted.

The most general procedure for the preparation of mono-α-cationic phosphines is treatment of chloro(dialkyl/diaryl)phosphines with the appropriate Lewis bases.[21] This process often uses halide abstractors, such as trimethylsilyl triflate, to generate a transient phosphenium cation, which is immediately trapped by the base. This strategy can also furnish di- and tri-α-cationic phosphines, when dichlorophosphines and trichlorophosphine are treated with the base.[22] Monocationic phosphine **1.21** was prepared by this protocol, using triphenylphosphine as base (Scheme 1-4, a).[21b] Other bases, such as pyridines[23] and *N*-heterocyclic carbenes[21a,24] can also be used in this type of reaction. The tricationic dimethylaminopyridinium-phosphine **1.22** was prepared by Weiss *et.al* in 1991, which represented the first described tricationic phosphine (Scheme 1-4, b).[22b]

For the preparation of the imidazolium-substituted phosphines a similar strategy can be applied, but the use of the free *N*-heterocyclic carbenes can be avoided by employing masked carbenes. Phosphine **1.24** was prepared by Weigand *et al.*, who treated a solution of trichlorophosphine with the silylated carbene **1.23** (Scheme 1-4, c).[25] Another method which gives access to imidazolium-substituted phosphines, consists of *N*-methylation of the corresponding imidazole-substituted phosphines, however the methylating agent has to be

selective in the presence of the phosphine moiety.[26] In analogy to the synthesis of their monocationic counterparts, both of these approaches are also amenable for the preparation of bis(imidazolium)phosphines. Dicationic phosphine **1.26** was prepared by Chauvin *et al. via* double alkylation of bis(imidazole)phosphine **1.25** (Scheme 1-4, d).[26c]

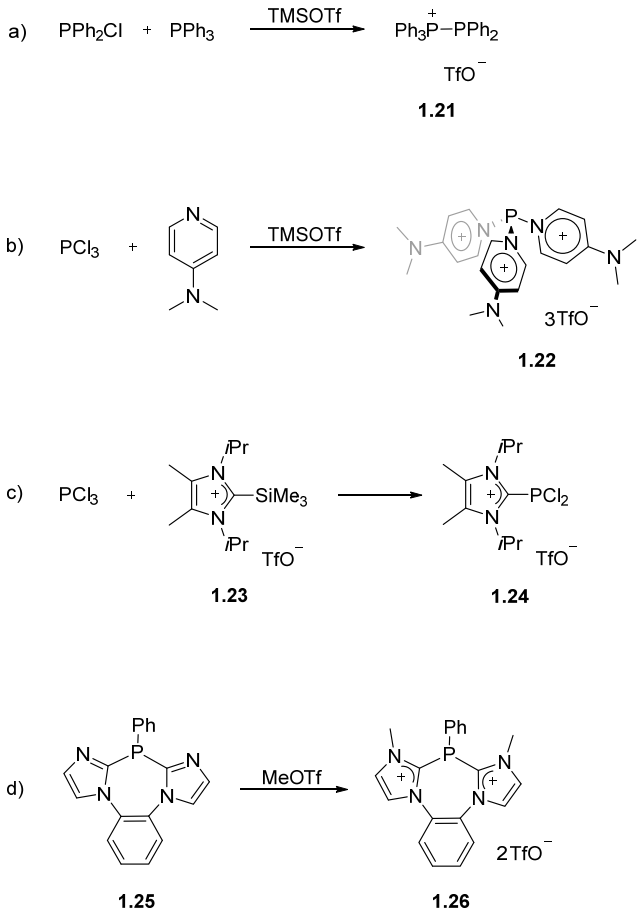

Scheme 1-4. a) Synthesis of monocationic phosphine **1.21**. b) Synthesis of tricationic phosphine **1.22.** c) Synthesis of monocationic phosphine **1.24.** c) Synthesis of dicationic phosphine **1.26**.

Our group has developed an alternative route for the synthesis of cationic phosphines, which involves condensation of secondary alkyl- or arylphosphines with the corresponding chloro-substituted "onium" cations following an aromatic nucleophilic substitution mechanism.[7] This protocol was also used for the synthesis of two new families of cationic phosphines, cyclopropenium and pyridinium phosphines (scheme 1-5). Among α-cationic ligands, pyridinium phosphines are very attractive for catalytic applications, since the pyridinium moiety allows for significant steric and electronic fine-tuning of the resulting phosphine.[27]

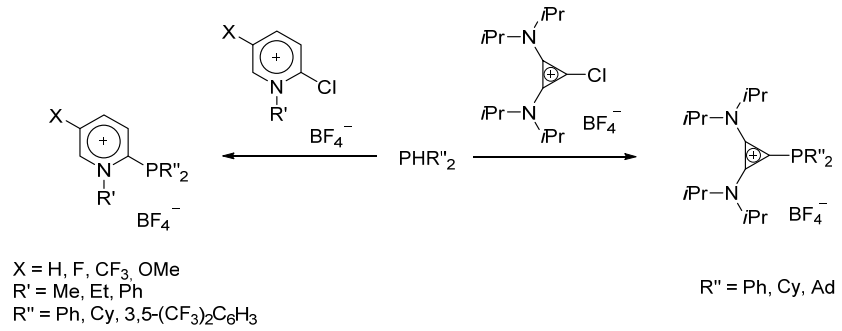

Scheme 1-5. Synthesis of cyclopropenium- and pyridinium-phosphines.

The Tolman stereoelectronic map shown in Figure 1-6 contains calculated (blue points) and experimental[28] (red points) values, for both neutral (black) and representative cationic phosphines (green). Among the monocationic series, pyridinium-substituted phosphines exhibit the poorest donor properties, being more inferior than triaryl- and trialkyl-phosphites. Imidazolium phosphines have similar donor properties to phosphites, while cyclopropenium ones are slightly stronger donor ligands. The highest stretching frequency value, which even surpasses that of PF_3 and $P(CF_3)_3$, was calculated for the bis(imidazolium)-phosphine **1.26**. Hence it was predicted to be the strongest π-acceptor ligand among the series. However, no coordination complexes of this cation have been reported to date, since the weak donor abilities prevent any ligation to metals.

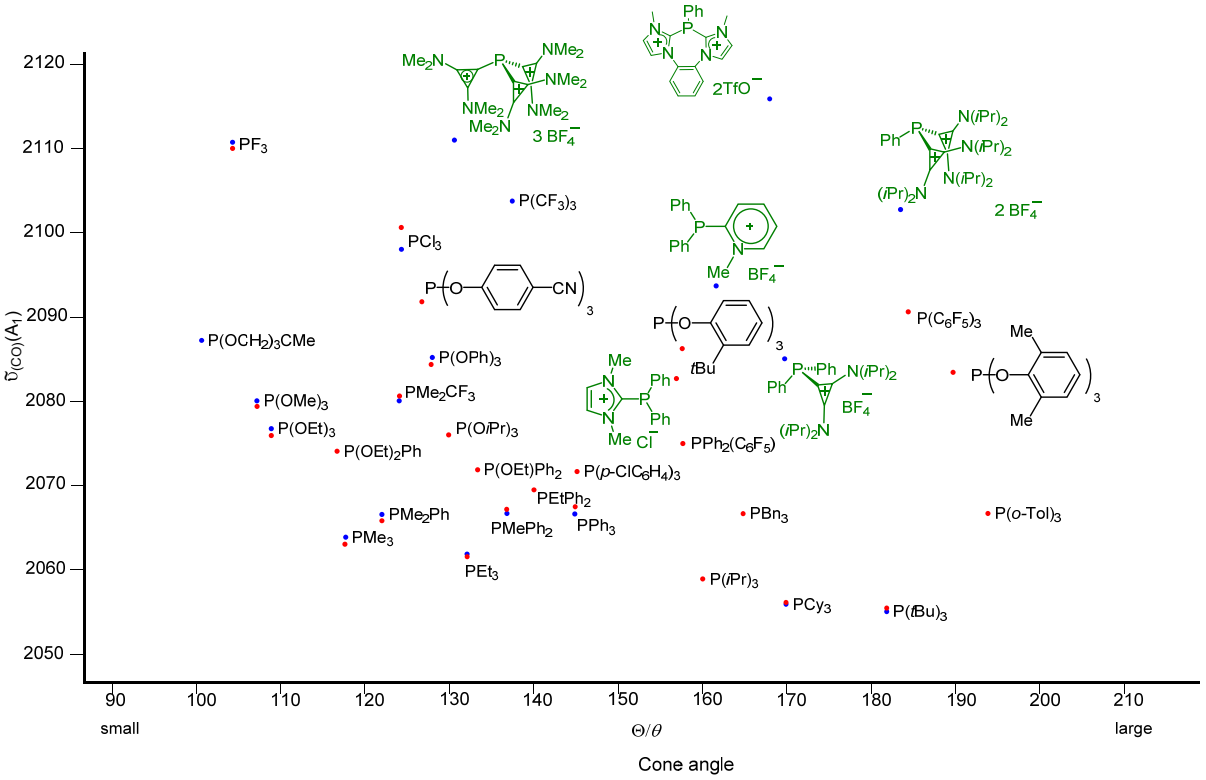

Figure 1-6. Tolman stereoelectronic map containing experimental (red points) and calculated (blue points) values for neutral (black) and cationic phosphines (green), all referring to $[Ni(CO)_3PR_3]$ complexes.

A number of catalytic processes have benefited from the phosphite surrogate nature of cationic phosphines and their high solubility in ionic liquids that facilitates catalyst recovery. The Neghisi cross-coupling of the arylzinc reagent **1.27** with aryl halide **1.28** using a palladium(0) source and imidazolium phosphine **1.30** is an example (Scheme 1-6).[29] In this case the desired product **1.29** was obtained in 91 % yield using a toluene/1-butyl-2,3-dimethylimidazolium (bdmim) tetrafluoroborate biphasic mixture, which allowed for a simple work-up and easy separation of the catalyst. However, attempts to reuse the palladium catalytic system showed that the yield drops by 20 % after the third cycle.

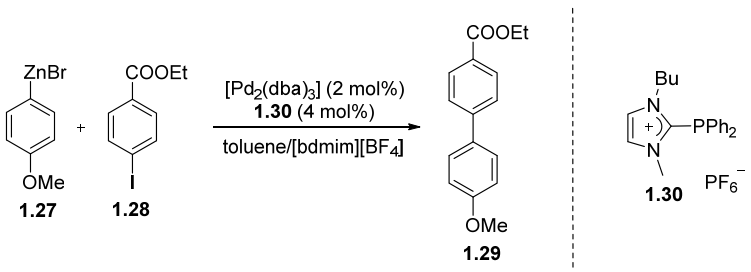

Scheme 1-6. Negishi cross-coupling of **1.27** with **1.28** using cationic ligand **1.30**.

An additional example is the hydrogenation reaction of meta-chloronitrobenzene **1.31** performed in 1-butyl-3-methylimidazolium (bmim) tetrafluoroborate using the platinum complex of **1.30** (Scheme 1-7). Employing 4 mol % catalyst loading, full conversion was obtained after 48 hours; more importantly, the desired product **1.32** could be extracted with diethylether from the ionic liquid phase containing the catalyst. The remaining bmim phase was then reloaded with substrate, affording constantly high conversions in up to seven cycles.

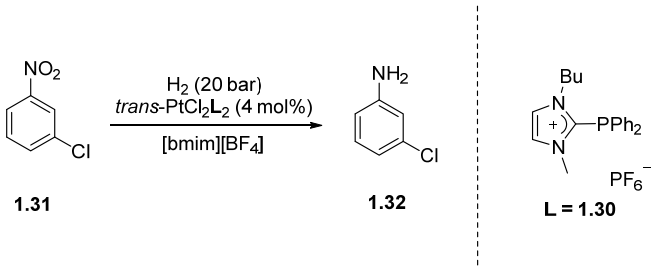

Scheme 1-7. Hydrogenation of **1.31** using cationic ligand **1.30**.

As shown in the Tolman stereoelectronic map in Figure 1-6, *N*-alkylated pyridinium phosphines are the strongest π-acceptor ligands among the monocationic series. Their outstanding performance, when compared to classical π-acceptor ligands, was demonstrated in the hydroarylation of propargyl aryl ether **1.33** to chromene **1.34** (Scheme 1-8). This is an ideal transformation to test cationic ligands, since its mechanism suggests that a platinum catalyst with enhanced π-acidity should facilitate the process. While less than 10 % conversion can be achieved after 10 minutes when employing $PtCl_4$ or $PtCl_2$ catalysts, the use of precatalyst **1.35**, in combination with a silver salt as chloride abstractor, affords full conversion after 10 minutes.

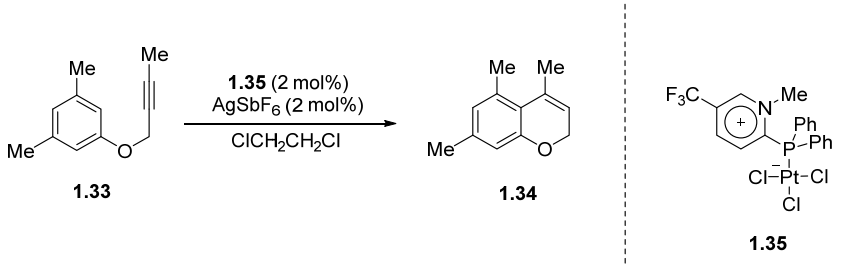

Scheme 1-8. Hydroarylation of propargyl aryl ether **1.33** using precatalyst **1.35**.

1.1.3. Cyclopropenium-Substituted Phosphines

The cyclopropenium-substituted phosphines presented in this section belong to the group of α-cationic phosphines. These compounds were first synthesized by a previous PhD student in our group.[30] Before giving an overview of their synthesis, electronic properties and catalytic applications, a brief historical background of cyclopropenium cations will be described.

1.1.3.1. Cyclopropenium Cation

In 1952 it was theoretically predicted that in addition to the well-known aromatic compounds that contain six or more π-electrons, the cyclopropenium cation with two π-electrons should also be aromatic.[31] This non-benzoid system also obeys Hückel's "4n + 2" rule, when n = 0. Five years later, Breslow reported the synthesis of the room temperature stable triphenylcyclopropenium tetrafluoroborate **1.36**, which was the first isolated example of this simple aromatic ring (Figure 1-7).[32] This discovery demonstrated that cyclopropenium cations can be isolated despite of their high ring strain.

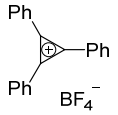

1.36

Figure 1-7. Triphenylcyclopropenium tetrafluoroborate **1.36** prepared by Breslow.

Dialkylamino-substituted cyclopropenium ions represent a popular subclass of this family, as they benefit from extra stabilization of the positive charge through the π-electron donating ability of the nitrogen atoms. The first aminocyclopropenium cation ever synthesized was reported by Yoshida in 1971,[33] when he observed that addition of an excess of dimethyl- or diethylamine to tetrachlorocyclopropene **1.37**, gave the corresponding triaminocyclopropenium ions **1.38** and **1.39**. In contrast, when the more sterically hindered diisopropylamine is used, the process stops after the second substitution, yielding the chlorobis(diisopropylamino)cyclopropenium **1.40** (Scheme 1-9).[34]

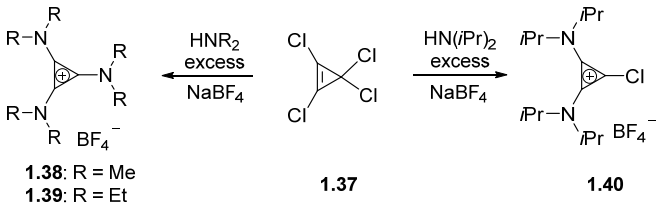

Scheme 1-9. Synthesis of aminocyclopropenium cations **1.38**-**1.40**.

This discovery was very interesting from a synthetic point of view, since **1.40** has a C-Cl bond that can be further functionalized. Thus, compound **1.40** can be used as starting material for the preparation of a large number of additional derivatives containing cyclopropenium cations. In fact, the easily accessible chlorocyclopropenium salt **1.40** was employed as source for the positively charged group in the preparation of α-cationic phosphines by our group.[30] Finally, it has to be mentioned that the small steric demand of the three-membered ring made the cyclopropenium cation very attractive for the synthesis of polycationic phosphines. In these cases however, ligation of the metal by the phosphine is not secured.

1.1.3.2. Synthesis

Cyclopropenium-substituted phosphines **1.41**-**1.46** are obtained as air-stable solids *via* the condensation of the chlorocyclopropenium salt **1.40** with a wide range of secondary phosphines (Scheme 1-10).[30a,30b] It is possible to describe these monocationic compounds using both, a covalent or a dative bonding model. Thus, compounds **1.41**-**1.46** can be seen as: (i) a phosphine containing a positively charged cyclopropenium substituent **A**, or as (ii) a phosphenium cation $[PR_2]^+$ stabilized by donation from a cyclopropenylidene ligand **B**.

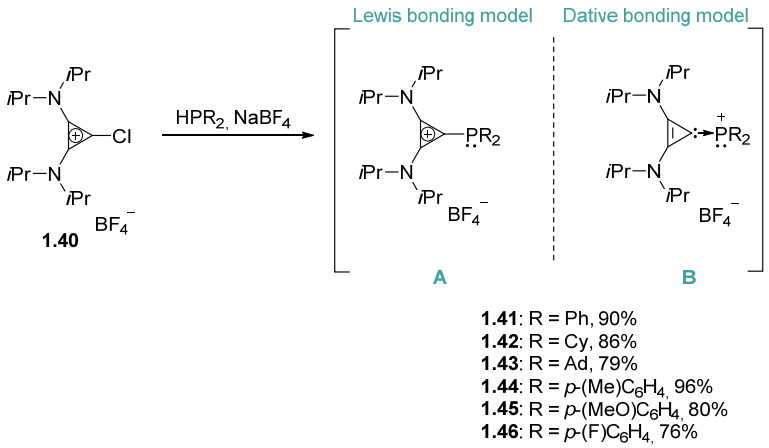

Scheme 1-10. Synthesis of α-cationic phosphines **1.41-1.46** and their bonding extremes **A** and **B**.

It was also envisaged that attachment of two or three positively charged groups to the phosphorus would result in phosphines able to mimic and even surpass the high π-acceptor properties of phosphites. Therefore, in an effort to improve the π-acceptor properties of the mono-α-cationic phosphines, further work in our group was then focused on the synthesis of di- and tricationic cyclopropenium-substituted phosphines.[20,30c]

Thus, compound **1.48** is prepared through a two-step sequence: treatment of chlorocyclopropenium salt **1.40** with a primary phosphine such as H_2PPh gives the secondary phosphine **1.47**, which after deprotonation with KHMDS and addition of a second equivalent of **1.40** affords the desired dication. Tricationic compounds **1.49** and **1.50** are obtained by a "reverse electron demand" –onium substituent strategy, making use of the silyl-substituted phosphines and chlorocyclopropenium salt **1.40** (Scheme 1-11). This synthetic route represents a variation of Bertrand's –onium substituent transfer methodology, where both reaction partners suffer from an umpolung of their original reactivity.[22a,35] In addition to multinuclear NMR spectroscopy, the connectivity of compounds **1.48** and **1.49** was confirmed by single crystal X-ray diffraction analysis. The low yields of the trications **1.49** and **1.50** are probably due to the steric demand of the cyclopropenium moiety, as replacement of the isopropyl groups by methyl groups on each nitrogen atom produces a significant increase of the yield (68 %).

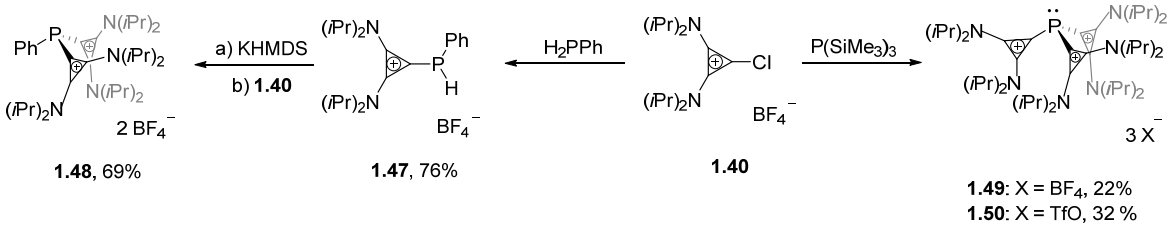

Scheme 1-11. Synthesis of cyclopropenium-substituted di-and trications **1.48-1.50**.

1.1.3.3. Electronic Properties

The donor properties of these unique monocationic phosphines were determined by measurement of the CO stretching frequencies of the rhodium complexes, of the general formula $[RhCl(CO)L_2](BF_4)_2$ (L = phosphine). These experimental values, summarized in table 1-1, are suggestive of slightly weaker donor abilities than that of neutral phosphines. As

expected, the phosphine containing *para*-fluoro-substituted phenyl groups is the weakest donor among the series, while the electron-donating groups such as cyclohexyl and *para*-tolyl induce stronger σ-donor character. In contrast, the imidazolium-phosphine **1.51** reported by Andrieu, resembles the strongly π-accepting character of phosphites.[21c,21e,25,26b,36] The intermediate behavior of cationic phosphines **1.41**-**1.46**, can be explained by the stronger σ-donor and poorer π-acceptor character of the free cyclopropenylidenes when compared to NHCs.

Table 1-1. Carbonyl stretching frequencies of representative monocationic phosphine ligands, PCy_3, PPh_3, $P(OMe)_3$, and **1.51** in the $[RhCl(CO)L_2](BF_4)_2$-type complexes. L = ligand.

Ligand	Comment	$\tilde{\nu}$ CO (cm^{-1})
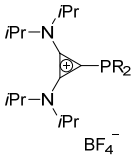	**1.41** R = Ph	1971
	1.42 R = Cy	1968
	1.44 R = *p*-(Me)C_6H_4	1969
	1.46 R = *p*-(F)C_6H_4	1976
PCy_3	-	1943
PPh_3	-	1962
$P(MeO)_3$	-	2011
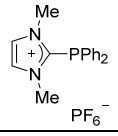	**1.51**	2003

In addition density functional theory (DFT) calculations on the B3LYP/6-31G* level were reported for polycations **1.48** and **1.49**.[20,30c,37] Several conclusions could be made: (i) the HOMO mainly has a lone pair character at phosphorus (**1.48**: 1.87e, **1.49**: 1.84e natural orbital occupancy), speaking for some Lewis base reactivity despite of the global +2 and +3 charges; (ii) the very low lying LUMO in both cases (**1.48**: -6.79 eV, **1.49**: -9.18 eV and $P(C_6F_5)_3$: -2.44 eV) is suggestive for very strong π-acceptor attributes.

The effect of a single and multiple positive charges on the frontier orbitals is shown in figure 1-8 where the calculated HOMO and LUMO orbitals for $P(OMe)_3$, $P(C_6F_5)_3$, mono-, di- and tricationic cyclopropenium-substituted phosphines are represented. Even the monocationic phosphine exhibits lower HOMO and LUMO energy levels than $P(OMe)_3$ and $P(C_6F_5)_3$, while the di- and tricationic phosphines display further decreased values.

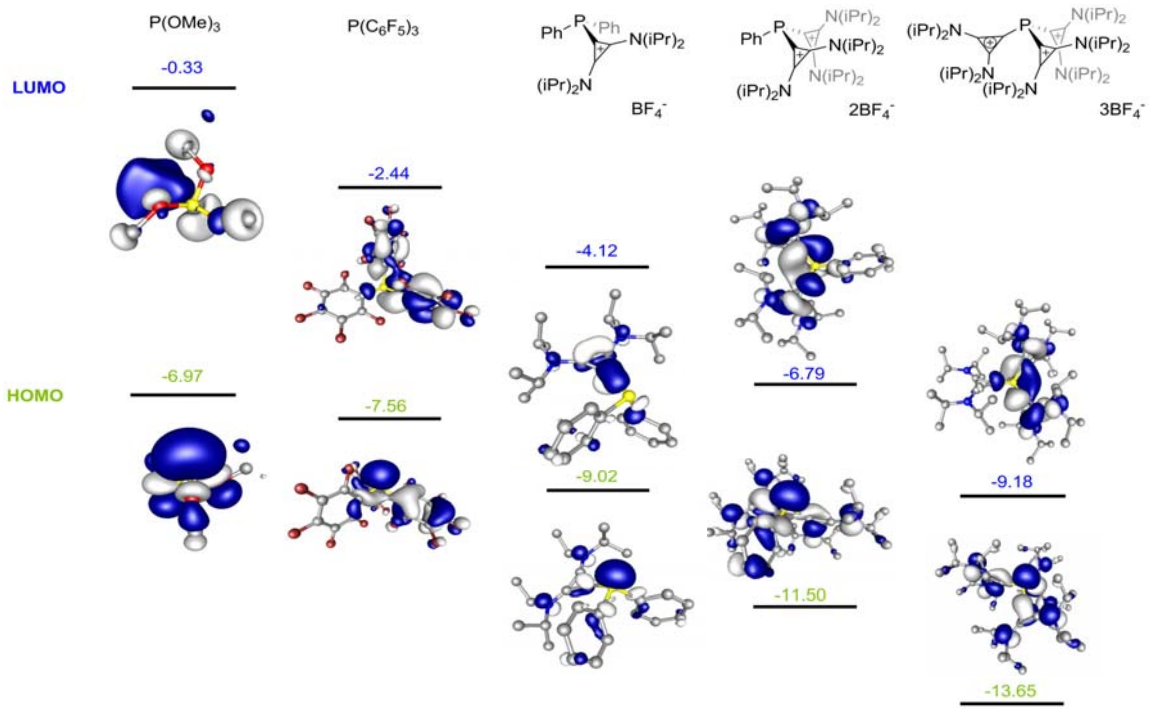

Figrue 1-8. Calculated HOMO and LUMO orbitals for $P(OMe)_3$, $P(C_6F_5)_3$, mono-, di- and tricationic cyclopropenium-substituted phosphines **1.41**, **1.48** and **1.49**, respectively on the B3LYP/6-311+G** level.

1.1.3.4. Application in Catalysis

The intermediate donor abilities of the monocationic cyclopropenium phosphines between neutral phosphines and phosphites was further supported by the performance of their gold complexes **1.52** and **1.53** (Figure 1-9) in several catalytic transformations.[30b]

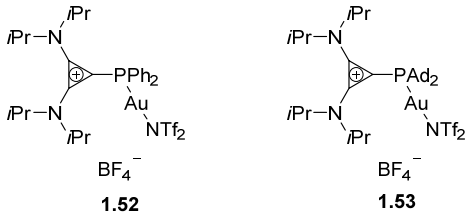

Figure 1-9. Cationic gold complexes **1.52** and **1.53**.

Some gold(I) catalyzed cyclization reactions are known to proceed through a number of possible pathways, depending on the σ-donor and π-acceptor properties of the ligand. An illustrative example is the cycloisomerization of allene-diene **1.54**: (i) electron poor ligands enhance the carbocationic nature of the intermediate **1.55**, providing product **1.56** by a 1,2-

alkyl shift; (ii) electron rich ligands afford compound **1.57** through a 1,2-hydride shift, owing to an increased carbene-like nature of intermediate **1.55** (Scheme 1-12).[38]

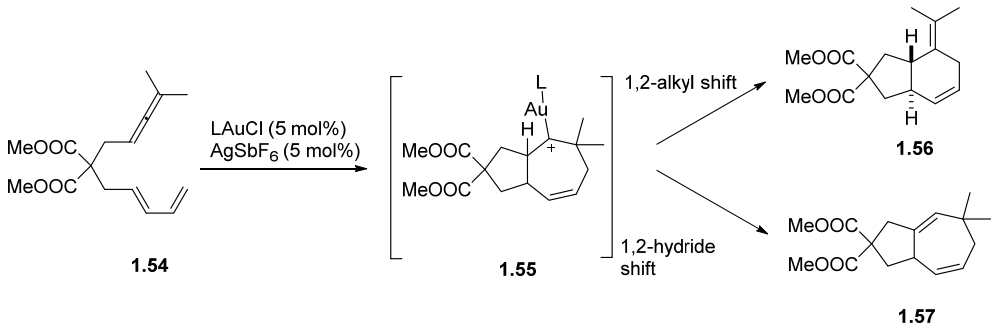

Scheme 1-12. Ligand effect on the gold(I) catalyzed cyclization of **1.54**.

While the use of standard gold(I) phosphine complexes, such as Me_3PAuCl and Ph_3PAuCl gives a mixture of products **1.56** and **1.57** in this reaction, the phosphite complex $(PhO)_3PAuCl$ favors the ring contraction by 1,2-alkyl shift. As expected, the electron rich NHC-based catalyst $IMesAuNTf_2$ (IMes = 1,3-bis(2,4,6-trimethylphenyl)imidazol-2-ylidene) favors the 1,2-hydride migration process. The selectivities obtained employing the gold complexes **1.52** and **1.53** lie between those of the commercially available phosphines and phosphites, being closer to the latter (Table 1-2). This finding corroborates the expectations, that the positive charge located at cyclopropenium groups lowers the donor abilities of the resulting phosphines, even though true phosphite-type behavior was not achieved.

Table 1-2. Cyclization reaction of **1.54** catalyzed by different gold complexes.

Catalyst	Reaction time	1.57/1.58 ratio	Yield
Me_3PAuCl	9h	55:45	84%
Ph_3PAuCl	3h	75:25	75%
$(PhO)_3PAuCl$	3h	97:3	98%
1.52	3h	87:13	92%
1.53	9h	61:39	64%
$IMesAuNTf_2$	3h	1:99	95%

Although the acceptor properties of monocationic cyclopropenium-substituted phosphines are similar to phosphites, they show a significant advantage owing to their saline nature. Hence, the recyclability of the Au(I) complex **1.52** was tested in the cycloisomerization

reaction of enyne **1.58** into diene **1.59** (Scheme 1-13), whereby the product could be easily extracted with diethylether, leaving behind the insoluble catalyst after filtration. Consecutive runs of the reaction gave consistently excellent yields in up to four cycles (98 to 95 %).[30a]

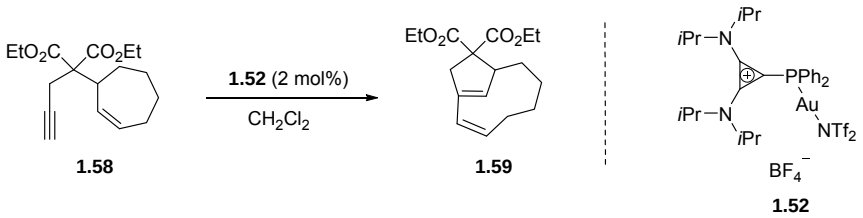

Scheme 1-13. Cycloisomerization of enyne **1.58**.

Encouraged by the calculated electronic properties of the di- and tricationic cyclopropenium phosphines **1.48** and **1.49**, suggesting strong π-acceptor properties, their Au(I)[20,30a] and Pt(II) complexes[30a,37] were tested as π-acid catalysts expecting an enhanced catalytic activity in processes requiring strong Lewis acidity at the metal center during the rate determining step.

To investigate if the dicationic phosphine-based Au(I) complexes could even surpass the reactivity of gold complexes bearing phosphite ancillary ligands, the Au(I) precatalyst **1.60** was then tested in the cycloisomerization of *ortho*-biaryl-substituted alkynes into bent phenanthrenes, containing substituents in both internal positions 4 and 5 (Scheme 1-14). These transformations are known to benefit from π-acidity at the metal center and therefore, they are ideal to explore π-acceptor ligands.[37,39]

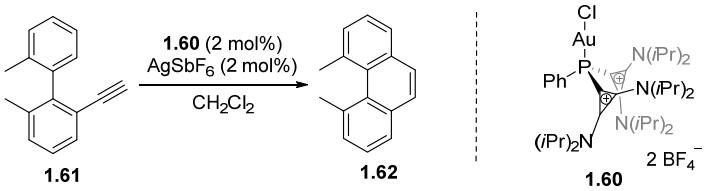

Scheme 1-14. Cycloisomerization of alkyne **1.61**.

Under the conditions shown in Scheme 1-14, substrate **1.61** was transformed into the desired product **1.62** after only 10 minutes in excellent yield (97%).[20] In sharp contrast, when the standard Au(I) catalysts Ph_3PAuCl and $(PhO)_3PAuCl$ were used, the conversion after the same time was minimal. Moreover, precatalyst **1.60** was also applied to the synthesis of a variety of naturally occurring phenanthrenes that belong to the *Orchidaceae* family.[40]

In spite of numerous examples where mono-, di- and tricationic cyclopropenium-substituted phosphines have proven favorable applicability in catalysis, some of their disadvantages are also apparent. Specifically, the dicationic Au(I) complex **1.60**, which exhibits excellent properties in the cycloisomerization of *ortho*-biaryl-substituted alkynes (Scheme 1-15),[20] slowly decomposes under the reaction conditions and therefore, is not effective if long reaction times are necessary. Finally, a last drawback of the described di- and tricationic catalysts is their insolubility in typical organic solvents owing to their highly charged nature, necessitating the use of polar solvents. Solutions to these inconveniences will be provided in the next chapter of this PhD thesis.

1.2. Scope of Thesis

This dissertation focuses on the design and synthesis of strong π-acceptor ligands, their coordination chemistry, and investigations into catalytic applications. For the reasons outlined in the introduction, the development of α-cationic phosphines which can not only mimic but also exceed the π-acceptor properties of phosphites and polyhalogenated phosphines is highly desirable. Moreover, stability issues also need to be taken into account.

In chapter two, entitled *Strong π-acceptor Monocationic Phosphines*, we aimed to overcome the stability issues. Hence, we decorated the phenyl rings of an already existing monocationic framework with strongly electron withdrawing groups (Figure 1-10, a, **A**). In addition, the cyclopropenium moiety was exchanged by a dihydroimidazolium ring, which is known to be a stronger π-acceptor (Figure 1-10, a, **B**). By decreasing the electron density on the central phosphorus atom in these ways, we avoided the necessity of two or three -onium substituents attached to the ligand in order to gain strong π-acceptor properties. This showed reduced destabilizing Coulombic repulsion between the ligand and the metal fragment, both bearing at least partial positive charge.

The goal of chapter three was to extend our synthetic methodology already optimized for the synthesis of cationic phosphines, to the preparation of nitrogen based isosteric structures. Our strategy is based on the reaction of a second equivalent of cyclopropenium cation with electron rich cyclopropenimines (Figure 1-10, b).

Finally, chapter four describes our efforts to design dicationic phosphines using bisimine stabilizing ligands. Because cyclopropenimines are predicted to be stronger bases than guanidines,[41] it was proposed that connection of these two imines by appropriate linkers resulting in chelate-type architectures would further stabilize the final phosphines. This represents a new realm in the chemistry of cyclopropenimines that has yet not been investigated (Figure 1-10, c).

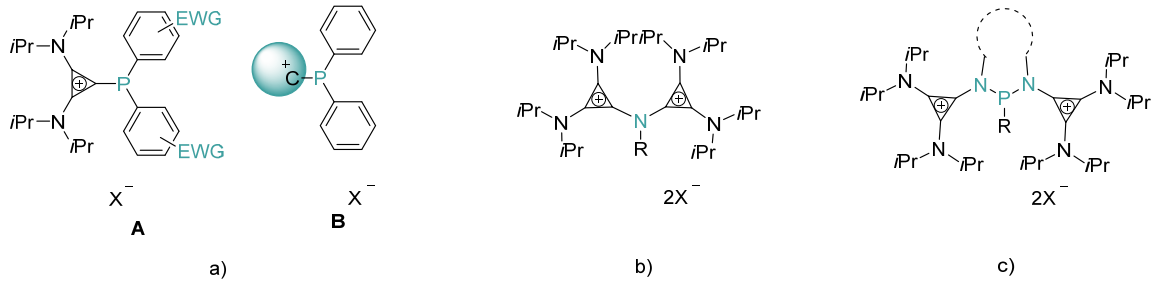

Figure 1-10. a) Design of new monocationic phosphines. b) Design of nitrogen analogs. c) Design of cyclopropenimine-substituted dicationic phosphines.

2. Strong π-acceptor Monocationic Phosphines

2.1. Introduction

In the vast realm of transition metal catalysis the choice of the ligand has a tremendous impact on the outcome of the reaction. Specifically, it often controls the reactivity of the resulting catalyst and the product selectivity, which underscores the importance of rational ligand design. Importantly for this thesis, the significance of ligands in catalysis endowed with strong π-acceptor properties lies in their capability to facilitate elementary steps of various transformations, such as reductive elimination, coordination of substrates to metal centers, nucleophilic attack on the coordinated substrates or deprotonation of the coordinated substrates. In the following each of these steps will be discussed in more detail.
Reductive elimination, the reverse of oxidative addition, is usually the last step of a catalytic cycle and leads directly to product formation. Prior to the reductive elimination in the catalytic cycle, the metal center is in a high oxidation state and hence strong π-acceptor ligands that deplete electron density from the already electron deficient metal center can facilitate this process. The palladium(II)-catalyzed arylation of α-branched secondary amines by Buchwald *et al.* shown in scheme 2-1 is evidence of this concept in practice.[42]

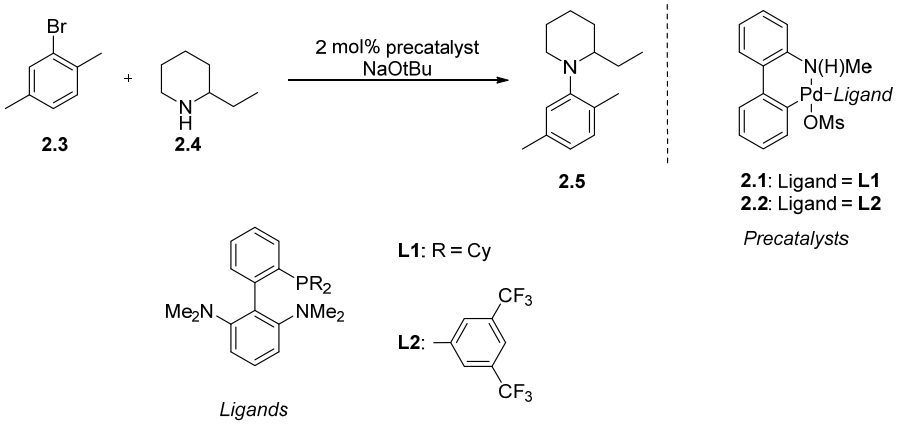

Scheme 2-1. Pd(II)-catalyzed arylation of **2.4** using precatalysts **2.1** and **2.2**.

One of the challenges in this C-N cross-coupling reaction is to overcome the competing β-hydride elimination, which may occur instead of the final reductive elimination step. The use of the electron rich biaryl phosphine ligand **2.1** affords a mixture of undesired (53 %) and desired (27 %, **2.5**) elimination products. Importantly, employing the more electron deficient

polyfluorinated ligand **2.2**, the side reaction can be suppressed and 85 % product **2.5** can be isolated.

A different elementary step that can also be enhanced by strong π-acceptor ligands is the coordination of unsaturated substrates to metal centers; in particular if the L ligand is positively charged (Scheme 2-2).[20,37] This step - consistently observed in π-acid catalysis mainly employing Au(I) and Pt(II) species - is usually precedented by treatment of the precatalyst **I** with silver salts (*e.g.* $AgBF_4$ or $AgSbF_6$) to obtain a coordination site at the metal center. The thus formed positively charged active catalyst **II** readily coordinates π-systems to form **III**; a process that can be facilitated by appending ligands able to withdraw electron density and hereby increase π-acidity at the metal center (Scheme 2-2).

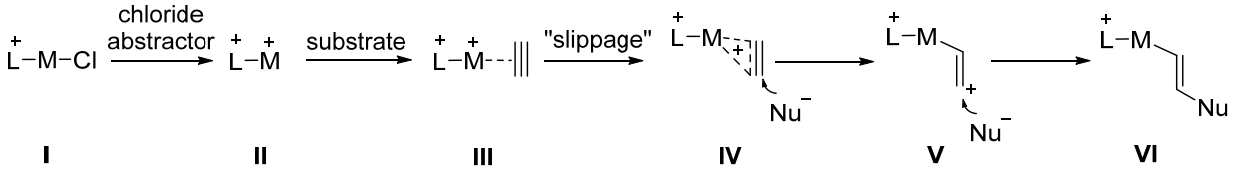

Scheme 2-2. Coordination of substrates to the metal center and nucleophilic attack on the coordinated substrate.[43]

The complexation of a π-system to the ligated metal center can be described using the Dewar-Chatt-Duncanson (DCD) model (Figure 2-1).[44] A σ-bonding interaction takes place due to constructive overlap between the bonding π orbital of the alkyne (substrate) and the empty, low lying d_{z^2} orbital on the metal (a). This is accompanied by π back-donation from a filled metal d orbital to the antibonding π* orbital of the alkyne (substrate) (b). It is also important to consider electrostatic interactions, which may play a significant part in describing the bonding situation, especially in the case of the charged metal fragments or ligands.[45]

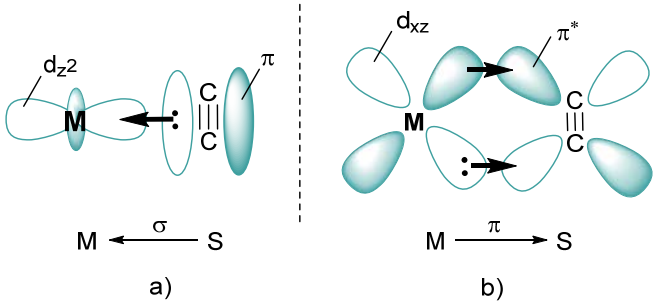

Figure 2-1. a) σ-Donation from a π orbital of an alkyne (S) into an empty d metal orbital; b) π back-donation from a filled metal d orbital into the π* alkyne (S) orbital.

High level theoretical calculations have shown that in general σ-donation gives the largest contribution to the orbital term (*ca.* 65 %).[45b,45c] The π-system therefore donates more electron density to the metal fragment than it gains through π back-bonding, resulting in an activation of the substrate towards nucleophilic attack. Additionally, computational studies have shown that a "slippage" of the ML_n fragment along the π-system of the substrate takes place (**IV** Scheme 2-2).[46]

Importantly, the nucleophilic attack on the coordinated substrate can similarly be promoted by strong π-acceptor ligands, since these ligands enhance the electrophilicity of the bound π-system through depletion of electron-density (**V**, **VI** Scheme 2-2). This is especially important, if the applied nucleophile is weak, such as arenes and olefins. Examples where strong π-acceptor ligands are employed to facilitate these elementary steps were discussed in sections **1.1.2** (Scheme 1-8) and **1.1.3.4** (Scheme 1-14) in the general introduction.

The last elementary step of a catalytic cycle that can benefit from strong π-acceptor ligands is the deprotonation of coordinated substrates, which is an important component in the field of C-H activation. Although various mechanistic views are present in the literature, a number of recent theoretical and experimental studies support that catalytic direct arylation reactions involve a concerted metalation-deprotonation (CMD) step.[47] This process includes deprotonation of the unfunctionalized arene and its simultaneous coordination to the metal. Ligand effect studies have shown that both inter- and intramolecular direct arylations benefit from the use of electron-poor phosphines, even though the electronic effect in the CMD still remains unclear.[48] A very recent example is the palladium catalyzed direct arylation of thiophene derivatives using Buchwald-type phosphines reported by Korenaga *et al.*, where kinetic isotope effect experiments validated CMD as rate-determining step (Scheme 2-3).[48a] While employing SPhos **2.9** as ligand only yielded 3 % of product **2.8**, the polyfluorinated SPhos derivative **2.10** afforded 90 % of the desired compound **2.8**. Interestingly, this performance even surpasses the more electron-poor ligand P(3,5-bis(trifluoromethyl)pyridine)$_3$, possibly due to additional stabilization of the catalyst through secondary Pd-arene interactions.

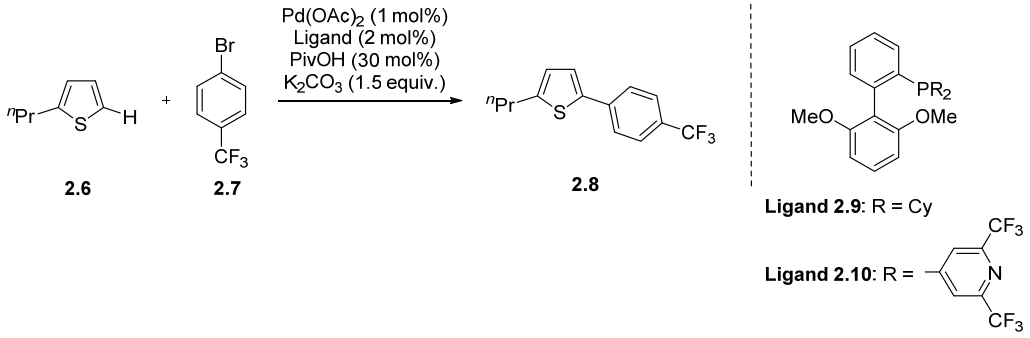

Scheme 2-3. Palladium(II)-catalyzed arylation of **2.6** using ligands **2.9** and **2.10**.

In conclusion, if in a catalytic process one of the mentioned elementary steps that can be facilitated by strong π-acceptor ligands is rate-determining, these ligands can be crucial to promote reactions or to permit novel transformations that may not be accessible otherwise.[49]

The disadvantages of the previously prepared cyclopropenium phosphines by our group, such as weak phosphorus-metal bond in case of polycations and relatively weak π-acceptor properties in case of monocations, prompted the design and utilization of the following two strategies for a second generation of new strong π-acceptor ligands.

Firstly, it was decided to incorporate trifluoromethyl groups onto the phenyl substituents of monocationic cyclopropenium phosphine **1.41**.[30a,30b] The more electron withdrawing substituents would then render the phosphorus atom more electron deficient, reducing its σ-donor ability and subsequently increasing its π-acceptor ability when bound to a metal.

Our second approach was to change the nature of the cationic substituent. Although the imidazolium-substituted phosphines are known to serve as ligands for different transition metals,[21e,24,26b,26c,50] the coordination chemistry of their saturated congeners, the dihydroimidazolium-phosphines still remains unexplored. The dihydroimidazolium moiety lacks a double bond in its backbone at the 4,5-position, hence in contrast to the imidazolium fragment it is not aromatic. As a consequence the positive charge is only delocalized between three atoms and should therefore confer stronger π-acceptor properties, when compared to the imidazolium fragment, which possesses a more evenly distributed positive charge across the ring. The proximity of both nitrogens of the dihydroimidazolium fragment to the phosphorus atom, coupled with easy, modular synthesis with respect to modifying the *N* substituents would also enable fine tuning of the electronic and steric properties of the resulting phosphine.

Π-acid catalysis, employing mainly Au(I) and Pt(II) species, is an excellent tool to generate structurally challenging natural products from simple unsaturated organic substrates.[43,49b,51] Furthermore, since the rate-determining step in these processes is often known to be the nucleophilic attack on the coordinated substrate, it is ideal to test π-acceptor ligands. Hence, to validate our newly prepared monocationic ligands, the platinum-catalyzed cycloisomerization of a biaryl alkyne was chosen as a model reaction. This represents rational ligand design for the synthesis of complex structures in further development of α-cationic phosphine ligands.

2.2. Results and Discussion

2.2.1. Synthesis

The synthesis of monocationic phosphines **1.41**-**1.46** was previously developed by our group.[30a,30b] Unfortunately, the direct condensation between a secondary phosphine and chlorocyclopropenium **1.40** could not be applied for the preparation of 3,5-bis(trifluoromethyl)phenyl-substituted phosphine **2.12**, as the low nucleophilicity of **2.11** prevents its attack on the cyclopropenium ring in **1.40**. Hence, deprotonation of the polyfluorinated secondary phosphine **2.11** by *n*BuLi is necessary to enhance the nucleophilicity and facilitate the desired transformation. After this change in the original protocol, compound **2.12** could be obtained in moderate, but reliable yield (38 %) (Scheme 2-4).[52a]

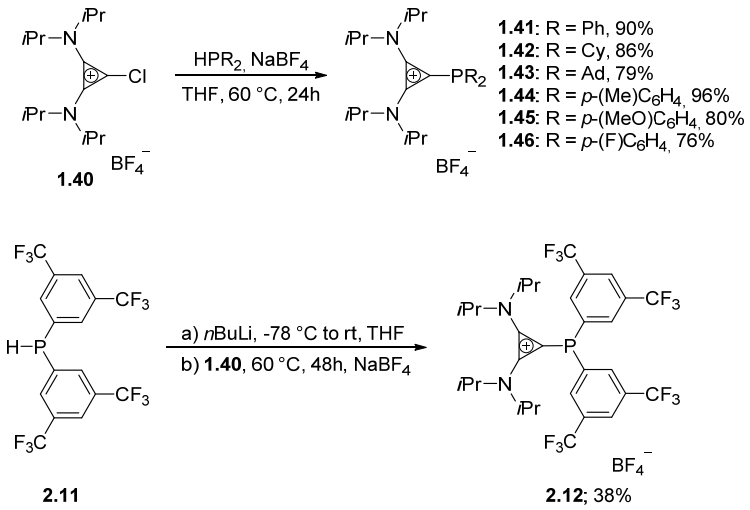

Scheme 2-4. Synthesis of cationic phosphines **1.41-1.46** and **2.12**.

The synthesis of dihydroimidazolium phosphines **2.14** and **2.15** follows the general method described by our group for the cyclopropenium-substituted phosphines that counts on a first condensation of chlorodihydroimidazolium salt **2.13** with the corresponding secondary phosphines and subsequent anion exchange (Scheme 2-5).[53]

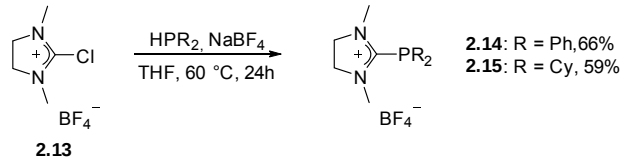

Scheme 2-5. Synthesis of phosphines **2.14** and **2.15**.

The connectivity of the new monocations **2.12**, **2.14** and **2.15** was first reflected by their characteristic $^{31}P\{^{1}H\}$ NMR signals (δ_P = -26.9, -14.6 and -10.4 ppm, respectively) and could subsequently be confirmed by X-ray diffraction analysis in the case of **2.15** (Figure 2-3). These data reveal that **2.15** adopts a conformation whereby the plane of the dihydroimidazolium ring bisects the C6-P1-C12 angle and the central phosphorus displays a pyramidal environment with retention of a non-bonding lone pair (sum of angles around the phosphorus: $\Sigma°P$ = 307.8°). The P1-C1 bond length of 1.860(2) Å has a similar value to the other phosphorus-carbon bond distances in the molecule (P1-C6 and P1-C12: 1.865(2) and 1.859(2) Å, respectively).

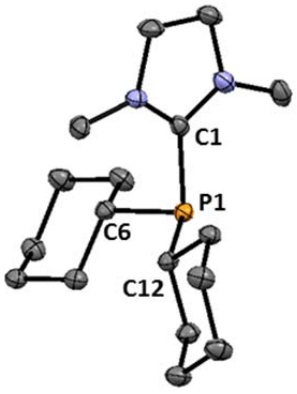

Figure 2-3. Solid-state structure of **2.15**. Hydrogen atoms and the anion are omitted for clarity; ellipsoids are set at 50 % probability.

2.2.2. Electronic Properties

As mentioned in the general introduction, the most widely accepted method to evaluate the combined σ-donor and π-acceptor abilities of phosphines is the CO stretching frequency analysis of their metal carbonyl complexes, introduced by Tolman[2]. Hence, we first aimed to evaluate the electronic properties of the newly prepared phosphines by the above mentioned method. Therefore, the corresponding rhodium complexes **2.16**-**2.18** were prepared in excellent yields by treating cationic phosphines **2.12**, **2.14** and **2.15** with $[RhCl(CO)_2]_2$ (Scheme 2-6). The formation of the new Rh-phosphine complexes was indicated by the appearance of characteristic doublet signals in their $^{31}P\{^1H\}$ NMR spectra: δ_P = 25.0 (d, $^1J_{RhP}$ = 136.5 Hz; **2.16**), 35.8 (d, $^1J_{RhP}$ = 132.0 Hz; **2.17**) and 50.1 (d, $^1J_{RhP}$ = 127.8 Hz; **2.18**) ppm. The obtained stretching frequency values suggest that compounds **2.12** ($\tilde{\nu}$ = 1991 cm^{-1}) and **2.14** ($\tilde{\nu}$ = 1993 cm^{-1}) are weaker donors than their previously reported counterparts **1.41**, **1.44**-**1.46** ($\tilde{\nu}$ = 1969 to 1976 cm^{-1}), due to the presence of electron withdrawing -CF_3 groups in **2.12** and the dihydroimidazolium moiety in **2.14**. Compound **2.15** ($\tilde{\nu}$ = 1971 cm^{-1}) is a slightly stronger donor than **2.12** and **2.14**, likely owing to the more electron donating cyclohexyl groups (Table 1-1). Surprisingly, these values are lower than the one measured for trimethyl phosphite (2011 cm^{-1}). This is unexpected and does not match our experimental results obtained during the studies of the catalytic activity of Au and Pt complexes derived from these phosphines, which will be shown at the end of this chapter. It is important to consider, however that the steric bulk of phosphites is much lower than that of all of the prepared cationic phosphines, therefore a comparison of their stretching frequency values - as explained in the introduction - may not be completely appropriate.

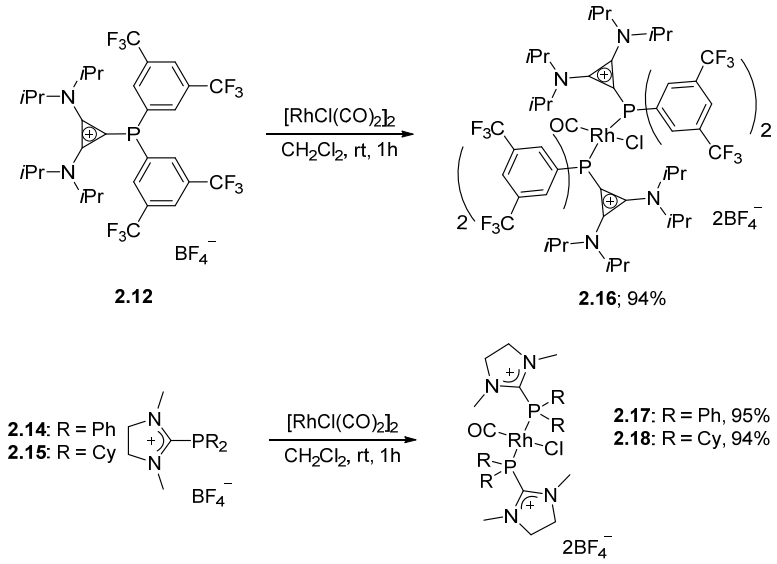

Scheme 2-6. Synthesis of $[RhCl(CO)L_2](BF_4)_2$-type complexes (L = ligand).

For these reasons an alternative experimental technique was chosen to rank the donor-acceptor properties of the prepared phosphines: determination of their oxidation potentials (E_p ox) by cyclic voltammetry.[54] In contrast to the classical CO stretching frequency analysis, the electrochemical method does not require the preparation of any metal complex; hence it is independent of steric factors.

Electron rich phosphines, having a quite high lying HOMO, are expected to be oxidized at low potential, while the oxidation should be more difficult for electron poor ones. Cationic phosphines are therefore expected to be oxidized at higher potentials than their neutral counterparts.

The oxidation potentials of the newly prepared phosphines **2.12**, **2.14**, **2.15** in addition to a number of controls are summarized in table 2-1. At a first glance these results are similar to the ones obtained from carbonyl stretching frequency, as phosphines **2.12** and **2.14** (E_p ox = 1.548 and 1.480 V, respectively) exhibit the weakest donor abilities among the series. However, there are subtle differences: the cyclic voltammetry measurements confirm the weak donor ability for all cationic phosphines (1.040 to 1.548 V) that now are very similar or even poorer than those exhibited by trimethyl phosphite (E_p ox = 1.287 V for $P(MeO)_3$). This ranking correlates much better with our observations in the catalytic activity of the phosphine-metal coordination complexes than the classical Tolman method and therefore, will be used throughout this thesis.

Table 2-1. Carbonyl stretching frequencies ($\tilde{\nu}$) for ligands **1.41**, **1.44-1.46**, **2.12**, **2.14**, **2.15**, PPh_3, $P(MeO)_3$ in the $[RhCl(CO)L_2](BF_4)_2$-type complexes (L = ligand) and oxidation potentials (E_p ox) for the free ligands.

Ligand	R	$\tilde{\nu}$ CO (cm^{-1}) $[RhCl(CO)L_2](BF_4)_2$	E_p ox (V)[a]
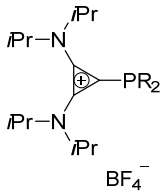	**1.41** R = Ph	1971	1.207
	1.44 R = *p*-(Me)C_6H_4	1969	-
	1.45 R = *p*-(OMe)C_6H_4	1969	1.040
	1.46 R = *p*-(F)C_6H_4	1976	1.246
	2.12 R = 3,5-$(CF_3)_2C_6H_3$	1991	1.548
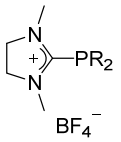	**2.14** R = Ph	1993	1.480
	2.15 R = Cy	1971	1.461
PPh_3		1979	0.687
$P(MeO)_3$		2011	1.287

[a] Oxidation potentials calibrated versus ferrocene/ferricinium, Bu_4NPF_6 (0.1 M) in CH_2Cl_2.

2.2.3. Coordination Properties

Although the synthesis of cyclopropenium-substituted salts **1.41**, **1.44**-**1.46** was already reported, their ability to form Pt(II) complexes has not been explored. Thus, reaction of **1.41**, **1.44**, **1.46** and **2.12** with one equivalent of $K_2[PtCl_4]$ yielded the corresponding trichloroplatinate complexes **2.19**-**2.22** (Scheme 2-7). The coordination of phosphorus to platinum was initially reflected by the diagnostic satellite signals in the $^{31}P\{^1H\}$ NMR spectra at δ_P = 3.1 ($^1J_{PtP}$ = 4021.5 Hz; **2.19**), 3.0 ($^1J_{PtP}$ = 4006.9 Hz; **2.20**), -0.01 ($^1J_{PtP}$ = 4031.2 Hz; **2.21**), 3.11 ($^1J_{PtP}$ = 4070.2 Hz; **2.22**) ppm. The phosphorus-platinum coupling constants increase in the order of increasing oxidation potential values of the free ligands as a consequence of the better π-acceptor properties in this order ($^1J_{PtP}$: **2.20** < **2.19** < **2.21** < **2.22**). Moreover, single crystals of **2.19**-**2.22** were grown and their structure was unambiguously determined by X-ray diffraction analysis.

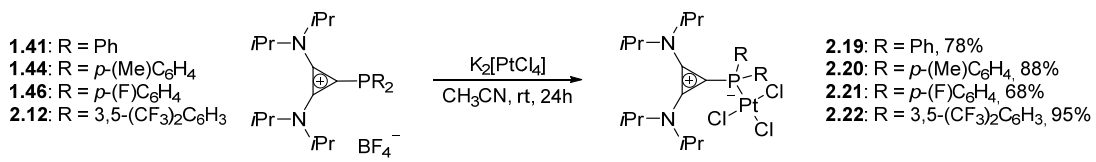

Scheme 2-7. Synthesis of Pt(II) complexes **2.19**-**2.22**.

Figure 2-4 shows the solid-state structures of the free ligand **1.44** and its Pt(II) complex **2.20**. Comparison of the C1-P1 bond lengths in these two compounds, 1.807(1) Å in **1.44** and 1.812(2) Å in **2.20,** reveals a slight bond elongation in the coordinated phosphine moiety when compared to the free ligand. This is probably due to cancellation of any back-donation from the phosphorus atom to the cyclopropenium ring upon its coordination to the metal center.

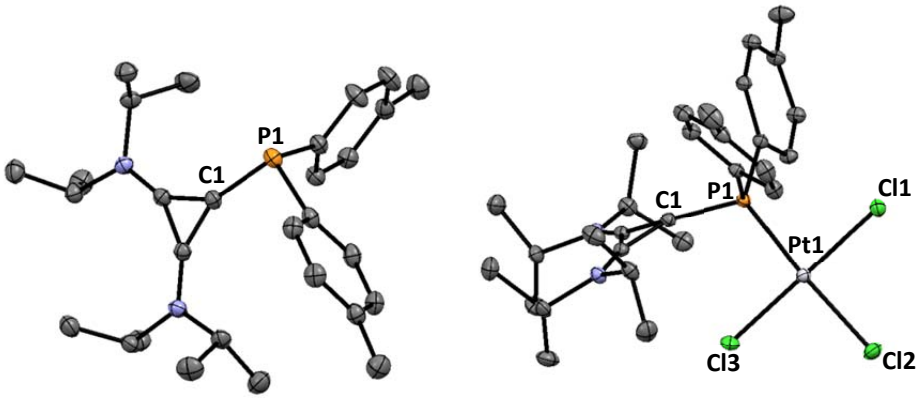

Figure 2-4. Solid-state structures of **1.44** (left) and **2.20** (right). Hydrogen atoms are omitted for clarity; ellipsoids are set at 50 % probability.

The solid-state structures of **2.19**, **2.21** and **2.22** are shown in figure 2-5. These data reveal that the same C1-P1 bond lengths in compounds **2.21** and **2.22** (1.799(4) and 1.797(1) Å, respectively) are slightly shorter than in **2.20** (*cf.* 1.812(2) Å). This suggests the presence of a stronger P1-C1 bond when the phosphorus atom is substituted by electron poor aromatic rings. Compound **2.19** also follows this trend with a slightly longer P1-C1 bond length (1.806(3) Å) than the one in **2.20** (*cf.* 1.812(2) Å), containing more electron rich phenyl substituents. As expected, the P1-Pt1 bond distance in this series of Pt(II) complexes is shortest in case of **2.22** (2.194(1) Å), while the more electron rich phosphines **2.19** and **2.20** exhibit slightly longer (2.201(1) and 2.207(1) Å, respectively) P1-Pt1 bonds. In contrast, **2.21** exhibits a slightly longer P1-Pt1 bond length than expected (2.219(1) Å), disagreeing the trend of the oxidation potentials of the free ligands.

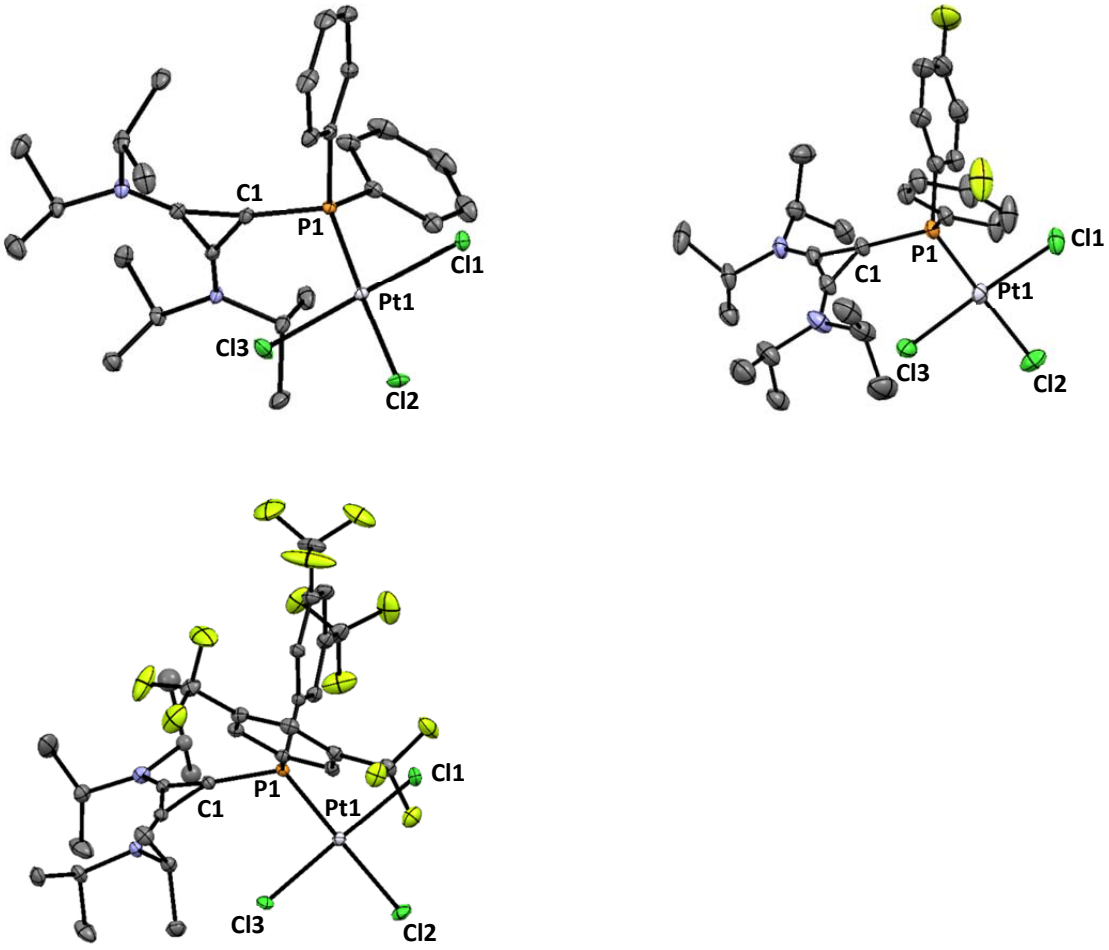

Figure 2-5. Solid-state structures of **2.19** (up, left), **2.21** (up, right) and **2.22** (down, left). Hydrogen atoms and solvent molecules are omitted for clarity; ellipsoids are set at 50 % probability.

Similarly, dihydroimidazolium-substituted phosphine **2.14** also coordinated Pt(II) to yield adduct **2.23** (Scheme 2-8), which possessed a $^{31}P\{^{1}H\}$ NMR spectrum with characteristic ^{195}Pt satellite signals: δ_P = 4.4 ($^{1}J_{PtP}$ = 3939.9 Hz). Its structure was also confirmed by X-ray diffraction analysis (Figure 2-6). The significantly longer C1-P1 bond distance in **2.23**, 1.874(5) Å, than in **2.19-2.22** (*cf.* 1.797(1)-1.812(2) Å), can be explained by the weaker σ-donor properties of the dihydroimidazolium moiety when compared to the cyclopropenium unit. Accordingly, **2.23** (2.212(1) Å) exhibits a slightly shorter P1-Pt1 bond legth when compared to the analogous cyclopropenium-substituted phosphine **2.19** (*cf.* 2.201(1) Å).

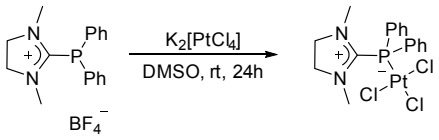

Scheme 2-8. Synthesis of Pt(II) complex **2.23**.

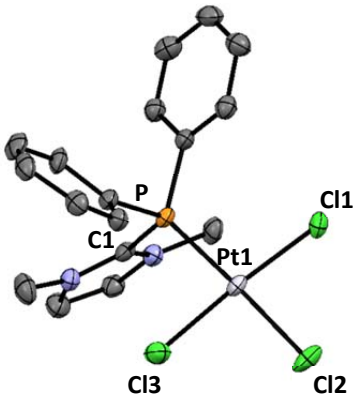

Figure 2-6. Solid-state structure of **2.23**. Hydrogen atoms and anions are omitted for clarity; ellipsoids are set at 50 % probability.

Cationic phosphines **1.41**-**1.46** were also shown to readily coordinate Au(I) centers;[30a,30b] therefore, we set out to examine the coordination of cations **2.12**, **2.14** and **2.15** to [AuCl] fragments. Thus, addition of one equivalent of [AuCl(SMe_2)] to a dichloromethane solution of the corresponding monocations afforded cleanly the desired Au(I) complexes **2.24**-**2.26** in excellent yields (Scheme 2-9). Coordination to the gold center was apparent from a significant downfield shift of the $^{31}P\{^{1}H\}$ NMR signals in comparison to the free ligand (δ = 19.8, 23.3 and 42.4 ppm for **2.24**, **2.25** and **2.26**, respectively; $\Delta\delta$ = 37.9 to 52.8 ppm). While complexes **2.25** and **2.26** are air stable, **2.24** has to be handled under inert atmosphere, probably due to the low electron density on the phosphorus atom.

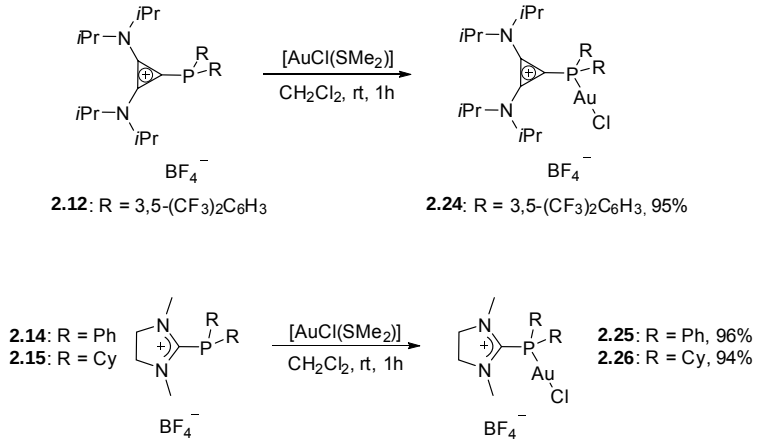

Scheme 2-9. Synthesis of Au(I) complexes **2.24-2.26**.

In addition, the corresponding [RhCl(cod)L](BF_4) type complex could be obtained (L = **2.14**) by stirring a dichloromethane solution of **2.14** with 0.5 equivalents of $[RhCl(cod)]_2$ (Scheme 2-10). The connectivity of **2.27** was not only implied by the doublet signal in the $^{31}P\{^1H\}$ NMR spectrum at δ = 29.9 ($^1J_{RhP}$ = 150.1 Hz) ppm, but also confirmed by X-ray diffraction analysis (Figure 2-7). These data reveal that the Rh1-C6 and Rh1-C7 bond distances (2.217(2) Å both) are significantly longer than the Rh1-C11 and Rh1-C10 (2.137(2) and 2.155(2) Å, respectively), indicative of a strong *trans*-influence from the cationic phosphine moiety.

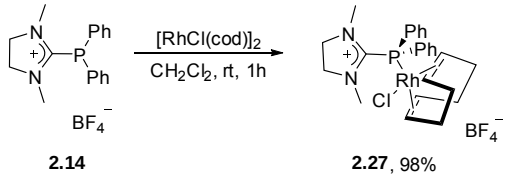

Scheme 2-10. Synthesis of Rh(I) complex **2.27**.

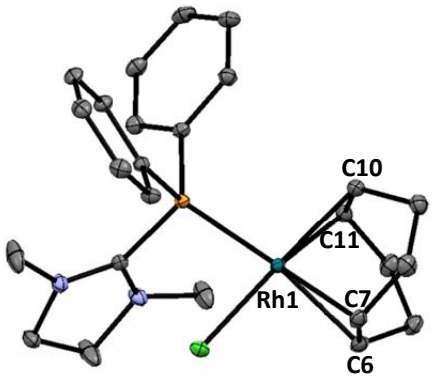

Figure 2-7. Solid-state structure of **2.27**. Hydrogen atoms and the anion are omitted for clarity; ellipsoids are set at 50 % probability.

To further understand the coordination properties of cyclopropenium-substituted phosphines, compounds **1.41** and **1.42** were treated with $[Pd_2(dba)_3]$ in dichloromethane at room temperature. Interestingly, the oxidative insertion of Pd(0) into the carbon-phosphorus bond took place, yielding the Pd(II) cyclopropenylidene complexes **2.28** and **2.29** (Scheme 2-11)**.** Although the upfield shifted signals observed by $^{31}P\{^{1}H\}$ NMR spectroscopy at δ_P = -130.6 (**2.28**) and -104.6 (**2.29**) ppm were already indicative of the presence of an anionic phosphide moiety in their structures, $[R_2P]^-$, the connectivity of these complexes could unambiguously be determined only after growing suitable crystals for X-ray diffraction analysis (Figure 2-6). These data show that the two Pd centers are interconnected by two phosphide moieties acting as μ_2 bridging ligands; the remaining coordination vacancies being occupied by acetonitrile, which was used as solvent for the crystallization.

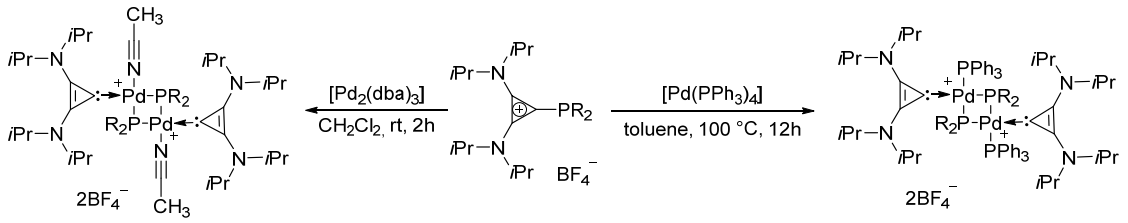

2.28: R = Ph, 44%
2.29: R = Cy, 38%

2.30: R = Ph, 73%

Scheme 2-11. Synthesis of the complexes **2.28-2.30**.

If palladium tetrakis-(triphenylphosphine) was employed as the Pd(0) source, the reaction evolved in a similar manner to yield **2.30**, however harsher conditions (toluene, 100 °C) were necessary (Scheme 2-11). In the $^{31}P\{^{1}H\}$ NMR spectrum of **2.30** in addition to the upfield shifted signal at δ_P = -168.9 (dd, $^{2}J_{PP\ trans}$ = 213.3 Hz, $^{2}J_{PP\ cis}$ = 108.8 Hz) ppm, characteristic of the phosphide region, a second signal at δ = 14.2 ppm is indicative of a different phosphorus atom in the molecule. The X-ray diffraction analysis revealed a similar structural core to **2.28**; however in this case the extra coordination site of each Pd atom is occupied by a triphenylphosphine ligand, instead of acetonitrile (Figure 2-8).

It is noteworthy to mention that the oxidative insertion of low-valent metals into C-Cl bonds of appropriate halo-iminium salts is a well-known process;[55] however, to the best of our knowledge, the insertion into the C-P bond of cyclopropenium salts is unprecedented. Furthermore compounds **2.28**-**2.30** exhibit $[R_2P]^-$ phosphide ligands, which may be beneficial for transformations where an electron rich environment is required.

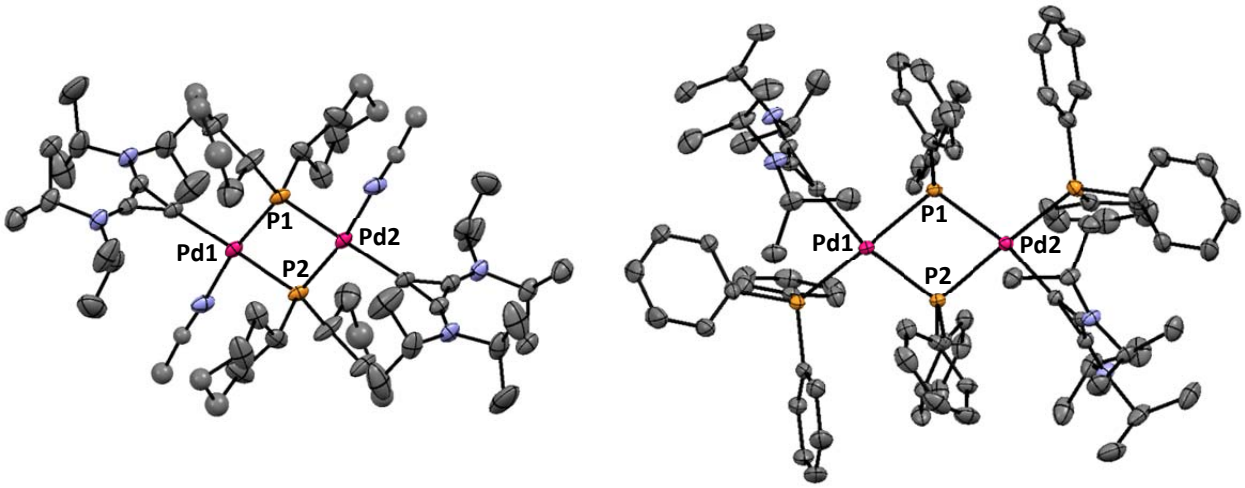

Figure 2-8. Solid-state structure of **2.18** (left) and **2.20** (right). Hydrogen atoms and anions are omitted for clarity; ellipsoids are set at 50 % probability.

2.2.4. Ligand Effect in Platinum(II) Catalysis

To study the catalytic performance of our newly prepared cationic ligands, we chose the platinum-catalyzed cyclization of 2-ethynyl-1,1'-binaphtalene **2.31** into pentahelicene **2.32** as a model reaction; first reported by Fürstner and coworkers (Scheme 2-12).[39,56] The 6-*endo*-dig cyclization takes place in the presence of $PtCl_2$, but long reaction times (24 h) are necessary to reach full conversion. In this transformation the rate determining step is known to be the nucleophilic attack of the aryl ring on the alkyne.[37,57] This is due to the fact that an aromatic ring, such as naphthalene, is a relatively weak nucleophile. Therefore, it can be envisaged that higher activation of the alkyne by a metal center with enhanced π-acidity should accelerate this reaction.

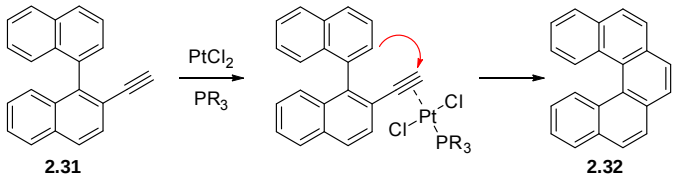

Scheme 2-12. Cyclization of 2-ethynyl-1,1'-binaphtalene **2.31** into pentahelicene **2.32.**

In order to test this hypothesis, the hydroarylation reaction of **2.31** was carried out in dichloroethane at 80 °C using 5 mol% of the trichloroplatinate complexes **2.19**, **2.21-2.23** and 5 mol% $AgBF_4$; the latter acting as a chloride abstractor, to generate the necessary

coordination vacancy at Pt. For comparison, the performance of some commercially available and the previously reported di- and tricationic cyclopropenium-substituted phosphines in this transformation is also shown in Figure 2-9.

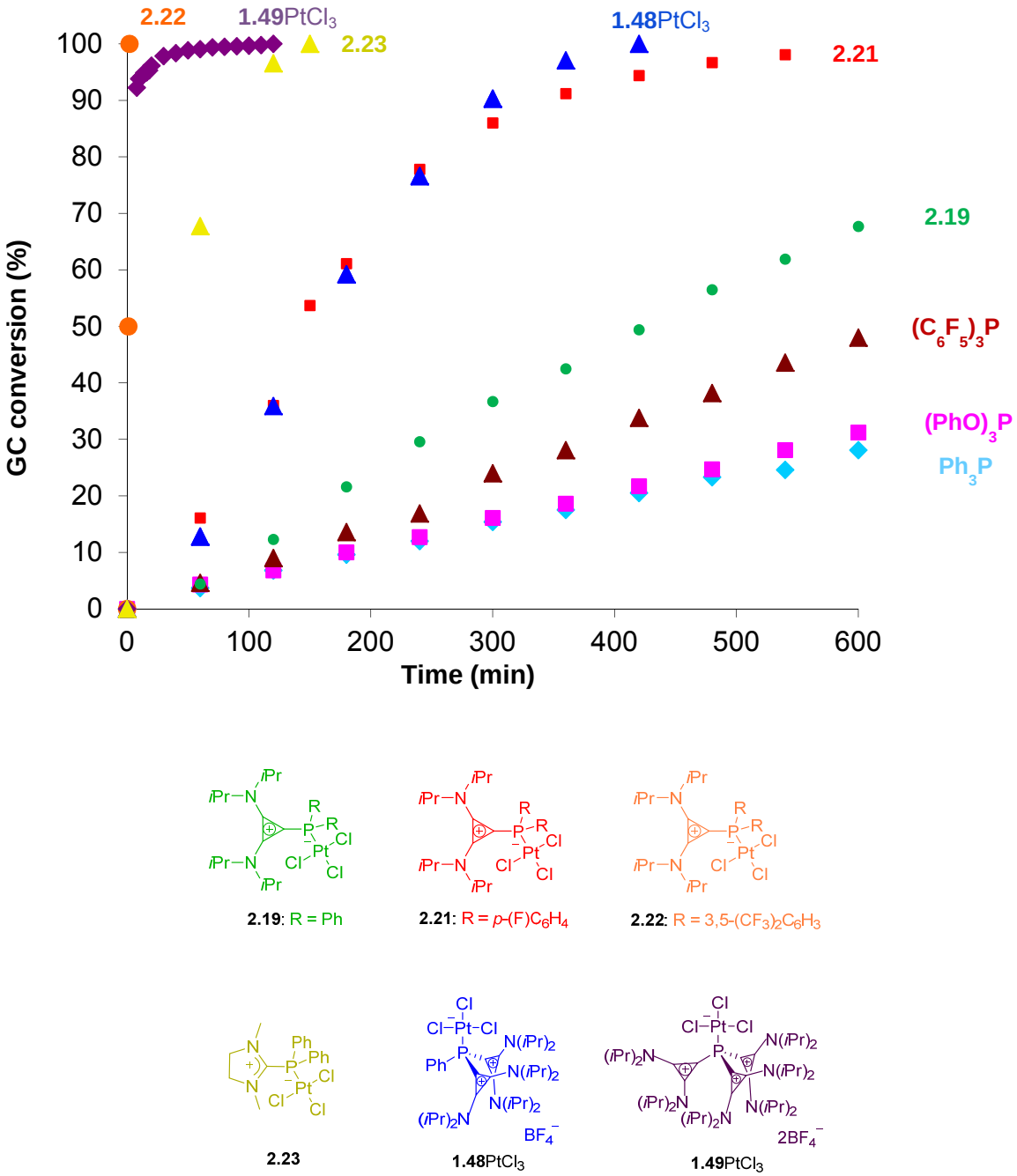

Figure 2-9. Ligand effect on the Pt-catalyzed cyclization of 2-ethynyl-1,1'-binaphtalene **2.31** into pentahelicene **2.32**.

As expected, both $(PhO)_3P$ (pink) and $(C_6F_5)_3P$ (brown) performed better than the less π-acceptor Ph_3P (light blue) in terms of reactivity, but all of these commercially available phosphines needed longer reaction times than the monocationic precatalyst **2.19** (green).

The Pt(II) complexes of the dicationic ligand, **1.48** (blue) and the monocationic phosphine, **2.21** (red), containing fluorophenyl substituents showed similar reactivities, but both induced a slower reaction than the newly prepared precatalysts **2.23** (yellow) and **2.22** (orange). To our delight the polyfluorinated precatalyst **2.22** satisfactorily afforded complete conversion to pentahelicene **2.32** in only two minutes, surpassing even the reactivity of the tricationic ligand in **1.49** (violet) under the standard reaction conditions. Since both the di- and tricationic ligands **1.48** and **1.49** (E_p ox = 1.541 V and 2.062 V, respectively) have similar or even higher oxidation potentials than polyfluorinated ligand **2.12** (E_p ox = 1.548 V), the superior reactivity of **2.22** is likely due to its higher solubility in dichloroethane.

The donor ability ranking of the described monocationic and commercially available phosphines, based on the conducted kinetic studies corresponds to the results of the cyclic voltammetry measurements presented earlier in this chapter. Discrepancies only appear in the case of highly insoluble catalysts.

2.2.5. Synthetic Applications

Encouraged by the outstanding catalytic reactivity of the π-acceptor ligand **2.12**, we decided to examine whether it could be employed in the synthesis of the naturally occurring phenanthrene derivative, 7-hydroxy-2,3,4,8-tetramethoxyphenanthrene **2.33**. Also named as Chrysotoxene, **2.33** was isolated from *Dendrobium aurantiacum* var. *denneanum* and *Tamus communis* and displayed moderate cytotoxicities (IC_{50} = 8.52 µM) against the HeLa cell line (Figure 2-10).[58]

Figure 2.10. Proposed structure of chrysotoxene **2.33**, *Dendrobium aurantiacum* var. *denneanum* (left) and *Tamus communis* (right).

The first step of our synthesis towards **2.33** was the Suzuki-coupling between the literature described 6-bromo-3-hydroxy-2-methoxybenzaldehyde **2.34**[59] and 2,3,4-trimethoxyphenyl

boronic acid **2.35** (68 % yield, Scheme 2-13). The resulting aldehyde **2.36** was subsequently transformed into the corresponding alkyne **2.37** using the Ohira-Bestmann reagent. Only moderate yield of **2.37** (52 %) was obtained due to the formation of a byproduct in this reaction, which after NMR spectroscopy and X-ray diffraction analysis was identified as benzofuran **2.38**. With alkyne **2.37** in hand, we performed the key hydroarylation using 5 mol% of **2.22** and $AgBF_4$ at 80 °C in dichloroethane, affording Chrysotoxene after only ten minutes in 88 % yield. Detailed 1D, 2D NMR spectra and crystallographic data (Figure 2-11) confirmed the structure of **2.33**, however, comparison of the ^{13}C NMR spectrum of the synthetic and natural samples show a significant mismatch for the resonance assigned to C2, which appears at δ = 152.0 and 148.0 ppm in the synthetic and natural product, respectively.

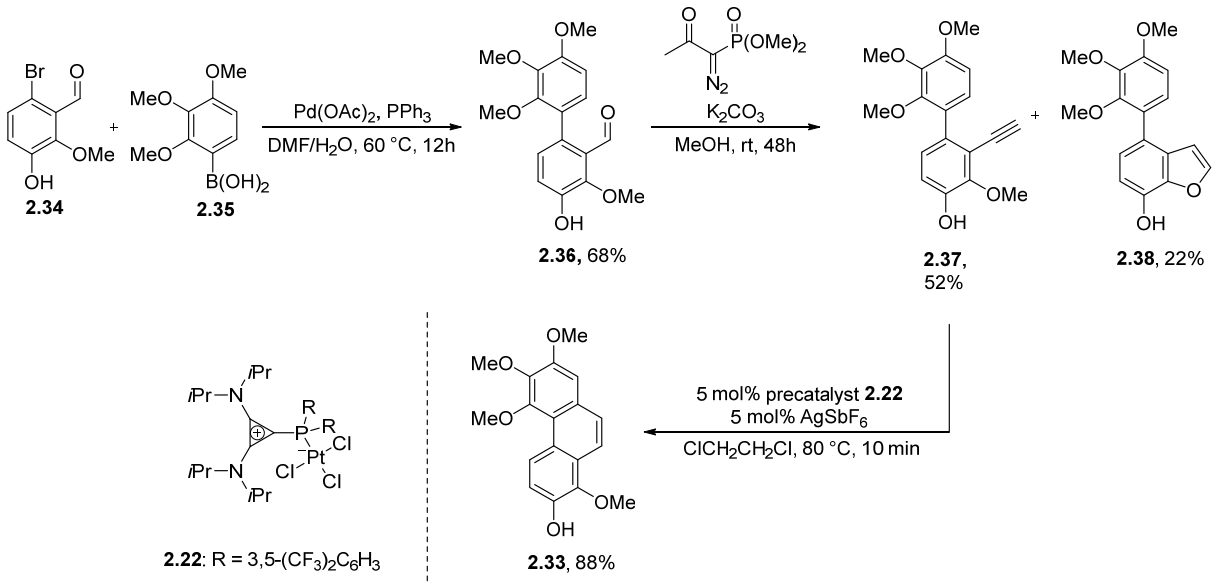

Scheme 2-13. Synthesis and proposed structure of Chrysotoxene **2.33**.

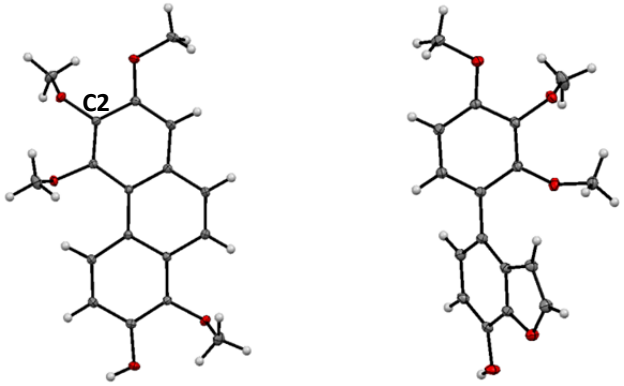

Figure 2-11. Solid-state structure of **2.33** and **2.38**. Ellipsoids are set at 50 % probability.

In view of the excellent catalytic reactivity of the Pt(II)-complex **2.22**, its synthetic relevance was further explored by our group. Phenanthrene derivative, **2.39**, was synthesized by a Masters student in our group, Tobias Deden, who applied precatalyst **2.22**, prepared during my PhD work, in the key 6-*endo*-dig cycloisomerization step depicted in Scheme 2-14.[52] Compound **2.39**, also named as Epimedoicarisoside A, was isolated from *Epimedium koreanum*[60] and is an interesting synthetic target, as biological studies revealed its cytotoxic effects on primary osteoblasts.[61]

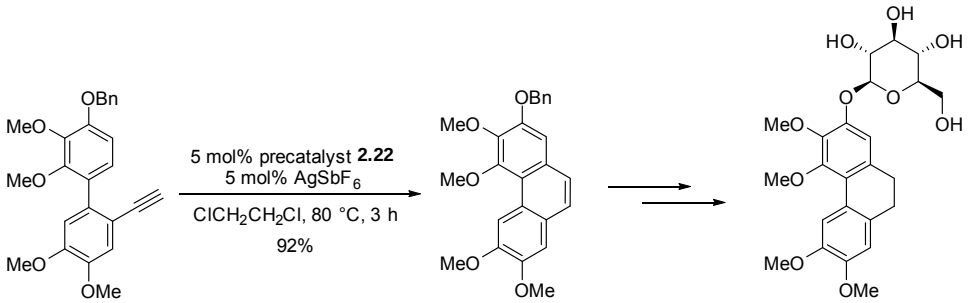

2.40 **2.41** **2.39**

Scheme 2-14. Proposed structure of Epimedoicarisoside A **2.39** and the key platinum-catalyzed step of its synthesis.

2.3. Conclusions

New strong π-acceptor ligands were prepared either by the use of polyfluorinated aromatic substituents on cyclopropenium derived phosphines (**2.12**) or through replacement of the cationic cyclopropenium moiety by the more electron withdrawing dihydroimidazolium unit

(**2.14** and **2.15**) (Figure 2-12). Evaluation of the donor properties by cyclic voltammetry measurements clearly showed higher oxidation potential values for the cationic phosphines (E_p ox = 1.461 to 1.548 V) when compared to the commercially available phosphite (E_p ox $P(OMe)_3$ = 1.287 V); a fact that was later corroborated by their catalytic performance in the Pt-catalyzed 6-*endo*-dig cyclization and could have been misrepresented if only CO stretching frequency analysis would have been considered.

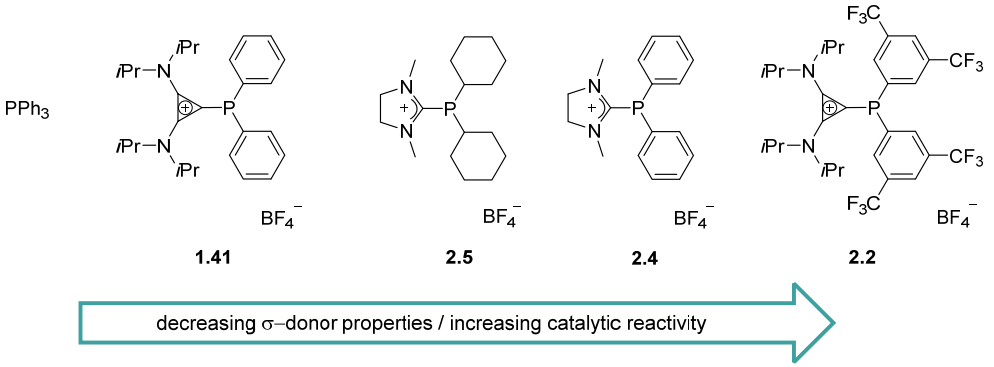

Figure 2-12. Designed and prepared monocationic strong π-acceptor phosphines **2.12**, **2.14**, **2.15**; PPh_3 and **1.41** in decreasing order of their σ-donor properties.

Despite exhibiting weak donor ability, all of the described ligands were shown to coordinate Au(I), Pt(II) and Rh(I) in excellent yields. In the case of Pd(0), unprecedented Pd insertion products were formed. Encouraged by the outstanding reactivity of the Pt(II) complex derived from the polyfluorinated precatalyst **2.22** in the model hydroarylation reaction, it was then applied to the synthesis of Chrysotoxene **2.33** and Epimedoicarisoside A **2.39**, both naturally occurring phenanthrene derivatives.

3. Cyclopropenium-Substituted Mono- and Polycationic Amines and Imines

3.1. Introduction

While there is a wide range of phosphorus-centered mono-, di- and trications displaying a variety of bonding motifs ($\mathbf{A_P}$-$\mathbf{E_P}$) reported in the literature,[62] the nitrogen-centered analogues are almost only limited to the monocationic $\mathbf{A_N}$-type ammonium salts. These mono- and polycationic compounds can be described by both Lewis and dative bonding models; the best structural representation being dependent on each specific system. The true electronic distribution however is probably somewhere in between the two extremes (Figure 3-1).

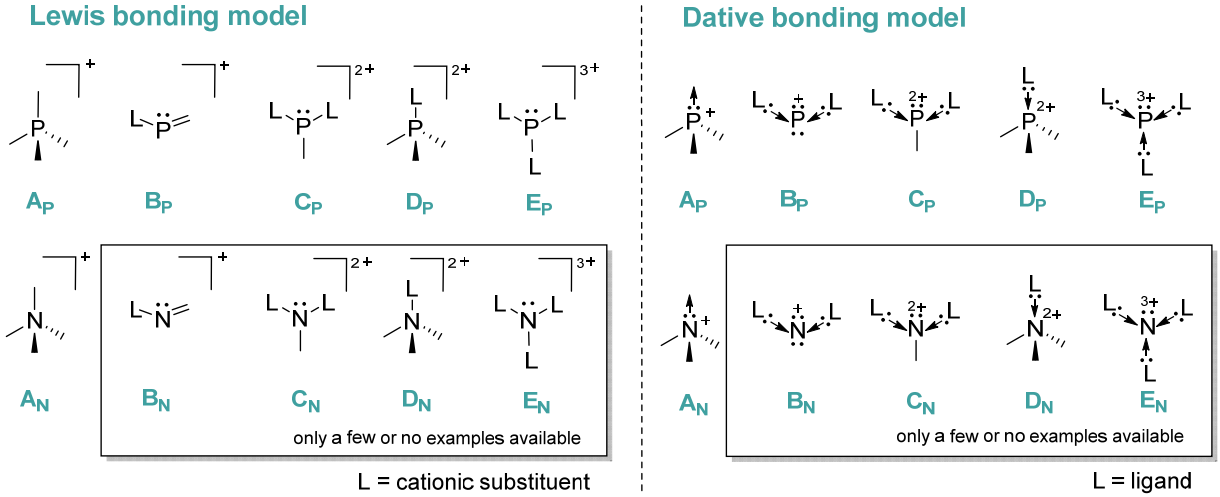

Figure 3-1. Known bonding environments of cationic phosphorus centers and plausible nitrogen analogues represented by both Lewis and dative bonding models.

A very large number of ammonium salts of general formula $\mathbf{A_N}$ are commercially available, others can be synthesized by quaternization of amines or nitrogen containing heterocycles with alkyl halides. Chiral ammonium salts have been extensively used in phase transfer catalysis[63] and have been employed as catalysts by the Ooi group for different reactions, such as asymmetric Mannich-type reactions,[64] stereoselective aza-Henry reactions[65] and aldol reactions.[66]

The $\mathbf{B_N}$-type species are much more rare. One of these compounds, the monocationic $OCNCO^+Sb_3F_{16}^-$ **3.2** was synthesized by Seppelt and coworkers[67] through fluoride abstraction from FOCNCO **3.1** by the Lewis acidic antimony pentafluoride. Its crystal structure reveals that the $OCNCO^+$ ion has a strongly bent structure (Φ_{C1N1C2} = 131°) in contrast to the linear carbon suboxide, C_3O_2 (Scheme 3-1).

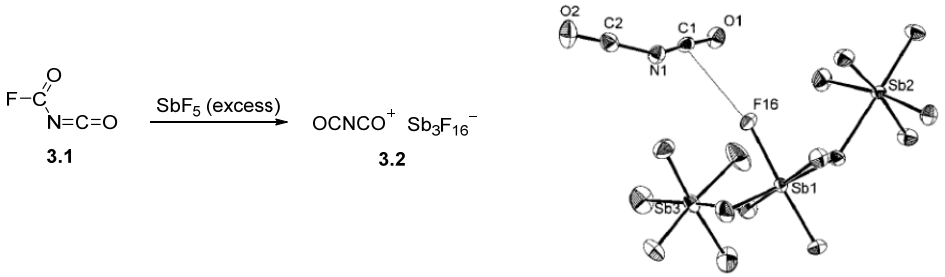

Scheme 3-1. Synthesis of the $\mathbf{B_N}$-type monocation **3.2** and its solid-state structure (C1-F16: 2.686 Å).[67]

Lyapkalo and coworkers[68] described a family of $\mathbf{B_N}$-type monocations, incorporating a fully substituted aromatic imidazolium fragment. The synthesis of **3.4-3.9** was accomplished by treating the corresponding chloroimidazolium salt **3.3** with *N,N,N,N*-tetramethylguanidine (**3.4**), aminotris(dimethylamino)phosphonium tetrafluoroborate (**3.5** and **3.6**) or with the corresponding aminoimidazolium salt (**3.7-3.9**) (Scheme 3-2). All these condensation reactions were carried out in presence of KF, which served as an activating agent by forming the more electrophilic fluoroimidazolium salt. On the other hand, KF also acted as a strong base, trapping protons and thus leading the process to completion.

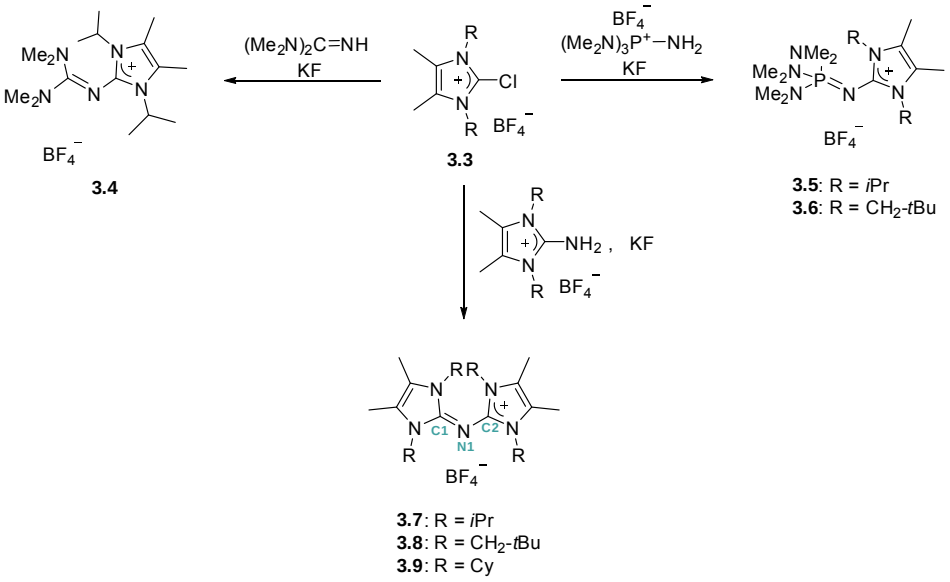

Scheme 3-2. Synthesis of $\mathbf{B_N}$-type monocations **3.4-3.9** incorporating imidazolium moieties.

These lipophilic cations can potentially be applied in phase transfer catalysis, where the aqueous base resistance of the catalyst is essential. Conventional organic cations often have limited stability towards solutions containing alkali hydroxides, therefore the organic phosphazenium cations developed by Schwesinger *et al.*[69] (*e.g.* **3.10**$^+$ and **3.11**$^+$, Figure 3-2) are currently the most attractive candidates in this regard. However, due to their high molecular weight and potential dermal toxicity,[70] the search for alternative cations with comparable or higher thermal stability and base resistance is required.

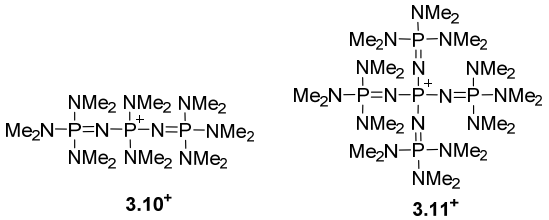

Figure 3-2. Phosphazenium cations **3.10**$^+$ and **3.11**$^+$.

Evaluation of the stability of monocations **3.4-3.9** under biphasic (toluene / 50 % aqueous KOH, 115° C) and homogeneous conditions (1M KOH in ethylene glycol, 197° C) revealed that their alkaline base resistance exceeds that of the conventional organic cations.[68] The neopentyl-substituted cations **3.6** and **3.8** proved to be the most stable cations of the studied series, which match the resistance of the phosphazenium cations developed by Schwesinger (*cf.* **3.10**$^+$ and **3.11**$^+$, Scheme 3-2). The enhanced aqueous base resistance of lipophilic cations **3.4-3.9** is likely the coupled result of the aromatic stabilization of the positive charge by the imidazolium moiety and the steric protection of the bulky *N*-alkyl substituents.

The steric bulk around the C1A and C4A atoms in **3.8** can be seen in the solid-state structure in Figure 3-3.[68] Both neopentyl groups of each imidazolium moiety are located on the same face of the ring, making the approach of a hydroxide nucleophile very difficult. This accounts for the highest base resistance observed for **3.8** within this family of compounds. Monocation **3.8** features an sp^2 hybridized exocyclic nitrogen atom and two imidazolium moieties with nearly identical bond lengths and angles (N1A-C1A: 1.333(3) and N1A-C4A: 1.336(3) Å), suggesting even distribution of the positive charge over both rings.

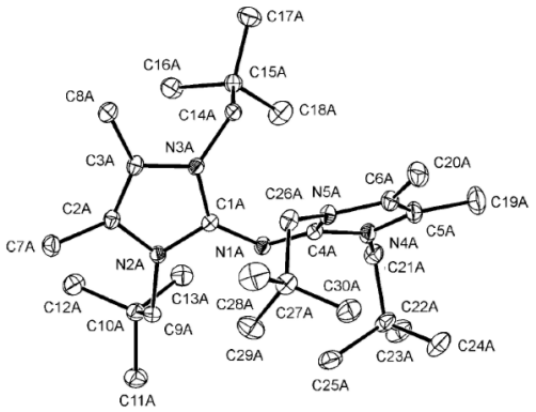

Figure 3-3. Solid-state structure of **3.8**. Hydrogen atoms and the anion are omitted for clarity; ellipsoids are set at 30 % probability.[68]

A few examples of $\mathbf{C_N}$-[71] and $\mathbf{D_N}$-type [72] dications have also been prepared, although they are not characterized by X-ray diffraction analysis. To the best of our knowledge tricationic structures with the general formula $\mathbf{E_N}$ were not known prior to this work. In an attempt to synthesize the monocationic compound **3.14**, Lyapkalo *et al.* obtained the $\mathbf{C_N}$-type dication **3.13**, as a double substitution side product.[71] As this was an undesired product, it was not further investigated (Scheme 3-3).

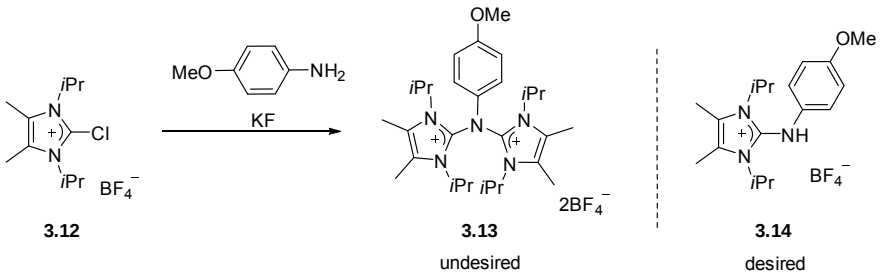

Scheme 3-3. Synthesis of $\mathbf{C_N}$-type dication **3.13.** Monocation **3.14**.

Compound **3.16,** belonging to the $\mathbf{D_N}$-type cations, was synthesized by our group by treatment of cyclopropenimine **3.15** with excess trimethyloxonium tetrafluoroborate. The fact that **3.15** reacts with two equivalents of the methylating reagent suggests its electron rich nature, which will be discussed in detail on the next pages (Scheme 3-4).

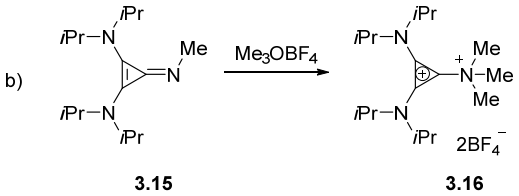

3.15 **3.16**

Scheme 3-4. Synthesis of $\mathbf{D_N}$-type dication **3.16**.

In light of the small number of $\mathbf{B_N}$**-,** $\mathbf{C_N}$**- and** $\mathbf{D_N}$-type nitrogen-centered cations reported in the literature and as a continuation of this thesis, it was decided to synthesize and study these new classes of cations centered on the lightest element of group 15. At first bis[(dialkylamino)cyclopropenimines] were chosen as source of the central nitrogen atom. We envisaged to engage them as nucleophiles in reaction with chlorocyclopropenium **1.40**, because of their electron rich nature predicted by theoretical calculations[41,73] and later proved experimentally.[72]

The first synthesis of bis[(dialkylamino)cyclopropenimines] was accomplished by Krebs and co-workers in 1984. Treatment of bis(dialkylamino)acetylenes with arylisocyanide **3.17** afforded the desired products **3.18** and **3.19** (Scheme 3-5, a).[74]

In 2010 a two-step synthesis of this type of cyclopropenimines was reported by our group.[72] Cyclopropenimines **3.20-3.24** were obtained in a modular procedure by condensation of the chlorocyclopropenium salt **1.40** with primary amines or anilines, followed by deprotonation with potassium hydride (Scheme 3-5, b). Cyclopropenimines can be depicted by both Lewis and dative bonding models (Scheme 3-4, b: **A** and **B**) where **B** explains their excellent first and second proton affinity; however, X-ray diffraction analysis suggests that in the ground state form **A** is preferred.

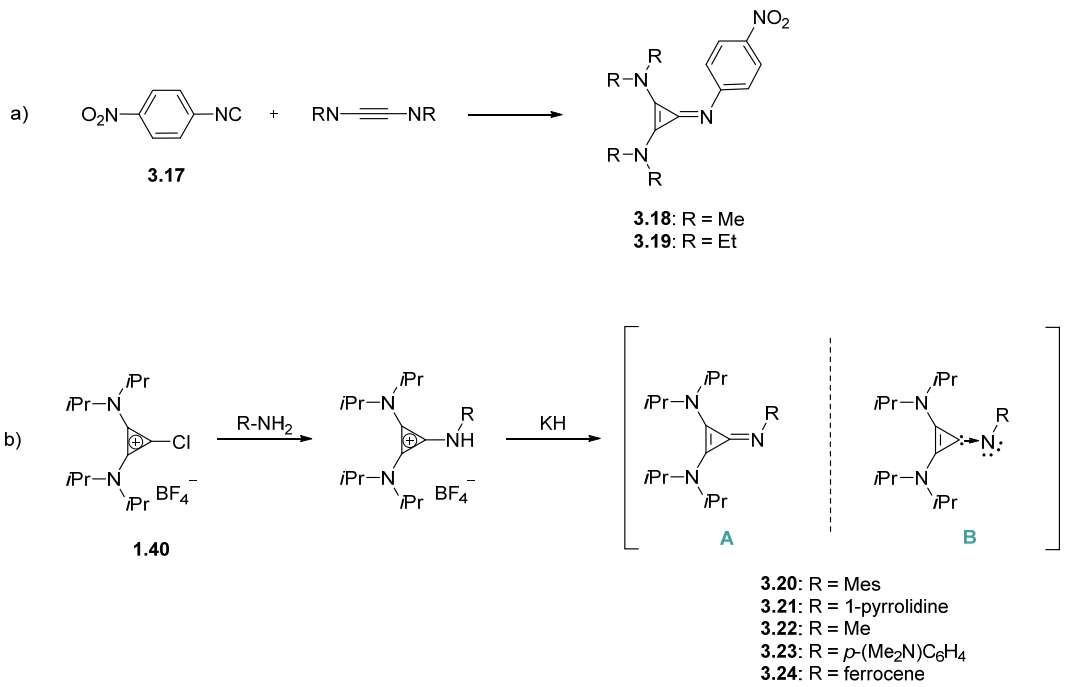

Scheme 3-5. a) Synthesis of cyclopropenimines **3.18** and **3.19**. b) Synthesis of cyclopropenimines **3.20**-**3.24** and their bonding extremes.

The excellent Brønsted basicity of the bis[(dialkylamino)cyclopropenimines) stems from the capability of the cyclopropenyl moiety to stabilize a positive charge by gaining aromaticity after protonation (Scheme 3-6), as illustrated by the solid-state structures of cyclopropenimine **3.20** and its protonated form **3.20H**$^{+}$.[72] In the free base **3.20**, the cyclopropenyl moiety has two longer (1.420(1) and 1.411(1) Å) and one shorter (1.371(1) Å) carbon-carbon bonds, while the C1-N1 bond distance (1.295(1) Å) is typical for a C=N double bond. These values suggest that the mesomeric structure **3.20a** gains importance. The bond lengths in the protonated form **3.20H**$^{+}$ significantly change: the three-membered ring now consists of three similar C-C bond lengths (1.379(2), 1.395(2) and 1.398(2) Å) and the C1-N1 bond distance is lengthened considerably to 1.334(2) Å. Therefore, compound **3.20H**$^{+}$ is better described by the mesomeric structure **3.20**$^{+}$**b** with an aromatic cyclopropenium moiety.

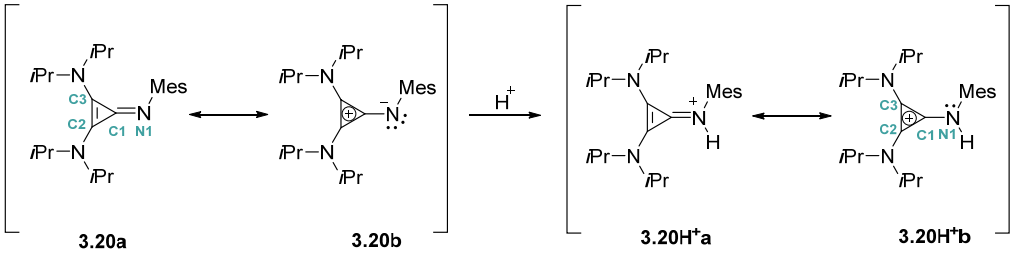

Scheme 3-6. Resonance structures of free cyclopropenimine **3.20** and protonated cyclopropenimine **3.20H**$^{+}$.

Stabilization of the positive charge in the cyclopropenyl moiety is evidence for the ability of cyclopropenimines to donate up to four electrons simultaneously to Lewis acids. This was proven experimentally in two different ways: as mentioned earlier, the methylation of imine **3.15** using excess of trimethyloxonium tetrafluoroborate yielded the dialkylated salt **3.16** (Scheme 3-5). Furthermore, the diimine **3.25** was able to react with two equivalents of $[PdCl_2(CH_3CN)_2]$ resulting in the dimetallic complex **3.26** (Scheme 3-7). Here, each nitrogen atom donates two electron pairs to two bridged palladium(II)-center. Density functional theory calculations corroborate the experimental findings: the HOMO and HOMO -1 of compounds **3.20-3.24** correspond to π- and σ-type lone pair orbitals with the maximum coefficients located on the central nitrogen atom (Figure 3-4).

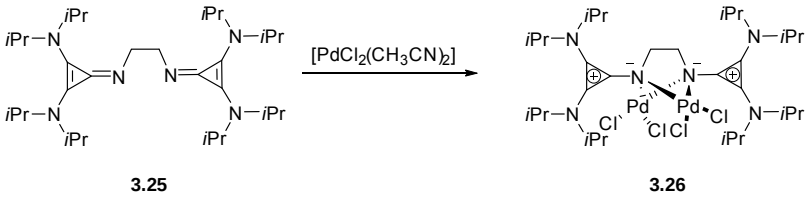

Scheme 3-7. Synthesis of bimetallic complex **3.26**.

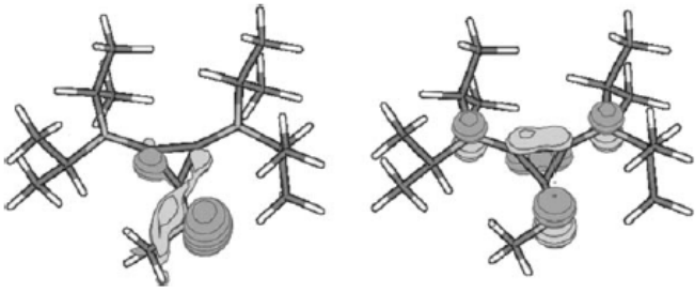

Figure 3-4. Highest occupied molecular orbitals of **3.22**: HOMO -1 (left) and HOMO (right).

Although the Brønsted basicity of cyclopropenimines had been predicted to be stronger than that of the guanidines[41] there were no experimental data in the literature until the report of Lambert *et al.* in 2012.[75] He measured the acidity of the conjugate acid (pK_{BH+}) of cyclopropenimine **3.30** (26.90) and found it to be comparable to the bicyclic guanidine **3.29** (26.03) and the phosphazene base **3.31** (26.98), both considered to be very strong "superbases".[76] Remarkably, cyclopropenimine **3.30** shows basicity 3 orders of magnitudes higher than a comparable guanidine **3.27** (23.56) (Scheme 3-8, a). Encouraged by these values they also investigated the performance of the chiral cyclopropenimine **3.32** in

Brønsted base catalysis; as a test transformation the Michael reaction of glycine imine **3.34** with methyl acrylate **3.35** was chosen. **3.32** was found to be a highly effective catalyst for this reaction: 10 mol % catalyst loading yielded the desired product in quantitative yield and with 98 % ee after 1 hour. In comparison, 20 % catalyst loading of guanidine **3.33** afforded the desired product **3.36** in quantitative yield and with 93 % ee only after 3 days. The optimized conditions were then applied to other Michael acceptors, such as *n*-butyl, *tert*-butyl and benzyl acrylates, all yielding quantitative yields and high enantioselectivity (Scheme 3-8, b, entries 1-3). Methyl vinyl ketone proceeded to full conversion in only 15 minutes, while acrylonitrile reacted much slower and with diminished enantioselectivity (Scheme 3-8, b, entries 4 and 5).

a)

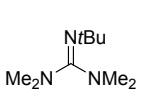

23.56 **3.27**

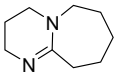

24.34 **3.28**

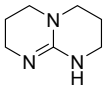

26.03 **3.29**

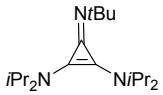

26.90 **3.30**

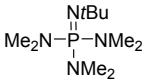

26.98 **3.31**

b)

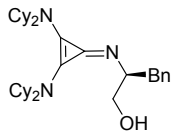

catalyst **3.32**

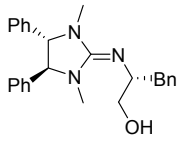

catalyst **3.33**

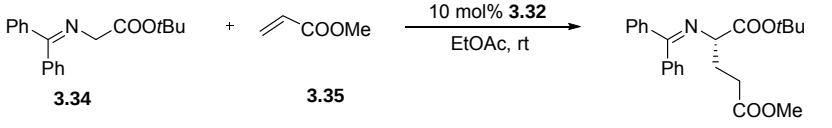

3.34 **3.35** **3.36**, 99% yield, 98% ee

entry	electrophile	time (h)	yield %	ee %
1	CO_2nBu	1.5	99	98
2	CO_2tBu	12	98	99
3	CO_2Bn	1	97	98
4	COMe	0.25	97	95
5	CN	30	97	77

Scheme 3-8. a) Basicity (pK_{BH+} values in acetonitrile) of cyclopropenimines **3.30** and several common strong organic bases. b) Catalysts **3.32** and **3.33**. Michael reaction of glycine imine **3.34** with methyl acrylate **3.35** catalyzed by cyclopropenimine **3.32** and reaction scope.[75]

Based on the structural features and reactivities of cyclopropenimines, all pointing towards their electron rich nature, we set out to use them as building blocks to access dicationic $\mathbf{C_N}$-type compounds. It would then be interesting to compare the structure and reactivity of these and related N-centered cations to their P-centered analogs, developed and extensively studied by our group (see the introduction of this thesis).

3.2. Results and Discussion

3.2.1. Synthesis

The corresponding cyclopropenimines for the preparation of the desired $\mathbf{C_N}$-type dications are synthesized by a procedure developed in our group.[72] Condensation of methylamine or anilines - bearing different substituents in the *para* position - with chlorocyclopropenium **1.40** and subsequent anion exchange affords the protonated cyclopropenimines **3.37-3.40** as air-stable solids in good yields.[77] Deprotonation of **3.37-3.40** with potassium hydride gives access to the free bases **3.41-3.44** in excellent yields (Scheme 3-9). This route, in contrast to the synthesis of imidazoline-2-imines developed by Tamm and coworkers, avoids the use of free carbenes.[78]

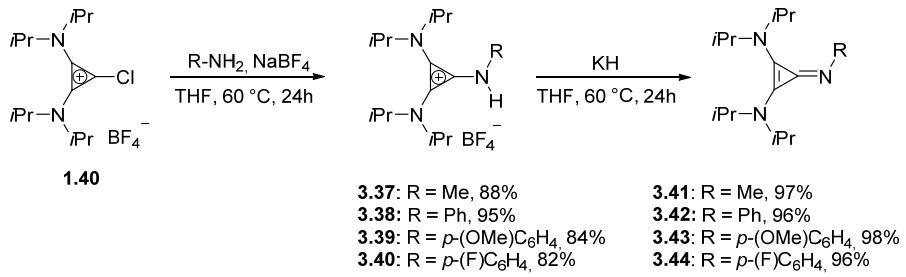

Scheme 3-9. Synthesis of cyclopropenimines **3.41-3.44**.

The connectivity of the protonated cyclopropenimine **3.38** was confirmed by X-ray diffraction analysis (Figure 3-5). These data reveal that, similarly to the previously isolated protonated cyclopropenimines[72], **3.38** possesses a cyclopropenium moiety with roughly equal C1-C2, C2-C3 and C1-C3 bond lengths (1.379(1), 1.401(1) and 1.375(1) Å, respectively) and a C1-N1 distance of 1.336(1) Å. The very similar C-C and the lengthened C1-N1 bonds support the aromatic character of the three-membered ring in **3.38**.

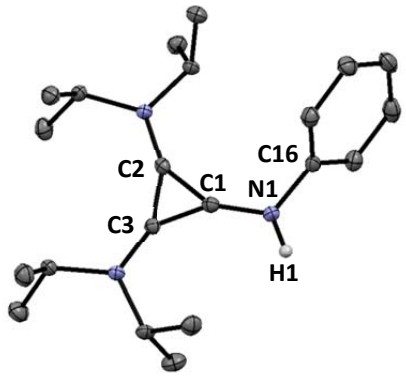

Figure 3-5. Solid-state structure of **3.38**. Hydrogen atoms (except that attached to N1) and the anion are omitted for clarity; ellipsoids are set at 50 % probability.

To our delight, the nucleophilic attack of cyclopropenimines **3.41-3.44** on the chlorinated carbon atom of another equivalent of **1.40** and subsequent anion exchange furnished the expected dicationic compounds **3.45-3.48** as air stable solids in each case (Scheme 3-10). In addition to this methodology, an alternative route for the synthesis of these dicationic compounds was also established, making use of the inverse –onium substituent strategy. Thus, by reaction of bis(sylilated)aniline **3.49** with two equivalents of chlorocyclopropenium salt **3.50** in tetrahydrofuran at 60 °C, dication **3.51** could be obtained in good yield (Scheme 3-9).

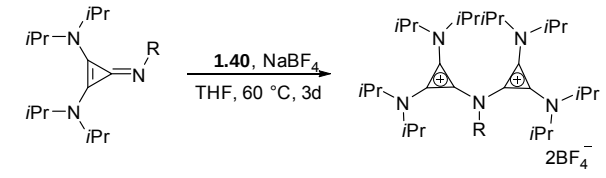

3.41: R = Me
3.42: R = Ph
3.43: R = *p*-(OMe)C$_6$H$_4$
3.44: R = *p*-(F)C$_6$H$_4$

3.45: R = Me, 49%
3.46: R = Ph, 81%
3.47: R = *p*-(OMe)C$_6$H$_4$, 80%
3.48: R = *p*-(F)C$_6$H$_4$, 70%

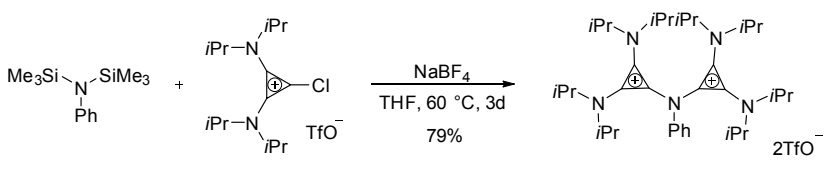

3.49 **3.50** **3.51**

Scheme 3-10. Synthesis of dications **3.50-3.53** and **3.56**.

The $^{15}N\{^1H\}$ NMR spectra recorded for the dications showed two signals at δ_N = -276.3 (NMe), -263.2 (N(*i*Pr)$_2$) ppm for **3.45** and -310.2 (NPh), -260.3 (N(*i*Pr)$_2$) ppm for **3.46**,

reflecting the two different nitrogen environments. As expected, the diisopropyl-substituted nitrogen atoms in these two compounds exhibit very similar chemical shifts, while the more electron poor central nitrogen atom in **3.46** (NPh) appears more downfield shifted than that of **3.45** (NMe). The connectivities of **3.45** and **3.51** were additionally confirmed by X-ray diffraction analysis (Figure 3-6).

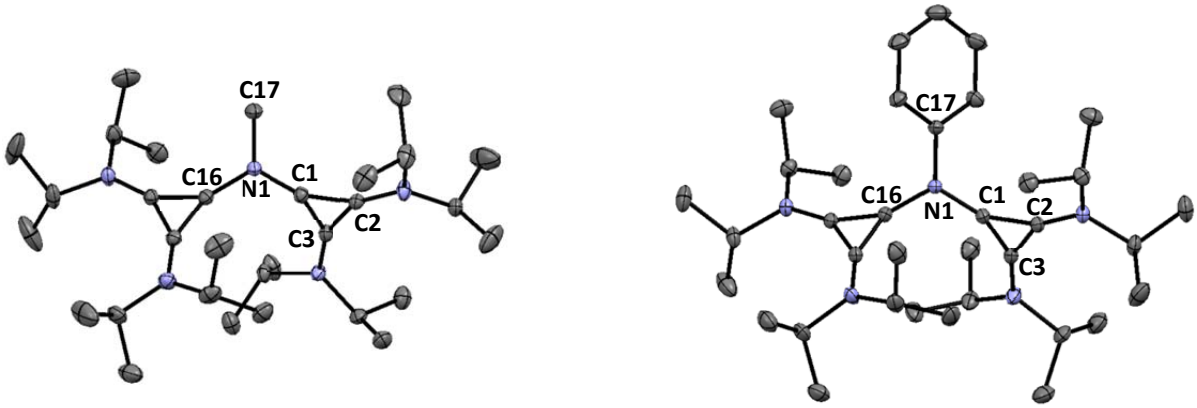

Figure 3-6. Solid-state structures of **3.45** (left) and **3.51** (right). Hydrogen atoms and anions are omitted for clarity; ellipsoids are set at 50 % probability.

In sharp contrast to their pyramidal P-centered analogues, compounds **3.45** and **3.51** exhibit a trigonal planar environment around the central nitrogen atom, with the sum of angles, **Σ°**N = 360.0°. Probably due to the large steric demand of the isopropyl substituents, in both molecules the cyclopropenium rings are tilted (average torsion angles: 48.8° for **3.45** and 50.1° for **3.51**). The N1-C1 and N1-C16 bond distances in dications **3.45** (1.362(2) and 1.379(2) Å, respectively) and **3.51** (1.385(2) and 1385(2) Å, respectively) have very similar values within a molecule, suggesting even distribution of the positive charges in both cases. Their considerably smaller values than the N1-C17 distances (1.476(2) Å for **3.45** and 1.433(2) Å for **3.51**) indicate a degree of back-donation from the central nitrogen atom. This is further supported by the trigonal planar arrangement of the central atom in these salts. The carbon-carbon bond lengths of the cyclopropenium moiety in cations **3.45** and **3.51** have a common feature: the C2-C3 distances (1.411(2) and 1.426(2) Å, respectively) are slightly longer when compared to C1-C2 and C1-C3 (1.377(2) to 1.381(2) Å), which are about the same length; however, the fact that all of them are shorter than a typical C(sp^2)-C(sp^2) single bond (1.460 Å)[79] speaks for delocalization of the π-electron system in the three membered ring. It is also worthwhile to mention that the nitrogen atoms of the diisopropyl

fragments show a planar environment in both of these compounds implying donation of the lone pairs of electrons into the cyclopropenium ring system.

Encouraged by the success achieved regarding the dications, the more challenging $\mathbf{E_N}$-type tricationic structures were addressed. Our first attempt was to use the inverse –onium substituent strategy. To this end, chlorocyclopropenium salt **1.40** was reacted with tris(trimethlysilyl)amine in tetrahydrofuran. Instead of the desired trication, a mixture of two compounds was formed. Separation by column chromatography yielded a compound with saline nature, in addition to the starting material **1.40**. After growing suitable single crystals for X-ray diffraction analysis from a mixture of CH_2Cl_2/Et_2O, the unknown salt could be identified as the monocationic compound **3.52**, containing two cyclopropenyl entities bridged by a central nitrogen atom.

As the above described transformation gives **3.52** in poor yield, a more straight-forward synthesis was established, employing potassium bis(trimethylsilyl)amide and two equivalents of cyclopropenium salt **1.40** to afford **3.52** in 68 % yield (Scheme 3-11). The $\mathbf{B_N}$-type monocation can be depicted by the two bonding models: an *N*-cyclopropenium cyclopropenylimine **3.52a** (Lewis bonding model) and an N^+ cation stabilized by simultaneous donation of two cyclopropenylidene moieties **3.52b** (dative bonding model, Scheme 3-11).

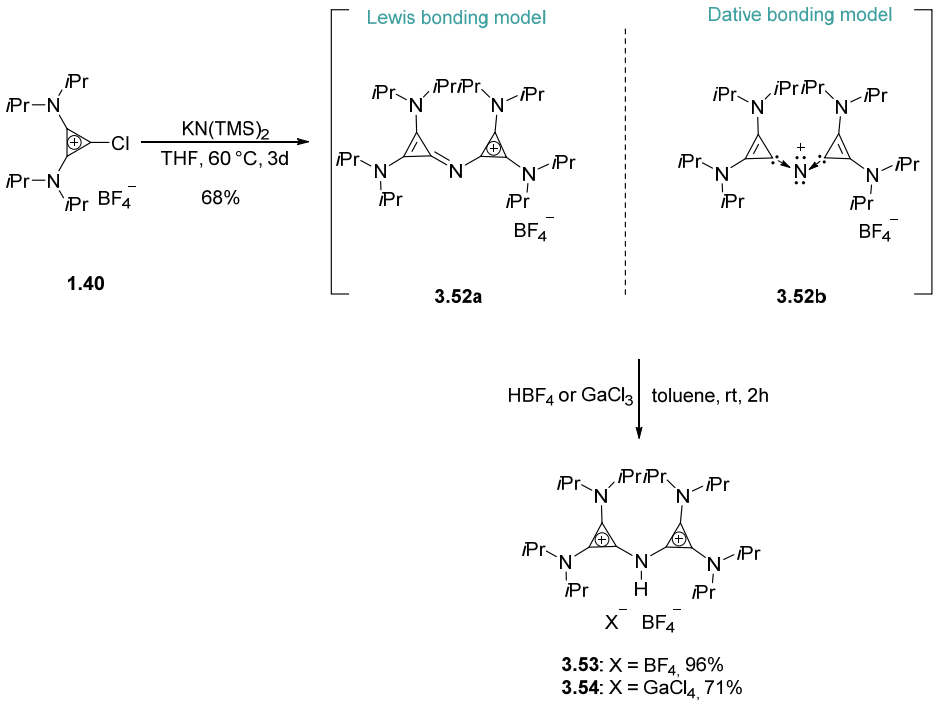

Scheme 3-11. Synthesis of monocation **3.52** and dications **3.53**, **3.54**; bonding extremes **3.52a** and **3.52b**.

The X-ray diffraction analysis revealed that the N1-C1 and N1-C16 bond lengths in the dicoordinate **3.52** are both 1.332(9) Å, which are shorter than the N(central)-C(cyclopropenyl) bonds in the previously described compounds **3.38**, **3.45** and **3.51**, implying a stronger back-donation from the central nitrogen to the three-membered rings. At the same time the two equal bond distances also suggest even delocalization of the positive charge over both rings. The same observation was made in the case of the imidazolium analogue of compound **3.52** (**3.8**, Figure 3-2), reported by Kunetskiy and coworkers,[68] where the N(central)-C(imidazolyl) bond lengths are 1.333(3) and 1.336(3) Å. The roughly equal C1-C2, C1-C3 and C2-C3 bond distances in **3.52** (1.389(1), 1.396(1) and 1.397(1) Å, respectively) correlate well with those in the protonated imine **3.20H$^+$** (Scheme 3-5), indicating the aromatic character of the cyclopropenium ring. The strongly bent structure of **3.52** ($\Phi_{C16N1C1}$ = 120°) resembles that of the first **B$_N$**-type monocation (**3.2**, Scheme 3-1) isolated by Seppelt and coworkers.[67] Similarly to the dicationic analogues, the two cyclopropenium moieties in **3.52** are tilted (average torsion angle 48.1°) (Figure 3-7).

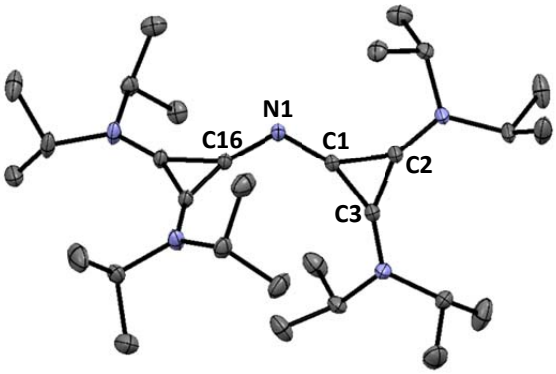

Figure 3-7. Solid-state structure of **3.52**. Hydrogen atoms and the anion are omitted for clarity; ellipsoids are set at 50 % probability.

The **B$_N$**-type monocation **3.52** exhibits two $^{15}N\{^1H\}$ NMR signals at δ_N = -291.6 (N central) and -279.6 (N(*i*Pr)$_2$) ppm, the chemical shift of the central nitrogen atom being in between those of dications **3.45** and **3.51**.

In an attempt to further study the reactivity of this monocation, it was also found that the lone pair of electrons of the central nitrogen atom in **3.52** can react with a proton: treatment with strong Brønsted acids such as HBF_4 or $HGaCl_4$ affords **C$_N$**-type dications **3.53** and **3.54** in good yields (Scheme 3-11). The fact that monocationic **3.52** can be purified by column chromatography and that it was only protonated in presence of strong acids confirmed its

weakly nucleophilic character. *N*-Protonation was immediately apparent from the broad, downfield shifted signal in the ^{1}H NMR spectra at δ = 8.28 (**3.53**) and 8.32 (**3.54**) ppm, and was subsequently confirmed by X-ray diffraction analysis in the case of **3.54** (Figure 3-8). The structure of **3.54** strongly resembles that of the previously described dications **3.45** and **3.51**. There is again a trigonal planar environment around the central nitrogen atom (sum of angles, **Σ °** N = 360.0°). Furthermore, similarly to **3.45** and **3.51**, the cyclopropenium moiety of **3.54** displays a slightly longer carbon-carbon bond distance (C2-C3: 1.409(3) Å) and two shorter ones (C1-C2 and C1-C3: 1.367(3) and 1.371(3) Å), all of them being shorter than a typical C(sp^2)-C(sp^2) single bond (1.460 Å)[79] suggesting delocalization of the π-electron system in the three membered ring. Interestingly, the N(central)-C(cyclopropenyl) bonds differ from each other (1.389(3) and 1.347(3) Å), which could be explained by crystal packing or loss of hyperconjugation when substituting a methyl (**3.45**) or phenyl (**3.51**) group by hydrogen.

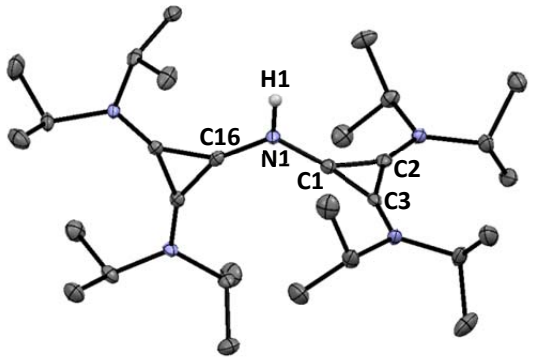

Figure 3-8. Solid-state structure of **3.54**. Hydrogen atoms (except that attached to N1) and anions are omitted for clarity; ellipsoids are set at 50 % probability.

Finally, the synthesis of the tricationic **E$_N$**-type structures was attempted again. In the case of the phosphorus-centered analogs the steric hindrance of the cyclopropenium moiety proved to be critical;[30a] therefore, we employed a sterically less demanding chlorocyclopropenium salt than **1.40**. Compound **3.55**, containing methyl substituents on the nitrogen atoms was then added to a solution of tris(trimethlysilyl)amine in tetrahydrofuran and stirred overnight (Scheme 3-12). Remarkably, our inverse onio-substituent-transfer strategy showed its synthetic utility also in this case. The isolated pale brown solid, obtained in 69 % yield, exhibits a downfield shifted signal in the ^{15}N{^{1}H} NMR spectrum at δ_N = -309.8 ppm for the central nitrogen atom, which is a very similar value to that of **3.51** (*cf.* δ_N = -310.2 ppm). The structure of the desired tricationic compound **3.56** was later unambiguously confirmed by X-

ray diffraction analysis (Figure 3-9). **3.56** can be depicted as an amine substituted by three cyclopropenium moieties **3.56a** and an N^{3+} cation stabilized by three cyclopropenylidenes **3.56b,** according to the Lewis and dative bonding models (Scheme 3-12).

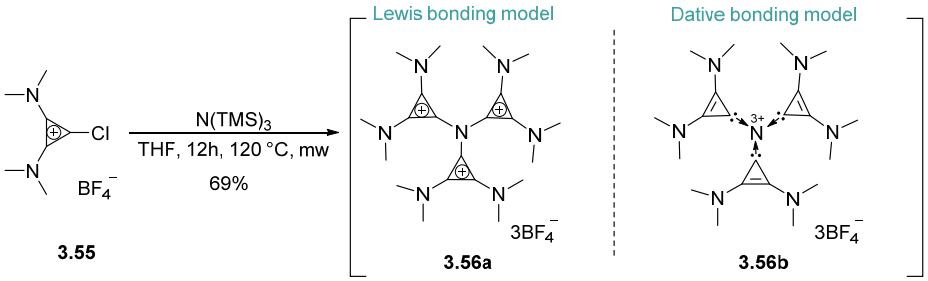

Scheme 3-12. Synthesis of trication **3.56** and bonding extremes **3.56a** and **3.56b**.

Similarly to the previously described tricoordinate compounds of this series, the central nitrogen of **3.56** adopts a trigonal planar environment in the solid-state (sum of angles, **Σ °** N = 359.8°), suggesting back-donation of the non-shared electron pair of the central nitrogen into the cyclopropenium rings (Figure 3-9). However, the significantly longer N(central)-C(cyclopropenyl) bond lengths (1.378(3), 1379(3) and 1.380(3) Å) than in **3.52** (*cf.* 1.332(9) Å) and the average torsion angle of 27.1° for the three cyclopropenium rings with respect to the coordination plane, indicate that this back-donation is quite weak. Similarly to all of the compounds of this family, the nitrogen atoms of the diisopropyl fragments show a planar environment, implying donation of the lone pairs of electrons into the cyclopropenium ring system. The carbon-carbon bond lengths of the cyclopropenium moiety also follow the previously observed trend in the dicationic compounds **3.45**, **3.51** and **3.53**: the C2-C3 distance (1.414(4) Å) is slightly longer than the C1-C2 and C1-C3 bonds (1.362(4) and 1.364(4) Å, respectively), however, all of them are shorter than a typical $C(sp^2)$-$C(sp^2)$ single bond (1.460 Å)[79].

Relevant bond lengths and angles for compounds **3.38**, **3.45, 3.51, 3.52, 3.54** and **3.56** are summarized in Table 3-1 for comparison.

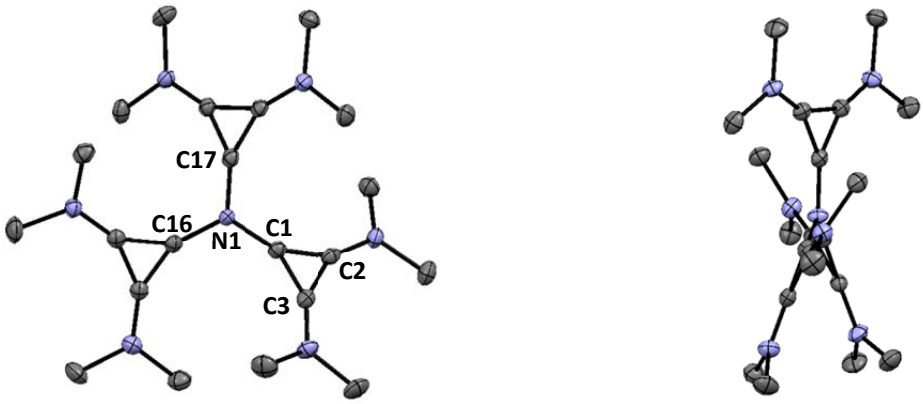

Figure 3-9. Solid state structures of **3.56** front (left) and side (right) view. Hydrogen atoms and anions are omitted for clarity; ellipsoids are set at 50 % probability.

Table 3-1. Selected bond lengths (Å) and angles (°) for compounds **3.38**, **3.45, 3.51, 3.52, 3.54** and **3.56**. Note that the bond lengths of the two (or three) cyclopropenium moieties in all of these compounds are roughly equal, therefore only one of them will be considered.

Compound	**3.38** $[LHN]^+$	**3.45** $[L_2NMe]^{2+}$	**3.51** $[L_2NPh]^{2+}$	**3.52** $[L_2N]^+$	**3.54** $[L_2NH]^{2+}$	**3.56** $[L_3N]^+$
N1-C1	1.336(1)	1.362(2)	1.385(2)	1.332(1)	1.389(3)	1.378(3)
N1-C16	1.432(1)	1.379(2)	1.385(2)	1.332(1)	1.347(3)	1.379(3)
N1-C17	-	1.476(2)	1.433(2)	-	-	1.380(3)
N1-H1	0.880	-	-	-	0.880	-
C1-C2	1.379(1)	1.380(2)	1.378(2)	1.389(1)	1.367(3)	1.362(4)
C1-C3	1.375(1)	1.377(2)	1.381(2)	1.396(1)	1.371(3)	1.364(4)
C2-C3	1.401(1)	1.411(2)	1.426(2)	1.397(1)	1.409(3)	1.414(4)
Σ°N	-	360.0	360.0	-	360.0	359.8

3.2.2. Electronic Properties

To evaluate the electronic properties of the novel amines and imine, it was decided to measure their oxidation potential using cyclic voltammetry (Table 3-2). These data reveal that, the monocationic **3.52** (E_p ox = 1.046 V) is the most electron rich compound within the series. This value is followed by the methyl-substituted dication **3.45** (E_p ox = 1.290 V), exhibiting weaker donor properties. Surprisingly, the highest oxidation potential values were

measured for the dicationic **3.51** (E_p ox = 1.560 V), which is slightly higher than the value recorded for the tricationic **3.56** (E_p ox = 1.406 V). However, it is worthwhile to mention that for the tricationic **3.56** a different solvent (acetonitrile) had to be used for the measurement due to solubility reasons, which can effect the oxidation potential.

Table 3-2. Oxidation potentials (E_p ox) of **3.45, 3.51**, **3.52**, **3.56**.

Compound	E_p ox (V)[a]
3.52 $[L_2N]^+$	1.046
3.45 $[L_2NMe]^{2+}$	1.290
3.51 $[L_2NPh]^{2+}$	1.560
3.56 $[L_3N]^{3+}$	1.406[b]

[a] Oxidation potentials calibrated versus ferrocene/ferricinium, Bu_4NPF_6 (0.1 M) in CH_2Cl_2. [b] Measured in CH_3CN.

In order to gain more insight into the electronic structure of compounds **3.45**, **3.51**, **3.52** and **3.56**, density functional calculations (DFT) were performed in cooperation with the theoretical chemistry department of our institute in the group of Professor Thiel. The geometry optimizations, carried out using Turbomole[80] (version 6.4) at the RI-BP86/def2-TZVP level,[81] closely match the experimental crystallographic data (Tables 3-1 and 3-3).

The calculated Wiberg bond indices - roughly equal for the di- and tricationic compounds **3.45**, **3.51** and **3.56** (1.06, 1.05 and 1.00, respectively) and significantly larger for the monocationic **3.52** (1.31) **-** corroborate our findings by the crystallographic data that the back-donation of the central nitrogen atom to the cyclopropenium moieties in dicoordinate **3.52** is the most pronounced. According to natural population analysis, the central nitrogen atom in these compounds bears a negative charge (-0.45 to -0.60 *e*), hence the cyclopropenium-substituted imine and amine Lewis bonding model description (**3.52a** and **3.56a)** is more appropriate than the cyclopropenylidene stabilized N^+ and N^{3+} (**3.52b** and **3.56b**) description derived from the dative bonding model (Schemes 3-10, 3-11 and Table 3-3).

Table 3-3. Computed bond distances (atBP86/def2-TZVP level), Wiberg bond indices and natural population analysis (at BP86/6-311+G** level). Note that the numbering of the atoms in the compounds is shown in Figures 3-6 - 3-9.

Compound	Bond distances (Å)		Wiberg bond indices (a.u.)	Natural charges (*e*)
	N1-C1/C16	N-C17	N1-C1/C16	Q(N)
3.52 $[L_2N]^+$	1.33	-	1.31	-0.60
3.45 $[L_2NMe]^{2+}$	1.38	1.48	1.06	-0.47
3.51 $[L_2NPh]^{2+}$	1.38	1.45	1.05	-0.47
3.56 $[L_3N]^{3+}$	1.40	-	1.00	-0.45

Inspection of the frontier orbitals reveals that the two highest occupied molecular orbitals of the dicoordinate **3.52** (HOMO and HOMO-1) correspond to π- and σ-type lone pair orbitals with maximum coefficients at the central nitrogen atom, which is in agreement with investigations for similar species reported by Frenking (Figure 3-10).[82]

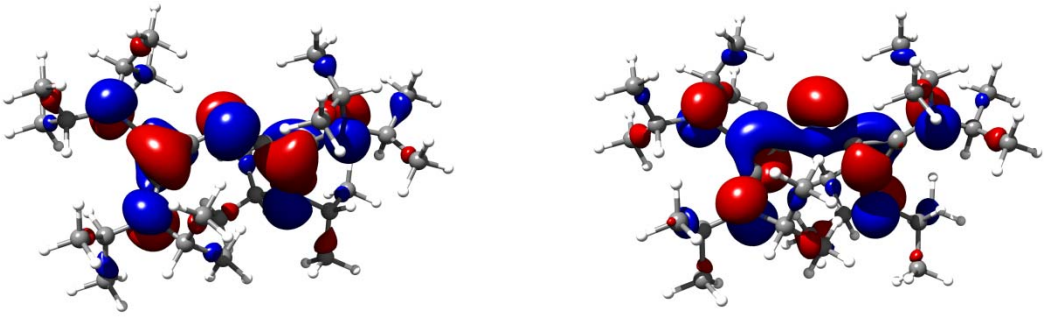

HOMO **HOMO-1**

Figure 3-10. HOMO and HOMO-1 of **3.52**.

Table 3-4 shows the calculated frontier molecular orbital energies for **3.45**, **3.51**, **3.52** and **3.56**. As expected, the tricationic **3.56** has the lowest lying HOMO and LUMO orbitals (-13.783 and -10.415 eV, respectively), implying the weakest donor and strongest acceptor properties. These values are followed by the two dications **3.45** and **3.51** with intermediate orbital energies, while the monocation **3.52** exhibits the highest HOMO and LUMO orbital energies (-7.074 and -3.364 eV, respectively).

Table 3-4. Molecular orbital energies at BP86/def2-TZVP level.

Compound	HOMO (eV)	LUMO (eV)
3.52 $[L_2N]^+$	-7.074	-3.364
3.45 $[L_2NMe]^{2+}$	-10.657	-7.213
3.51 $[L_2NPh]^{2+}$	-10.516	-7.111
3.56 $[L_3N]^{3+}$	-13.783	-10.415

3.3. Conclusions

In conclusion, it was possible to extend our previous work on the design and study of phosphorus-centered cations to their nitrogen-centered analogues. The inverse –onium substituent-strategy developed for the P-centered analogues[30c] could be applied to the preparation of N-centered **B_N-**, **C_N-** and **E_N**-type mono-, di- and trications **3.52**, **3.51** and **3.56.** Among other methods, cations **3.45**, **3.46**, **3.52** and **3.56** were characterized by $^{15}N\{^1H\}$ NMR spectroscopic measurements and by X-ray diffraction analysis. These data reveal that the new di- and tricationic compounds - in sharp contrast to their P-centered pyramidal analogues - all display a trigonal planar environment around the central nitrogen atom (sum of angles around the nitrogen: Σ°N = 359.8 to 360.0°). Furthermore **3.45**, **3.46** and **3.53** represent the first solid-state structures of an N-centered dication, while **3.56** is the first N-centered trication reported ever (Figure 3-11).

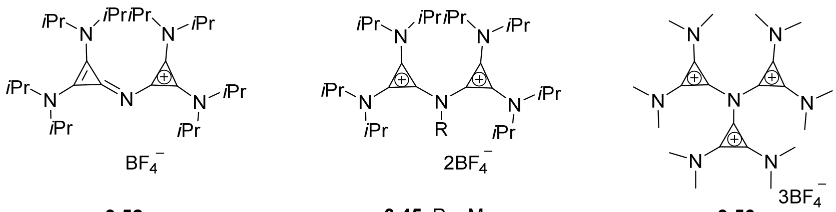

3.52

3.45: R = Me
3.46: R = Ph
3.47: R = *p*-(OMe)C_6H_4
3.48: R = *p*-(F)C_6H_4
3.53: R = H

3.56

Figure 3-11. Isolated N-centered mono- and polycations **3.52**, **3.45-3.48**, **3.53** and **3.56**.

The electronic properties of the novel nitrogen cations were evaluated by cyclic voltammetry and density functional theory calculations. The theoretical calculations corroborate the experimental crystallographic data, suggesting that the best structural description of these novel cations is the Lewis bonding model, whereby a partial negative charge could be located on the central nitrogen atom in all cases.

4. Cyclopropenimine-Substituted Dicationic Phosphines

4.1. Introduction

While singly charged α-cationic phosphines are relatively prevalent, their polycationic counterparts remain less represented, due to their high reactivity, which often precludes structural characterization. Furthermore, owing to their highly charged nature and therefore weak donor abilities, most of them do not coordinate metal centers. This phenomenon is demonstrated by the dicationic phosphines employing imidazolium moieties as charged substituents.[21e,25,83] In contrast, dicationic cyclopropenium-substituted phosphines do exhibit coordination chemistry,[20] as mentioned in the general introduction, due to the higher energy LUMOs of the cyclopropenium group when compared to that of the imidazolium substituents (Figure 4-1).[7]

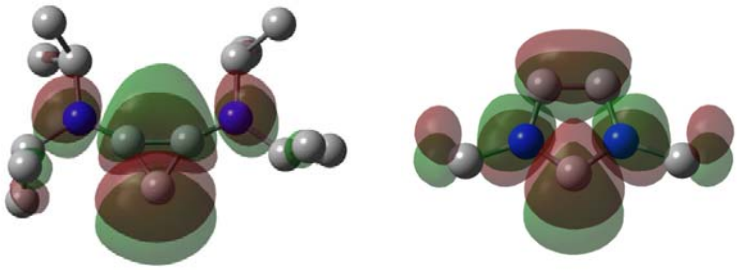

E = -0.1388 eV E = -0.1847 eV

Figure 4-1. LUMOs of 1,2-bis(diisopropylamino)cyclopropenium (left) and 1,3-dimethylimidazolium (right) at the B3LYP/6-31G* level.

Bis-imidazolium phosphines **4.3** and **4.4** were prepared and structurally characterized by Andrieu *et al.* by treatment of 1,3-disubstituted imidazolium-2-carboxylates **4.1** and **4.2** with dichlorophenylphosphine.[21e] In an attempt to evaluate the potential of imidazolium-2-carboxylates in the synthesis of other dicationic phosphines, dichloro-(diethylamino)phosphine was also used by the same authors as electrophilic phosphorus source. Interestingly, instead of the desired dicationic compound, the mono-imidazolium phosphine **4.5** was isolated. A possible explanation for this reaction outcome is the low solubility of **4.5** in dichloromethane, employed as reaction solvent, preventing its further reactivity with the remaining excess of imidazolium-2-carboxylate. On the other hand, the low electrophilicity of the central phosphorus atom that has an electron-donating amino group as substituent may also inhibit the attack of a second carbene (Scheme 4-1).

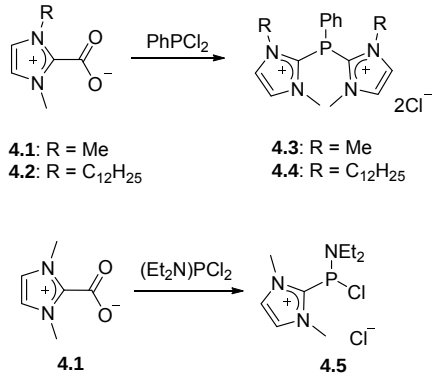

Scheme 4-1. Synthesis of bis-imidazolium phosphines **4.3** and **4.4** and mono-imidazolium phosphine **4.5**.

The synthesis and solid-state structure of the analogous bis-imidazolium phosphine **4.7**, having a chloro-substituent on the central phosphorus was reported by Weigand *et al.*[25] Compound **4.7** was obtained via an –onium substituent transfer strategy,[22a,35] treating the masked carbene **4.6** with phosphorus trichloride. Subsequently, the chloro-substituent in **4.7** was displaced with –CN and $-N_3$ groups when reacted with the corresponding trimethylsilyl reagents, affording the first examples of a dicationic phosphorus cyanide **4.8** or azide **4.9** (Scheme 4-2, a). Furthermore, the structure of these compounds could unambiguously be confirmed by X-ray diffraction analysis, revealing a pyramidalized central phosphorus atom in both cases.

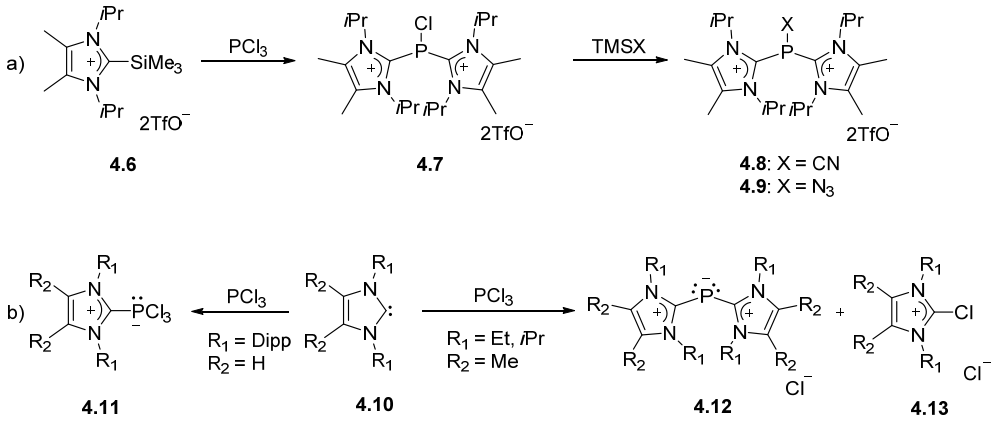

Scheme 4-2. a) Synthesis bis-imidazolium phosphines **4.7-4.9**. b) Reaction of free carbenes with PCl_3.

On the contrary, the reaction of the free carbenes with electrophilic phosphorus sources does not lead to the formation of dicationic phosphines of this type. Bulky carbenes form hypervalent adducts, such as **4.11**, which do not react further[84], while sterically less

demanding carbenes favor the formation of a reductive pathway resulting in **4.12** and **4.13** (Scheme 4-2, b).[62e,85]

In order to enhance the stability of the resulting polycationic phosphines through the chelate effect, bi- and tridentate ancillary ligands have also been employed. In particular, a family of dicationic phosphines were prepared and structurally characterized in our group using dicoordinating (**4.14** and **4.15**) and scorpionate (**4.16** and **4.17**) ligands (Scheme 4-3).[86] Compounds **4.18-4.20** were synthesized through the –onium substituent transfer concept, treating a dichloromethane solution of the bis(pyrazolyl)methane **4.14** with different dichlorophosphines in the presence of trimethylsilyl triflate. Dication **4.21** was prepared in a similar manner, using a bis(oxazoline) ligand, which is particularly interesting since it might offer a route for the preparation of chiral, enantiopure dicationic phosphines. The C2-symmetric bis(oxazolines) are widely used ligands in asymmetric homogeneous catalysis being especially effective for carbon-carbon bond forming reactions.[87] The stability of compounds **4.22** and **4.23** further increases due to the presence of the negatively charged boron atom in the ligand probably due to an attractive Coulombic interaction between the P-center and the ligand. The solid-state structures of this family of dications reveal a pyramidal phosphorus center indicative of retention of a lone pair of electrons on this atom. Despite this fact, no coordination of this series of dicationic phosphines **4.18-4.23** could be observed, likely owing to the high positively charged nature and therefore low lying HOMO of these polycations.

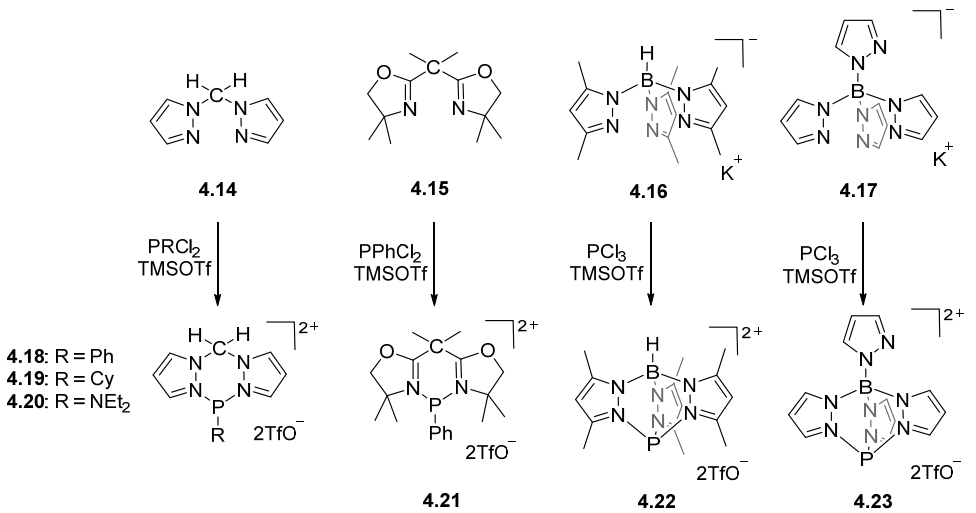

Scheme 4-3. Synthesis of dicationic phosphines **4.18-4.23.**

Alternative chelating structures based on the methylene linked bis(guanidine) **4.24** were prepared by Coles *et al.* to stabilize the electrophilic phosphorus center in compounds such as **4.25**. These salts were obtained through treatment of a dichloromethane solution of **4.24** with dichlorophenylphosphine.[88] Interestingly, despite of the low pyramidalization at phosphorus (51.7 %), **4.25** showed Lewis basic properties; its treatment with $[PtCl(PEt_3)(\mu\text{-}Cl)]_2$ yielded the corresponding platinum(II) complex **4.26** (Scheme 4-4).

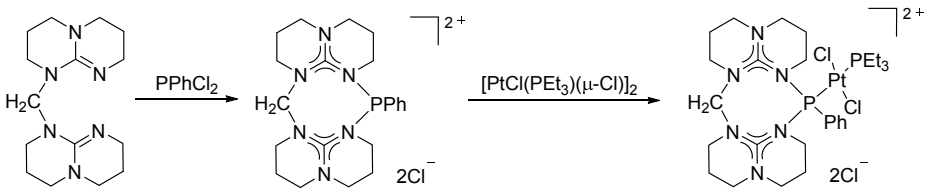

4.24 **4.25** **4.26**

Scheme 4-4. Synthesis of bis-guanidinium phosphine **4.25** and its Pt(II)-complex **4.26**.

The excellent basicity of cyclopropenimines, which is similar to that of bicyclic guanidines, (mentioned in chapter 3) renders them ideal for stabilization of electrophilic moieties. In this context we envisaged that the connection of two cyclopropenimines would result in chelate-type architectures efficient enough to stabilize electrophilic phosphorus centers. Furthermore, the presence of two strongly electron-donating cyclopropenimines would yield phosphines able to coordinate metal centers. The coordination chemistry of bis(cyclopropenimines) towards main group elements remains unexplored; in contrast, several metal complexes of the related bis(imidazoline)imines are known[89] and they have recently also been used in the stabilization of boron centers (Figure 4-2).[90]

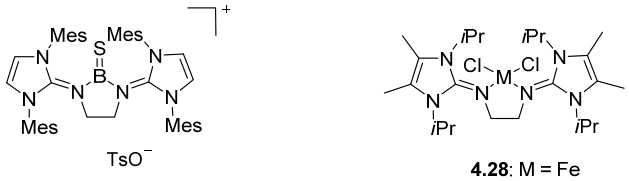

Figure 4-2. Bis(imidazoline)imine-stabilized boron center **4.27** and selected examples of bis(imidazoline)imine metal complexes **4.28**-**4.30**.

4.2. Results and Discussion

4.2.1. Synthesis

The desired bis(cyclopropenimines) are obtained in a two-step synthesis. Condensation of 1,8-diaminonaphthalene or 1,2-diaminobenzene with two equivalents of chlorocyclopropenium salt **1.40** in the presence of triethylamine gives bis(cyclopropenium) salts **4.27** and **4.28** as air-stable crystalline materials. Subsequent deprotonation with potassium hydride gives access to diimines **4.29** and **4.30** in excellent yields (Scheme 4-5). Dichloromethane/diethylether solvent mixture was used to crystallize the dicationic **4.28**, while slow evaporation of a pentane solution of the free base **4.29** afforded suitable single crystals for X-ray diffraction analysis.[91] During the preparation of these compounds, Dudding *et al.* reported the synthesis of **4.27** and **4.29** obtained through a very similar route.[92]

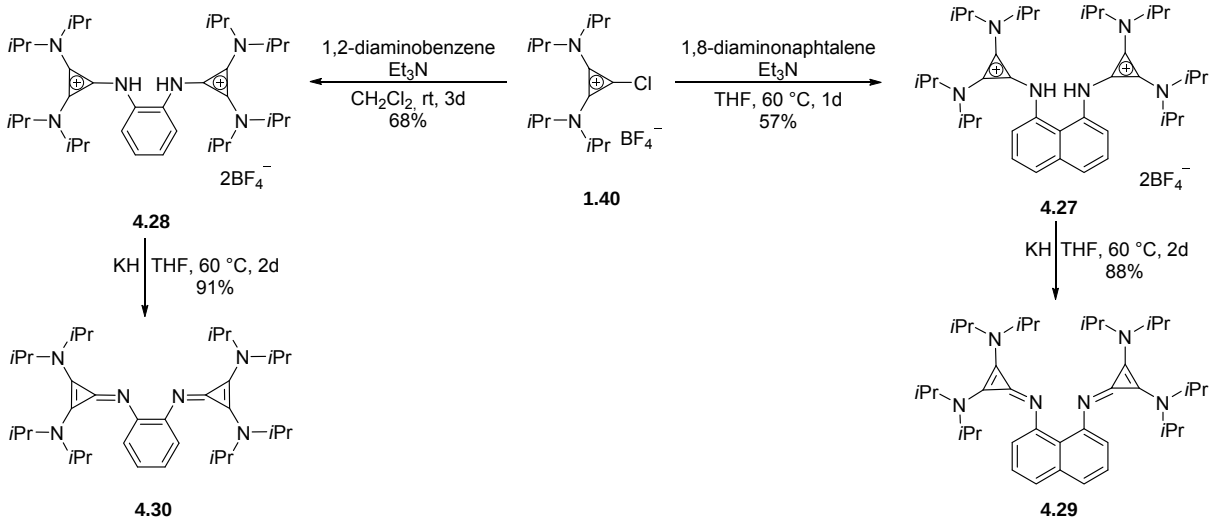

Scheme 4-5. Synthesis of diimines **4.29** and **4.30**.

The solid state structures of **4.28** and **4.29** are shown in Figure 4-3 while the relevant bond distances (Å) are listed in Table 4-1. Compound **4.28** features three similar carbon-carbon bond lengths in both cyclopropenium moieties (1.376(2), 1.377(2) and 1.396(2) Å in both rings) indicating their aromatic character. The two nitrogen-carbon distances, (both N1-C1 and N2-C4 are 1.335(2) Å) typical for N(sp^2)- C(sp^2) single bonds, also support this idea. In contrast, the three-membered rings in the free base **4.29** exhibit two longer and a shorter C-C bond (1.421(2), 1.406(2), 1.374(2) Å in both rings) indicative for loss of the aromatic character. In addition, the N1-C1 and N2-C4 bond distances are significantly shorter (both

1.297(2) Å), inferring the double bond character of this interaction. An interesting feature of the free base **4.29** is the highly strained structure arising from the repulsion between the lone-pairs of electrons of N1 and N2. This manifests in a twisted naphthalene backbone (N1-C7-C9-N2 torsion angle 30.7°) instead of the ideal planarity, which also avoids steric clash between the two relatively bulky isopropyl groups. The high basicity of **4.29** originates from the relief of the strain upon protonation, which also generates aromaticity in the three-membered ring.

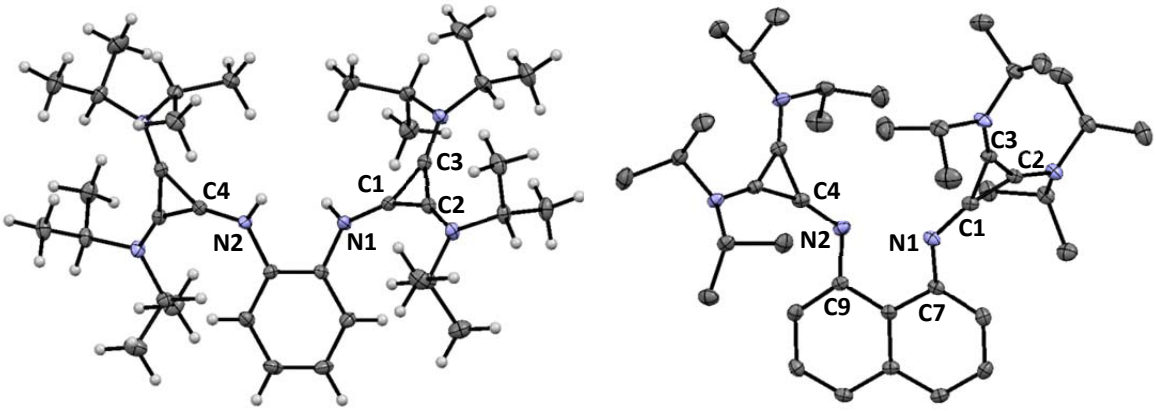

Figure 4-3. Solid-state structures of **4.28** (left) and **4.29** (right). Hydrogen atoms (for **4.29**) and anions (for **4.28**) are omitted for clarity; ellipsoids are set at 50 % probability.

Table 4-1. Selected bond lengths (Å) for compounds **4.28** and **4.29**.

Compound	N1-C1	N2-C4	C1-C2	C1-C3	C2-C3
4.28	1.335(2)	1.335(2)	1.376(2)	1.377(2)	1.396(2)
4.29	1.297(2)	1.297(2)	1.421(2)	1.406(2)	1.374(2)

With the bis(cyclopropenimines) in hand, we investigated their ability to stabilize P(III)-centers. Following the -onium substituent transfer methodology,[22a,35] chlorinated phosphines such as $PhPCl_2$, $CyPCl_2$, PCl_3 and $(Et_2N)PCl_2$ were added to a dichloromethane solution of the prepared diimines, in the presence of two equivalents of trimethylsilyl triflate. To our delight, washing the crude mixtures with diethylether and subsequent recrystallization from dichloromethane/diethylether solvent mixtures, afforded the desired compounds **4.31-4.36** in good yields (Scheme 4-6). Coordination of the chelating ligands to phosphorus was indicated by the $^{31}P\{^1H\}$ NMR spectra of the novel compounds at δ_P = 72.1 (**4.31**), 79.2 (**4.32**), 84.6 (**4.33**), 69.8 (**4.34**), 98.5 (**4.35**) and 126.3 (**4.36**) ppm and subsequently confirmed by X-ray diffraction analysis in the cases of **4.31-4.33**, **4.35** and **4.36.**

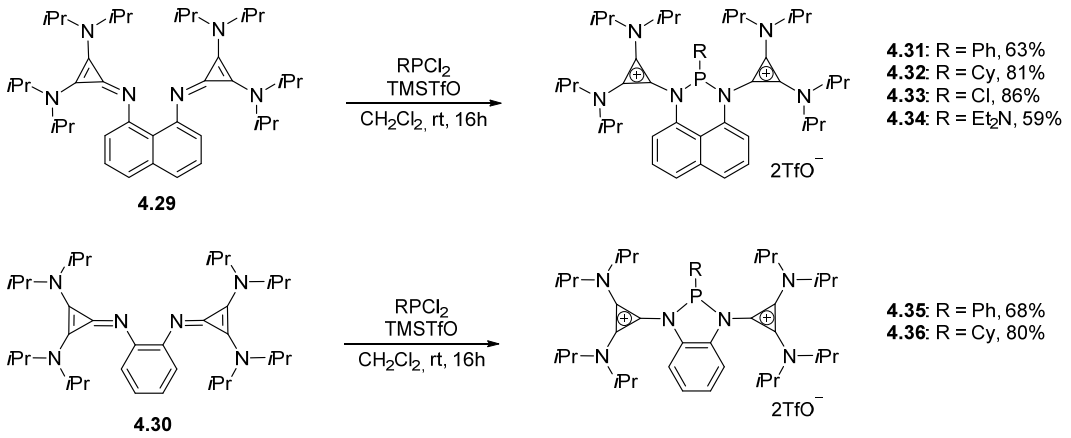

Scheme 4-6. Synthesis of P(III)-centered dications **4.31-4.36**.

The solid state structures of **4.31-4.33, 4.35** and **4.36** are shown in figure 4-4 while the relevant bond distances (Å) and angles (°) are listed in Table 4-2. The degree of pyramidalization[93] at the central phosphorus in all of these compounds is 72.4, 71.7, 72.3, 75.6 and 75.3 % for **4.31-4.33, 4.35** and **4.36**, respectively and suggests retention of the non-bonding electron-pair at this atom.

The P1-C1 bond distances in **4.31** (1.828(3) Å) and **4.32** (1.844(2) Å) are comparable although longer in **4.32**. This is probably due to the presence of the sp^3 and sp^2 hybridized carbon atoms in the cyclohexyl and phenyl groups, respectively. The same trend can be observed in compounds **4.35** and **4.36** (1.820(2) and 1.827(5) Å, respectively). The P1-N1 and P1-N2 bond distances have similar values in **4.31** and **4.32** (1.725(2) to 1.731(1) Å), but slightly decrease in **4.33** (1.703(2) and 1.711(2) Å, respectively) probably owing to the stronger donation of the imine groups to the more electron deficient phosphorus atom in **4.33**, having a chloro-substituent. Dications **4.35** and **4.36**, containing the benzene backbone, depict the longest P1-N1 and P2-N2 distances (1.738(4) to 1.768(2) Å). This is probably due to the formation of a 5-membered ring instead of the 6-membered one derived from the naphthyl skeleton.

An interesting feature of this family of compounds is the linear arrangement of the Cl1 or C1, P1 and O1 (the oxygen atom is part of the triflate anion) atoms. The P1-O1 distance of 2.884 Å in **4.33**, which is remarkably shorter than the sum of the van der Waals radii (3.21 Å), is the shortest among this series of compounds, likely due to the electronegativity of the chloro-substituent attached to the phosphorus atom. These parameters indicate donation of electron density from the triflate anion to the σ*(P-Cl) orbital and reveal Lewis acid character at the phosphorus atom. The longer P1-O1 distances in **4.31**, **4.32** and **4.35** (3.476, 3.596 and 3.179 Å, respectively) suggest that similar interactions, although weaker, can be

found between the triflate counteranions and the σ*(P-C) orbital as well. Interestingly, despite of their steric bulk, both bis(diisopropyl)cyclopropenium-substituents reside on the same side of the naphthalene or benzene plane in all of these molecules, except for **4.36**. Although these dicationic compounds have similar structural attributes, the phosphorus atom is bended away significantly more from the naphthalene plane than from that of the benzene (torsion angles for **4.31**-**4.33**, **4.35** and **4.36**: 48.6, 50.1, 40.4, 14.9 and 9.6°) probably due to the reduced steric hindrance derived from the formation of a 5-membered ring.

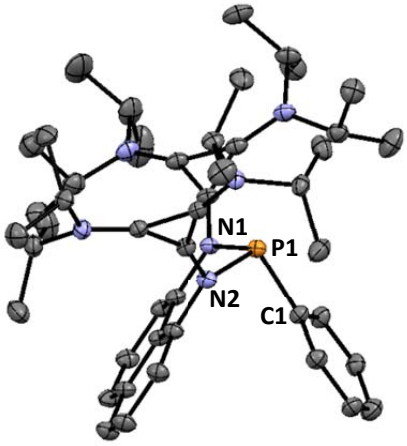

4.31

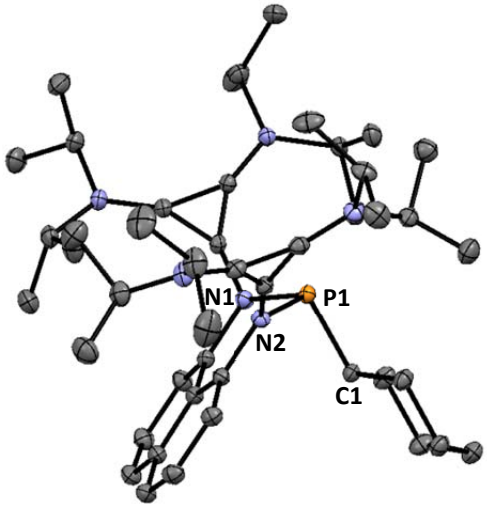

4.32

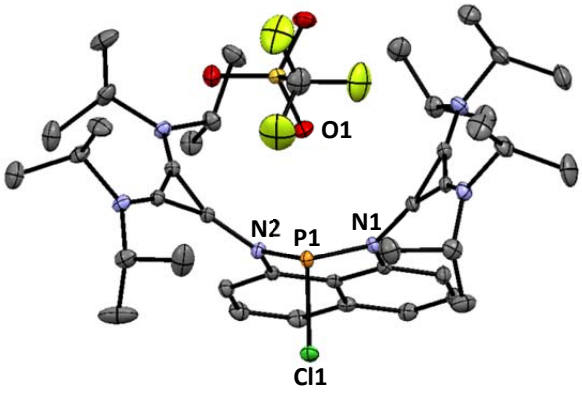

4.33

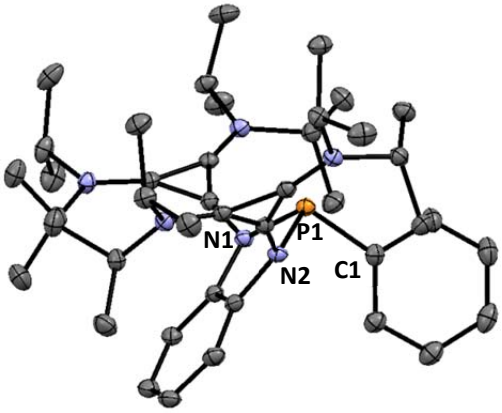

4.35

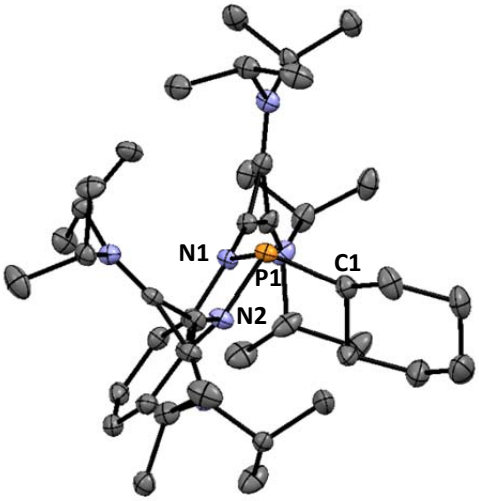

4.36

Figure 4-4. Solid-state structures of **4.31-4.33, 4.35** and **4.36** from top to bottom, left to right. Hydrogen atoms and anions (except for **4.33**) are omitted for clarity; ellipsoids are set at 50 % probability.

Table 4-2. Selected bond lengths (Å) and angles (°) and degree of pyramidalization (DP)[93] for compounds **4.31-4.33, 4.35** and **4.36.**

Compound	P1-C1	P1-N1	P1-N2	DP (%)
4.31 R = Ph	1.828(3)	1.725(2)	1.727(2)	72.4
4.32 = Cy	1.844(2)	1.728(1)	1.737(1)	71.7
4.33 = Cl	2.094(1) (**P1-Cl1**)	1.703(2)	1.711(2)	72.3
4.35 = Ph	1.820(2)	1.762(2)	1.768(2)	75.7
4.36 = Cy	1.827(5)	1.759(4)	1.738(4)	75.3

It is worth to mention that derivative **4.33** is especially versatile from a synthetic point of view since the chloro-substituent can easily be exchanged by –CN, –SPh or $–N_3$ groups using the corresponding silylated reagents (Scheme 4-7).[25,94] The displacement of the chloro-substituent in **4.33** was reflected by a significant change in the $^{31}P\{^{1}H\}$ NMR spectra: δ_P = 16.6 (**4.37**), 91.0 (**4.38**) and 74.0 (**4.39**) ppm (*cf.* δ_P = 84.6 ppm for **4.33**).

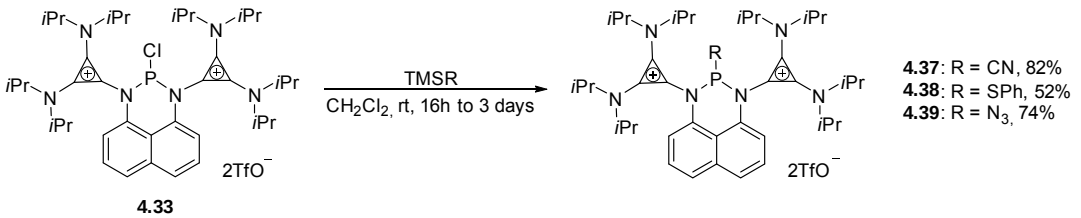

4.33

Scheme 4-7. Synthesis of P(III)-centered dications **4.37-4.39**.

4.2.2. Electronic Properties

As in the previous chapters, in order to evaluate the donor abilities of the novel dicationic phosphines, cyclic voltammetry measurements were carried out. The oxidation potentials (E_p ox) of **4.31-4.39** are shown in Table 4-3.

Table 4-3. Oxidation potentials of compounds **4.31-4.39**, PCy_3, PPh_3 and $P(MeO)_3$.

Compound	E_p ox (V)[a]	Compound	E_p ox (V)
4.31 R = Ph	0.944	**4.37** R = CN	1.147
4.32 R = Cy	0.940	**4.38** R = SPh	0.965
4.33 R = Cl	1.034	**4.39** R = N_3	1.052
4.34 R = Et_2N	0.818	PCy_3	0.542
4.35 R = Ph	0.854	PPh_3	0.687
4.36 R = Cy	0.826	$P(MeO)_3$	1.287

[a] Oxidation potentials calibrated versus ferrocene/ferricinium, Bu_4NPF_6 (0.1 M) in CH_2Cl_2.

Compounds **4.31** and **4.32** (E_p ox = 0.944 and 0.940 V, respectively) depict higher oxidation potentials when compared to their benzene containing counterparts **4.35** and **4.36** (E_p ox = 0.854 and 0.826 V, respectively). This suggests that diimine **4.29** - containing the naphthalene backbone - donates electron density to the central atom less efficiently than **4.30**. Probably the larger torsion angles observed in the solid-state structure of dications **4.31-4.33** hinder an efficient orbital overlap between the central P-atom and the flanking nitrogens. As expected, the oxidation potential values decrease within a given architecture, when employing strongly electron donating groups such as cyclohexyl (**4.32** and **4.36**, E_p ox = 0.940 and 0.826 V) or diethylamine (**4.34**, E_p ox = 0.818 V). Following this trend, attachment of electron withdrawing groups - such as cyano or chloro - on the central phosphorus atom, imparts weaker donor abilities, increasing the oxidation potentials of the corresponding dications (**4.37** and **4.33**, E_p ox = 1.147 and 1.034 V, respectively). Comparing these data to the oxidation potentials of PCy_3, PPh_3 and $P(MeO)_3$ (E_p ox = 0.542, 0.687 and 1.287 V, respectively), we can conclude that the newly prepared phosphines have intermediate donor abilities between phosphines and phosphites. This is remarkable, considering their dicationic nature and is likely due to the excellent ability of the bis(cyclopropenimines) to transfer electron density onto the central phosphorus.

4.2.3. Coordination Properties

As the cyclic voltammetry measurements indicated that the new dicationic phosphines were likely able to form coordination complexes, we next investigated their reactivity towards metal centers. Reaction of **4.31, 4.32** and **4.34-4.36** in dichloromethane with one equivalent of (Me_2S)AuCl yielded the corresponding Au(I) complexes **4.40-4.44** in excellent yields (Scheme 4-8). The coordination of gold by the phosphorus atom was initially reflected by the downfield shifted signals in the $^{31}P\{^1H\}$ NMR spectra at δ_P = 77.1 (**4.40**), 97.5 (**4.41**), 79.1 (**4.42**), 100.1 (**4.43**) and 127.1 (**4.44**) ppm. Moreover, single crystals of **4.40** and **4.41** were grown from a dichloromethane/diethylether solvent mixture and their structure was unambiguously confirmed by X-ray diffraction analysis.

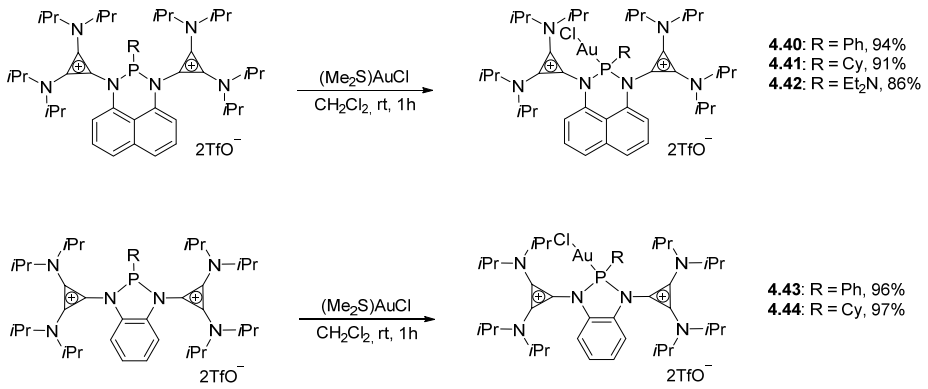

Scheme 4-8. Synthesis of Au(I) complexes **4.40-4.44**.

The solid state structures of **4.40** and **4.41** are shown in Figure 4-5 while the relevant bond distances (Å) and angles (°) are listed in Table 4-4. Similarly to the free ligands **4.31** and **4.32**, the P1-C1 bond length in **4.41** (1.827(2) Å) is longer than that in **4.40** (1.801(2) Å), probably owing to the sp^3 hybridized carbon atom of the cyclohexyl group in **4.41**. However, both of these bond lengths are shorter in comparison to the corresponding free ligands **4.31** and **4.32** (*cf.* 1.828(3) and 1.844(2) Å, respectively**)**, suggesting a stronger P1-C1 bond when the phosphorus atom is involved in coordination to the gold(I)-center. The P1-N1 and P1-N2 bond lengths in the gold complexes **4.40**, **4.41** (1.690(1) to 1.701(2) Å) are significantly shortened when compared to the free ligands **4.31** and **4.32** (*cf.* 1.725(2) to 1.737(1) Å), indicating an enhanced donation of the diimine to the central phosphorus, which is more Lewis acidic after coordinating to gold. The P1-Au1-Cl1 angles in both **4.40** (176°) and **4.41** (174°) are in agreement with the linear structure.

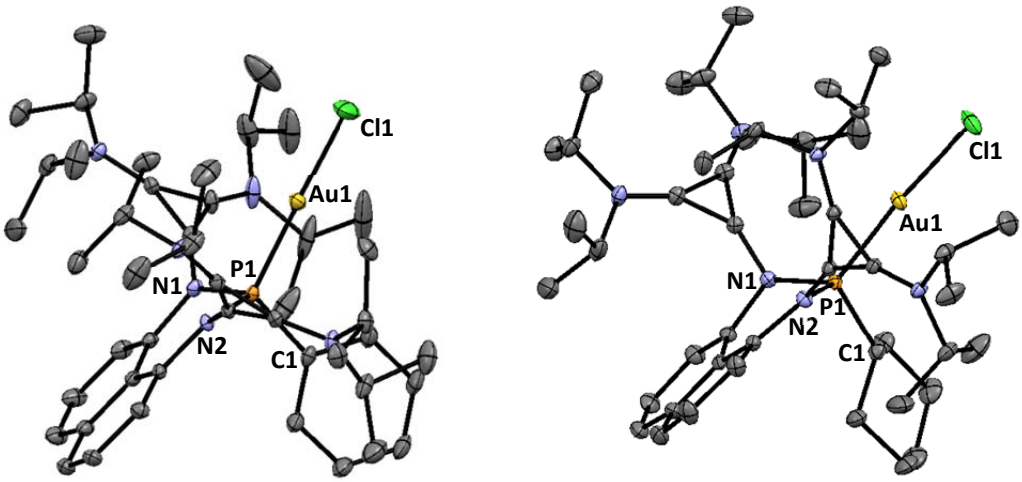

Figure 4-5. Solid-state structures of **4.40** (left) and **4.41** (right). Hydrogen atoms and anions are omitted for clarity; ellipsoids are set at 50 % probability

Table 4-4. Selected bond lengths (Å) and angles (°) for compounds **4.40** and **4.41**.

Compound	P1-C1	P1-N1	P1-N2	$\Phi_{P1Au1Cl1}$
4.40 = Ph	1.801(2)	1.690(1)	1.696(2)	176
4.41= Cy	1.827(2)	1.698(2)	1.701(2)	174

To further extend the coordination chemistry of these dications, the silver derivative **4.45** was prepared analogously from **4.31** but employing AgTfO as a metal source (Scheme 4-9). Although no crystal structure could be obtained, the coordination of the silver by the phosphorus atom was indicated by the broad doublet signal in the $^{31}P\{^{1}H\}$ NMR spectrum at δ_P = 69.1 ($^{1}J_{AgP}$ = 716 Hz) ppm. Unfortunately, our attempt to synthesize the corresponding trichloroplatinate complexes failed, most likely due to the bulkiness of the ligand, which encumbers the approach of the sterically more demanding metal fragment.

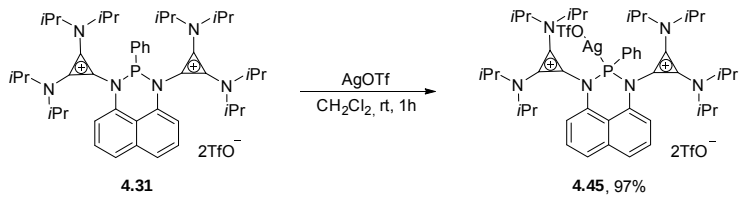

4.31 **4.45**, 97%

Scheme 4-9. Synthesis of Ag(I) complex **4.45**.

4.2.4. Oxidation Reactions

In light of the low oxidation potentials measured for the dicationic phosphines, we envisaged that oxidations to afford analogous P(V) species would be observable. Thus, a dichloromethane solution of **4.31** was treated with *m*-chloroperbenzoic acid, affording cleanly the desired dicationic oxide **4.46** in 92 % yield (Scheme 4-10). The product formation was first suggested by the significant upfield shift in the $^{31}P\{^{1}H\}$ NMR spectra from δ_P = 72.1 ppm (**4.31**) to -0.1 ppm (**4.46**) and later unambiguously confirmed by X-ray diffraction analysis (Figure 4-6). Although peracids have previously been used for the oxidation of monocationic phosphines[95], oxidation of dicationic analogues with this procedure is unknown.

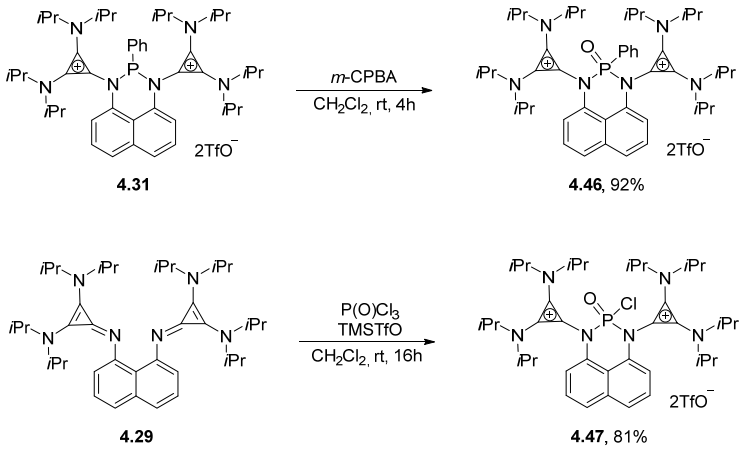

4.31 **4.46**, 92%

4.29 **4.47**, 81%

Scheme 4-10. Synthesis of dicationic P(V)-oxides **4.46** and **4.47**.

The solid-state structure revealed that the dicationic oxide **4.46**, similarly to the gold complexes **4.40** and **4.41,** has shorter P1-N1 and P1-N2 distances (1.692(2) and 1.683(2) Å, respectively) than the corresponding P(III)-compound **4.31** (*cf.* 1.725(2) and 1.727(2) Å), as the nitrogen atoms donate stronger to the highly oxidized P(V)-center. The same trend can be observed in the case of the P1-C1 bond distance of this molecule (1.803(2) Å), which is significantly shorter than the one in the corresponding phosphine **4.31** (*cf.* 1.828(3) Å). The P1-O1 distance in **4.46** (1.468(1) Å) is slightly shorter than that reported for triphenylphosphine (1.479(2) Å), likely due to the stronger back-donation from the oxygen to the phosphorus induced by the two positive charges.[96]

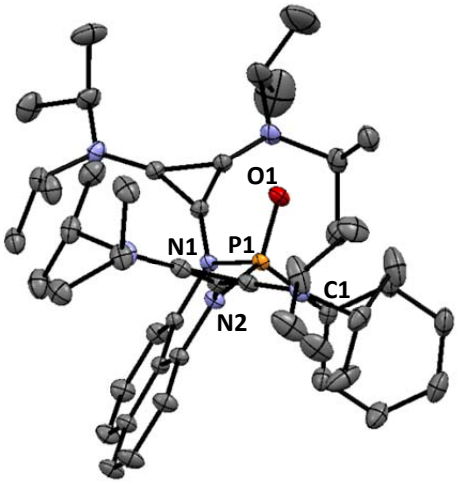

Figure 4-6. Crystal structure of **4.46**. Hydrogen atoms and anions are omitted for clarity; ellipsoids are set at 50 % probability.

For the preparation of the dicationic P(V)-oxide **4.47** having a chloro-substituent, we developed an alternative route, in order to avoid the use of the air and moisture sensitive chloro-substituted phosphine **4.33.** Treatment of the free base **4.29** with phosphoryl chloride in the presence of trimethylsilyl triflate afforded **4.47** in 81 % yield (Scheme 4-10).
Finally, as continuation of our reactivity studies regarding oxidations, we also attempted the preparation of a difluorinated P(V) dication, using XeF_2 as the oxidating agent. Addition of XeF_2 to a dichloromethane solution of **4.35** in a glovebox furnished **4.48** in 45 % yield after several recrystallizations. **4.48** exhibits a triplet signal in the $^{31}P\{^{1}H\}$ NMR spectrum at δ_P = -49.8 ppm with a relatively high $^{1}J_{PF}$ = 940 Hz coupling constant, consistent with the attachment of two fluorine atoms to the central phosphorus (Scheme 4-11).

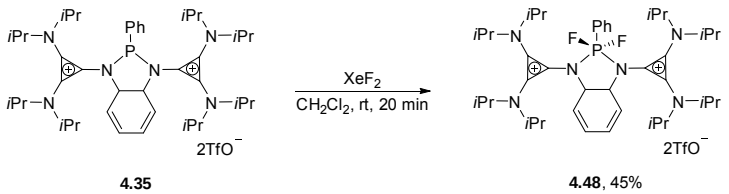

4.35 **4.48**, 45%

Scheme 4-11. Synthesis of dicationic P(V)-oxide **4.48**.

4.3. Conclusions

A series of bis[(dialkylamino)cyclopropenimine]-stabilized dicationic phosphines have been described where both imines were connected through naphthalene or benzene architectures. Dications **4.31-4.36** were isolated by treatment of the chelate-type diimines **4.29** or **4.30** with a variety of dichlorophosphines in the presence of trimethylsilyl triflate using the –onium substituent transfer strategy. The chloro-derivative **4.33** was found to undergo substitution reactions with several silylated reagents delivering dicationic phosphines **4.37-4.39**, bearing cyano, thiophenol and azido functionalities (Figure 4-7).

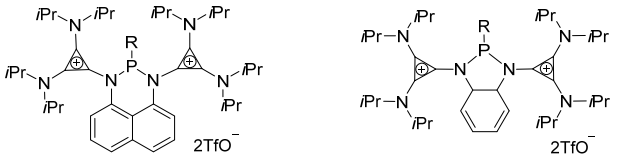

4.31: R = Ph **4.37**: R = CN
4.32: R = Cy **4.38**: R = SPh
4.33: R = Cl **4.39**: R = N_3
4.34: R = Et_2N

4.35: R = Ph
4.36: R = Cy

Figure 4-7. Prepared P(III)-centered dications **4.31-4.39**.

The evaluation of the σ-donor and π-acceptor properties by cyclic voltammetry revealed that all of the prepared dicationic phosphines (E_p ox = 0.818 to 1.147 V) have intermediate behavior between PPh_3 (E_p ox = 0.687 V) and $P(OMe)_3$ (E_p ox = 1.287 V). Their strong donor abilities - despite of their dicationic nature - prompted us to investigate their coordination chemistry. Thus, the phenyl-, cyclohexyl- and diethylamine-substituted dicationic phosphines **4.31**, **4.32** and **4.34-4.36** were shown to form the corresponding Au(I) and Ag(I) complexes in excellent yields. In line with the low oxidation potentials measured for the novel phosphines, P(V)-centered dications **4.46-4.48** could also be prepared employing strong oxidants, such as metachloroperbenzoic acid or xenon difluoride (Figure 4-8).

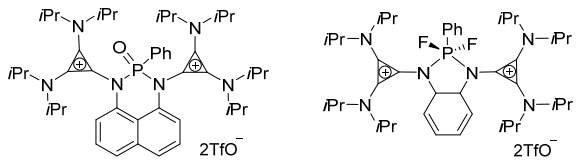

4.46: R = Ph
4.47: R = Cl

4.48

Figure 4-8. Prepared P(V)-centered dications **4.46-4.48**.

5. Experimental Section

5.1. General Experimental Methods

All manipulations were carried out under an inert atmosphere either in flame-dried glassware on a Schlenk line or in an MBraun Labmaster 130 Glovebox. All solvents were purified by distillation over the drying agents indicated and were transferred under argon: THF, Et_2O (Mg/anthracene), CH_2Cl_2, (CaH_2), pentane, hexane, toluene (Na/K), MeOH (Mg, stored over MS 3Å). DMF, DMSO, CH_3CN and Et_3N were dried by an adsorption solvent purification system based on molecular sieves. PCl_3 and TMSOTf were distilled under argon prior to use. All other commercially available compounds (Aldrich, Alfa Aesar, Fluka, ABCR, Acros, Fischer) were used as received. 2,3-bis(diisopropylamino)-1-chlorocyclopropenium tetrafluoroborate **1.40**,[97] bis[3,5-bis(trifluoromethyl)phenyl]phosphine **2.11**,[98] 2-chloro-1,3-dimethyldihyroimidazolium tetrafluoroborate **2.13**,[99] 6-bromo-3-hydroxy-2-methoxybenzaldehyde **2.34**,[59] *N,N*-Bis(trimethylsilyl)aniline **3.49**,[100] 2,3-dimethylamino-1-chlorocyclopropenium tetrafluoroborate **3.55**[101] were prepared according to literature procedures.

5.2. General Experimental Instrumentation

Samples for solution ^{1}H, $^{13}C\{^{1}H\}$, $^{11}B\{^{1}H\}$, $^{31}P\{^{1}H\}$, $^{19}F\{^{1}H\}$ NMR spectroscopy were recorded on a Bruker AV 600, AV 400 or DPX 300. ^{1}H and $^{13}C\{^{1}H\}$ chemical shifts (δ) are given in ppm relative to TMS, coupling constants (*J*) in Hz. The solvent signals in the spectra were used as references and the chemical shifts converted to the TMS scale. For a selection of compounds, ^{15}N chemical shifts were also obtained in a ^{1}H, ^{15}N-HMBC at natural abundance on a Bruker AV 600 equipped with a TCI cryoprobe; this experiment was typically run for 5 hours with transfer delays optimized for 2 to 5 Hz heteronuclear couplings. For most samples, the 5-bond heteronuclear coupling $^{5}J_{^{15}N\text{-}^{1}H}$ was large enough to obtain the signal from the central nitrogen. These chemical shifts are indirectly referenced to the signal from $CH_3{}^{15}NO_2$.

Mass spectrometry samples were measured by the department for mass spectrometry at the Max-Planck-Institut für Kohlenforschung. The following equipment was used: MS (EI): Finnigan MAT 8200 (70 eV), ESI-MS: Finnigan MAT 95. Accurate mass determinations: Bruker

APEX III FT-MS (7 T magnet). Analytical measurements by gas chromatography were conducted with an Agilent 6890A device with an Agilent 5973 Mass Selective Detector. Analytical and preparative high performance liquid chromatography (HPLC) was performed in the HPLC department of the Max-Planck-Institut für Kohlenforschung. The following devices were used: LC-20 and LC-10 (Schimadzu). Thin layer chromatography (TLC) was performed on Macherey-Nagel precoated plates (POLYGRAM SIL/uv254). Detection was achieved under UV light (254 nm). Flash chromatography was perfomed with Merck silica gel 60 (40-63 μm).

The IR spectra were recorded on the Spectrum One (Perkin-Elmer) spectrometer and the Alpha Platinum ATM (Bruker) at room temperature, wavenumbers ($\tilde{\nu}$) are given in cm^{-1}; all measurements were carried out on solid samples.

X-Ray diffraction analysis was performed in the department “Chemische Kristallographie” in the Max-Planck-Institut für Kohlenforschung, which is directed by Prof. Christian Lehmann. The X-ray intensity data were measured on a Bruker AXS Proteum X8 and a Bruker AXS Apex II diffractometers. These were equipped with a Cu and Mo FR591 rotating anode, respectively, and multilayer X-ray optics. The APEX2[102] software was used to operate both diffractometers. The data were integrated with SAINT[103] and corrected for absorption effects based on Gaussian numerical integration and scaled with SADABS.[104] The crystal structures were solved by direct methods using SHELXS-97 and refined with SHELXL-2014.[105]

Melting or decomposition points were determined by placing the sample in capillaries and heating using a Büchi Melting Point B-540 heater.

The oxidation peak potentials for the cyclic voltammetry measurements are reported in V and calibrated versus ferrocene/ferrocinium, Bu_4NPF_6 (0.1M) in CH_2Cl_2 or CH_3CN, as stated.

Elemental analysis measurements were carried out at the microanalysis laboratories Kolbe in Mülheim an der Ruhr.

5.3. Synthetic Details

Compound **2.12**

A solution of bis[3,5-bis(trifluoromethyl)phenyl]phosphine (1.00 g, 2.18 mmol) in dry THF (15 mL) was cooled to -78 °C, then *n*BuLi (1.6 M in hexane, 1.4 mL, 2.18 mmol) was added and the resulting mixture was stirred for 2 hours at this temperature. Chlorocyclopropenium salt **1.40** (782 mg, 2.18 mmol) was then added to the reaction and the mixture allowed to warm up slowly to room temperature and further stirred at 60 °C for 2 days. After cooling to ambient temperature, the solvent was evaporated, the residue suspended in CH_2Cl_2 (20 mL) and washed with saturated aq. $NaBF_4$ solution (3 x 15 mL). After drying over Na_2SO_4, the organic phase was concentrated and the residue purified by column chromatography (CH_2Cl_2/acetone: 90/10) to afford the title compound as a pale yellow solid (653 mg, 38 %).

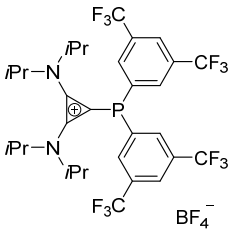

^{1}H NMR (400 MHz, $CDCl_3$) δ = 1.11 (d, *J* = 6.8 Hz, 12H), 1.41 (d, *J* = 6.8 Hz, 12H), 3.48 (sept, *J* = 6.8 Hz, 2H), 4.16 (sept, *J* = 6.8 Hz, 2H), 7.93 (s, 2H), 7.95 (s, 2H), 8.02 (s, 2H) ppm.

^{31}P{^{1}H} NMR (162 MHz, $CDCl_3$) δ = -26.9 ppm.

^{19}F{^{1}H} NMR (282 MHz, CD_2Cl_2) δ = -151.5, -63.1 ppm.

^{13}C{^{1}H} NMR (101 MHz, $CDCl_3$) δ = 20.8, 20.8, 21.2, 52.8, 54.6, 99.4 (d, J_{PC} = 61.4 Hz), 122.7 (q, J_{FC} = 273.3 Hz), 124.8-125.1 (m), 133.3 (dq, J_{FC} = 34.3 Hz, J_{PC} = 7.1 Hz), 133.9 (dq, J_{FC} = 21.9 Hz, J_{PC} = 3.6 Hz), 134.3 (d, J_{PC} = 15.4 Hz), 140.0 ppm.

HRMS *calcd*. for $[C_{31}H_{34}N_2F_{12}P]^+$: 693.226254; *found* 693.226826.

IR (solid) $\tilde{\nu}$ = 681, 704, 845, 899, 1057, 1095, 1122, 1180, 1278, 1353, 1459, 1567, 1867, 2981 cm^{-1}.

Compound **2.14**

Ph_2PH (2.4 mL, 13.61 mmol) was added to a solution of chlorodihydroimidazolium salt **2.13** (1.00 g, 4.54 mmol) in dry THF (18 mL) and the resulting mixture was stirred at 60 °C for 1 day. After cooling to room temperature, the solvent was evaporated and the residue diluted with CH_2Cl_2 (6 mL). $NaBF_4$ (2.50 g, 22.70 mmol) was then added to the suspension and stirred at room temperature for 1 hour. After filtration, the filtrate was concentrated and the residue purified by column chromatography (CH_2Cl_2/MeOH: 97/3) to give the title compound as a transparent oil (1.11 g, 66 %).

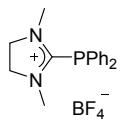

^{1}H NMR (300 MHz, $CDCl_3$) δ = 2.85 (s, 6H), 4.05 (d, *J* = 1.1 Hz, 4H), 7.50-7.58 (m, 10H) ppm.

^{31}P{^{1}H} NMR (121 MHz, CD_2Cl_2) δ = -14.6 ppm.

^{13}C{^{1}H} NMR (101 MHz, $CDCl_3$) δ = 35.8 (d, J_{PC} = 9.2 Hz), 52.1, 126.8 (d, J_{PC} = 6.0 Hz), 130.2 (d, J_{PC} = 8.3 Hz), 131.6, 134.2 (d, J_{PC} = 21.6 Hz), 168.9 (d, J_{PC} = 53.6 Hz) ppm.

HRMS *calcd.* for $[C_{17}H_{20}N_2P]^+$: 283.135864; *found* 283.135696.

IR (solid) $\tilde{\nu}$ = 695, 747, 934, 996, 1033, 1045, 1296, 1411, 1436, 1480, 1569, 2940, 3055 cm^{-1}.

Compound **2.15**

Cy_2PH (2.2 mL, 10.89 mmol) was added to a solution of chlorodihydroimidazolium salt **2.13**

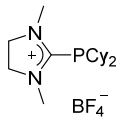

(800 mg, 3.63 mmol) in dry THF (15 mL) and the resulting mixture was stirred at 60 °C for 1 day. After cooling to room temperature, the solvent was evaporated, the residue washed with Et_2O (3 x 8 mL) and diluted with CH_3CN (5 mL). $NaBF_4$ (2.00 g, 18.15 mmol) was then added to the suspension and stirred at room temperature for 12 hours. The solvent was then evaporated and the product extracted with CH_2Cl_2. Evaporation of the solvent and purification of the residue by column chromatography (CH_2Cl_2/acetone: 90/10) gave the title compound as a white solid (819 mg, 59 %).

^{1}H NMR (400 MHz, CD_2Cl_2) δ = 1.67-1.43 (m, 10H), 1.46-1.56 (m, 2H), 1.65-1.74 (m, 2H), 1.74-1.85 (m, 4H), 1.85-1.94 (m, 2H), 2.27-2.39 (m, 2H), 3.31 (s, 6H), 3.98 (s, 4H) ppm.

^{31}P{^{1}H} NMR (162 MHz, CD_2Cl_2) δ = -10.4 ppm.

^{13}C{^{1}H} NMR (101 MHz, CD_2Cl_2) δ = 25.9, 26.5 (d, J_{PC} = 25.3 Hz), 26.6 (d, J_{PC} = 19.3 Hz), 30.6 (d, J_{PC} = 8.0 Hz), 32.0 (d, J_{PC} = 24.2 Hz), 33.9 (d, J_{PC} = 14.9 Hz), 36.4 (d, J_{PC} = 11.9 Hz), 51.8, 171.3 (d, J_{PC} = 63.8 Hz) ppm.

HRMS *calcd.* for $[C_{17}H_{32}N_2P]^+$: 295.229762; *found* 295.229690.

IR (solid) $\tilde{\nu}$ = 483, 517, 633, 852, 890, 933, 1032, 1046, 1093, 1203, 1300, 1341, 1411, 1447, 1525, 1579, 2846, 2932 cm^{-1}.

Compound **2.16**

To a solution of the cationic phosphine **2.12** (70 mg, 0.09 mmol) in CH_2Cl_2 (1.5 mL), $[RhCl(CO)_2]_2$ (9 mg, 0.02 mmol) was added and the reaction mixture was stirred for 2 hours at room temperature. After removal of the solvents *in vacuo*, the solid residue was washed with pentane (2 x 1 mL) and dried, affording the desired product as a yellow solid (36 mg, 93 %).

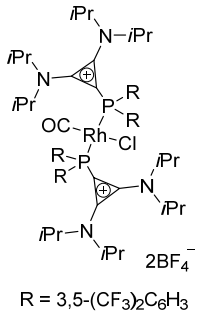

^{1}H NMR (400 MHz, $CDCl_3$) δ = 1.06 (d, *J* = 6.9 Hz, 24H), 1.39 (d, *J* = 6.9 Hz, 24H), 3.49 (sept, *J* = 6.9 Hz, 4H), 4.20 (sept, *J* = 6.9 Hz, 4H), 8.21 (s, 4H), 9.02 (t, *J* = 5.8 Hz, 8H) ppm.

^{31}P{^{1}H} NMR (162 MHz, CD_2Cl_2) δ = 25.0 (d, J_{RhP} = 136.5 Hz) ppm.

^{19}F{^{1}H} NMR (282 MHz, CD_2Cl_2) δ = -150.3, -150.2, -63.2 ppm.

The sample decomposes during the ^{13}C NMR measurement.

ESI-MS: 1639 m/z, $[C_{63}H_{68}BClF_{28}N_4OP_2Rh]$ $[M\text{-}BF_4^-]$

IR (solid) $\tilde{\nu}$ = 681, 701, 901, 1051, 1095, 1121, 1181, 1278, 1354, 1457, 1561, 1863, 1991, 2981 cm^{-1}.

Compound **2.17**

$[RhCl(CO)_2]_2$ (13 mg, 0.03 mmol) was added to a solution of cationic phosphine **2.14** (48 mg, 0.13 mmol) in CH_2Cl_2 (1 mL) and the resulting mixture was stirred at room temperature for 1 hour. The solvent was then evaporated affording the desired product as a yellow solid (56 mg, 95 %).

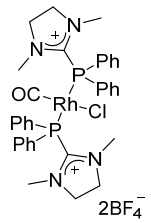

^{1}H NMR (300 MHz, CD_2Cl_2) δ = 2.89 (s, 12H), 4.14 (s, 8H), 7.62-7.76 (m, 12H), 8.00-8.11 (m, 8H) ppm.

^{31}P{^{1}H} NMR (121 MHz, CD_2Cl_2) δ = 35.8 (d, J_{RhP} = 132.0 Hz) ppm.

^{13}C{^{1}H} NMR (101 MHz, CD_2Cl_2) δ = 37.6, 52.9, 124.7 (t, J_{PC} = 24.7 Hz), 130.7 (t, J_{PC} = 5.8 Hz), 134.0, 135.5 (t, J_{PC} = 7.5 Hz), 164.1 (t, J_{PC} = 13.0 Hz), 185.3 (dt, J_{RhC} = 70.4 Hz, J_{PC} = 16.4 Hz) ppm.

HRMS *calcd.* for $[C_{35}H_{40}BClF_4N_4OP_2Rh]^+$: 819.145939; *found* 819.145265.

IR (solid) $\tilde{\nu}$ = 691, 731, 750, 931, 997, 1034, 1047, 1296, 1410, 1437, 1481, 1580, 1993, 2941 cm^{-1}.

Compound **2.18**

$[RhCl(CO)_2]_2$ (25 mg, 0.07 mmol) was added to a solution of cationic phosphine **2.15** (100 mg, 0.26 mmol) in CH_2Cl_2 (1 mL) and the resulting mixture was stirred at room temperature for 1 hour. The solvent was then evaporated affording the desired product as a yellow solid (115 mg, 94 %).

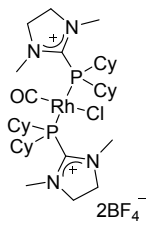

^{1}H NMR (400 MHz, CD_2Cl_2) δ = 1.28-1.50 (m, 12H), 1.59-1.72 (m, 4H), 1.73-1.86 (m, 8H), 1.92-2.10 (m, 16H), 2.62-2.73 (m, 4H), 3.58 (s, 12H), 4.10 (s, 8H) ppm.

^{31}P{^{1}H} NMR (162 MHz, CD_2Cl_2) δ = 50.1 (d, J_{RhP} = 127.8 Hz) ppm.

^{13}C{^{1}H} NMR (101 MHz, $(CD_3)_2SO$) δ = 25.4, 25.9 (br), 26.3 (br), 29.2 (br), 30.0 (br), 34.6 (br), 38.6 (br), 52.5, 161.4, 184.0 (dt, J_{RhC} = 72.1 Hz, J_{PC} = 16.2 Hz) ppm.

HRMS *calcd.* for $[C_{35}H_{64}N_4OBClF_4P_2Rh]^+$: 843.331561; *found* 843.332700.

IR (solid) $\tilde{\nu}$ = 480, 519, 571, 640, 743, 848, 931, 1019, 1040, 1292, 1448, 1557, 1962, 1971, 2854, 2930 cm^{-1}.

Compound **2.19**

K_2PtCl_4 (122 mg, 0.30 mmol) was added to a solution of cationic phosphine **1.41** (150 mg, 0.30 mmol) in dry DMSO (4 mL) and the mixture was stirred at room temperature. After 1 day CH_2Cl_2 (9 mL) was added to the solution to precipitate the inorganic salts. Filtration and removal of the solvents from the filtrate yielded the desired product as a yellow solid (134 mg, 63 %).

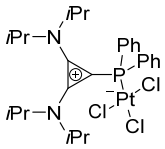

^{1}H NMR (400 MHz, CD_2Cl_2) δ = 0.88 (d, *J* = 6.8 Hz, 12H), 1.31 (d, *J* = 6.8 Hz, 12H), 3.49 (sept, *J* = 6.8 Hz, 2H), 4.04 (sept, *J* = 6.8 Hz, 2H), 7.51-7.60 (m, 6H), 8.27-8.34 (m, 4H) ppm.

^{31}P{^{1}H} NMR (162 MHz, CD_2Cl_2) δ = 3.3 (J_{PtP} = 4034.6 Hz) ppm.

^{13}C{^{1}H} NMR (101 MHz, CD_2Cl_2) δ = 20.5, 21.6, 41.4, 100.7 (d, J_{PC} = 43.4 Hz), 125.7 (d, J_{PC} = 66.9 Hz), 129.2 (d, J_{PC} = 11.9 Hz), 132.9 (d, J_{PC} = 2.2 Hz), 136.3 (d, J_{PC} = 12.0 Hz), 138.1 ppm.

HRMS *calcd*. for $[C_{29}H_{41}N_3Cl_2PPt]^+$: 727.205780; *found* 727.205790. $[M^+-Cl+CH_3CN]$

IR (solid) $\tilde{\nu}$ = 517, 575, 697, 893, 1029, 1096, 1146, 1183, 1534, 1375, 1435, 1549, 1866, 2933, 2977 cm^{-1}.

Compound **2.20**

K_2PtCl_4 (43 mg, 0.10 mmol) was added to a solution of cationic phosphine **1.44** (51 mg, 0.09 mmol) in dry CH_3CN (3 mL) and the mixture was stirred at room temperature. After 1 day the solvents were evaporated and the residue was extracted with CH_2Cl_2 (5 x 2 mL). Removal of the solvents and recrystallization from CH_3CN/Et_2O gave the desired product as an orange solid (62 mg, 88 %).

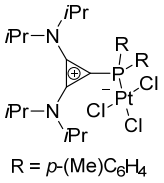

^{1}H NMR (400 MHz, CD_2Cl_2) δ = 0.90 (d, *J* = 6.7 Hz, 12H), 1.32 (d, *J* = 6.7 Hz, 12H), 2.41 (s, 6H), 3.53 (sept, *J* = 6.7 Hz, 2H), 4.04 (sept, *J* = 6.7 Hz, 2H), 7.35 (dd, *J* = 7.9 Hz, 2.3 Hz, 4H), 8.16 (dd, *J* = 12.4 Hz, 8.1 Hz, 4H) ppm.

^{31}P{^{1}H} NMR (162 MHz, CD_2Cl_2) δ = 3.0 (J_{PtP} = 4006.9 Hz) ppm.

^{13}C{^{1}H} NMR (101 MHz, CD_2Cl_2) δ = 20.6, 21.6 (d, J_{PC} = 1.4), 21.7, 52.2 (br), 54.9 (br), 101.9 (d, J_{PC} = 42.0 Hz), 122.7 (d, J_{PC} = 69.2 Hz), 129.9 (d, J_{PC} = 12.3 Hz), 136.3 (d, J_{PC} = 12.3 Hz), 138.2 (d, J_{PC} = 8.0 Hz), 143.8 (d, J_{PC} = 2.7 Hz).

HRMS *calcd*. for $[C_{29}H_{42}N_2Cl_2PPt]^+$: 714.210531; *found* 714.211157.

IR (solid) $\tilde{\nu}$ = 665, 678, 711, 814, 896, 1011, 1030, 1098, 1149, 1186, 1316, 1352, 1375, 1449, 1497, 1551, 1597, 1865, 2934, 2978 cm^{-1}.

Compound **2.21**

K_2PtCl_4 (128 mg, 0.31 mmol) was added to a solution of cationic phosphine **1.46** (150 mg, 0.28 mmol) in dry CH_3CN (4 mL) and the mixture was stirred at room temperature. After 1 day the solvents were evaporated and the residue was extracted with CH_2Cl_2 (5 x 4 mL). Removal of the solvents and recrystallization from CH_3CN/Et_2O gave the desired product as a yellow solid (158 mg, 68 %).

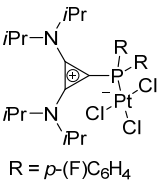

^{1}H NMR (400 MHz, CD_3CN) δ = 0.91 (d, *J* = 6.8 Hz, 12H), 1.30 (d, *J* = 6.8 Hz, 12H), 3.56 (sept, *J* = 6.8 Hz, 2H), 4.11 (sept, *J* = 6.8 Hz, 2H), 7.34 (dt, *J* = 8.9, 1.9 Hz, 4H), 8.31-8.40 (m, 4H) ppm.

^{31}P{^{1}H} NMR (162 MHz, CD_3CN) δ = -0.1 (J_{PtP} = 4031.2 Hz) ppm.

^{19}F{^{1}H} NMR (282 MHz, CD_3CN) δ = -107.8 ppm.

^{13}C{^{1}H} NMR (101 MHz, CD_2Cl_2) δ = 20.7, 21.7, 52.3 (br), 100.3 (d, J_{PC} = 43.7 Hz), 116.6 (dd, J_{PC} = 21.6, 13.3 Hz), 121.8 (dd, J_{PC} = 69.8, 3.4 Hz), 138.2 (d, J_{PC} = 8.6 Hz), 138.8 (dd, J_{PC} = 13.9, 8.9 Hz), 165.7 (dd, J_{PC} = 255.7, 2.8 Hz) ppm.

HRMS *calcd*. for $[C_{27}H_{36}Cl_4F_2N_2PPt]^-$: 792.097748; *found* 792.098455.

IR (solid) $\tilde{\nu}$ = 685, 714, 815, 894, 1011, 1031, 1095, 1160, 1229, 1260, 1354, 1375, 1452, 1495, 1550, 1588, 1866, 2977 cm^{-1}.

Compound **2.22**

K_2PtCl_4 (87 mg, 0.21 mmol) was added to a solution of cationic phosphine **2.12** (150 mg, 0.19 mmol) in dry CH_3CN (4 mL) and the mixture was stirred at room temperature. After 1 day the solvent was evaporated and the residue extracted with CH_2Cl_2 (3 x 3 mL). Removal of the solvent *in vacuo* afforded the desired product as a yellow solid (182 mg, 95 %).

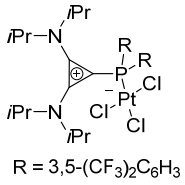

^{1}H NMR (400 MHz, CD_2Cl_2) δ = 0.98 (d, *J* = 6.8 Hz, 12H), 1.39 (d, *J* = 6.9 Hz, 12H), 3.61 (sept, *J* = 6.8 Hz, 2H), 4.16 (sept, *J* = 6.8 Hz, 2H), 8.16 (s, 2H), 8.70 (s, 2H), 8.73 (s, 2H) ppm.

^{31}P{^{1}H} NMR (121 MHz, CD_2Cl_2) δ = 3.1 (J_{PtP} = 4070.2 Hz) ppm.

^{19}F{^{1}H} NMR (282 MHz, CD_2Cl_2) δ = -63.2 ppm.

^{13}C{^{1}H} NMR (101 MHz, CD_2Cl_2) δ = 20.7, 21.7, 55.5 (br), 95.8 (d, J_{PC} = 47.5 Hz), 122.9 (q, J_{FC} = 273.3 Hz), 127.1-127.4 (m), 128.7 (d, J_{PC} = 65.1 Hz), 132.9 (dq, J_{FC} = 34.3 Hz, J_{PC} 11.8 Hz), 135.7-136.1 (m), 138.9 (d, J_{PC} = 7.8 Hz) ppm.

HRMS *calcd*. for $[C_{31}H_{34}Cl_4F_{12}N_2PPt]^-$: 1028.066206; *found* 1028.067766.

IR (solid) $\tilde{\nu}$ = 680, 698, 845, 894, 910, 1031, 1096, 1120, 1179, 1276, 1354, 1455, 1560, 1865, 2983 cm^{-1}.

Compound **2.23**

K_2PtCl_4 (112 mg, 0.27 mmol) was added to a solution of cationic phosphine **2.14** (100 mg, 0.27 mmol) in dry CH_3CN (3 mL) and the mixture was stirred at room temperature for 16 hours. The solvent was then evaporated and the residue recrystallized from DMSO/CH_2Cl_2 affording the desired product as a yellow solid (122 mg, 77 %).

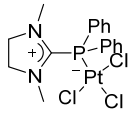

^{1}H NMR (300 MHz, $(CD_3)_2SO$) δ = 2.62 (s, 6H), 3.95 (s, 4H), 7.56-7.76 (m, 6H), 8.26-8.43 (m, 4H) ppm.

31.8 (2188.0 Hz) ppm.

^{31}P{^{1}H} NMR (121 MHz, $(CD_3)_2SO$) δ = 4.4 (J_{PtP} = 3939.9 Hz) ppm.

$^{13}C\{^1H\}$ NMR (101 MHz, $(CD_3)_2SO$) δ = 36.6 (d, J_{PC} = 2.4 Hz), 52.0 (d, J_{PC} = 2.5 Hz), 124.0 (d, J_{PC} = 62.7 Hz), 129.1 (d, J_{PC} = 12.0 Hz), 132.9 (d, J_{PC} = 2.8 Hz), 135.5 (d, J_{PC} = 12.2 Hz), 162.6 (d, J_{PC} = 42.5 Hz) ppm.

HRMS *calcd.* for $[C_{19}H_{26}Cl_2N_2OPPtS]^+$: 626.051010; *found* 626.052329. $[M^+$-Cl+$(CD_3)_2SO)]$

IR (solid) $\tilde{\nu}$ = 494, 516, 625, 694, 707, 748, 766, 847, 934, 996, 1089, 1121, 1191, 1285, 1414, 1433, 1522, 1578, 2944 cm^{-1}.

Compound **2.24**

$[AuCl(SMe_2)]$ (37 mg, 0.13 mmol) was added to a solution of cationic phosphine **2.12** (98 mg, 0.13 mmol) in dry CH_2Cl_2 (1 mL) and the resulting mixture was stirred at room temperature for 1 hour. The solvent was then evaporated affording the desired product as a white solid (121 mg, 95 %).

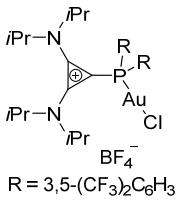

^1H NMR (400 MHz, CD_2Cl_2) δ = 1.09 (d, *J* = 6.9 Hz, 12H), 1.45 (d, *J* = 6.9 Hz, 12H), 3.48 (sept, *J* = 6.9 Hz, 2H), 4.22 (sept, *J* = 6.9 Hz, 2H), 8.23 (s, 2H), 8.63 (s, 2H), 8.66 (s, 2H) ppm.

$^{31}P\{^1H\}$ NMR (162 MHz, CD_2Cl_2) δ = 19.8 ppm.

$^{19}F\{^1H\}$ NMR (282 MHz, CD_2Cl_2) δ = -150.0, -149.9, -63.2 ppm.

$^{13}C\{^1H\}$ NMR (101 MHz, CD_2Cl_2) δ = 21.4, 21.6, 55.7 (br), 90.8 (d, J_{PC} = 54.2 Hz), 123.7 (q, J_{FC} = 272.9 Hz), 129.1-129.4 (m), 129.2 (d, J_{PC} = 66.4 Hz), 133.8 (dq, J_{FC} = 34.2 Hz, J_{PC} = 13.2 Hz), 135.8 (d, J_{PC} = 14.1 Hz), 140.2 (d, J_{PC} = 6.7 Hz) ppm.

HRMS *calcd.* for $[C_{31}H_{34}N_2AuClF_{12}P]^+$: 925.161662; *found* 925.160975.

IR (solid) $\tilde{\nu}$ = 681, 897, 1029, 1052, 1096, 1122, 1182, 1278, 1355, 1457, 1571, 1866, 2985 cm^{-1}.

Compound **2.25**

$[AuCl(SMe_2)]$ (81 mg, 0.27 mmol) was added to a solution of cationic phosphine **2.14** (100 mg, 0.27 mmol) in dry CH_2Cl_2 (1 mL) and the resulting mixture was stirred at room temperature for 1 hour. The solvent was then evaporated affording the desired product as a white solid (156 mg, 96 %).

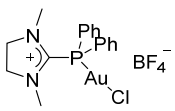

^1H NMR (400 MHz, CD_2Cl_2) δ = 2.78 (s, 6H), 4.11 (s, 4H), 7.64-7.77 (m, 6H), 8.04 (dd, *J* = 14.8, 7.5 Hz, 4H) ppm.

$^{31}P\{^1H\}$ NMR (162 MHz, CD_2Cl_2) δ = 23.3 ppm.

$^{13}C\{^{1}H\}$ NMR (101 MHz, CD_2Cl_2) δ = 37.2 (d, J_{PC} = 4.1 Hz), 53.4 (d, J_{PC} = 2.5 Hz), 122.5 (d, J_{PC} = 61.5 Hz), 131.2 (d, J_{PC} = 13.2 Hz), 135.0 (d, J_{PC} = 2.7 Hz), 135.8 (d, J_{PC} = 17.0 Hz), 161.0 (d, J_{PC} = 34.0 Hz) ppm.

HRMS *calcd.* for $[C_{17}H_{20}N_2AuClP]^+$: 515.071269; *found* 515.071361.

IR (solid) $\tilde{\nu}$ = 689, 750, 931, 996, 1034, 1047, 1095, 1296, 1410, 1438, 1482, 1524, 1585, 2941, 3060 cm^{-1}.

Compound **2.26**

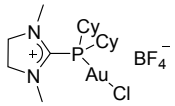

[AuCl(SMe$_2$)] (62 mg, 0.21 mmol) was added to a solution of cationic phosphine **2.15** (80 mg, 0.21 mmol) in dry CH_2Cl_2 (1 mL) and the resulting mixture was stirred at room temperature for 1 hour. The solvent was then evaporated affording the desired product as a white solid (121 mg, 94 %).

^{1}H NMR (400 MHz, CD_3CN) δ = 1.25-1.37 (m, 2H), 1.39-1.54 (m, 6H), 1.56-1.65 (m, 2H), 1.68-1.79 (m, 4H), 1.80-1.92 (m, 4H), 2.10-2.19 (m, 2H), 2.74-2.86 (m, 2H), 3.51 (s, 6H), 3.95 (s, 4H) ppm.

$^{31}P\{^{1}H\}$ NMR (162 MHz, CD_3CN) δ = 42.4 ppm.

$^{13}C\{^{1}H\}$ NMR (101 MHz, CD_3CN) δ = 25.7 (d, J_{PC} = 1.5 Hz), 26.3 (d, J_{PC} = 16.9 Hz), 26.6 (d, J_{PC} = 13.4 Hz), 30.8, 33.4 (d, J_{PC} = 6.5 Hz), 36.5 (d, J_{PC} = 27.4 Hz), 38.6 (d, J_{PC} = 3.3 Hz), 53.7, 160.5 (d, J_{PC} = 23.9 Hz) ppm.

HRMS *calcd.* for $[C_{17}H_{32}N_2AuClP]^+$: 527.165167; 527.165410.

IR (solid) $\tilde{\nu}$ = 506, 519, 711, 755, 801, 930, 958, 1036, 1051, 1092, 1263, 1304, 1448, 1577, 2854, 2931 cm^{-1}.

Compound **2.27**

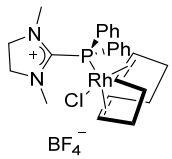

[RhCl(cod)]$_2$ (39 mg, 0.08 mmol) was added to a solution of cationic phosphine **2.14** (59 mg, 0.16 mmol) in CH_2Cl_2 (1 mL) and the resulting mixture was stirred at room temperature for 1 hour. The solvent was then evaporated affording the desired product as an orange solid (96 mg, 98 %).

^{1}H NMR (300 MHz, CD_2Cl_2) δ = 2.09-2.25 (m, 4H), 2.34-2.54 (m, 4H), 3.02 (s, 6H), 4.02 (br, 2H), 4.06 (br, 4H), 5.72 (br, 2H), 7.53-7.74 (m, 10H) ppm.

$^{31}P\{^{1}H\}$ NMR (121 MHz, CD_2Cl_2) δ = 29.9 (d, J_{RhP} = 150.1 Hz) ppm.

$^{13}C\{^1H\}$ NMR (101 MHz, CD_2Cl_2) δ = 29.1, 33.3 (d, J_{RhC} = 2.6 Hz), 37.5 (d, J_{RhC} = 4.3 Hz), 52.8, 73.2 (d, J_{RhC} = 13.0 Hz), 108.2 (dd, J_{RhC} = 12.1 Hz, J_{PC} = 7.1 Hz), 125.3 (d, J_{PC} = 41.4 Hz), 130.5 (d, J_{PC} = 10.5 Hz), 133.4 (d, J_{PC} = 2.0 Hz), 135.1 (d, J_{PC} = 13.1 Hz), 165.7 (d, J_{PC} = 18.4 Hz) ppm.

HRMS *calcd.* for $[C_{25}H_{32}ClN_2PRh]^+$: 529.104119; *found* 529.104598.

IR (solid) $\tilde{\nu}$ = 692, 730, 749, 816, 870, 932, 996, 1035, 1048, 1189, 1294, 1336, 1409, 1435, 1480, 1520, 1574, 2882 cm^{-1}.

Compound **2.28**

A mixture of compound **1.41** (77 mg, 0.15 mmol) and $Pd_2(dba)_3$ (70 mg, 0.08 mmol) was

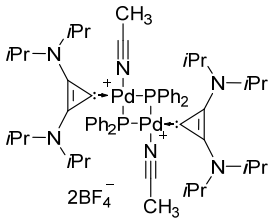

evacuated for 10 minutes, then dry CH_2Cl_2 (3 mL) was added and the suspension stirred at room temperature for 2 hours. After this time the solvent was removed *in vacuo* and the residue washed with Et_2O (4 x 2 mL). Recrystallization of the crude product from CH_3CN/Et_2O gave the title compound as a yellow solid (44 mg, 44 %).

^1H NMR (400 MHz, CD_2Cl_2) δ = 0.97 (br, 24H), 1.10 (br, 24H), 2.04 (s, 6H), 3.71 (sept, *J* = 6.7 Hz, 8H), 7.34-7.41 (m, 8H), 7.43-7.49 (m, 4H), 7.74-7.82 (m, 8H) ppm.

$^{31}P\{^1H\}$ NMR (162 MHz, CD_2Cl_2) δ = -130.6 ppm.

$^{13}C\{^1H\}$ NMR (101 MHz, CD_2Cl_2) δ = 2.8, 21.7 (br), 50.2 (br), 51.8 (br), 117.1, 129.1-129.4 (m), 130.7, 133.1-133.6 (m), 134.6-134.9 (m), 137.6, 148.2 ppm.

ESI-MS (neg.): 1075 m/z, $[C_{43}H_{54}B_2F_8N_4P_2Pd_2]^-$

IR (solid) $\tilde{\nu}$ = 695, 745, 941, 1030, 1049, 1134, 1154, 1185, 1200, 1327, 1350, 1372, 1389, 1403, 1434, 1452, 1487, 1850, 2876, 2936, 2979 cm^{-1}.

Compound **2.29**

A mixture of compounds **1.42** (79 mg, 0.15 mmol) and $Pd_2(dba)_3$ (69 mg, 0.08 mmol) was

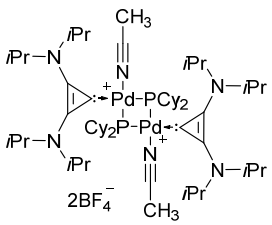

evacuated for 10 minutes. Dry CH_2Cl_2 (3 mL) was then added and the resulting suspension stirred at room temperature for 2 hours. After removal of the solvents *in vacuo*, the residue was washed with Et_2O (4 x 2 mL) and recrystallized from CH_3CN/Et_2O to give the desired compound as a yellow solid (33 mg, 38 %).

^1H NMR (400 MHz, CD_2Cl_2) δ = 1.14-1.65 (m, 70H), 1.71-2.10 (m, 20H), 2.25 (s, 6H), 2.28-2.38 (m, 2H), 4.14 (br, 8H) ppm.

$^{31}P\{^{1}H\}$ NMR (162 MHz, CD_2Cl_2) δ = -104.6 ppm.

$^{13}C\{^{1}H\}$ NMR (101 MHz, CD_2Cl_2) δ = 22.1 (br), 22.4-22.8 (m), 26.5, 27.4-27.9 (m), 31.5, 33.6, 36.5, 51.0, 151.1 ppm.

ESI-MS: 1099 m/z, $[C_{44}H_{82}B_2F_8N_5PPd_2]^+$

IR (solid) $\tilde{\nu}$ = 729, 849, 890, 1004, 1030, 1049, 1107, 1138, 1155, 1185, 1209, 1325, 1348, 1369, 1450, 1484, 1843, 2855, 2930, 2973 cm^{-1}.

Compound **2.30**

A mixture of compounds **1.41** (52 mg, 0.10 mmol) and $Pd(PPh_3)_4$ (116 mg, 0.10 mmol) was evacuated for 10 minutes. Dry toluene (4 mL) was then added and the suspension stirred at 100 °C overnight. After removal of the solvents the residue was washed with Et_2O (4 x 2 mL). Recrystallization of the crude product from CH_2Cl_2/Et_2O, gave the title compound as a yellow solid (128 mg, 73 %).

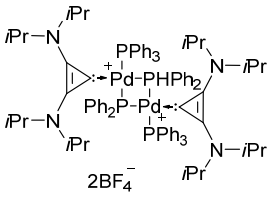

^{1}H NMR (400 MHz, CD_2Cl_2) δ = 0.38 (br, 12H), 0.67 (br, 12H), 1.04 (d, *J* = 6.4 Hz, 12H), 1.11 (d, *J* = 6.0 Hz, 12H), 3.20 (sept, *J* = 6.3 Hz, 4H), 3.69 (sept, *J* = 6.3 Hz, 4H), 6.55-6.73 (m, 12H), 7.02-7.60 (m, 38H) ppm.

$^{31}P\{^{1}H\}$ NMR (162 MHz, CD_2Cl_2) δ = -168.9 (dd, $J_{PP\ trans)}$ = 213.3, $J_{PP\ cis}$ = 108.8 Hz), 14.2 (dd, $J_{PP\ trans}$ = 213.3, $J_{PP\ cis}$ = 108.8 Hz) ppm.

$^{13}C\{^{1}H\}$ NMR (101 MHz, CD_2Cl_2) δ = 22.0, 22.4, 51.4 (br), 128.7-129.3 (m), 129.6 (br), 131.2, 131.5 (br), 133.4-133.9 (m), 134.3 (br), 147.8 ppm.

ESI-MS: 1665 m/z, $[C_{90}H_{106}BF_4N_4P_4Pd_2]^+$

IR (solid) $\tilde{\nu}$ = 693, 739, 895, 999, 1031, 1049, 1088, 1151, 1185, 1318, 1345, 1372, 1433, 1451, 1488, 1841, 2976, 3058 cm^{-1}.

Compound **2.33**

A hot solution (80 °C) of alkyne **2.37** (40 mg, 0.13 mmol) in 2.5 mL dry dichloroethane was transferred to a Schlenk containing precatalyst **2.22** (6.3 mg, 6 µmol, 5 mol%) and $AgSbF_6$ (2.2 mg, 6 µmol, 5 mol%). After stirring for 10 minutes at this temperature, the mixture was filtered through silica, the solvent evaporated and the residue purified by flash chromatography (hexane/ethyl acetate:

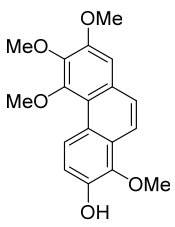

2/1). The sample thus obtained was 90 % pure by NMR. Analytical purity was obtained by preparative HPLC separation.

^{1}H NMR (400 MHz, $CDCl_3$) δ = 3.98 (s, 3H), 4.01 (s, 3H), 4.01 (s, 3H), 4.03 (s, 3H), 5.75 (s, 1H), 7.09 (s, 1H), 7.31 (d, *J* = 9.3 Hz, 1H), 7.64 (d, *J* = 9.3 Hz, 1H), 7.88 (d, *J* = 9.3 Hz, 1H), 9.24 (d, *J* = 9.3 Hz, 1H) ppm.

^{13}C{^{1}H} NMR (151 MHz, $CDCl_3$) δ = 56.0, 60.3, 61.3, 62.1, 105.5, 116.4, 119.5, 119.5, 124.3, 124.9, 126.5, 127.5, 128.9, 141.0, 143.2, 145.6, 152.0, 152.1 ppm.

HRMS *calcd.* for $[C_{18}H_{18}O_5Na]^+$: 337.104643; *found* 337.104323. $[M+Na^+]$

IR (solid) $\tilde{\nu}$ = 699, 716, 766, 780, 799,816, 837, 852, 899, 944, 978, 990, 1043, 1052, 1105, 1144, 1193, 1225, 1268, 1294, 1322, 1341, 1353, 1392, 1433, 1475, 1574, 1608, 2838, 2931, 2960, 3009, 3451 cm^{-1}.

Compound **2.36**

A suspension of compounds **2.34** (1.40 g, 6.10 mmol), **2.35** (1.55 g, 7.30 mmol), $Pd(OAc)_2$ (68 mg, 0.30 mmol) and PPh_3 (80 mg, 0.30 mmol) was stirred in DMF/H_2O (10/1, 66 mL) mixture at 60 °C overnight. After removal of the solvents *in vacuo*, the residue was suspended in H_2O (40 mL) and extracted with EtOAc (3 x 50 mL). After drying over Na_2SO_4, the organic phase was concentrated and purified by column chromatography (hexane/ethyl acetate: 10/1) to afford the title compound as a white solid (1.30 g, 68 %).

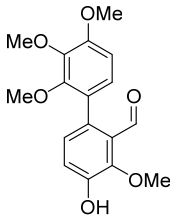

^{1}H NMR (400 MHz, $CDCl_3$) δ = 3.57 (s, 3H), 3.90 (s, 3H), 3.90 (s, 3H), 3.97 (s, 3H), 6.07 (s, 1H), 6.73 (d, *J* = 8.5 Hz, 1H), 6.93 (d, *J* = 8.5 Hz, 1H), 7.02 (d, *J* = 8.3 Hz, 1H), 7.21 (d, *J* = 8.3 Hz, 1H), 9.84 (s, 1H) ppm.

^{13}C{^{1}H} NMR (101 MHz, $CDCl_3$) δ = 56.2, 60.7, 61.2, 63.2, 107.5, 120.0, 125.2, 125.6, 127.2, 127.7, 134.5, 142.1, 146.6, 149.0, 151.3, 154.0, 191.4 ppm.

HRMS *calcd*. for $[C_{17}H_{18}O_6Na]^+$: 341.099561; *found* 341.099485. $[M+Na^+]$

IR (solid) $\tilde{\nu}$ = 705, 803, 827, 929, 986, 1002, 1032, 1088, 1127, 1163, 1176, 1213, 1275, 1403, 1426, 1442, 1474, 1591, 1698, 2843, 2953, 3398 cm^{-1}.

Compound **2.37**

Aldehyde **2.36** (1.00 g, 3.14 mmol), *Ohira-Bestmann* reagent (907 mg, 4.71 mmol) and K_2CO_3 (870 mg, 6.29 mmol) were stirred in MeOH (45 mL) at room temperature during 12 hours. After this time not consumed starting material could be observed by TLC, therefore more *Ohira-Bestmann* reagent (907 mg, 4.71 mmol) and K_2CO_3 (870 mg, 6.29 mmol) were added and the mixture was stirred for 12 extra hours. After removal of the solvents *in vacuo*, the residue was suspended in H_2O (30 mL) and extracted with EtOAc (3 x 40 mL). After drying over Na_2SO_4, the organic phase was concentrated and purified by column chromatography (hexane/ethyl acetate: 20/1) to afford a mixture of compounds **2.27** and **2.28** which was separated by HPLC (MeOH/H_2O: 60/40, flow rate 50 mL/min, τ_{16} = 1.43 min, τ_{17} = 1.76 min) (**2.27**: 510 mg, 52 %; **2.28**: 210 mg, 23 %).

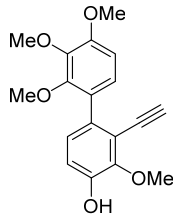

^{1}H NMR (400 MHz, $CDCl_3$) δ = 3.23 (s, 1H), 3.68 (s, 3H), 3.90 (s, 3H), 3.91 (s, 3H), 4.06 (s, 3H), 5.77 (s, 1H), 6.69 (d, *J* = 8.6, 1H), 6.95 (d, *J* = 8.4 Hz, 1H), 6.96 (d, *J* = 8.6 Hz, 1H), 6.99 (d, *J* = 8.3 Hz, 1H) ppm.

^{13}C{^{1}H} NMR (101 MHz, $CDCl_3$) δ = 56.1, 61.1, 61.2, 61.5, 78.9, 85.1, 106.7, 115.4, 115.8, 125.7, 126.6, 127.1, 135.0, 142.2, 147.8, 148.7, 151.9, 153.4 ppm.

HRMS *calcd*. for $[C_{18}H_{18}O_5Na]^+$: 337.104644; *found* 337.104888. $[M+Na^+]$

IR (solid) $\tilde{\nu}$ = 670, 691, 789, 812, 827, 901, 925, 975, 999, 1010, 1038, 1091, 1125, 1230, 1272, 1290, 1329, 1411, 1433, 1462, 1484, 1576, 1599, 2827, 2934, 3279, 3370 cm^{-1}.

Compound **2.38**

It was obtained as a side product during the synthesis of compound **2.37**.

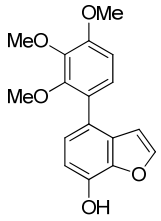

^{1}H NMR (400 MHz, $CDCl_3$) δ = 3.55 (s, 3H), 3.92 (s, 3H), 3.96 (s, 3H), 5.49 (s, 1H), 6.73 (d, *J* = 2.2 Hz, 1H), 6.76 (d, *J* = 8.6 Hz, 1H), 6.88 (d, *J* = 8.0 Hz, 1H), 7.05 (d, *J* = 8.6 Hz, 1H), 7.15 (d, *J* = 8.1 Hz, 1H), 7.60 (d, *J* = 2.1 Hz, 1H) ppm.

^{13}C{^{1}H} NMR (101 MHz, $CDCl_3$) δ = 56.2, 61.0, 61.3, 107.5, 108.0, 110.5, 124.2, 124.6, 125.6, 126.8, 128.6, 140.4, 142.6, 143.1, 144.7, 151.6, 153.1 ppm.

HRMS *calcd*. for $[C_{17}H_{16}O_5Na]^+$: 323.088998; *found* 323.088746. $[M+Na^+]$

IR (solid) $\tilde{\nu}$ = 681, 753, 780, 807, 826, 878, 911, 936,, 949, 1006, 1035, 1044, 1089, 1114, 1165, 1178, 1220, 1231, 1264, 1293, 1333, 1411,1436, 1460, 1481, 1593, 2839, 2941, 3266 cm^{-1}.

Compound **3.38**

Aniline (0.3 mL, 2.79 mmol) was added to a stirred suspension of chlorocyclopropenium salt

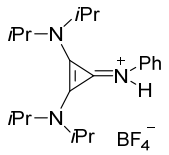

1.40 (500 mg, 1.39 mmol) in dry THF (11 mL) and the resulting mixture was stirred at 60 °C for 1 day. After cooling to room temperature, the solvent was evacuated and the residue suspended in CH_2Cl_2 (25 mL) and washed with a saturated aq. $NaBF_4$ solution (2 x 20 mL). Once dried over Na_2SO_4, the organic phase was concentrated and washed with Et_2O (2 x 4 mL) affording **3.38** as a pale brown solid (395 mg, 95 %).

^{1}H NMR (400 MHz, CD_2Cl_2) δ = 1.27 (d, *J* = 6.8 Hz, 24H), 3.76 (sept, *J* = 6.8 Hz, 4H), 7.22-7.27 (m, 3H), 7.38-7.44 (m, 2H), 7.90 (br, 1H) ppm.

^{13}C{^{1}H} NMR (101 MHz, CD_2Cl_2) δ = 22.2, 51.5, 112.9, 117.2, 123.2, 126.5, 129.9, 139.4 ppm.

HRMS *calcd.* for $[C_{21}H_{34}N_3]^+$: 328.274720; *found* 328.274461.

IR (solid) $\tilde{\nu}$ = 703, 767, 801, 895, 949, 991, 1032, 1045, 1062, 1080, 1109, 1146, 1193, 1205, 1234, 1354, 1377, 1450, 1468, 1504, 1527, 1595, 2937, 2977, 3300 cm^{-1}.

Compound **3.39**

4-Methoxyaniline (246 mg, 2.00 mmol) was added to a stirred suspension of

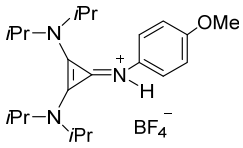

chlorocyclopropenium salt **1.40** (359 mg, 1.00 mmol) in dry THF (8 mL) and the resulting mixture stirred at 60 °C for 1 day. After cooling to room temperature, the precipitate was filtered off and the filtrate concentrated. The residue was suspended in CH_2Cl_2 (20 mL) and washed with a saturated aq. $NaBF_4$ solution (2 x 20 mL). After drying over Na_2SO_4, the organic phase was concentrated and washed with Et_2O (2 x 4 mL) affording **3.39** as a pale violet solid (375 mg, 84 %).

^{1}H NMR (400 MHz, CD_2Cl_2) δ = 1.25 (d, *J* = 6.8 Hz, 24H), 3.70 (sept, *J* = 6.8 Hz, 4H), 3.81 (s, 3H), 6.93 (d, *J* = 8.8 Hz, 2H), 7.22 (d, *J* = 8.8 Hz, 2H), 7.61 (br, 1H) ppm.

^{13}C{^{1}H} NMR (101 MHz, CD_2Cl_2) δ = 22.1, 51.3, 56.0, 114.1, 115.0, 115.9, 126.6, 131.7, 159.1 ppm.

HRMS *calcd.* for $[C_{22}H_{36}N_3O]^+$: 358.285286; *found* 358.285019.

IR (solid) $\tilde{\nu}$ = 670, 718, 782, 804, 829, 848, 948, 1038, 1141, 1192, 1212, 1236, 1296, 1353, 1372, 1450, 1505, 2972, 3294 cm^{-1}.

Compound **3.40**

4-Fluoroaniline (0.1 mL, 1.11 mmol) was added to a stirred suspension of chlorocyclopropenium salt **1.40** (200 mg, 0.56 mmol) in dry THF (4 mL) and the resulting mixture stirred at 60 °C for 1 day. After cooling to room temperature, the precipitate was filtered off, suspended in CH_2Cl_2 (10 mL) and extracted with saturated aq. $NaBF_4$ solution (3 x 15 mL). After drying over Na_2SO_4, the organic phase was concentrated and washed with Et_2O (2 x 4 mL) affording **3.40** as a white solid (199 mg, 82 %).

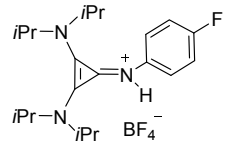

^{1}H NMR (300 MHz, CD_2Cl_2) δ = 1.27 (d, *J* = 6.8 Hz, 24H), 3.73 (sept, *J* = 6.8 Hz, 4H), 7.06-7.15 (m, 2H), 7.23-7.31 (m, 2H), 7.90 (br, 1H) ppm.

^{13}C{^{1}H} NMR (101 MHz, CD_2Cl_2) δ = 22.1, 51.5, 113.1, 116.6 (d, J_{FC} = 23.1 Hz), 116.7, 125.9 (d, J_{FC} = 8.5 Hz), 135.5 (d, J_{FC} = 2.9 Hz), 161.4 (d, J_{FC} = 245.4 Hz) ppm.

^{19}F{^{1}H} NMR (282 MHz, CD_2Cl_2) δ = -151.1, -151.0, -116.2 ppm.

HRMS *calcd.* for $[C_{21}H_{33}FN_3]^+$: 346.265297; *found* 346.265205.

IR (solid) $\tilde{\nu}$ = 670, 717, 794, 832, 1010, 1040, 1059, 1142, 1156, 1191, 1214, 1351, 1365, 1390, 1449, 1470, 1505, 1525, 2942, 2974, 3294 cm^{-1}.

Compound **3.42**

3.42 was obtained by deprotonation of **3.38**: Salt **3.38** (374 mg, 0.90 mmol) was added to a suspension of KH (72 mg, 1.80 mmol) in dry THF (7 mL) and the mixture was then stirred at 60 °C overnight. After cooling to room temperature, the organic solvent was evaporated *in vacuo* and the remaining solid extracted with Et_2O (2 x 15 mL). Concentration of the combined ethereal extracts afforded **3.42** as a white solid (283 mg, 96 %).

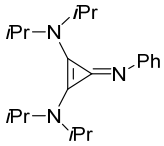

^{1}H NMR (400 MHz, CD_2Cl_2) δ = 1.23 (d, *J* = 6.8 Hz 24H), 3.68 (sept, *J* = 6.8 Hz, 4H), 6.68-6.74 (m, 1H), 6.80-6.85 (m, 2H), 7.10-7.15 (m, 2H) ppm.

^{13}C{^{1}H} NMR (101 MHz, CD_2Cl_2) δ = 22.5, 49.9, 114.9, 118.8, 122.8, 125.3, 128.6, 156.4 ppm.

^{15}N{^{1}H} NMR (61 MHz, CD_3CN) δ = -289.4 (-*N*(*i*Pr)$_2$), -231.5 (=*N*Ph) ppm.

HRMS *calcd.* for $[C_{21}H_{34}N_3]^+$: 328.274718; *found* 328.274436. [M+H$^+$]

IR (solid) $\tilde{\nu}$ = 698, 752, 819, 888, 951, 994, 1039, 1049, 1129, 1165, 1202, 1218, 1270, 1323, 1365, 1438, 1471, 1482, 1511, 2871, 2933, 2968 cm^{-1}.

Melting point: 122-123 °C.

Compound **3.43**

3.43 was obtained by deprotonation of **3.39**: Salt **3.39** (379 mg, 0.85 mmol) was added to a suspension of KH (68 mg, 1.70 mmol) in dry THF (7 mL) and the mixture was then stirred at 60 °C overnight. After cooling to room temperature, the organic solvent was evaporated *in vacuo* and the remaining solid extracted with Et_2O (2 x 15 mL). Concentration of the combined ethereal extracts afforded the title compound as a light brown solid (298 mg, 98 %).

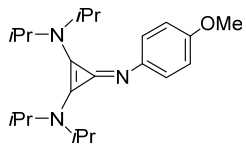

^{1}H NMR (400 MHz, CD_2Cl_2) δ = 1.21 (d, *J* = 6.8 Hz, 24H), 3.65 (sept, *J* = 6.8 Hz, 4H), 3.72 (s, 3H), 6.71 (d, *J* = 9.0 Hz, 2H), 6.76 (d, *J* = 9.0 Hz, 2H) ppm.

^{13}C{^{1}H} NMR (101 MHz, CD_2Cl_2) δ = 22.5, 49.8, 55.9, 114.1, 114.4, 123.5, 125.7, 149.9, 153.6 ppm.

HRMS *calcd.* for $[C_{22}H_{36}N_3O]^+$: 358.285285; *found* 358.285110. $[M+H^+]$

IR (solid) $\tilde{\nu}$ = 674, 709, 726, 776, 809, 837, 876, 958, 1027, 1041, 1098, 1119, 1133, 1158, 1223, 1258, 1313, 1364, 1433, 1463, 1495, 1522, 1881, 2936, 2971 cm^{-1}.

Melting point: 123-124 °C.

Compound **3.44**

3.44 was obtained by deprotonation of **3.40**: Salt **3.40** (347 mg, 0.80 mmol) was added to a suspension of KH (64 mg, 1.60 mmol) in THF (7 mL) and the mixture was then stirred at 60 °C overnight. After cooling to room temperature, the organic solvent was evaporated *in vacuo* and the remaining solid extracted with Et_2O (2 x 15 mL). Concentration of the combined ethereal extracts afforded the title compound as a white solid (265 mg, 96 %).

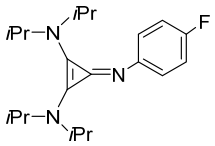

^{1}H NMR (400 MHz, CD_2Cl_2) δ = 1.22 (d, *J* = 6.8 Hz, 24H), 3.65 (sept, *J* = 6.8 Hz, 4H), 6.72-6.89 (m, 4H) ppm.

^{13}C{^{1}H} NMR (101 MHz, CD_2Cl_2) δ = 22.4, 49.9, 114.5, 114.8 (d, J_{FC} = 21.8 Hz), 123.4 (d, J_{FC} = 7.6 Hz), 125.5 (br), 152.7, 157.3 (d, J_{FC} = 234.4 Hz) ppm.

^{19}F{^{1}H} NMR (282 MHz, CD_2Cl_2) δ = -127.9 ppm.

HRMS *calcd.* for $[C_{21}H_{33}N_3F]^+$: 346.265296; *found* 346.265212. $[M+H^+]$

IR (solid) $\tilde{\nu}$ = 676, 719, 786, 819, 841, 950, 1040, 1049, 1085, 1130, 1166, 1202, 1217, 1274, 1320, 1363, 1436, 1485, 1515, 1893, 2874, 2934, 2975 cm^{-1}.

Melting point: 132-133 °C.

Compound **3.45**

Compound **3.41** (93 mg, 0.35 mmol) was added to a stirred suspension of

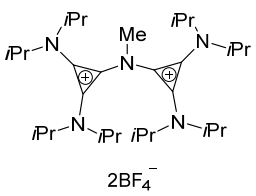

chlorocyclopropenium salt **1.40** (126 mg, 0.35 mmol) in dry THF (4 mL) and the resulting mixture was stirred at 60 °C for 3 days. After cooling to room temperature, the solvent was evacuated and the residue suspended in CH_2Cl_2 (9 mL) and filtered. After concentration of the filtrate, the residue was washed with Et_2O (3 x 3 mL) and recrystallized from CH_2Cl_2/Et_2O to afford the desired compound as a white solid (106 mg, 49 %).

^{1}H NMR (400 MHz, CD_2Cl_2) δ = 1.37 (d, *J* = 6.8 Hz, 48H), 3.65 (s, 3H), 3.94 (sept, *J* = 6.8 Hz, 8H) ppm.

^{13}C{^{1}H} NMR (101 MHz, CD_2Cl_2) δ = 21.9, 41.7, 53.1, 108.8, 126.9 ppm.

^{15}N{^{1}H} NMR (61 MHz, CD_3CN) δ = -276.3 (-*N*Me), -263.2 (-*N*(*i*Pr)$_2$) ppm.

HRMS *calcd.* for **[**$C_{31}H_{59}B_1F_4N_5]^+$: 588.479409; *found* 588.479646.

IR (solid) $\tilde{\nu}$ = 708, 739, 875, 892, 1033, 1045, 1093, 1142, 1181, 1206, 1351, 1396, 1455, 1548, 1916, 2940, 2978 cm^{-1}.

Elemental analysis (%) *calcd.* for $C_{31}H_{59}B_2F_8N_5$: C: 55.12, H: 8.80, N: 10.37; *found*: C: 54.78, H: 8.84, N: 10.25.

Melting point: 259 °C (decomposition).

Compound **3.46**

Compound **3.42** (132 mg, 0.40 mmol) was added to a stirred suspension of

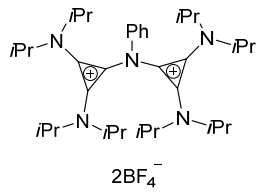

chlorocyclopropenium salt **1.40** (144 mg, 0.40 mmol) in dry THF (4 mL) and the resulting mixture was stirred at 60 °C for 3 days. After cooling to room temperature, the solvent was evacuated and the residue suspended in CH_2Cl_2 (9 mL) and washed with a saturated aq. $NaBF_4$ solution (3 x 8 mL). After drying over Na_2SO_4, the organic phase was concentrated. Recrystallization of the residue from CH_2Cl_2/Et_2O afforded the desired compound as a white solid (281 mg, 81 %).

^{1}H NMR (400 MHz, CD_2Cl_2) δ = 1.10 (br, 24H), 1.40 (br, 24H), 3.69 (br, 4H), 4.08 (br, 4H), 7.37-7.44 (m, 1H), 7.55-7.62 (m, 2H), 7.64-7.69 (m, 2H) ppm.

^{13}C{^{1}H} NMR (101 MHz, CD_2Cl_2) δ = 21.2, 22.7, 50.2, 56.6, 105.2, 125.6, 127.9, 129.7, 131.7, 139.1 ppm.

$^{15}N\{^1H\}$ NMR (61 MHz, CD_3CN) δ = -310.2 (-*N*Ph), -260.3 (-*N*(*i*Pr)2) ppm.

HRMS *calcd.* for $[C_{36}H_{61}BF_4N_5]^+$: 650.496812; *found* 650.497078.

IR (solid) $\tilde{\nu}$ = 697, 731, 766, 886, 1033, 1046, 1140, 1191, 1205, 1240, 1350, 1376, 1448, 1464, 1558, 1914, 2940, 2982 cm^{-1}.

Elemental analysis (%) *calcd.* for $C_{36}H_{61}B_2F_8N_5$: C: 58.63, H: 8.34, N: 9.50; *found*: C: 58.39, H: 8.39, N: 9.45.

Melting point: 219 °C (decomposition).

Compound **3.47**

Compound **3.43** (125 mg, 0.35 mmol) was added to a stirred suspension of

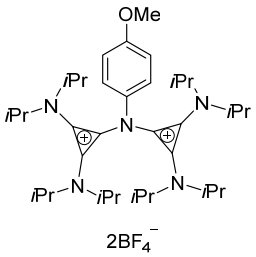

chlorocyclopropenium salt **1.40** (126 mg, 0.35 mmol) in dry THF (4 mL) and the resulting mixture was stirred at 60 °C for 3 days. After cooling to room temperature, the solvent was evacuated and the residue suspended in CH_2Cl_2 (9 mL) and washed with a saturated aq. $NaBF_4$ solution (3 x 8 mL). After drying over Na_2SO_4, the organic phase was concentrated and washed with Et_2O (3 x 3 mL). Recrystallization of the residue from CH_2Cl_2/Et_2O afforded the desired compound as a pale violet solid (214 mg, 80 %).

^1H NMR (400 MHz, CD_2Cl_2) δ = 1.11 (br, 24 H), 1.39 (br, 24 H), 3.70 (br, 4H), 3.82 (s, 3H), 4.05 (br, 4H), 7.07 (d, *J* = 9.0 Hz, 2H), 7.52 (d, *J* = 9.0 Hz, 2H) ppm.

$^{13}C\{^1H\}$ NMR (101 MHz, CD_2Cl_2) δ = 21.1, 22.6, 50.1, 56.2, 56.6, 105.7, 116.6, 127.4, 127.4, 131.6, 160.7 ppm.

HRMS *calcd.* for $[C_{37}H_{63}BF_4N_5O]^+$: 680.507393; *found* 680.507756.

IR (solid) $\tilde{\nu}$ = 665, 729, 835, 886, 1047, 1141, 1159, 1207, 1261, 1305, 1350, 1376, 1452, 1508, 1561, 1915, 2940, 2983 cm^{-1}.

Melting point: 249 °C (decomposition).

Compound **3.48**

Compound **3.44** (100 mg, 0.35 mmol) was added to a stirred suspension of

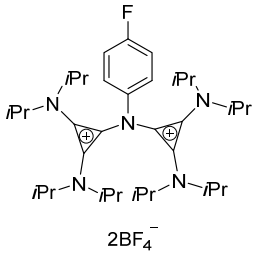

chlorocyclopropenium salt **1.40** (126 mg, 0.35 mmol) in dry THF (4 mL) and the resulting mixture stirred at 60 °C for 3 days. After cooling to room temperature, the solvent was evacuated and the residue suspended in CH_2Cl_2 (9 mL) and extracted with a saturated aq. $NaBF_4$

solution (3 x 8 mL). After drying over Na_2SO_4, the organic phase was concentrated, washed with Et_2O (3 x 3 mL) and crystallization of the residue from CH_2Cl_2/Et_2O afforded the desired compound as a white solid (186 mg, 70 %).

^{1}H NMR (400 MHz, CD_2Cl_2) δ = 1.12 (br, 24H), 1.39 (br, 24H), 3.70 (br, 4H), 4.06 (br, 4H), 7.25-7.32 (m, 2H), 7.66-7.73 (m, 2H) ppm.

^{13}C{^{1}H} NMR (101 MHz, CD_2Cl_2) δ = 21.1, 22.6, 50.2, 56.6, 105.0, 118.5 (d, J_{FC} = 23.4 Hz), 127.8, 128.0 (d, J_{FC} = 9.0 Hz), 135.1 (d, J_{FC} = 2.2 Hz), 162.8 (d, J_{FC} = 250.4 Hz) ppm.

^{19}F{^{1}H} NMR (282 MHz, CD_2Cl_2) δ = -151.8, -151.7, -111.4 ppm.

HRMS *calcd.* for $[C_{36}H_{60}BF_5N_5]^+$: 668.485637; *found* 668.486347.

IR (solid) $\tilde{\nu}$ = 664, 816, 844, 884, 1032, 1046, 1157, 1191, 1206, 1220, 1351, 1376, 1453, 1505, 1563, 1912, 2983 cm^{-1}.

Compound **3.51**

N,N-bis(trimethylsilyl)aniline (95 mg, 0.40 mmol) was added to a stirred suspension of

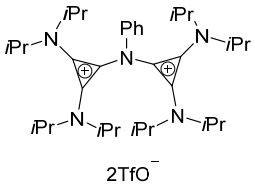

chlorocyclopropenium salt **3.50** (340 mg, 0.80 mmol) in dry THF (4 mL) and the resulting mixture was stirred at 60 °C for 3 days. After cooling to room temperature, the solvent was evacuated and the residue washed with THF (3 x 4 mL). Compound **3.51** was obtained as a white solid (233 mg, 79 %).

^{1}H NMR (400 MHz, CD_2Cl_2) δ = 1.10 (d, *J* = 4.6 Hz, 24H), 1.40 (d, *J* = 4.4 Hz, 24H), 3.70 (brs, 4H), 4.08 (brs, 4H), 7.38-7.44 (m, 1H), 7.55-7.61 (m, 2H) 7.65-7.69 (m, 2H) ppm.

^{13}C NMR (101 MHz, CD_2Cl_2) δ = 21.0, 21.3, 22.6, 22.8, 50.0, 50.1, 56.5, 56.6, 105.1, 121.5 (q, *J* = 321.9 Hz), 125.6, 127.9, 129.7, 131.6, 139.1 ppm.

HRMS *calcd.* for $[C_{37}H_{61}N_5O_3F_3S]^+$: 712.444170; *found* 712.444513.

IR (solid) $\tilde{\nu}$ = 697, 753, 762, 885, 1020, 1031, 1140, 1207, 1222, 1264, 1344, 1375, 1446, 1461, 1563, 1592, 1911, 2941, 2990 cm^{-1}.

Compound **3.52**

Chlorocyclopropenium salt **1.40** (500 mg, 1.39 mmol) was added to a suspension of KHMDS (139 mg, 0.70 mmol) in dry THF (17 mL) and the mixture was stirred for a day at 60 °C. Additional amounts of KHMDS (80 mg, 0.40 mmol) were added after 24 and 48 hours maintaining the temperature at 60 °C. Finally, the organic solvents were evaporated in vacuum and the residue purified by column chromatography (CH_2Cl_2/MeOH: 97/3), affording the title compound as a pale yellow solid (207 mg, 52 %).

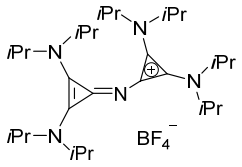

^{1}H NMR (400 MHz, CD_2Cl_2) δ = 1.27 (d, *J* = 6.8 Hz, 48H), 3.71 (sept, *J* = 6.8 Hz, 8H) ppm.

^{13}C{^{1}H} NMR (101 MHz, CD_2Cl_2) δ = 22.3, 51.0, 121.5, 123.4 ppm.

^{15}N{^{1}H} NMR (61 MHz, CD_2Cl_2) δ = -291.6 (-*N*central), -279.6 (-*N*(*i*Pr)$_2$) ppm.

HRMS *calcd.* for $[C_{30}H_{56}N_5BF_4]$: 573.456491; *found* 573.456110.

IR (solid) $\tilde{\nu}$ = 752, 800, 879, 1022, 1045, 1089, 1129, 1161, 1194, 1217, 1260, 1335, 1361, 1387, 1455, 1478, 2876, 2936, 2978 cm^{-1}.

Melting point: 175-176 °C.

Compound **3.53**

Tetrafluoroboric acid diethyl ether complex (24 µL, 0.18 mmol) was added to a stirred suspension of monocation **3.52** (103 mg, 0.18 mmol) in dry DCM (4 mL) and the resulting solution was stirred at room temperature. After 2 hours the solvent was evacuated and the residue dried, affording the title compound as a pale yellow solid (114 mg, 96 %).

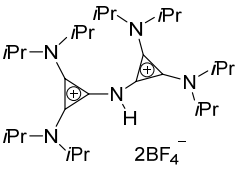

^{1}H NMR (400 MHz, $CDCl_3$) δ = 1.35 (d, *J* = 6.7 Hz, 48H), 3.95 (br, 8H), 8.28 (br, 1H) ppm.

^{13}C{^{1}H} NMR (101 MHz, $CDCl_3$) δ = 21.8, 52.5 (br), 104.7, 125.6 ppm.

HRMS *calcd.* for $[C_{30}H_{57}B_3F_{12}N_5]^-$: 748.473724; *found* 748.473016.

IR (solid) $\tilde{\nu}$ = 762, 892, 1048, 1138, 1190, 1207, 1263, 1349, 1377, 1395, 1456, 1503, 1551, 1917, 2940, 2980, 3313 cm^{-1}.

Melting point: 223-224 °C.

Compound **3.54**

Monocation **3.52** (57 mg, 0.10 mmol) was added to a stirred suspension of $GaCl_3$ (35 mg, 0.20 mmol) in dry toluene (3 mL) and the resulting solution stirred at room temperature for 14 hours. The solvent was then evacuated and the residue extracted with CH_3CN (5 mL). Removal of the solvents under vacuum afforded the title compound as a pale yellow solid (56 mg, 71 %).

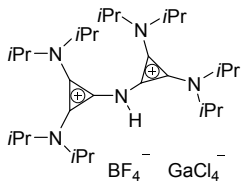

^{1}H NMR (400 MHz, CD_2Cl_2) δ = 1.37 (d, *J* = 6.7 Hz, 48H), 3.90 (br, 8H), 8.32 (br, 1H) ppm.

^{13}C{^{1}H} NMR (101 MHz, CD_2Cl_2) δ = 21.9, 105.4, 126.0 ppm.

HRMS *calcd.* for: $[C_{30}H_{57}N_5GaCl_4]^+$ 696.262383; *found* 696.262350.

IR (solid) $\tilde{\nu}$ = 764, 894, 987, 1066, 1143, 1194, 1208, 1262, 1346, 1375, 1391, 1454, 1471, 1516, 1539, 1588, 1919, 2938, 2987, 3234 cm^{-1}.

Melting point: 222-223 °C.

Compound **3.55**

This compound was prepared similarly to the already known perchlorate analogue.[101] Oxalyl chloride (2.32 g, 18.28 mmol) was slowly added directly to a flask containing neat 2,3-bis(dimethylamino)-2-cyclopropen-1-one (800 mg, 5.71 mmol) at 0 °C and the mixture was stirred at room temperature for 15 minutes. After removing the excess of oxalyl chloride in vacuum, a pale brown solid was obtained. A dry CH_3CN (5 mL) solution of this solid (879 mg, 4.50 mmol) was added to a suspension of $NaBF_4$ (494 mg, 4.50 mmol) in dry CH_3CN (5 mL). The mixture was stirred for 2 hours at room temperature and then placed into the fridge for 30 minutes. The precipitate formed was filtered off and evaporation of the solvent from the filtrate gave the desired product as a pale brown solid (842 mg, 76 %).

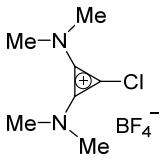

^{1}H NMR (400 MHz, CD_3CN) δ = 3.17 (s, 6H), 3.19 (s, 6H) ppm.

^{13}C{^{1}H} NMR (101 MHz, CD_3CN) δ = 41.9, 42.5, 92.0, 135.4 ppm.

HRMS *calcd.* for $[C_{14}H_{24}N_4BCl_2F_4]^+$: 405.141129; *found* 405.141423. [2M-BF_4^-]

IR (solid) $\tilde{\nu}$ = 727, 797, 1030, 1096, 1213, 1238, 1278, 1391, 1418, 1409, 1451, 1635, 1729, 1954, 2950 cm^{-1}.

Melting point: 108-109 °C.

Compound **3.56**

Tris(trimethylsilyl)amine (150 mg, 0.60 mmol) was added to a stirred suspension of

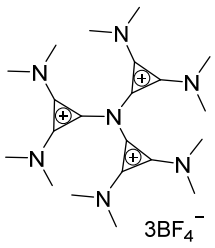

chlorocyclopropenium salt **3.55** (47 mg, 0.20 mmol) in dry THF (3 mL) and the resulting mixture was stirred at 120 °C for 13 hours in a microwave oven. After cooling to room temperature, the solvents were removed by filtration and the precipitate thus obtained was washed with THF (4 x 4 mL). Recrystallization of the residue from CH_3CN/Et_2O afforded the desired compound as a pale brown solid (53 mg, 41 %).

^{1}H NMR (400 MHz, CD_3CN) δ = 3.13 (s, 18H), 3.23 (s, 18H) ppm.

^{13}C{^{1}H} NMR (101 MHz, CD_3CN) δ = 42.8, 43.5, 99.6, 128.1 ppm.

^{15}N{^{1}H} NMR (61 MHz, CD_3CN) δ = -309.8 ppm (-*N*central).

HRMS *calcd.* for $[C_{21}H_{36}B_2F_8N_7]^+$: 560.310541; *found* 560.310449.

IR (solid) $\tilde{\nu}$ = 790, 1027, 1230, 1406, 1501, 1627, 1980, 2952 cm^{-1}.

Elemental analysis (%) *calcd.* for $C_{21}H_{36}B_3F_{12}N_7$: C: 38.99, H: 5.61, N: 15.15; *found*: C: 38.16, H: 5.73, N: 14.57.

Melting point: 235 °C (decomposition).

Compound **4.27**

Triethylamine (0.9 mL, 11.13 mmol) and chlorocyclopropenium salt **1.40** (4 g, 11.13 mmol)

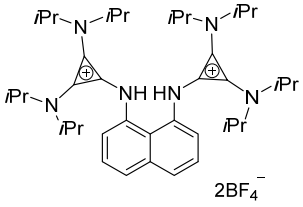

were added to a stirred solution of 1,8-diaminonaphtalene (0.80 g, 5.06 mmol) in dry THF (18 mL) and the resulting mixture was heated at 60 °C for 1 day. After cooling to room temperature, the solvent was removed under vacuum, the residue suspended in CH_2Cl_2 (40 mL) and washed with a saturated aq. $NaBF_4$ solution (3 x 50 mL). The organic phase was dried over Na_2SO_4 and concentrated. Finally, the desired compound was obtained by recrystallizing from CH_2Cl_2/Et_2O as a light brown solid (2.34 g, 57 %).

^{1}H NMR (400 MHz, CD_2Cl_2) δ = 1.21 (d, *J* = 6.8 Hz, 48H), 3.69 (sept, *J* = 6.8 Hz, 8H), 7.24 (d, *J* = 7.9 Hz, 2H), 7.54 (t, *J* = 7.9 Hz, 2H), 7.84 (d, *J* = 7.9 Hz, 2H), 8.44 (s, 2H) ppm.

^{13}C{^{1}H} NMR (101 MHz, CD_2Cl_2) δ = 22.0, 51.7, 112.7, 119.0, 123.4, 124.6, 126.7, 128.6, 135.8, 136.9 ppm.

HRMS *calcd.* for $[C_{40}H_{64}N_6BF_4]^+$: 715.521500; *found* 715.521611.

IR (solid) $\tilde{\nu}$ = 518, 729, 763, 830, 1031, 1049, 1078, 1136, 1192, 1212, 1280, 1344, 1452, 1497, 1536, 2937, 2981, 3310, 3360 cm^{-1}.

Compound **4.28**

Triethylamine (0.6 mL, 4.07 mmol) and chlorocyclopropenium salt **1.40** (1.46 g, 4.07 mmol) were added to a stirred solution of *o*-phenylenediamine (200 mg, 1.85 mmol) in dry CH_2Cl_2 (8 mL) and the resulting mixture was stirred at room temperature for 3 days. The mixture was then diluted with CH_2Cl_2 (10 mL), and washed with a saturated aq. $NaBF_4$ solution (3 x 20 mL). The organic phase was dried over Na_2SO_4 and concentrated. Finally, the desired compound was obtained by recrystallizing from CH_2Cl_2/Et_2O as a white solid (953 mg, 68 %).

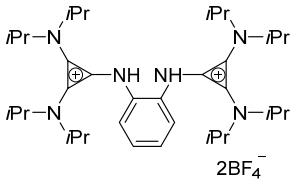

^{1}H NMR (400 MHz, $CDCl_3$) δ = 1.29 (d, *J* = 6.8 Hz, 48H), 3.71 (sept, *J* = 6.8 Hz, 8H), 7.21 (br, 4H), 8.05 (s, 2H) ppm.

^{13}C{^{1}H} NMR (101 MHz, $CDCl_3$) δ = 22.1, 50.9, 112.6, 115.6, 125.8, 126.3, 134.5 ppm.

HRMS *calcd.* for $[C_{36}H_{62}N_6BF_4]^+$: 665.505961; *found* 665.505720.

IR (solid) $\tilde{\nu}$ = 521, 780, 1014, 1047, 1066, 1141, 1218, 1288, 1350, 1367, 1452, 1500, 1520, 2934, 2960, 2983, 3321 cm^{-1}.

Compound **4.29**

Dicationic salt **4.27** (2.00 g, 2.49 mmol) was added to a stirred suspension of KH (800 mg, 19.94 mmol) in dry THF (20 mL) and the resulting suspension was heated at 60 °C for 2 days. After cooling to room temperature, the solvent was removed under vacuum and the residue extracted with Et_2O. Concentration of the combined ethereal extracts afforded the title compound as a light brown solid (1.37 g, 88 %).

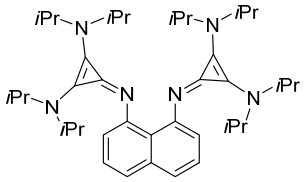

^{1}H NMR (400 MHz, $CDCl_3$) δ = 1.29 (d, *J* = 6.8 Hz, 48H), 3.83 (sept, *J* = 6.8 Hz, 8H), 6.48 (dd, *J* = 6.1, 2.4 Hz, 2H), 7.21 – 7.25 (m, 4H) ppm.

^{13}C{^{1}H} NMR (101 MHz, $CDCl_3$) δ = 22.4, 51.1, 113.0, 117.6, 118.5, 120.4, 120.7, 126.0, 136.9, 146.1 ppm.

HRMS *calcd.* for $[C_{40}H_{63}N_6]^+$: 627.510550; *found* 627.510867. $[M+H^+]$

IR (solid) $\tilde{\nu}$ = 505, 559, 758, 826, 914, 1024, 1120, 1133, 1161, 1218, 1308, 1363, 1432, 1483, 1529, 1888, 2870, 2930, 2963, 3042 cm^{-1}.

Compound **4.30**

Dicationic salt **4.28** (1.00 g, 1.33 mmol) was added to a stirred suspension of KH (426 mg, 10.63 mmol) in dry THF (10 mL) and the resulting mixture was heated at 60 °C for 2 days. After cooling to room temperature, the solvent was evaporated and the residue extracted with Et_2O. Concentration of the combined ethereal extracts afforded the title compound as a light red solid (696 mg, 91 %).

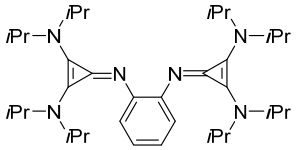

^{1}H NMR (400 MHz, CD_2Cl_2) δ = 1.18 (d, *J* = 6.8 Hz, 48H), 3.60 (sept, *J* = 6.8 Hz, 8H), 6.61 (dd, *J* = 5.7, 3.5 Hz, 2H), 6.70 (dd, *J* = 5.7, 3.5 Hz, 2H) ppm.

^{13}C{^{1}H} NMR (101 MHz, CD_2Cl_2) δ = 22.4, 49.5, 113.7, 119.6, 122.8, 124.2, 149.0 ppm.

HRMS *calcd.* for $[C_{36}H_{61}N_6]^+$: 577.495217; *found* 577.494840. [M+H$^+$]

IR (solid) $\tilde{\nu}$ = 497, 741, 1022, 1037, 1130, 1158, 1193, 1214, 1271, 1301, 1320, 1365, 1441, 1469, 1489, 1621, 2872, 2931, 2967 cm^{-1}.

Compound **4.31**

$PhPCl_2$ (130 µL, 0.96 mmol) and TMSOTf (346 µL, 1.91 mmol) were added to a solution of the free base **4.29** (500 mg, 0.80 mmol) in dry CH_2Cl_2 (5 mL) and the resulting mixture was stirred at room temperature for 16 hours. The solvent was then evaporated and the residue washed with Et_2O (3 x 7 mL). Recrystallization from CH_2Cl_2/Et_2O gave the title compound as a white solid (516 mg, 63 %).

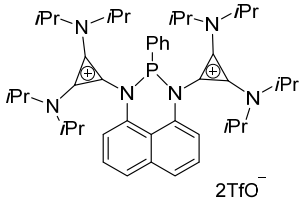

^{1}H NMR (400 MHz, CD_2Cl_2) δ = 1.35 (br, 48H), 3.88 (br, 8H), 7.11-7.18 (m, 3H), 7.23-7.31 (m, 4H), 7.52 (t, *J* = 8.2 Hz, 2H), 7.65 (d, *J* = 8.2 Hz, 2H) ppm.

^{31}P{^{1}H} NMR (121 MHz, CD_2Cl_2) δ = 72.1 ppm.

^{13}C{^{1}H} NMR (101 MHz, CD_2Cl_2) δ = 22.2, 53.0, 110.9 (d, J_{PC} = 28.9 Hz), 119.3, 120.9, 121.4 (q, J_{FC} = 321.2 Hz), 125.0 (d, J_{PC} = 28.9 Hz), 126.9, 127.0, 129.3 (d, J_{PC} = 4.2 Hz), 130.3 (d, J_{PC} = 17.1 Hz), 130.6, 134.2, 134.7 (d, J_{PC} = 7.3 Hz), 135.1 ppm.

HRMS *calcd.* for $[C_{47}H_{67}N_6O_3F_3PS]^+$: 883.467370; *found* 883.467960.

IR (solid) $\tilde{\nu}$ = 427, 515, 572, 635, 747, 766, 828, 987, 1029, 1141, 1220, 1262, 1355, 1374, 1445, 1537, 2939, 2976 cm^{-1}.

Compound **4.32**

$CyPCl_2$ (147 µL, 0.96 mmol) and TMSOTf (346 µL, 1.91 mmol) were added to a solution of the free base **4.29** (500 mg, 0.80 mmol) in dry CH_2Cl_2 (5 mL) and the resulting mixture was stirred at room temperature for 16 hours. The solvent was then removed under vacuum and the residue washed with Et_2O (3 x 7 mL). Recrystallization from CH_2Cl_2/Et_2O gave the title compound as a light brown solid (673 mg, 81 %).

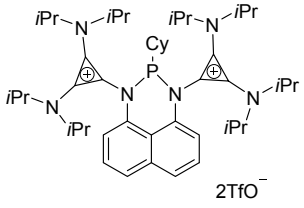

^{1}H NMR (400 MHz, CD_2Cl_2) δ = 0.71-0.85 (m, 2H), 1.01-1.19 (m, 2H), 1.31 (br, 48H), 1.51-1.74 (m, 7H), 3.85 (br, 8H), 7.24 (d, *J* = 8.0 Hz, 2H), 7.65 (t, *J* = 8.0 Hz, 2H), 7.86 (d, *J* = 8.0 Hz, 2H) ppm.

^{31}P{^{1}H} NMR (162 MHz, CD_2Cl_2) δ = 79.2 ppm.

^{13}C{^{1}H} NMR (101 MHz, CD_2Cl_2) δ = 22.3, 22.4, 22.4, 25.8, 26.3 (d, J_{PC} = 12.5 Hz), 27.5, (d, J_{PC} = 18.1 Hz), 37.8 (d, J_{PC} = 11.8 Hz), 53.5, 54.2, 111.6 (d, J_{PC} = 25.3 Hz), 119.6, 121.2, 121.4 (q, J_{FC} = 321.7 Hz), 124.6 (d, J_{PC} = 4.2 Hz), 127.3, 127.5, 133.4, 135.1 ppm.

HRMS *calcd.* for $[C_{47}H_{73}N_6O_3F_3PS]^+$: 889.514910; *found* 889.514330.

IR (solid) $\tilde{\nu}$ = 516, 575, 635, 729, 769, 830, 989, 1031, 1143, 1221, 1269, 1348, 1439, 1464, 1528, 1544, 2938, 2978 cm^{-1}.

Elemental Analysis (%) *calcd.* C: 55.48, H: 7.08, N: 8.09, P: 2.98; *found* C: 55.21, H: 7.22, N: 7.96, P: 2.73.

Compound **4.33**

PCl_3 (84 µL, 0.96 mmol) and TMSOTf (346 µL, 1.91 mmol) were added to a solution of the free base **4.29** (500 mg, 0.80 mmol) in dry CH_2Cl_2 (5 mL) and the resulting mixture was stirred at room temperature for 16 hours. The solvent was then removed under vacuum and the residue washed with Et_2O (3 x 7 mL). Recrystallization from CH_2Cl_2/Et_2O gave the title compound as a light brown solid (683 mg, 86 %).

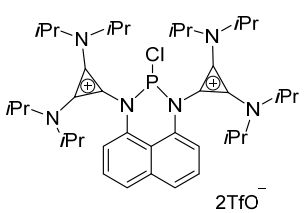

^{1}H NMR (400 MHz, CD_2Cl_2) δ = 0.98 (br, 12H), 1.42 (br, 30H), 1.60 (br, 6H), 3.44 (br, 2H), 3.92 (br, 4H), 4.19 (br, 2H), 7.06 (d, *J* = 8.0 Hz, 2H), 7.64 (t, *J* = 8.0 Hz, 2H), 7.82 (d, *J* = 8.0 Hz, 2H) ppm.

^{31}P{^{1}H} NMR (162 MHz, CD_2Cl_2) δ = 84.6 ppm.

^{13}C{^{1}H} NMR (101 MHz, CD_2Cl_2) δ = 21.0 (br), 21.7, 22.0, 22.4, 22.8, 49.6, 53.0, 53.4, 55.8, 106.1 (d, J_{PC} = 35.5 Hz), 117.6, 118.1, 121.2 (q, J_{FC} = 321.2), 126.7, 127.6, 128.0, 131.3, 135.4 ppm.

HRMS *calcd.* for $[C_{41}H_{62}N_6O_3ClF_3PS]^+$: 841.398050; *found* 841.397688.

IR (solid) $\tilde{\nu}$ = 451, 635, 762, 822, 972, 1030, 1145, 1255, 1358, 1376, 1448, 1556, 1918, 2940, 2979 cm^{-1}.

Compound **4.34**

$N(Et_2)PCl_2$ (139 µL, 0.96 mmol) and TMSOTf (346 µL, 1.91 mmol) were added to a solution of the free base **4.29** (500 mg, 0.80 mmol) in dry CH_2Cl_2 (5 mL) and the resulting mixture was stirred at room temperature for 16 hours. The solvent was then evaporated and the residue washed with Et_2O (3 x 7 mL). Recrystallization from CH_2Cl_2/Et_2O gave the title compound as a light brown solid (482 mg, 59 %).

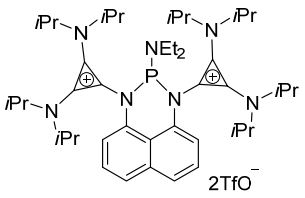

^{1}H NMR (400 MHz, CD_2Cl_2) δ = 0.78 (t, *J* = 7.0 Hz, 6H), 1.32 (br, 48H), 2.88 (q, *J* = 7.0 Hz, 2H), 2.91 (q, J = 7.0 Hz, 2H), 3.85 (br, 8H), 7.05 (d, *J* = 7.9 Hz, 2H), 7.60 (t, *J* = 7.9 Hz, 2H), 7.71 (d, *J* = 7.9 Hz, 2H) ppm.

^{31}P{^{1}H} NMR (162 MHz, CD_2Cl_2) δ = 69.8 ppm.

^{13}C{^{1}H} NMR (101 MHz, CD_2Cl_2) δ = 14.2 (d, J_{PC} = 3.8 Hz), 22.1, 42.6 (d, J_{PC} = 20.4 Hz), 53.0, 110.0, (d, J_{PC} = 32.3 Hz), 117.7, 118.7, 121.3 (q, J_{FC} = 321.3 Hz), 125.6, 126.1 (d, J_{PC} = 6.1 Hz), 128.1, 134.9, 135.3 ppm.

HRMS *calcd.* for $[C_{45}H_{72}N_7O_3F_3PS]^+$: 878.510159; *found* 878.510500.

IR (solid) $\tilde{\nu}$ = 515, 572, 636, 766, 1029, 1141, 1263, 1351, 1442, 1536, 2937, 2978 cm^{-1}.

Compound **4.35**

$PhPCl_2$ (85 µL, 0.62 mmol) and TMSOTf (226 µL, 1.25 mmol) were added to a solution of the free base **4.30** (300 mg, 0.52 mmol) in dry CH_2Cl_2 (3 mL) and the resulting mixture was stirred at room temperature for 16 hours. The solvent was then removed under vacuum and the remaining residue washed with Et_2O (3 x 5 mL). Recrystallization from CH_2Cl_2/Et_2O gave the title compound as a white solid (333 mg, 65 %).

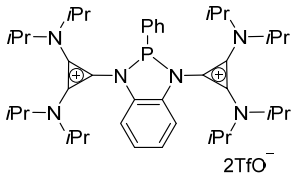

^{1}H NMR (400 MHz, CD_2Cl_2) δ = 1.23 (d, *J* = 6.7 Hz, 24H), 1.28 (d, *J* = 6.7 Hz, 24H), 3.82 (br, 8H), 7.20 (dd, *J* = 5.8, 3.3 Hz, 2H), 7.28 (dd, *J* = 5.8, 3.3 Hz, 2H), 7.36-7.42 (m, 2H), 7.49-7.58 (m, 3H) ppm.

^{31}P{^{1}H} NMR (162 MHz, CD_2Cl_2) δ = 98.5 ppm.

^{13}C{^{1}H} NMR (101 MHz, CD_2Cl_2) δ = 21.8, 21.8, 22.1, 52.7, 107.1 (d, J_{PC} = 22.4 Hz), 117.2, 121.4 (q, J_{FC} = 321.3 Hz), 125.6, 127.3, 129.7 (d, J_{PC} = 8.9 Hz), 131.2 (d, J_{PC} = 27.8 Hz), 134.1, 137.1 (d, J_{PC} = 3.0 Hz), 138.7 (d, J_{PC} = 31.3 Hz) ppm.

HRMS *calcd.* for $[C_{43}H_{65}N_6O_3F_3PS]^+$: 883.452310; *found* 883.451790.

IR (solid) $\tilde{\nu}$ = 434, 515, 635, 1028, 1141, 1260, 1354, 1444, 1536, 2977 cm^{-1}.

Compound **4.36**

$CyPCl_2$ (96 µL, 0.62 mmol) and TMSOTf (226 µL, 1.25 mmol) were added to a solution of the free base **4.30** (300 mg, 0.52 mmol) in dry CH_2Cl_2 (3 mL) and the resulting mixture was stirred at room temperature for 16 hours. The solvent was then removed under vacuum and the residue thus obtained washed with Et_2O (3 x 5 mL). Recrystallization from CH_2Cl_2/Et_2O gave the title compound as a light brown solid (412 mg, 80 %).

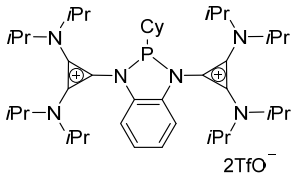

^{1}H NMR (400 MHz, CD_2Cl_2) δ = 0.99-1.22 (m, 5H), 1.36 (d, *J* = 6.8 Hz, 24H), 1.37 (d, *J* = 6.8 Hz, 24H), 1.63-1.82 (m, 6H), 3.89 (sept, *J* = 6.8 Hz, 8H), 7.22-7.29 (m, 4H) ppm.

^{31}P{^{1}H} NMR (162 MHz, CD_2Cl_2) δ = 126.3 ppm.

^{13}C{^{1}H} NMR (101 MHz, CD_2Cl_2) δ = 22.1, 22.1, 22.1, 22.5, 26.0, 26.7 (d, J_{PC} = 10.7 Hz), 27.1 (d, J_{PC} = 13.0 Hz), 45.5 (d, J_{PC} = 25.1 Hz), 51.5, 53.2, 109.5 (d, J_{PC} = 18.7 Hz), 118.2, 121.4 (q, J_{FC} = 321.9 Hz), 125.0, 126.0, 138.2 ppm.

HRMS *calcd.* for $[C_{43}H_{71}N_6O_3F_3PS]^+$: 839.499260; *found* 839.498740.

IR (solid) $\tilde{\nu}$ = 515, 634, 749, 1028, 1136, 1210, 1255, 1348, 1359, 1451, 1472, 1536, 1562, 1916, 2933, 2981 cm^{-1}.

Elemental Analysis (%) *calcd.* C: 53.43, H: 7.24, N: 8.50, P 3.13; *found* C: 53.70, H: 7.27, N: 8.38, P: 3.30.

Compound **4.37**

TMSCN (19 µL, 0.15 mmol) was added to a stirred solution of compound **4.33** (126 mg, 0.13 mmol) in dry CH_2Cl_2 (1 mL) and the resulting mixture was stirred at room temperature for 16 hours. The solvent was then evaporated and the residue washed with Et_2O (2 x 3 mL) affording the title compound as a light brown solid (102 mg, 82 %).

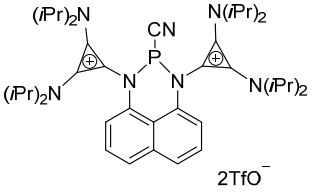

^{1}H NMR (400 MHz, CD_2Cl_2) δ = 0.92 (d, *J* = 6.3 Hz, 6H), 0.97 (d, *J* = 6.3 Hz, 6H), 1.42 (d, *J* = 6.3 Hz, 30H), 1.61 (d, *J* = 6.3 Hz, 6H), 3.36 (sept, *J* = 6.3 Hz, 2H), 3.87 (sept, *J* = 6.3 Hz, 4H), 4.23 (sept, *J* = 6.3 Hz, 2H), 7.22 (d, *J* = 8.0 Hz, 2H), 7.68 (t, *J* = 8.0 Hz, 2H), 7.90 (d, *J* = 8.0 Hz, 2H) ppm.

^{31}P{^{1}H} NMR (162 MHz, CD_2Cl_2) δ = 16.6 ppm.

^{13}C{^{1}H} NMR (101 MHz, CD_2Cl_2) δ = 20.6, 20.8, 21.6, 21.8, 22.0, 22.2, 22.5, 23.6, 48.4, 52.3, 54.0, 56.4, 106.6 (d, J_{PC} = 36.9 Hz), 118.2 (d, J_{PC} = 103.5 Hz), 118.4, 119.4, 121.2 (q, J_{FC} = 321.3 Hz), 127.3, 127.5 (d, J_{PC} = 15.1 Hz), 127.6, 133.5, 135.7 ppm.

HRMS *calcd.* for $[C_{42}H_{62}N_7O_3F_3PS]^+$: 832.431908; *found* 832.431720.

IR (solid) $\tilde{\nu}$ = 516, 566, 635, 760, 823, 1029, 1145, 1254, 1355, 1375, 1450, 1465, 1559, 1918, 2882, 2937, 2978 cm^{-1}.

Compound **4.38**

TMSSPh (32 µL, 0.17 mmol) was added to a stirred solution of compound **4.33** (150 mg, 0.15 mmol) in dry CH_2Cl_2 (1 mL) and the resulting mixture was stirred at room temperature for 16 hours. The solvent was then evaporated and the residue washed with Et_2O (2 x 3 mL) affording the title compound as a light brown solid (84 mg, 52 %).

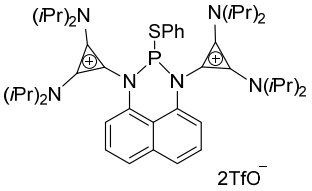

^{1}H NMR (400 MHz, CD_2Cl_2) δ = 1.27 (br, 48H), 3.75 (br, 8H), 7.19 (d, *J* = 7.9 Hz, 2H), 7.36-7.43 (m, 5H), 7.69 (t, *J* = 7.9 Hz, 2H), 7.89 (d, *J* = 7.9 Hz, 2H) ppm.

^{31}P{^{1}H} NMR (162 MHz, CD_2Cl_2) δ = 91.0 ppm.

$^{13}C\{^1H\}$ NMR (101 MHz, CD_2Cl_2) δ = 22.1, 53.4 (br), 108.9 (d, J_{PC} = 29.3 Hz), 119.2, 120.2, 121.3 (q, J_{FC} = 321.3 Hz), 125.5 (bs), 127.0 (d, J_{PC} = 12.1 Hz), 127.2, 127.5, 130.5, 133.4, 135.3, 136.2, 136.2 ppm.

HRMS *calcd.* for $[C_{47}H_{67}N_6O_3F_3PS_2]^+$: 915.440032; *found* 915.439430.

IR (solid) $\tilde{\nu}$ = 517, 636, 752, 824, 1029, 1143, 1261, 1353, 1376, 1441, 1543, 2976 cm^{-1}.

Compound **4.39**

$TMSN_3$ (24 µL, 0.18 mmol) was added to a stirred solution of compound **4.33** (150 mg, 0.15 mmol) in dry CH_2Cl_2 (1 mL) and the resulting mixture was stirred at room temperature for 3 days. The solvent was then evaporated and the residue washed with Et_2O (2 x 3 mL) affording the title compound as a light brown solid (111 mg, 74 %).

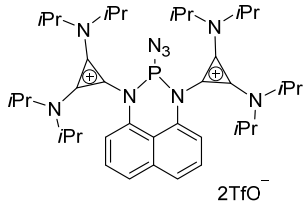

^1H NMR (400 MHz, CD_2Cl_2) δ = 0.97 (br, 12H), 1.43 (br, 36H), 3.40 (br, 2H), 3.90 (br, 4H), 4.19 (br, 2H), 7.06 (d, *J* = 7.9 Hz, 2H), 7.63 (t, *J* = 7.9 Hz. 2H), 7.81 (d, *J* = 7.9 Hz, 2H) ppm.

$^{31}P\{^1H\}$ NMR (162 MHz, CD_2Cl_2) δ = 74.0 ppm.

$^{13}C\{^1H\}$ NMR (101 MHz, CD_2Cl_2) δ = 21.0 (br), 22.4, 56.1, 107.2 (d, J_{PC} = 34.2 Hz), 117.6, 118.2, 121.3 (q, J_{FC} = 320.5 Hz), 126.6-128.5 (br), 126.7, 127.6, 131.8, 135.4 ppm.

HRMS *calcd.* for $[C_{41}H_{62}N_9O_3F_3PS]^+$: 848.438056; *found* 848.437900.

IR (solid) $\tilde{\nu}$ = 516, 635, 765, 825, 1030, 1135, 1256, 1345, 1376, 1451, 1550, 1921, 2120, 2361, 2981 cm^{-1}.

Compound **4.40**

[AuCl(SMe$_2$)] (57 mg, 0.19 mmol) was added to a solution of compound **4.31** (200 mg, 0.19 mmol) in dry CH_2Cl_2 (2 mL) and the resulting mixture was stirred at room temperature for 1 hour. The solvent was then evaporated affording the desired product as a white solid (231 mg, 94 %).

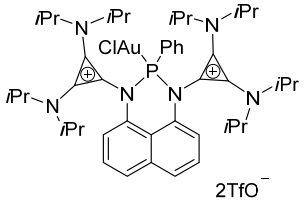

^1H NMR (400 MHz, CD_2Cl_2) δ = 0.90 (d, *J* = 6.8 Hz, 6H), 1.01 (d, *J* = 6.8 Hz, 6H), 1.12 (d, *J* = 6.8 Hz, 6H), 1.32 (d, *J* = 6.8 Hz, 6H), 1.40 (d, *J* = 6.8 Hz, 6H), 1.48 (d, *J* = 6.8 Hz, 18H), 3.54 (sept, *J* = 6.8 Hz, 2H), 3.69 (sept, *J* = 6.8 Hz, 2H), 4.08 (sept, *J* = 6.8 Hz, 2H), 4.28 (sept, *J* = 6.8 Hz, 2H), 7.43 (td, *J* = 7.9, 3.7 Hz, 2H), 7.55 (dd, *J* =

15.9, 7.9 Hz, 2H), 7.60 (d, *J* = 7.8 Hz, 2H), 7.66 (t, *J* = 7.9 Hz, 1H), 7.78 (t, *J* = 7.8 Hz, 2H), 7.86 (d, *J* = 7.8 Hz, 2H) ppm.

$^{31}P\{^{1}H\}$ NMR (162 MHz, CD_2Cl_2) δ = 77.1 ppm.

$^{13}C\{^{1}H\}$ NMR (101 MHz, CD_2Cl_2) δ = 20.3, 21.0, 21.6, 21.7, 22.7, 22.8, 23.1, 25.0, 49.5, 53.8, 55.3, 57.4, 102.9 (d, J_{PC} = 16.0 Hz), 116.1, 119.2, 121.4 (q, J_{FC} = 321.0 Hz), 127.1, 129.1, 130.7 (d, J_{PC} = 14.3 Hz), 131.3 (d, J_{PC} = 3.9 Hz), 131.5 (d, J_{PC} = 1.5 Hz), 132.3, 132.6 (d, J_{PC} = 20.3 Hz), 132.9, 134.5 (d, J_{PC} = 1.9 Hz), 135.6, 136.1 (d, J_{PC} = 2.4 Hz) ppm.

HRMS *calcd.* for $[C_{45}H_{67}N_6O_3AuClF_3PS]^+$: 1115.403366; *found* 1115.402800.

IR (solid) $\tilde{\nu}$ = 515, 596, 636, 709, 754, 822, 1029, 1141, 1222, 1258, 1348, 1376, 1449, 1570, 1895, 2937, 2980 cm^{-1}.

Elemental Analysis (%) *calcd.* C: 45.55, H: 5.34, N: 6.64, P: 2.45; *found* C: 45.02, H: 5.24, N: 6.35, P: 2.62.

Compound **4.41**

[AuCl(SMe$_2$)] (57 mg, 0.19 mmol) was added to a solution of compound **4.32** (200 mg, 0.19 mmol) in dry CH_2Cl_2 (2 mL) and the resulting mixture was stirred at room temperature for 1 hour. The solvent was then evaporated affording the desired product as a light brown solid (245 mg, 91 %).

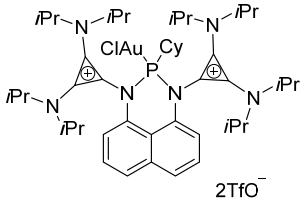

^{1}H NMR (400 MHz, CD_2Cl_2) δ = 0.86 (d, *J* = 6.2 Hz, 6H), 1.06 (d, *J* = 6.2 Hz, 6H), 1.10-1.34 (m, 5H), 1.37-1.45 (m, 12H), 1.56 (d, *J* = 6.2 Hz, 12H), 1.61 (d, *J* = 6.2 Hz, 12H), 1.75-1.89 (m, 5H), 2.19-2.34 (m, 1H), 3.28 (sept, *J* = 6.2 Hz, 2H), 4.13 (sept, *J* = 6.2 Hz, 2H), 4.34 (bs, 4H), 7.77 (t, *J* = 7.7 Hz, 2H), 7.85 (d, *J* = 7.7 Hz, 2H), 7.91 (d, *J* = 7.7 Hz, 2H) ppm.

$^{31}P\{^{1}H\}$ NMR (162 MHz, CD_2Cl_2) δ = 97.5 ppm.

$^{13}C\{^{1}H\}$ NMR (101 MHz, CD_2Cl_2) δ = 21.4, 21.6, 22.2, 22.5, 23.4, 23.9, 25.1, 25.9 (d, J_{PC} = 17.2 Hz), 27.0 (d, J_{PC} = 3.6 Hz), 40.8 (d, J_{PC} = 46.2 Hz), 53.1, 54.0, 54.2, 56.0, 106.5 (d, J_{PC} = 10.8Hz), 117.7 (d, J_{PC} = 2.8Hz), 121.4 (q, J_{FC} = 321.3 Hz), 122.1 (d, J_{PC} = 1.7 Hz), 128.2, 128.8, 130.5, 131.8, 135.3 ppm.

HRMS *calcd.* for $[C_{47}H_{73}N_6O_3AuF_3PS]$: 1121.450865; *found* 1121.449140.

IR (solid) $\tilde{\nu}$ = 516, 635, 759, 826, 992, 1029, 1143, 1222, 1258, 1350, 1376, 1441, 1536, 1571, 1894, 2936, 2979 cm^{-1}.

Compound **4.42**

[AuCl(SMe$_2$)] (25 mg, 0.09 mmol) was added to a solution of compound **4.34** (89 mg, 0.09 mmol) in dry CH_2Cl_2 (1 mL) and the resulting mixture was stirred at room temperature for 1 hour. The solvent was then evaporated and the residue washed with Et_2O. The desired product was isolated as a light brown solid (94 mg, 86 %).

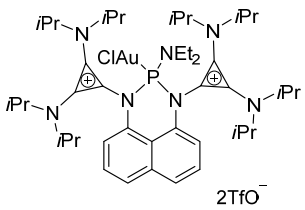

^{1}H NMR (400 MHz, CD_2Cl_2) δ = 0.85 (d, *J* = 6.8 Hz, 6H), 0.91 (t, *J* = 7.0 Hz, 6H), 1.20 (d, *J* = 6.8 Hz, 6H), 1.40 (d, *J* = 6.8 Hz, 6H), 1.46 (d, *J* = 6.8 Hz, 6H), 1.51-1.59 (m, 24H), 3.22 (overlap of two quartets, *J* = 7.0 Hz, 4H), 3.56 (sept, *J* = 6.8 Hz, 2H), 4.12 (bs, 4H), 4.24 (sept, *J* = 6.8 Hz, 2H), 7.63 (d, *J* = 7.8 Hz, 2H), 7.71 (d, *J* = 7.8 Hz, 2H), 7.76 (t, *J* = 7.8 Hz, 2H) ppm.

^{31}P{^{1}H} NMR (162 MHz, CD_2Cl_2) δ = 79.1 ppm.

^{13}C{^{1}H} NMR (101 MHz, CD_2Cl_2) δ = 13.7 (d, J_{PC} = 3.0 Hz), 20.8, 21.3, 22.1, 22.5, 23.4, 24.4, 42.4 (d, J_{PC} = 9.4 Hz), 51.4, 56.2, 104.6 (d, J_{PC} = 17.1 Hz), 118.9, 121.3 (q, J_{FC} = 322.5 Hz), 126.7, 129.1, 130.5 (d, J_{PC} = 5.2 Hz), 132.6, 132.8, 135.3 ppm.

HRMS *calcd.* for $[C_{45}H_{72}N_7O_3AuClF_3PS]^+$: 1110.445564; *found* 1110.446680.

IR (solid) $\tilde{\nu}$ = 516, 636, 799, 821, 1029, 1147, 1260, 1353, 1377, 1447, 1565, 1890, 2973 cm^{-1}.

Compound **4.43**

[AuCl(SMe$_2$)] (29 mg, 0.10 mmol) was added to a solution of compound **4.35** (95 mg, 0.10 mmol) in dry CH_2Cl_2 (1 mL) and the resulting mixture was stirred at room temperature for 1 hour. The solvent was then evaporated affording the desired product as a white solid (113 mg, 96 %).

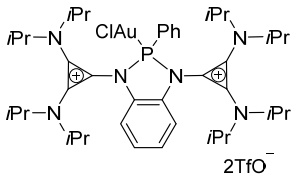

^{1}H NMR (400 MHz, CD_2Cl_2) δ = 0.43 (br, 6H), 0.99 (br, 6H), 1.06 (br, 6H), 1.25-1.61 (m, 30H), 3.47 (br, 2H), 3.82 (br, 2H), 4.07 (br, 2H), 4.19 (br, 2H), 7.27 (dd, *J* = 5.6, 3.2 Hz, 2H), 7.52 (dd, *J* = 5.6, 3.2 Hz, 2H), 7.60 (td, *J* = 7.8, 3.3 Hz, 2H), 7.81 (t, *J* = 7.8 Hz, 1H), 8.01 (dd, *J* = 16.1, 7.8 Hz, 2H) ppm.

^{31}P{^{1}H} NMR (162 MHz, CD_2Cl_2) δ = 100.1 ppm.

^{13}C{^{1}H} NMR (101 MHz, CD_2Cl_2) δ = 20.2, 21.4, 21.6, 22.3, 22.8, 25.4, 49.1, 49.4, 57.6, 58.2, 97.9 (d, J_{PC} = 14.8 Hz), 115.5, 121.3 (q, J_{FC} = 321.2 Hz), 125.9, 130.9 (d, J_{PC} = 14.2 Hz), 132.6 (d, J_{PC} = 2.9 Hz), 133.4 (d, J_{PC} = 21.6 Hz), 135.6 (d, J_{PC} = 59.4 Hz), 135.6, 137.7 ppm.

HRMS *calcd.* for $[C_{43}H_{65}N_6O_3AuClF_3PS]^+$: 1065.387715; *found* 1065.388470.

IR (solid) $\tilde{\nu}$ = 516, 594, 636, 756, 922, 1029, 1106, 1143, 1200, 1222, 1259, 1351, 1376, 1454, 1577, 1901, 2980 cm^{-1}.

Compound **4.44**

[AuCl(SMe_2)] (30 mg, 0.10 mmol) was added to a solution of compound **4.36** (100 mg, 0.10 mmol) in dry CH_2Cl_2 (1 mL) and the resulting mixture was stirred at room temperature for 1 hour. The solvent was then evaporated affording the desired product as a white solid (120 mg, 97 %).

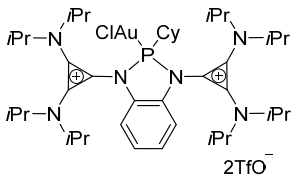

^{1}H NMR (400 MHz, CD_2Cl_2) δ = 1.08-1.35 (m, 5H), 1.46 (d, *J* = 6.7 Hz, 48H), 1.69-1.78 (m, 1H), 1.82-1.91 (m, 2H), 1.99-2.10 (m, 2H), 2.30-2.41 (m, 1H), 4.04 (br, 8H), 7.29 (dd, *J* = 5.8, 3.2 Hz, 2H), 7.41 (dd, *J* = 5.8, 3.2 Hz, 2H) ppm.

^{31}P{^{1}H} NMR (162 MHz, CD_2Cl_2) δ = 127.1 ppm.

^{13}C{^{1}H} NMR (101 MHz, CD_2Cl_2) δ = 22.2, 22.4, 22.5, 25.6, 26.2 (d, J_{PC} = 16.1 Hz), 26.7, 49.2 (d, J_{PC} = 30.1 Hz), 54.3, 101.9 d (J_{PC} = 9.1 Hz), 116.6, 121.3 d (J_{FC} = 321.3 Hz), 126.8, 134.8, 134.8 ppm.

HRMS *calcd.* for $[C_{43}H_{71}N_6O_3AuClF_3PS]^+$: 1071.434666; *found* 1071.435150.

IR (solid) $\tilde{\nu}$ = 516, 594, 635, 758, 919, 1029, 1144, 1194, 1221, 1261, 1346, 1375, 1449, 1571, 1892, 2937, 2980 cm^{-1}.

Compound **4.45**

AgOTf (25 mg, 0.09 mmol) was added to a solution of compound **4.31** (100 mg, 0.09 mmol) in dry CH_2Cl_2 (2 mL) and the resulting mixture was stirred at room temperature for 16 hours. The solvent was then evaporated affording the desired product as a white solid (121 mg, 97 %).

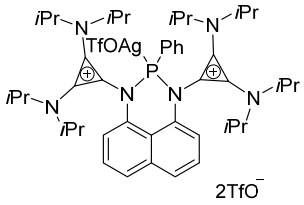

^{1}H NMR (400 MHz, CD_2Cl_2) δ = 0.63-1.07 (m, 18H), 1.42 (br, 30H), 3.22 (br, 2H), 3.70 (br, 2H), 4.03 (br, 2H), 4.25 (br, 2H), 6.96 (d, *J* = 7.9 Hz, 2H), 7.38 (td, *J* = 8.1, 2.7 Hz, 2H), 7.52-7.63 (m, 3H), 7.71 (t, *J* = 7.9 Hz, 2H), 7.85 (d, *J* = 7.9 Hz, 2H) ppm.

^{31}P{^{1}H} NMR (162 MHz, CD_2Cl_2) δ = 69.1 (d, J_{AgP} = 715.8 Hz) ppm.

^{13}C{^{1}H} NMR (101 MHz, CD_2Cl_2) δ = 19.9, 21.2, 21.5, 22.4, 23.1, 23.7, 48.5, 52.3, 55.2, 57.8, 101.8 (d, J_{PC} = 21.6 Hz), 116.3, 116.5, 120.9 (q, J_{FC} = 319.7 Hz), 126.4, 128.4, 130.5 (d, J_{PC} = 13.2 Hz), 132.6, 132.6, 132.9, 133.9 (d, J_{PC} = 20.9 Hz), 135.3, 136.0 ppm.

HRMS *calcd.* for $[C_{48}H_{67}N_6O_6AgF_6PS]^+$: 1139.324956; *found* 1139.325840.

IR (solid) $\tilde{\nu}$ =515, 594, 635, 795, 1020, 1071, 1095, 1150, 1222, 1259, 1347, 1377, 1450, 1569, 1896, 2963 cm^{-1}.

Compound **4.46**

m-CPBA (43 mg, 0.19 mmol) was added to a solution of compound **4.31** (200 mg, 0.19 mmol) in dry CH_2Cl_2 (2 mL) and the resulting mixture was stirred at room temperature for 4 hours. The solvent was then evaporated and the residue washed with Et_2O (3 x 4 mL) affording the desired product (186 mg, 92 %).

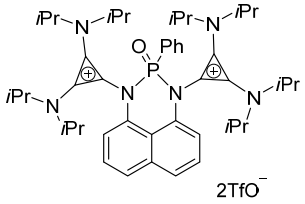

^{1}H NMR (400 MHz, CD_2Cl_2) δ = 0.77 (br, 6H), 0.90 (br, 12H), 1.27-1.52 (m, 30H), 3.32 (br, 2H), 3.70 (br, 2H), 4.00 (br, 2H), 4.25 (br, 2H), 7.35 (d, *J* = 7.7 Hz, 2H), 7.39-7.46 (m, 2H), 7.54 (dd, *J* = 14.1, 7.7 Hz, 2H), 7.64 (t, *J* = 7.7 Hz, 1H), 7.76 (t, *J* = 7.7 Hz, 2H), 7.82 (d, *J* = 7.7 Hz, 2H) ppm.

^{31}P{^{1}H} NMR (162 MHz, CD_2Cl_2) δ = -0.1 ppm.

^{13}C{^{1}H} NMR (101 MHz, CD_2Cl_2) δ = 20.5, 21.3, 21.7, 22.4, 49.2, 53.0, 54.7, 57.4, 100.2 (d, J_{PC} = 4.7 Hz), 115.2, 116.7 (d, J_{PC} = 4.3 Hz), 121.4 (q, J_{FC} = 321.2 Hz), 126.2, 129.0, 129.2, 130.2 (d, J_{PC} = 15.2 Hz), 130.8, 131.3 (d, J_{PC} = 10.6 Hz), 133.0, 133.5 (d, J_{PC} = 1.9 Hz), 134.4, 135.2 (d, J_{PC} = 2.9 Hz), 135.8 ppm.

HRMS *calcd.* for $[C_{47}H_{67}N_6O_4F_3PS]^+$: 899.462875; *found* 899.462410.

IR (solid) $\tilde{\nu}$ = 516, 573, 636, 713, 754, 823, 994, 1029, 1065, 1139, 1222, 1258, 1348, 1377, 1449, 1567, 1901, 2941, 2980 cm^{-1}.

Compound **4.47**

$POCl_3$ (36 µL, 0.38 mmol) and TMSOTf (139 µL, 0.77 mmol) were added to a solution of compound **4.29** (200 mg, 0.32 mmol) in dry CH_2Cl_2 (2 mL) and the resulting mixture was stirred at room temperature for 16 hours. The solvent was then evaporated and the residue washed with Et_2O (3 x 3 mL). Recrystallization from CH_2Cl_2/Et_2O gave the title compound as a light brown solid (259 mg, 81 %).

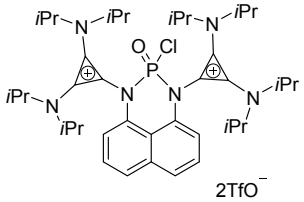

^{1}H NMR (400 MHz, CD_2Cl_2) δ = 0.92 (d, *J* = 6.7 Hz, 6H), 1.25 (d, *J* = 6.7 Hz, 6H), 1.37 (d, *J* = 6.7 Hz, 6H), 1.42 (d, *J* = 6.7 Hz, 6H), 1.45-1.82 (m, 18H), 1.54 (d, *J* = 6.7 Hz, 6H), 3.72 (sept, *J* = 6.7

Hz, 2H), 3.93 (sept, *J* = 6.7 Hz, 2H), 4.11 (sept, *J* = 6.7 Hz, 2H), 4.31 (sept, *J* = 6.7 Hz, 2H), 7.58 (d, *J* = 7.7 Hz, 2H), 7.76 (t, *J* = 7.7 Hz, 2H), 7.81 (d, *J* = 7.7 Hz, 2H) ppm.

^{31}P{^{1}H} NMR (162 MHz, CD_2Cl_2) δ = -8.9 ppm.

^{13}C{^{1}H} NMR (101 MHz, CD_2Cl_2) δ = 20.1, 21.1, 21.4, 21.9, 21.99, 22.2, 22.4, 22.9, 48.7, 52.9, 55.6, 58.0, 97.2 (d, J_{PC} = 3.7 Hz), 115.7 (d, J_{PC} = 3.9 Hz), 117.2 (d, J_{PC} = 5.8 Hz), 121.4 (q, J_{FC} = 321.1 Hz), 126.8, 129.0, 132.0, 133.1 (d, J_{PC} = 4.6 Hz), 134.7, 135.9 ppm.

HRMS *calcd.* for $[C_{41}H_{62}N_6O_4ClF_3PS]^+$: 857.392603; *found* 857.392260.

IR (solid) $\tilde{\nu}$ = 516, 599, 636, 765, 829, 1009, 1030, 1077, 1146, 1224, 1260, 1348, 1377, 1449, 1575, 1907, 2941, 2984 cm^{-1}.

Compound **4.48**

XeF_2 (30 mg, 0.18 mmol) was added to a stirred solution of compound **4.35** (160, 0.16 mmol) in dry CH_2Cl_2 (1 mL) in a glovebox and the resulting mixture was stirred at room temperature for 20 minutes. Et_2O (0.5 mL) was then slowly added to the CH_2Cl_2 solution, causing precipitation of the crude product. After filtration, the solid was recrystallized from CH_2Cl_2/Et_2O, affording the title compound as a white microcrystalline solid (74 mg, 45 %).

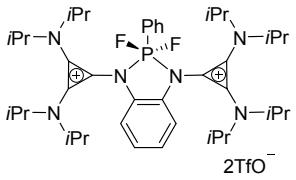

^{1}H NMR (400 MHz, CD_2Cl_2) δ = 1.20 (br, 48H), 3.87 (br, 8H), 7.16-7.24 (m, 4H), 7.50-7.59 (m, 2H), 7.65-7.74 (m, 3H) ppm.

^{31}P{^{1}H} NMR (162 MHz, CD_2Cl_2) δ = -49.8 (t, J_{PF} = 940.4 Hz) ppm.

^{13}C{^{1}H} NMR (101 MHz, CD_2Cl_2) δ = 21.6, 53.8, 54.0, 54.3, 103.4, 113.3 (d, J_{PC} = 7.1 Hz), 121.5 (q, J_{FC} = 321.2 Hz), 124.7, 128.7 (d, J_{PC} = 14.9 Hz), 130.0 (d, J_{PC} = 19.8 Hz), 131.3 (d, J_{PC} = 12.9 Hz), 132.3 (dt, J_{PC} = 236.1 Hz, J_{FC} = 25.5 Hz), 133.1, 135.1 (d, J_{PC} = 3.9 Hz) ppm.

^{19}F{^{1}H} NMR (282 MHz, CD_2Cl_2) δ = -78.8, -34.3 (d, J_{PF} = 940.4 Hz) ppm.

HRMS *calcd.* for $[C_{43}H_{65}N_6O_3F_5PS]^+$: 871.449117; *found* 871.449530.

IR (solid) $\tilde{\nu}$ = 516, 530, 563, 600, 636, 729, 752, 815, 886, 941, 1029, 1135, 1222, 1262, 1347, 1455, 1497, 1568, 1905, 2940, 2980 cm^{-1}.

6. Bibliography

(1) R. H. Crabtree, *The Organometallic Chemistry of the Transition Metals, 6*; Yale University, N. H., Connecticut, Ed.; John Wiley & Sons, Inc.: Hoboken, NJ, USA, **2014**, p 98.

(2) C. A. Tolman, *Chem. Rev.* **1977**, *77*, 313.

(3) R. Dorta, E. D. Stevens, C. D. Hoff, S. P. Nolan, *J. Am. Chem. Soc.* **2003**, *125*, 10490.

(4) U. Christmann, R. Vilar, *Angew. Chem. Int. Ed.* **2005**, *44*, 366.

(5) a) J. F. Hartwig, *Inorg. Chem.* **2007**, *46*, 1936; b) T. E. Barder, S. L. Buchwald, *J. Am. Chem. Soc.* **2007**, *129*, 12003.

(6) a) F. W. Bennett, G. R. A. Brandt, H. J. Emeleus, R. N. Haszeldine, *Nature* **1950**, *166*, 225; b) T. Drews, D. Rusch, S. Seidel, S. Willemsen, K. Seppelt, *Chem. Eur. J.* **2008**, *14*, 4280.

(7) M. Alcarazo, *Chem. Eur. J.* **2014**, *20*, 7868.

(8) D. J. Cole-Hamilton, *Science* **2003**, *299*, 1702.

(9) D. P. Curran, *Angew. Chem. Int. Ed.* **1998**, *37*, 1174.

(10) a) W. Leitner, *Acc. Chem. Res.* **2002**, *35*, 746; b) D. Prajapati, M. Gohain, *Tetrahedron* **2004**, *60*, 815.

(11) V. I. Pârvulescu, C. Hardacre, *Chem. Rev.* **2007**, *107*, 2615.

(12) a) W. A. Herrmann, C. W. Kohlpaintner, *Angew. Chem. Int. Ed. Engl.* **1993**, *32*, 1524; b) N. Pinault, D. W. Bruce, *Coord. Chem. Rev.* **2003**, *241*, 1.

(13) K. H. Shaughnessy, *Chem. Rev.* **2009**, *109*, 643.

(14) R. T. Smith, M. C. Baird, *Inorg. Chim. Acta* **1982**, *62*, 135.

(15) B. Mohr, D. M. Lynn, R. H. Grubbs, *Organometallics* **1996**, *15*, 4317.

(16) K. H. Shaughnessy, *Eur. J. Org. Chem.* **2006**, *2006*, 1827.

(17) M. Berthod, C. Saluzzo, G. Mignani, M. Lemaire, *Tetrahedron: Asymmetry* **2004**, *15*, 639.

(18) K. H. Shaughnessy, R. S. Booth, *Org. Lett.* **2001**, *3*, 2757.

(19) R. B. DeVasher, L. R. Moore, K. H. Shaughnessy, *J. Org. Chem.* **2004**, *69*, 7919.

(20) J. Carreras, G. Gopakumar, L. Gu, A. Gimeno, P. Linowski, J. Petuškova, W. Thiel, M. Alcarazo, *J. Am. Chem. Soc.* **2013**, *135*, 18815.

(21) a) N. Kuhn, J. Fahl, D. Bläser, R. Boese, *Z. Anorg. Chem.* **1999**, *625*, 729; b) N. Burford, P. J. Ragogna, R. McDonald, M. J. Ferguson, *J. Am. Chem. Soc.* **2003**, *125*, 14404; c) J. Andrieu, M. Azouri, P. Richard, *Inorg. Chem. Commun.* **2008**, *11*, 1401; d) E. Digard, J. Andrieu, H. Cattey, *Inorg. Chem. Commun.* **2012**, *25*, 39; e) M. Azouri, J. Andrieu, M. Picquet, H. Cattey, *Inorg. Chem.* **2009**, *48*, 1236; f) Y. Canac, N. Debono, L. Vendier, R. Chauvin, *Inorg. Chem.* **2009**, *48*, 5562; g) Y. Canac, C. Maaliki, I. Abdellah, R. Chauvin, *New J. Chem.* **2012**, *36*, 17; h) C. Barthes, C. Lepetit, Y. Canac, C. Duhayon, D. Zargarian, R. Chauvin, *Inorg. Chem.* **2013**, *52*, 48.

(22) a) G. Bouhadir, R. W. Reed, R. Réau, G. Bertrand, *Heteroat. Chem.* **1995**, *6*, 371; b) R. Weiss, S. Engel, *Synthesis* **1991**, *1991*, 1077.

(23) N. Burford, P. Losier, A. D. Phillips, P. J. Ragogna, T. S. Cameron, *Inorg. Chem.* **2003**, *42*, 1087.

(24) N. Kuhn, G. Henkel, M. Göhner, *Z. Anorg. Chem.* **1999**, *625*, 1415.

(25) J. J. Weigand, K.-O. Feldmann, F. D. Henne, *J. Am. Chem. Soc.* **2010**, *132*, 16321.

(26) a) A. A. Tolmachev, A. A. Yurchenko, A. S. Merculov, M. G. Semenova, E. V. Zarudnitskii, V. V. Ivanov, A. M. Pinchuk, *Heteroat. Chem.* **1999**, *10*, 585; b) N. Debono, Y. Canac, C. Duhayon, R. Chauvin, *Eur. J. Inorg. Chem.* **2008**, *2008*, 2991; c) I. Abdellah, N. Debono, Y. Canac, L. Vendier, R. Chauvin, *Chem. Asian. J.* **2010**, *5*, 1225.

(27) H. Tinnermann, C. Wille, M. Alcarazo, *Angew. Chem. Int. Ed.* **2014**, *53*, 8732.

(28) D. G. Gusev, *Organometallics* **2009**, *28*, 763.

(29) J. Sirieix, M. Oßberger, B. Betzemeier, P. Knochel, *Synlett* **2000**, *2000*, 1613.

(30) a) J. Petuškova, *Synthesis of Phosphorus(III)-Centered Cations and Their Applications as Ligands*, **2012**; b) J. Petuškova, H. Bruns, M. Alcarazo, *Angew. Chem. Int. Ed.* **2011**, *50*, 3799; c) J. Petuškova, M. Patil, S. Holle, C. W. Lehmann, W. Thiel, M. Alcarazo, *J. Am. Chem. Soc.* **2011**, *133*, 20758.

(31) J. D. Roberts, A. Streitwieser, C. M. Regan, *J. Am. Chem. Soc.* **1952**, *74*, 4579.

(32) R. Breslow, *J. Am. Chem. Soc.* **1957**, *79*, 5318.

(33) Z. Yoshida, Y. Tawara, *J. Am. Chem. Soc.* **1971**, *93*, 2573.

(34) J. S. Bandar, T. H. Lambert, *Synthesis* **2013**, *45*, 2485.

(35) R. Reed, R. Réau, F. Dahan, G. Bertrand, *Angew. Chem. Int. Ed. Engl.* **1993**, *32*, 399.

(36) a) S. Saleh, E. Fayad, M. Azouri, J.-C. Hierso, J. Andrieu, M. Picquet, *Adv. Synth. Catal.* **2009**, *351*, 1621; b) I. Abdellah, C. Lepetit, Y. Canac, C. Duhayon, R. Chauvin, *Chem. Eur. J.* **2010**, *16*, 13095.

(37) J. Carreras, M. Patil, W. Thiel, M. Alcarazo, *J. Am. Chem. Soc.* **2012**, *134*, 16753.

(38) a) I. Alonso, B. Trillo, F. López, S. Montserrat, G. Ujaque, L. Castedo, A. Lledós, J. L. Mascareñas, *J. Am. Chem. Soc.* **2009**, *131*, 13020; b) P. Mauleón, R. M. Zeldin, A. Z. González, F. D. Toste, *J. Am. Chem. Soc.* **2009**, *131*, 6348; c) D. Benitez, E. Tkatchouk, A. Z. Gonzalez, W. A. Goddard, F. D. Toste, *Org. Lett.* **2009**, *11*, 4798.

(39) V. Mamane, P. Hannen, A. Fürstner, *Chem. Eur. J.* **2004**, *10*, 4556.

(40) A. Kovács, A. Vasas, J. Hohmann, *Phytochemistry* **2008**, *69*, 1084.

(41) a) Z. B. Maksić, B. Kovačević, *J. Phys. Chem. A* **1999**, *103*, 6678; b) Z. Gattin, B. Kovačević, Z. B. Maksić, *Eur. J. Org. Chem.* **2005**, *2005*, 3206.

(42) N. H. Park, E. V. Vinogradova, D. S. Surry, S. L. Buchwald, *Angew. Chem. Int. Ed.* **2015**, *54*, 8259.

(43) A. Fürstner, *Acc. Chem. Res.* **2014**, *47*, 925.

(44) a) J. Chatt, L. A. Duncanson, *J. Chem. Soc.* **1953**, 2939; b) M. J. S. Dewar, *Bull. Soc. Chim. Fr.* **1951**, *18*, C71.

(45) a) T. Ziegler, A. Rauk, *Inorg. Chem.* **1979**, *18*, 1558; b) R. H. Hertwig, W. Koch, D. Schröder, H. Schwarz, J. Hrušák, P. Schwerdtfeger, *J. Phys. Chem.* **1996**, *100*, 12253; c) M. S. Nechaev, V. M. Rayón, G. Frenking, *J. Phys. Chem. A* **2004**, *108*, 3134.

(46) O. Eisenstein, R. Hoffmann, *J. Am. Chem. Soc.* **1981**, *103*, 4308.

(47) a) L. Ackermann, *Chem. Rev.* **2011**, *111*, 1315; b) D. Lapointe, K. Fagnou, *Chem. Lett.* **2010**, *39*, 1118; c) M. Wakioka, Y. Nakamura, Y. Hihara, F. Ozawa, S. Sakaki, *Organometallics* **2014**, *33*, 6247.

(48) a) T. Korenaga, R. Sasaki, K. Shimada, *Dalton Trans.* **2015**; b) T. Korenaga, N. Suzuki, M. Sueda, K. Shimada, *J. Organomet. Chem.* **2015**, *780*, 63.

(49) a) A. S. K. Hashmi, *Chem. Rev.* **2007**, *107*, 3180; b) A. Fürstner, P. W. Davies, *Angew. Chem. Int. Ed.* **2007**, *46*, 3410; c) E. Jiménez-Núñez, A. M. Echavarren, *Chem. Rev.* **2008**, *108*, 3326; d) A. S. K. Hashmi, M. Rudolph, *Chem. Soc. Rev.* **2008**, *37*, 1766; e) A. Fürstner, *Chem. Soc. Rev.* **2009**, *38*, 3208; f) A. S. K. Hashmi, *Angew. Chem. Int. Ed.* **2010**, *49*, 5232.

(50) a) M. Azouri, J. Andrieu, M. Picquet, P. Richard, B. Hanquet, I. Tkatchenko, *Eur. J. Inorg. Chem.* **2007**, 4877; b) C. Maaliki, Y. Canac, C. Lepetit, C. Duhayon, R. Chauvin, *RSC Adv.* **2013**, *3*, 20391.

(51) A. Fürstner, *Chem. Soc. Rev.* **2009**, *38*, 3208.

(52) a) Á. Kozma, T. Deden, J. Carreras, C. Wille, J. Petuškova, J. Rust, M. Alcarazo, *Chem. Eur. J.* **2014**, *20*, 2208; b) T. Deden, *Application of a dicationic ligand in the gold catalyzed cycloisomerization of ortho-alkynylated biaryls*, **2013**.

(53) E. Haldon, Á. Kozma, H. Tinnermann, L. Gu, R. Goddard, M. Alcarazo, *Dalton Trans.* **2016**.

(54) a) A. B. P. Lever, *Inorg. Chem.* **1990**, *29*, 1271; b) A. B. P. Lever, *Inorg. Chem.* **1991**, *30*, 1980; c) S. Leuthäußer, D. Schwarz, H. Plenio, *Chem. Eur. J.* **2007**, *13*, 7195.

(55) a) D. Kremzow, G. Seidel, C. W. Lehmann, A. Fürstner, *Chem. Eur. J.* **2005**, *11*, 1833; b) Z. Yoshida, *Pure Appl. Chem.* **1982**, *54*, 1059; c) N. J. Hardman, M. B. Abrams, M. A. Pribisko, T. M. Gilbert, R. L. Martin, G. J. Kubas, R. T. Baker, *Angew. Chem. Int. Ed.* **2004**, *43*, 1955.

(56) a) A. Fürstner, V. Mamane, *Chem. Commun.* **2003**, 2112; b) A. Fürstner, V. Mamane, *J. Org. Chem.* **2002**, *67*, 6264.

(57) E. Soriano, J. Marco-Contelles, *Organometallics* **2006**, *25*, 4542.

(58) a) L. Yang, Y. Wang, G. Zhang, F. Zhang, Z. Zhang, Z. Wang, L. Xu, *Biomed. Chromtogr.* **2007**, *21*, 687; b) A. Kovács, P. Forgo, I. Zupkó, B. Réthy, G. Falkay, P. Szabó, J. Hohmann, *Phytochemistry* **2007**, *68*, 687.

(59) T. Nakanishi, M. Suzuki, *J. Nat. Prod.* **1998**, *61*, 1263.

(60) W.-K. Li, J.-Q. Pan, M.-J. Lü, R.-Y. Zhang, P.-G. Xiao, *Phytochemistry* **1995**, *39*, 231.

(61) D. Zhang, Y. Cheng, J. Zhang, X. Wang, N. Wang, X. Yao, *Pharmaceutical Biology* **2008**, *46*, 185.

(62) a) K.-O. Feldmann, J. J. Weigand, *Angew. Chem. Int. Ed.* **2012**, *51*, 6566; b) J. L. Dutton, P. J. Ragogna, *Coord. Chem. Rev.* **2011**, *255*, 1414; c) N. Burford, P. J. Ragogna, *J. Chem. Soc., Dalton Trans.* **2002**, 4307; d) C. A. Dyker, N. Burford, *Chem. Asian. J.* **2008**, *3*, 28; e) B. D. Ellis, C. L. B. Macdonald, *Coord. Chem. Rev.* **2007**, *251*, 936.

(63) T. Ooi, K. Maruoka, *Angew. Chem. Int. Ed.* **2007**, *46*, 4222.

(64) a) D. Uraguchi, K. Koshimoto, T. Ooi, *J. Am. Chem. Soc.* **2008**, *130*, 10878; b) D. Uraguchi, K. Koshimoto, C. Sanada, T. Ooi, *Tetrahedron: Asymmetry* **2010**, *21*, 1189.

(65) a) K. Oyaizu, D. Uraguchi, T. Ooi, *Chem. Commun.* **2015**, *51*, 4437; b) D. Uraguchi, K. Oyaizu, H. Noguchi, T. Ooi, *Chem. Asian. J.* **2015**, *10*, 334; c) D. Uraguchi, K. Oyaizu, T. Ooi, *Chem. Eur. J.* **2012**, *18*, 8306.

(66) D. Uraguchi, K. Koshimoto, T. Ooi, *J. Am. Chem. Soc.* **2012**, *134*, 6972.

(67) I. Bernhardi, T. Drews, K. Seppelt, *Angew. Chem. Int. Ed.* **1999**, *38*, 2232.

(68) R. A. Kunetskiy, I. Císařová, D. Šaman, I. M. Lyapkalo, *Chem. Eur. J.* **2009**, *15*, 9477.

(69) a) R. Schwesinger, R. Link, P. Wenzl, S. Kossek, *Chem. Eur. J.* **2006**, *12*, 438; b) R. Schwesinger, R. Link, P. Wenzl, S. Kossek, M. Keller, *Chem. Eur. J.* **2006**, *12*, 429.

(70) A. Pleschke, A. Marhold, M. Schneider, A. Kolomeitsev, G. V. Röschenthaler, *J. Fluorine Chem.* **2004**, *125*, 1031.

(71) R. A. Kunetskiy, S. M. Polyakova, J. Vavřík, I. Císařová, J. Saame, E. R. Nerut, I. Koppel, I. A. Koppel, A. Kütt, I. Leito, I. M. Lyapkalo, *Chem. Eur. J.* **2012**, *18*, 3621.

(72) H. Bruns, M. Patil, J. Carreras, A. Vázquez, W. Thiel, R. Goddard, M. Alcarazo, *Angew. Chem. Int. Ed.* **2010**, *49*, 3680.

(73) D. Barić, Z. B. Maksić, *J. Phys. Org. Chem.* **2003**, *16*, 753.

(74) A. Krebs, A. Güntner, S. Versteylen, S. Schulz, *Tetrahedron Lett.* **1984**, *25*, 2333.

(75) J. S. Bandar, T. H. Lambert, *J. Am. Chem. Soc.* **2012**, *134*, 5552.

(76) I. Kaljurand, A. Kütt, L. Sooväli, T. Rodima, V. Mäemets, I. Leito, I. A. Koppel, *J. Org. Chem.* **2005**, *70*, 1019.

(77) Á. Kozma, G. Gopakumar, C. Farès, W. Thiel, M. Alcarazo, *Chem. Eur. J.* **2013**, *19*, 3542.

(78) M. Tamm, D. Petrovic, S. Randoll, S. Beer, T. Bannenberg, P. G. Jones, J. Grunenberg, *Org. Biomol. Chem.* **2007**, *5*, 523.

(79) F. H. Allen, O. Kennard, D. G. Watson, L. Brammer, A. G. Orpen, R. Taylor, *J. Chem. Soc. Perkin Trans. 2* **1987**, S1.

(80) R. Ahlrichs, M. Bär, M. Häser, H. Horn, C. Kölmel, *Chem. Phys. Lett.* **1989**, *162*, 165.

(81) a) A. D. Becke, *Phys. Rev. A.* **1988**, *38*, 3098; b) J. P. Perdew, *Phys. Rev. B.* **1986**, *33*, 8822; c) F. Weigend, R. Ahlrichs, *Phys. Chem. Chem. Phys.* **2005**, *7*, 3297.

(82) M. A. Celik, R. Sure, S. Klein, R. Kinjo, G. Bertrand, G. Frenking, *Chem. Eur. J.* **2012**, *18*, 5676.

(83) C. Maaliki, C. Lepetit, Y. Canac, C. Bijani, C. Duhayon, R. Chauvin, *Chem. Eur. J.* **2012**, *18*, 7705.

(84) Y. Wang, Y. Xie, M. Y. Abraham, R. J. Gilliard, P. Wei, H. F. Schaefer, P. v. R. Schleyer, G. H. Robinson, *Organometallics* **2010**, *29*, 4778.

(85) B. D. Ellis, C. A. Dyker, A. Decken, C. L. B. Macdonald, *Chem. Commun.* **2005**, 1965.

(86) L. Gu, G. Gopakumar, P. Gualco, W. Thiel, M. Alcarazo, *Chem. Eur. J.* **2014**, *20*, 8575.

(87) a) G. Desimoni, G. Faita, K. A. Jørgensen, *Chem. Rev.* **2006**, *106*, 3561; b) A. K. Ghosh, P. Mathivanan, J. Cappiello, *Tetrahedron: Asymmetry* **1998**, *9*, 1.

(88) M. P. Coles, P. B. Hitchcock, *Chem. Commun.* **2007**, 5229.

(89) X. Wu, M. Tamm, *Coord. Chem. Rev.* **2014**, *260*, 116.

(90) D. Franz, E. Irran, S. Inoue, *Angew. Chem. Int. Ed.* **2014**, *53*, 14264.

(91) Á. Kozma, J. Rust, M. Alcarazo, *Chem. Eur. J.* **2015**, *21*, 10829.

(92) L. Belding, T. Dudding, *Chem. Eur. J.* **2014**, *20*, 1032.

(93) Z. B. Maksic, B. Kovacevic, *J. Chem. Soc. Perkin Trans. 2* **1999**, 2623.

(94) D. Michalik, A. Schulz, A. Villinger, N. Weding, *Angew. Chem. Int. Ed.* **2008**, *47*, 6465.

(95) C. Maaliki, C. Lepetit, C. Duhayon, Y. Canac, R. Chauvin, *Chem. Eur. J.* **2012**, *18*, 16153.

(96) K. Al-Farhan, *J. Crystallogr. and Spectr. Res.* **1992**, *22*, 687.

(97) R. Weiss, K. G. Wagner, C. Priesner, J. Macheleid, *J. Am. Chem. Soc.* **1985**, *107*, 4491.

(98) C. A. Busacca, J. C. Lorenz, P. Sabila, N. Haddad, C. H. Senanyake, In *Organic Syntheses*, John Wiley & Sons, Inc. **2003**.

(99) M. Kitamura, N. Tashiro, S. Miyagawa, T. Okauchi, *Synthesis* **2011**, *2011*, 1037.

(100) D. A. Pennington, P. N. Horton, M. B. Hursthouse, M. Bochmann, S. J. Lancaster, *Polyhedron* **2005**, *24*, 151.

(101) A. Landau, G. Seitz, *Chem. Ber.* **1991**, *124*, 665.

(102) APEX2 version 2.1-0, Bruker AXS Inc. Madison, **2004**.

(103) SAINT version 7.46a, Bruker AXS Inc. Madison **2004**.

(104) G. Sheldrick GM SADABS. University of Göttingen, Göttingen **1996**.

(105) G. Sheldrick GM, *Acta Cryst.* **2008**, *A64*, 112.

7. Appendices

7.1. List of Abbreviations

Ad	1-Adamantyl (-$C_{10}H_{15}$)
aq	aqueous
BINAP	(2,2'-bis(diphenylphosphino)-1,1'-binaphtyl)
br	broad
Bu	Butyl (-C_4H_9)
ca.	*circa* (approximately)
cf.	*confer* (compare)
cod	1,5-cyclooctadiene
Cy	cyclohexyl
d	doublet
dba	dibenzylideneacetone
dd	doublet of doublets
DCE	1,2-dichloroethane
DCM	dichloromethane
DFT	density functional theory
Dipp	2,6-diisopropylphenyl
DMF	dimethylformamide
DMSO	dimethyl sulfoxide
dt	doublet of triplets
e.g.	*exempli gratia* (for example)
ee	enantiomeric excess
E_p ox	oxidation potential (V)
eq	equivalent
ESI-MS	electrospray ionization mass spectrometry
Et	ethyl (-C_2H_5)
et al.	*et alii* (and others)
eV	electronvolt
g	gram
GC	gas cromatography

hr	hour(s)
HOMO	highest occupied molecular orbital
HPLC	high-performance liquid cromatography
HRMS	high resolution mass spectrometry
Hz	hertz
IMes	1,3-bis(2,4,6-trimethylphenyl)imidazol-2-ylidene
IR	infrared
*i*Pr	isopropyl (-CH(CH_3)$_2$)
J	coupling constant (Hz)
KHMDS	potassium hexamethyldisilazane
L	generalized ligand
LUMO	lowest unoccupied molecular orbital
m	multiplet
M	generalized metal; mol/L
Me	methyl (-CH_3)
MeO	methoxy
MeOH	methanol
Mes	2,4,6-trimethylphenyl; mesityl
MHz	megahertz
min	minute(s)
mg	milligram (10^{-3} gram)
mL	milliliter (10^{-3} litre)
mmol	millimol (10^{-3} mol)
mw	microwave
*n*BuLi	*normal* Butyllithium
NHC	*N*-heterocyclic carbene
NMR	nuclear magnetic resonance
p	*para*
Ph	phenyl (-C_6H_5)
ppm	parts per million
q	quartet
R	generalized substituent

rt	room temperature
s	singlet
sept	septet
t	triplet
*t*BuLi	*tertiary* butyllithium
td	triplet of doublets
Tf	triflate
THF	tetrahydrofurane
TLC	thin layer cromatography
TMS	trimethylsilyl
UV	ultra-violet
V	volt
vs.	*versus*
Å	Angstrom
°	degrees
°C	degrees Celsius
δ	chemical shift (ppm)
$\Delta\delta$	change in chemical shift
$\{^1H\}$	proton decoupled
ν	frequency
µL	microliter (10^{-6} litre)
θ	cone angle

7.2. Selected NMR Spectra

^{1}H NMR spectrum (400 MHz, $CDCl_3$) **2.12**

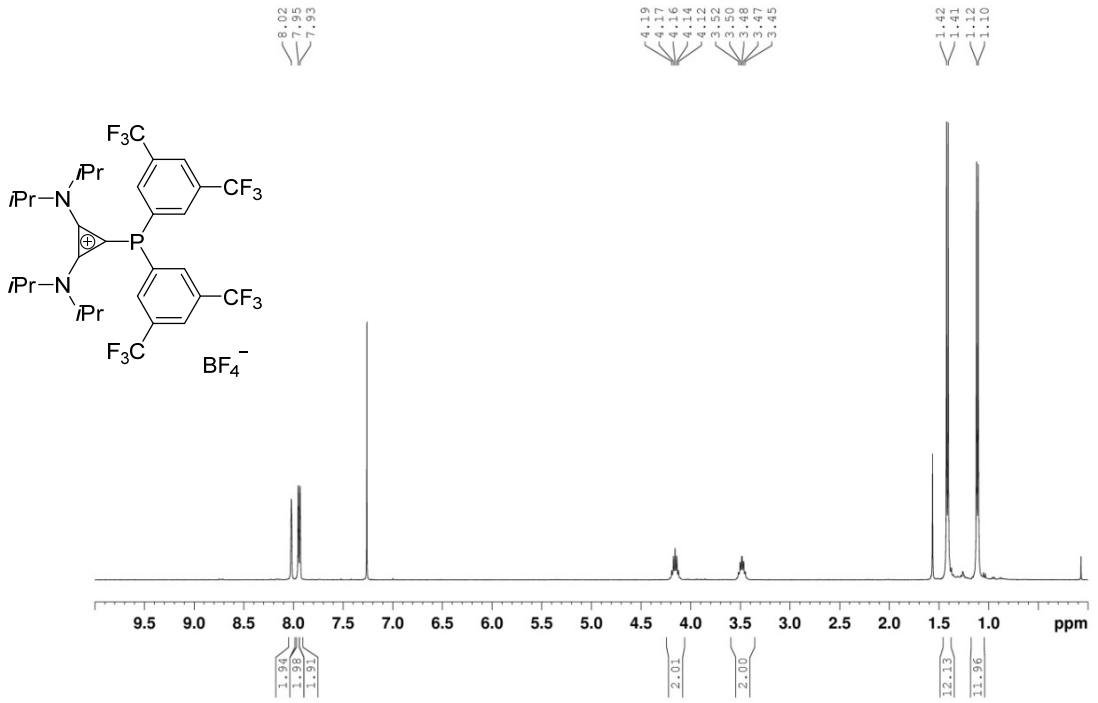

^{31}P{^{1}H} NMR spectrum (162 MHz, $CDCl_3$) **2.12**

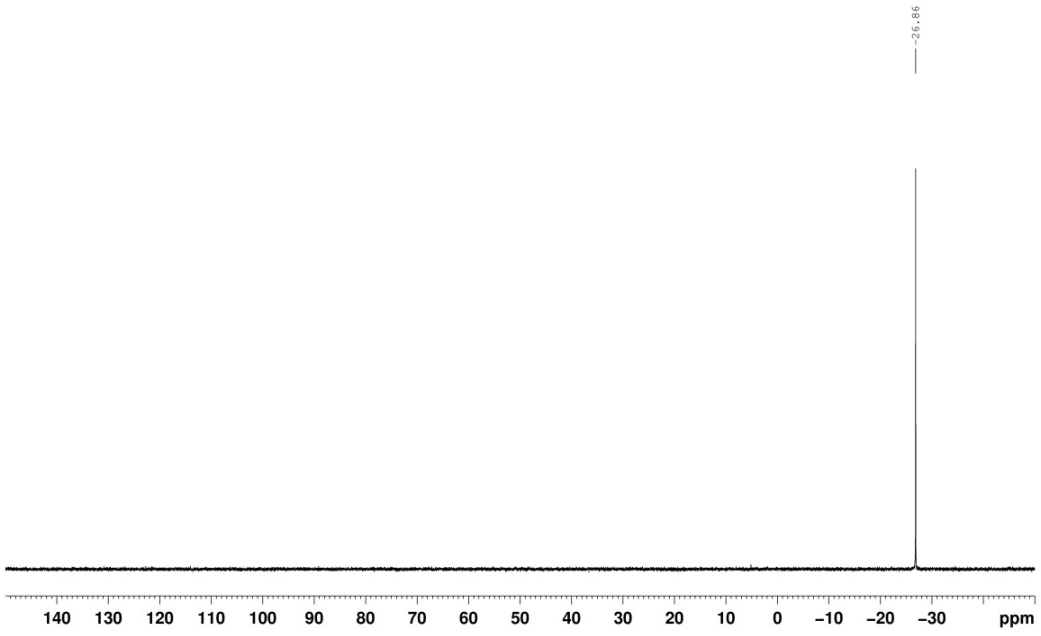

$^{19}F\{^{1}H\}$ NMR spectrum (282 MHz, CD_2Cl_2) **2.12**

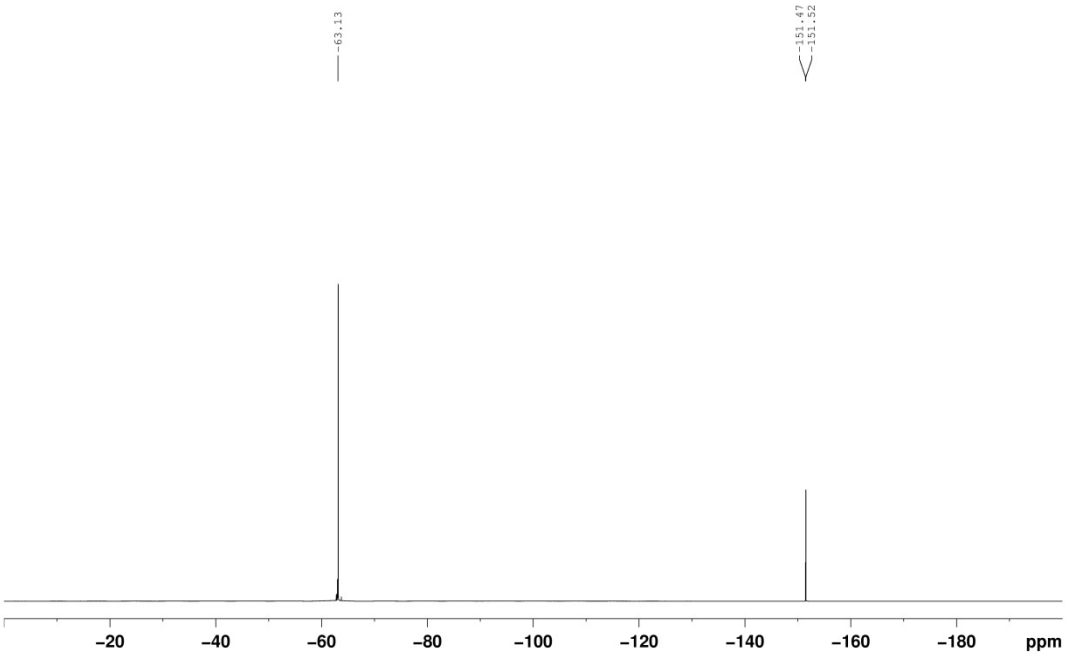

$^{13}C\{^{1}H\}$ NMR spectrum (101 MHz, $CDCl_3$) **2.12**

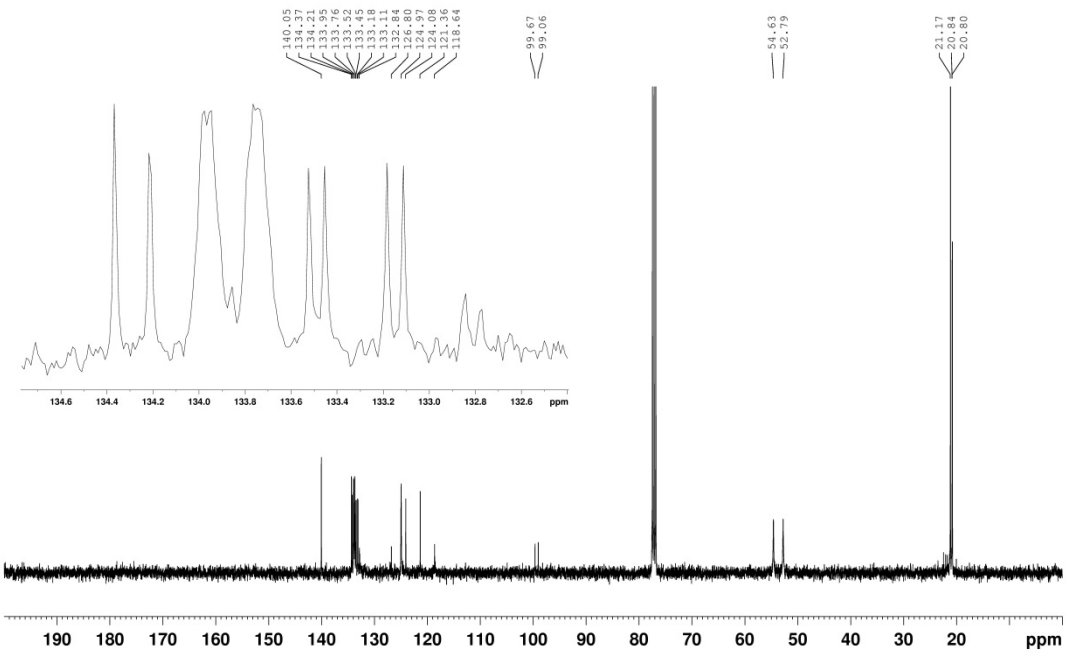

^{1}H NMR spectrum (300 MHz, $CDCl_3$) **2.14**

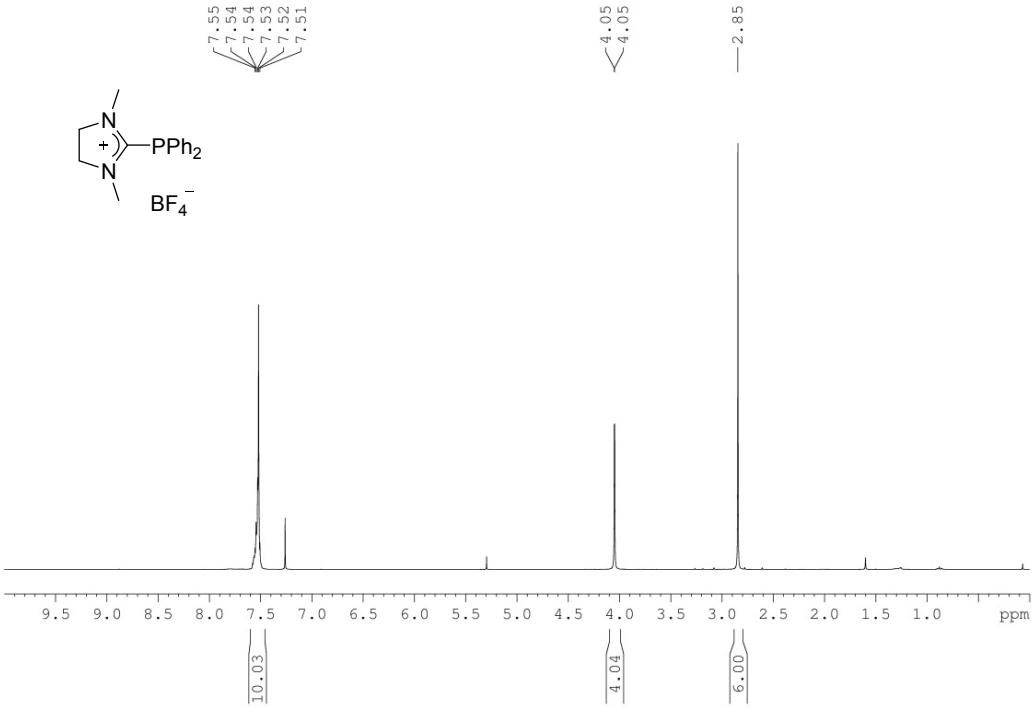

^{31}P{^{1}H} NMR spectrum (121 MHz, CD_2Cl_2) **2.14**

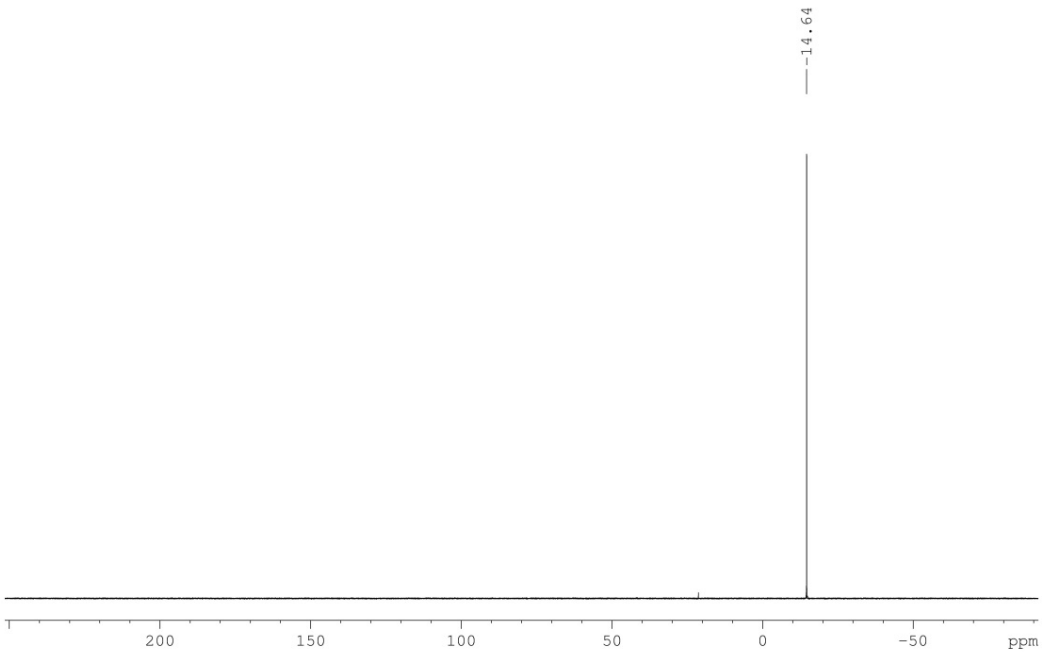

$^{13}C\{^{1}H\}$ NMR spectrum (101 MHz, $CDCl_3$) **2.14**

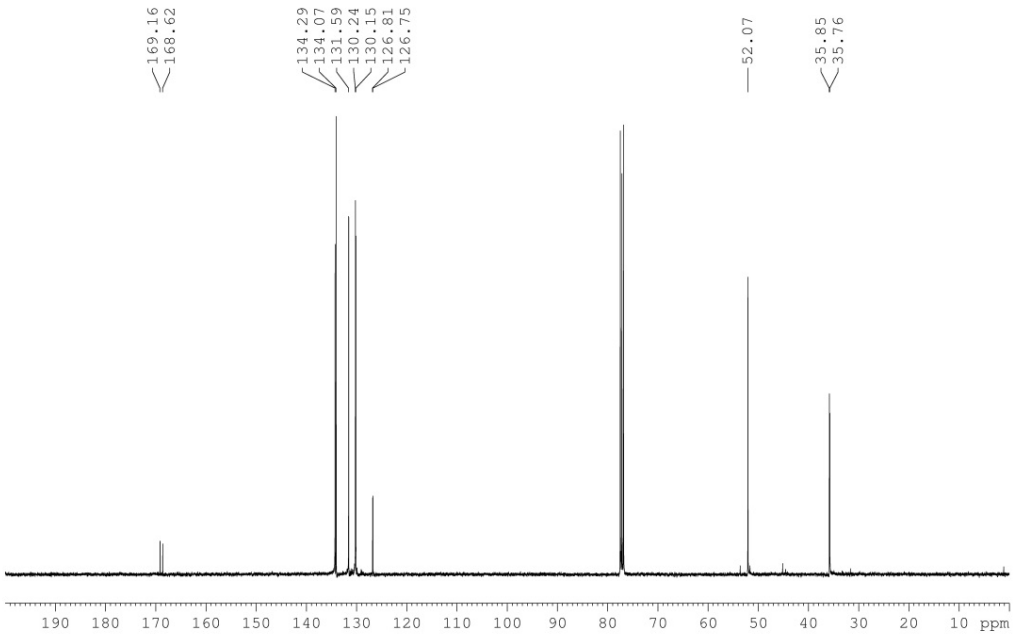

^{1}H NMR spectrum (400 MHz, CD_2Cl_2) **2.15**

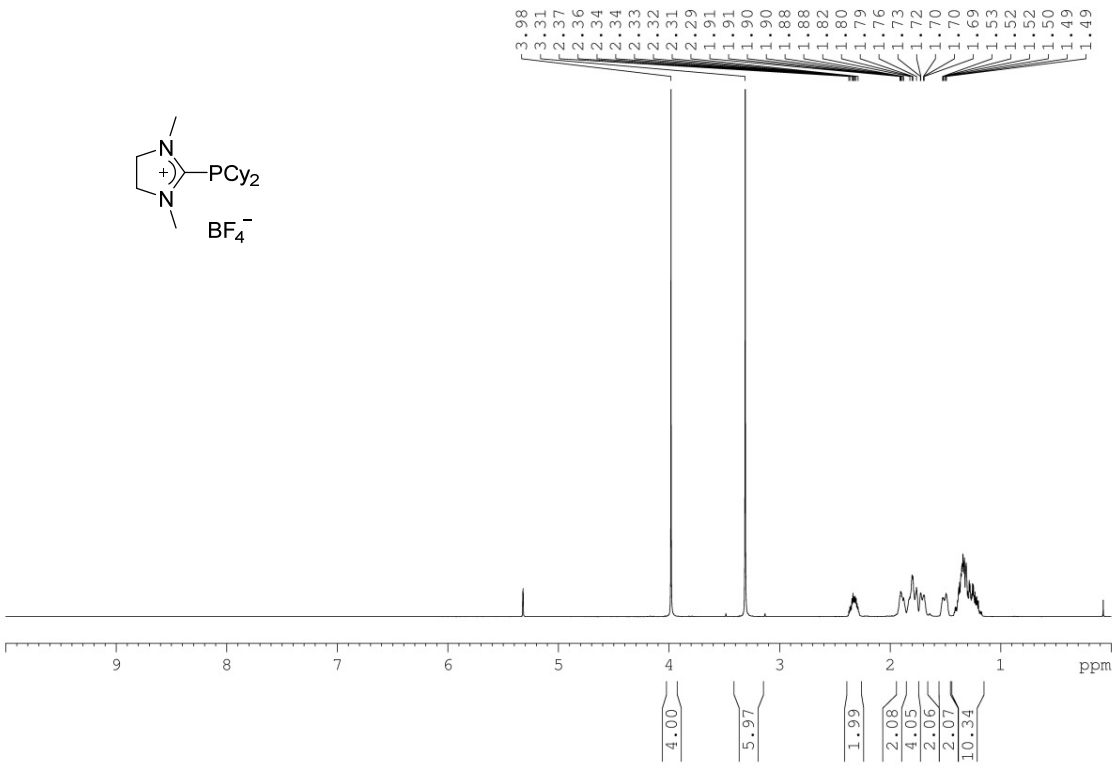

$^{31}P\{^{1}H\}$ NMR spectrum (162 MHz, CD_2Cl_2) **2.15**

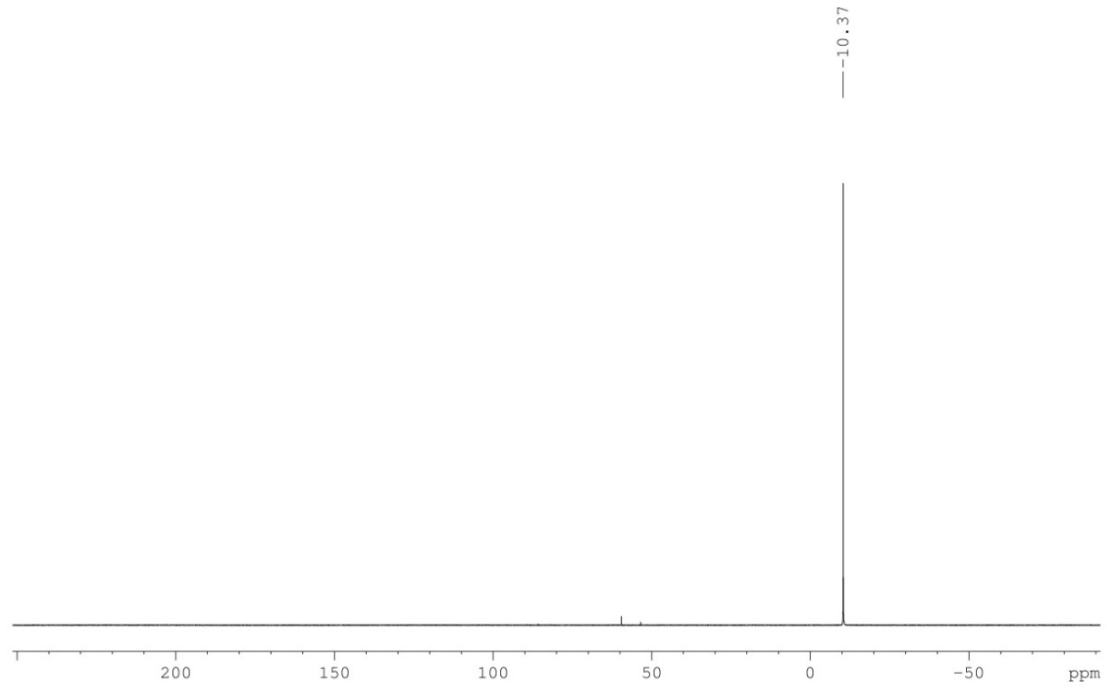

$^{13}C\{^{1}H\}$ NMR spectrum (101 MHz, CD_2Cl_2) **2.15**

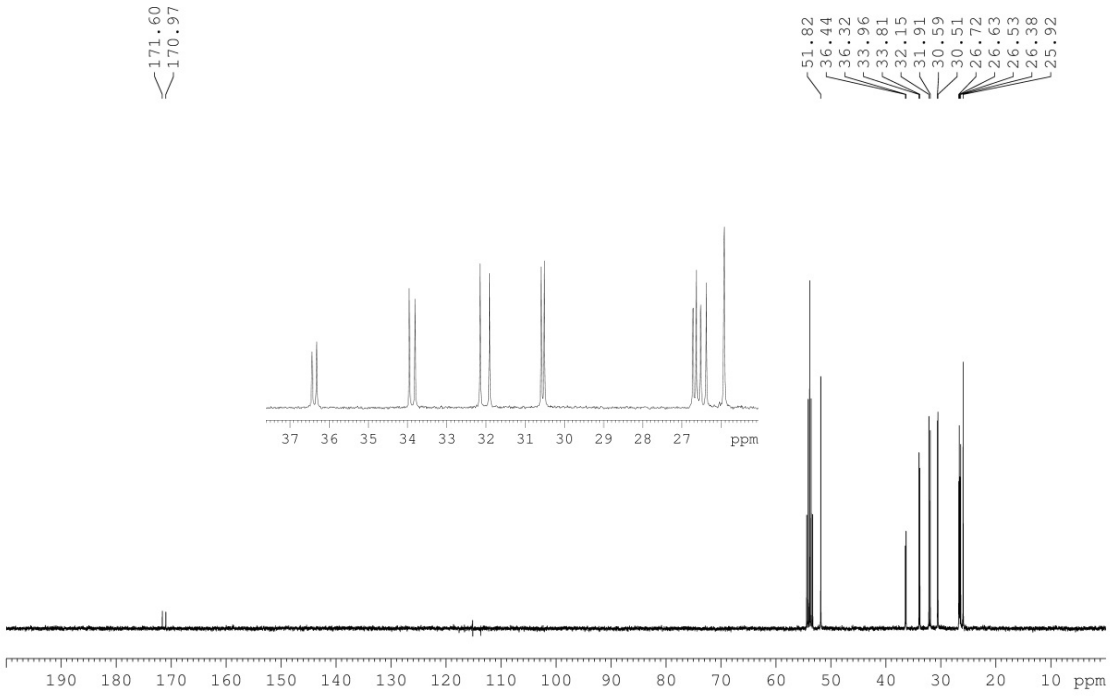

^{1}H NMR spectrum (400 MHz, $CDCl_3$) **2.16**

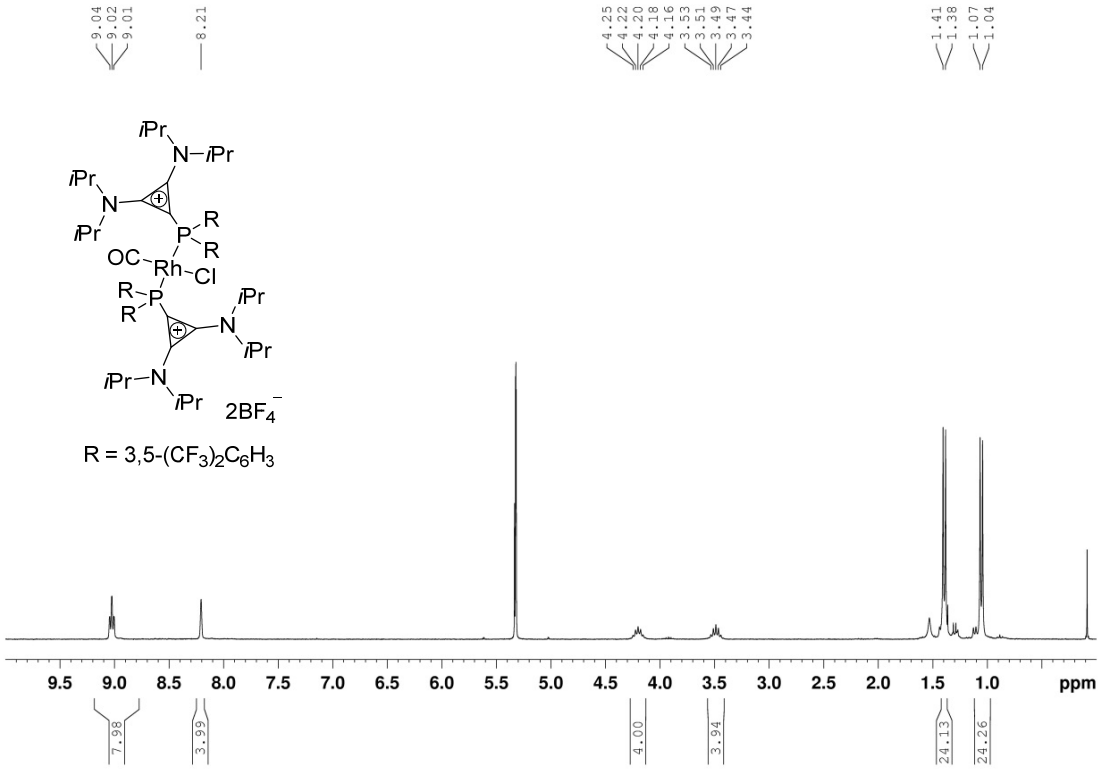

^{31}P NMR spectrum (162 MHz, CD_2Cl_2) **2.16**

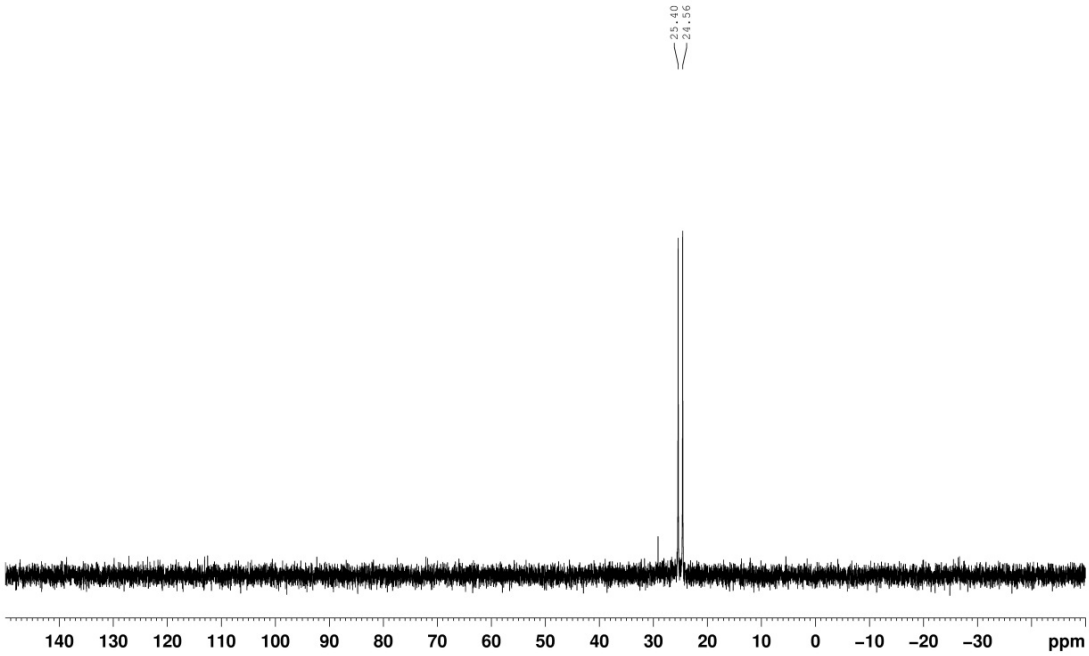

^{19}F NMR (282 MHz, CD_2Cl_2) **2.16**

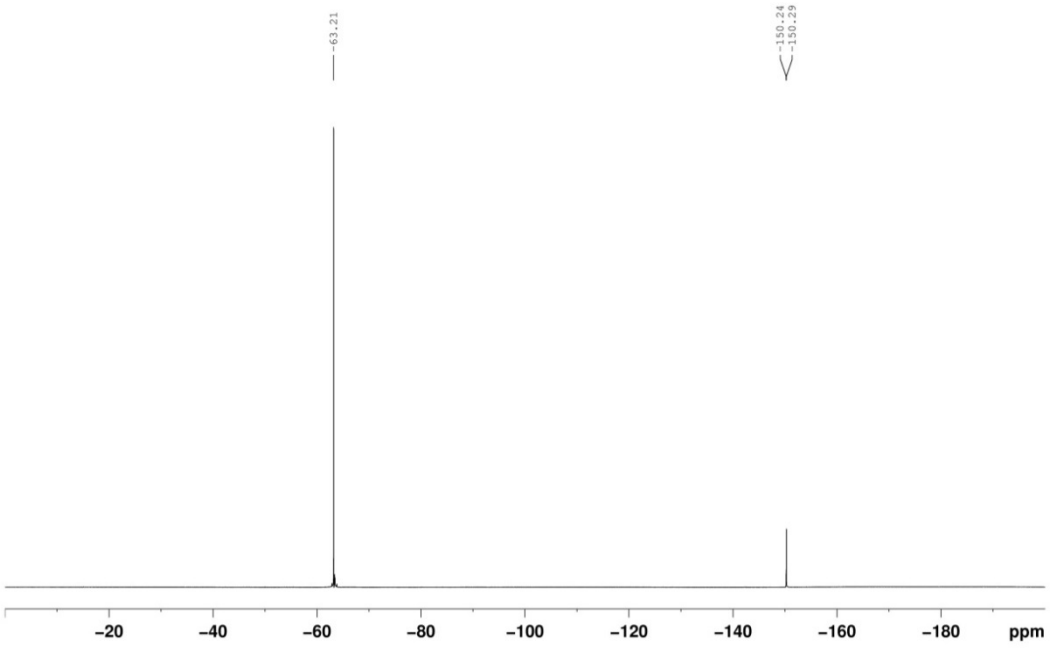

^{1}H NMR spectrum (300 MHz, CD_2Cl_2) **2.17**

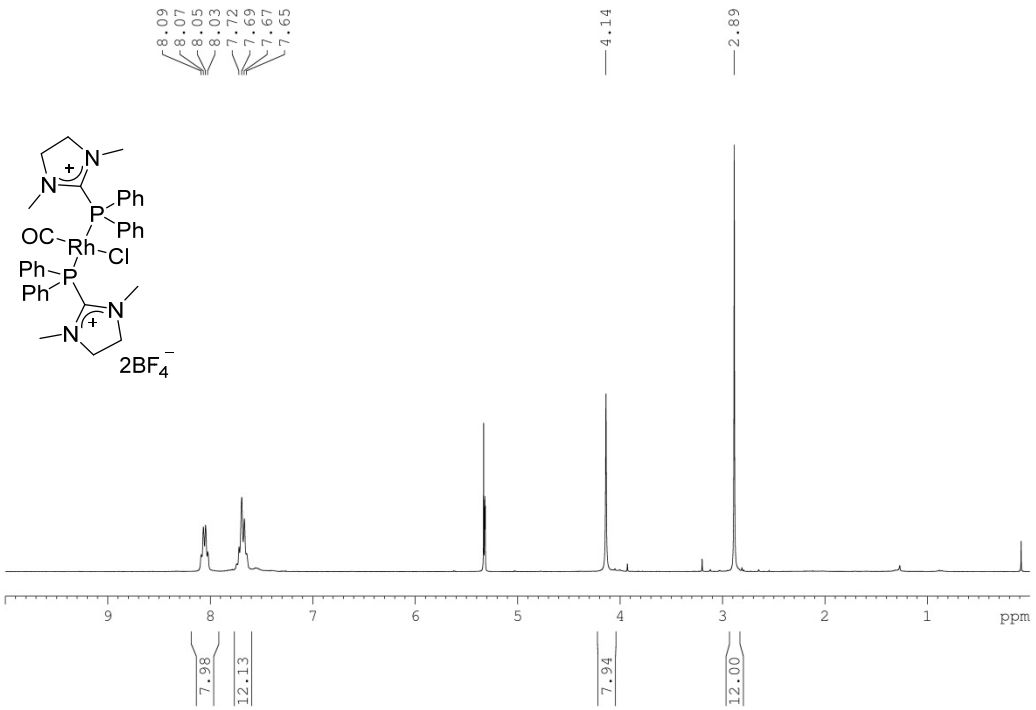

$^{31}P\{^{1}H\}$ NMR spectrum (121 MHz, CD_2Cl_2) **2.17**

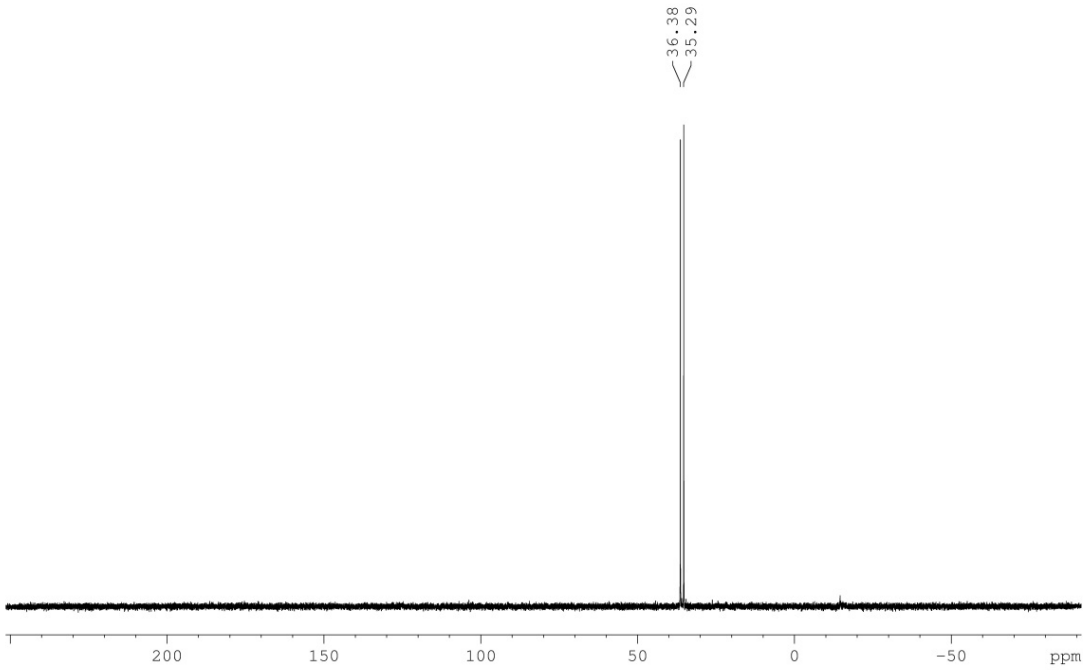

$^{13}C\{^{1}H\}$ NMR spectrum (101 MHz, CD_2Cl_2) **2.17**

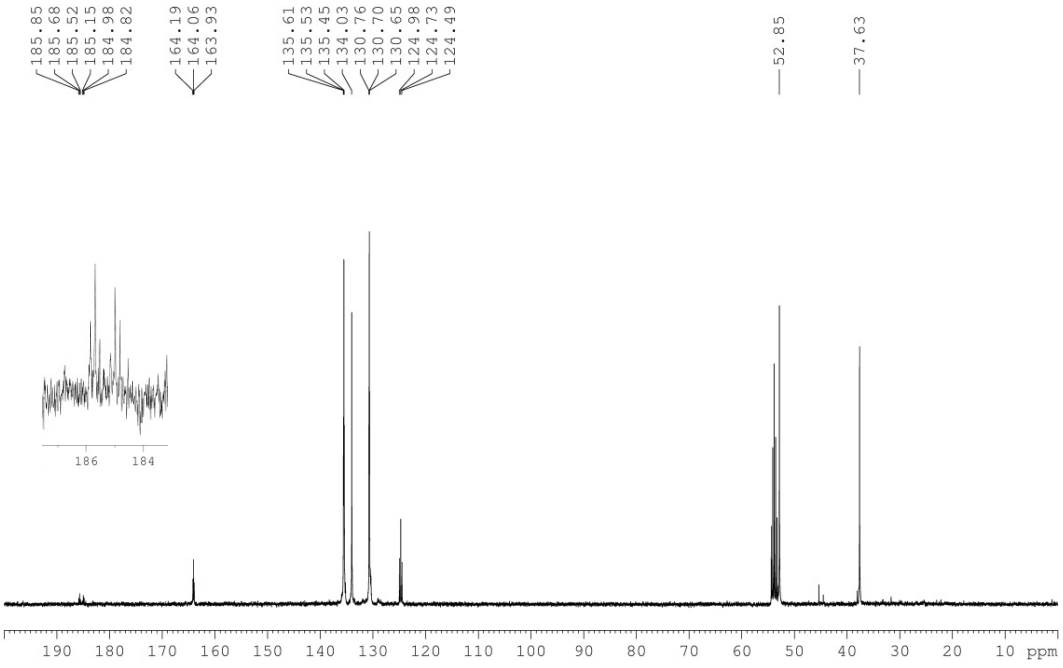

^{1}H NMR spectrum (400 MHz, CD_2Cl_2) **2.20**

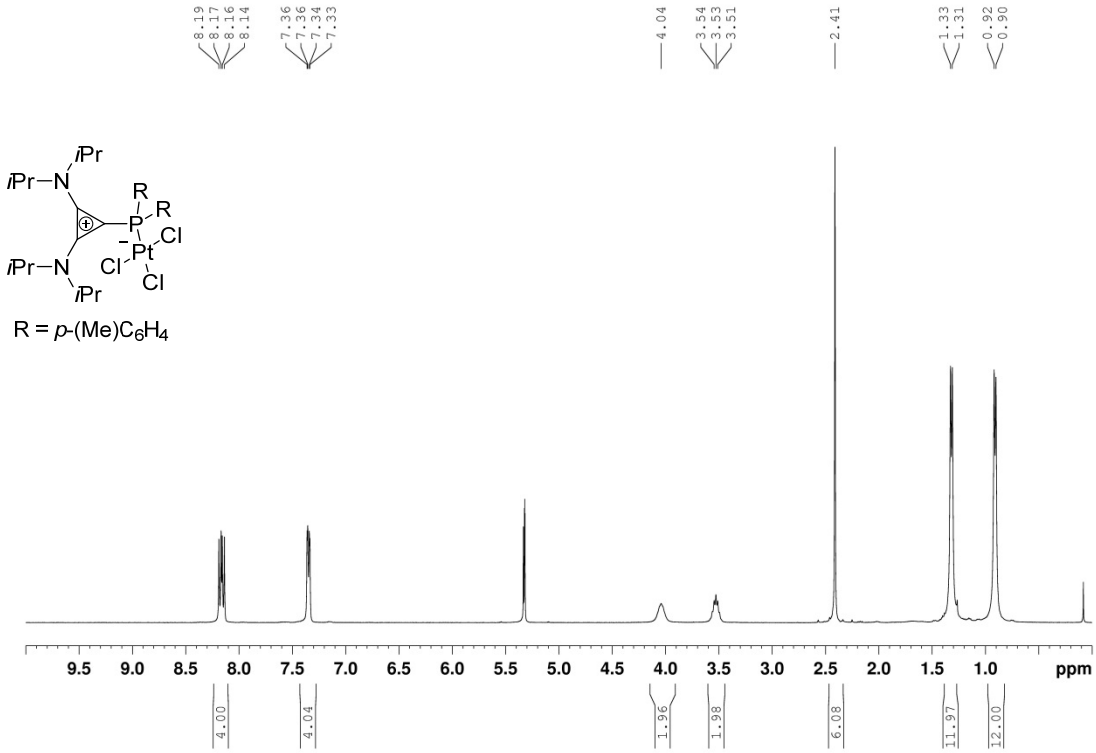

^{31}P NMR spectrum (162 MHz, CD_2Cl_2) **2.20**

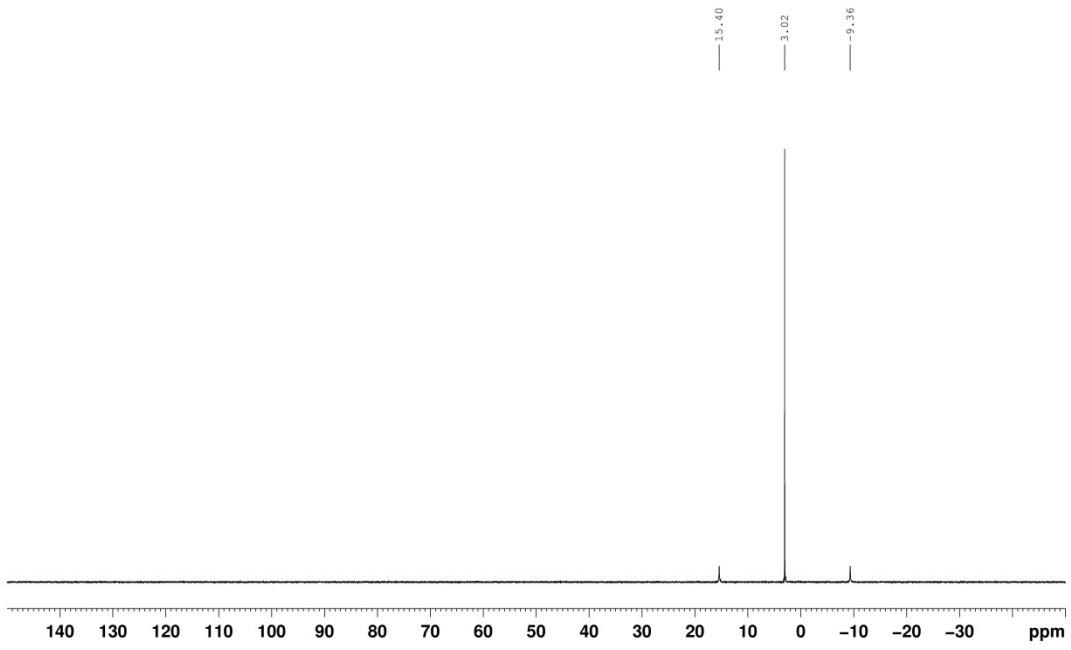

^{13}C NMR spectrum (101 MHz, CD_2Cl_2) **2.20**

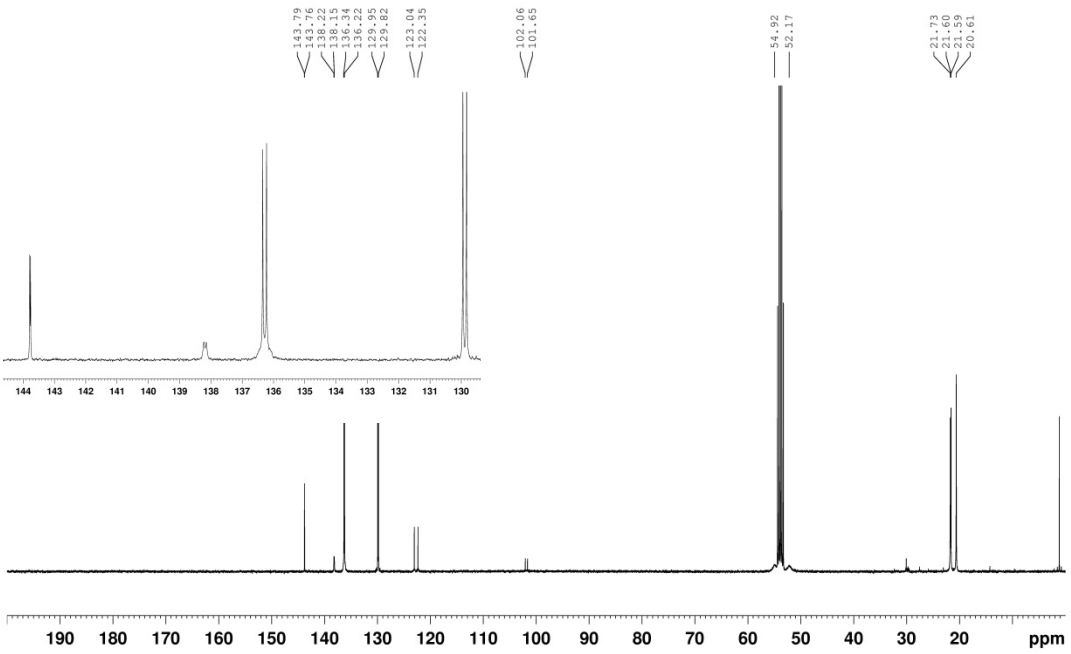

^{1}H NMR spectrum (400 MHz, CD_3CN) **2.21**

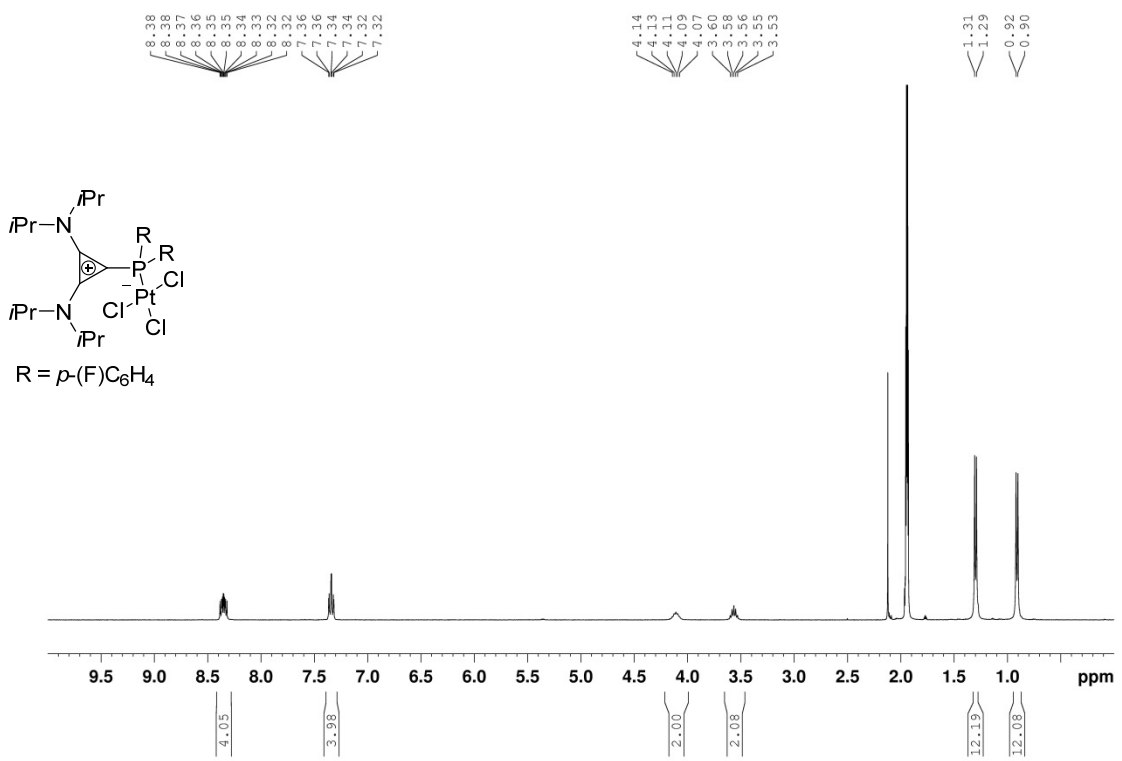

^{31}P NMR spectrum (162 MHz, CD_3CN) **2.21**

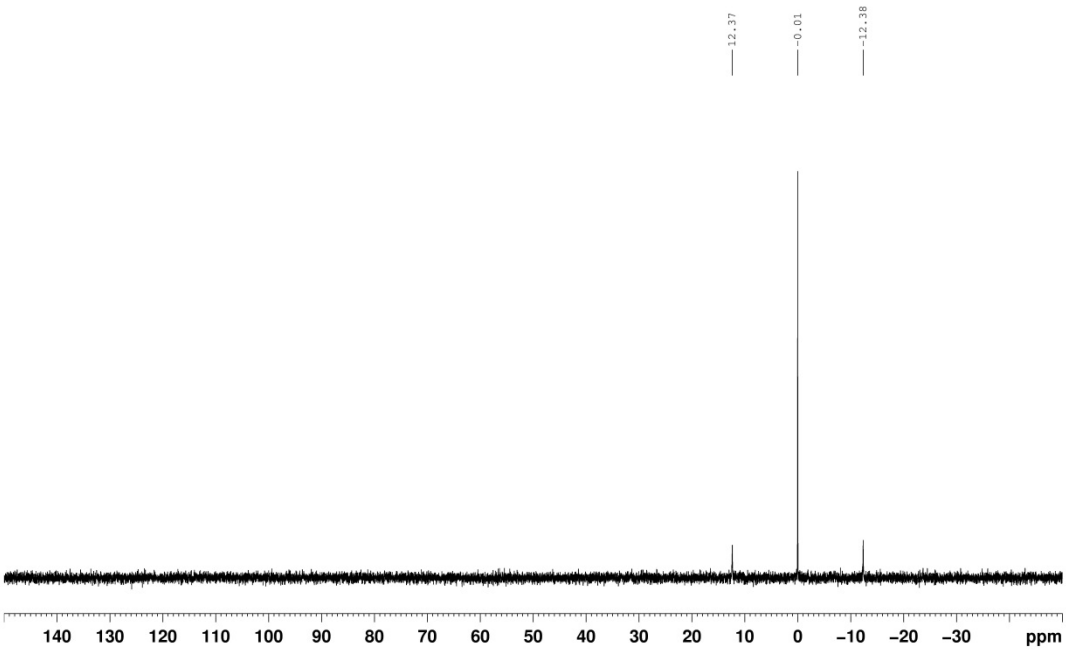

^{19}F NMR spectrum (282 MHz, CD_3CN) **2.21**

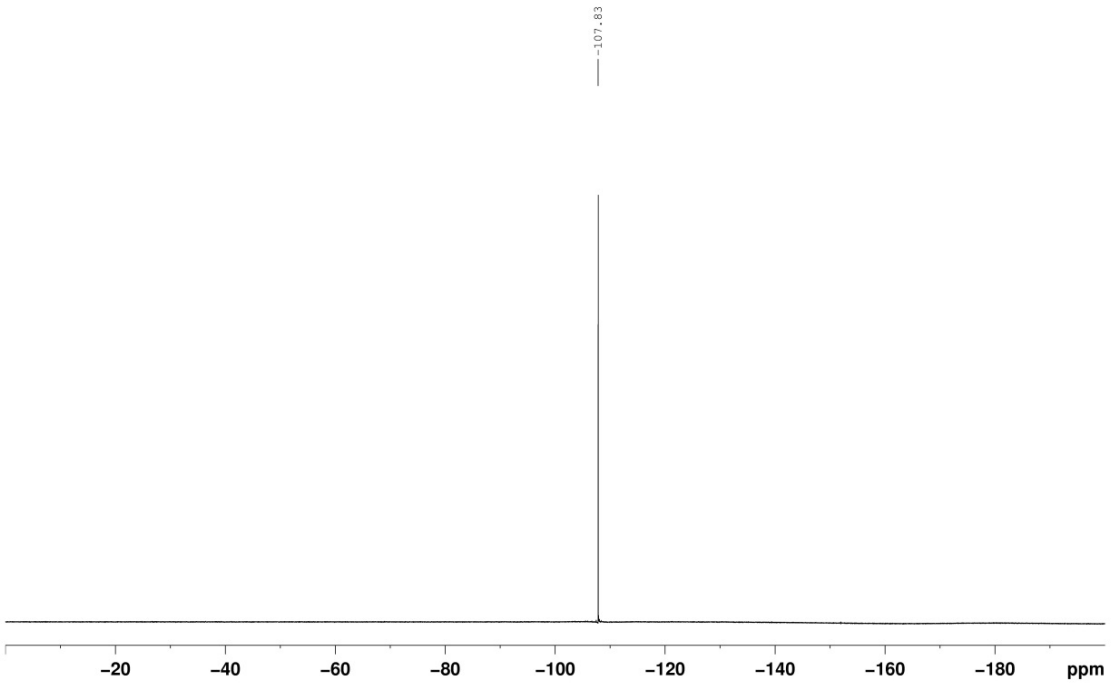

^{13}C NMR spectrum (101 MHz, CD_2Cl_2) **2.21**

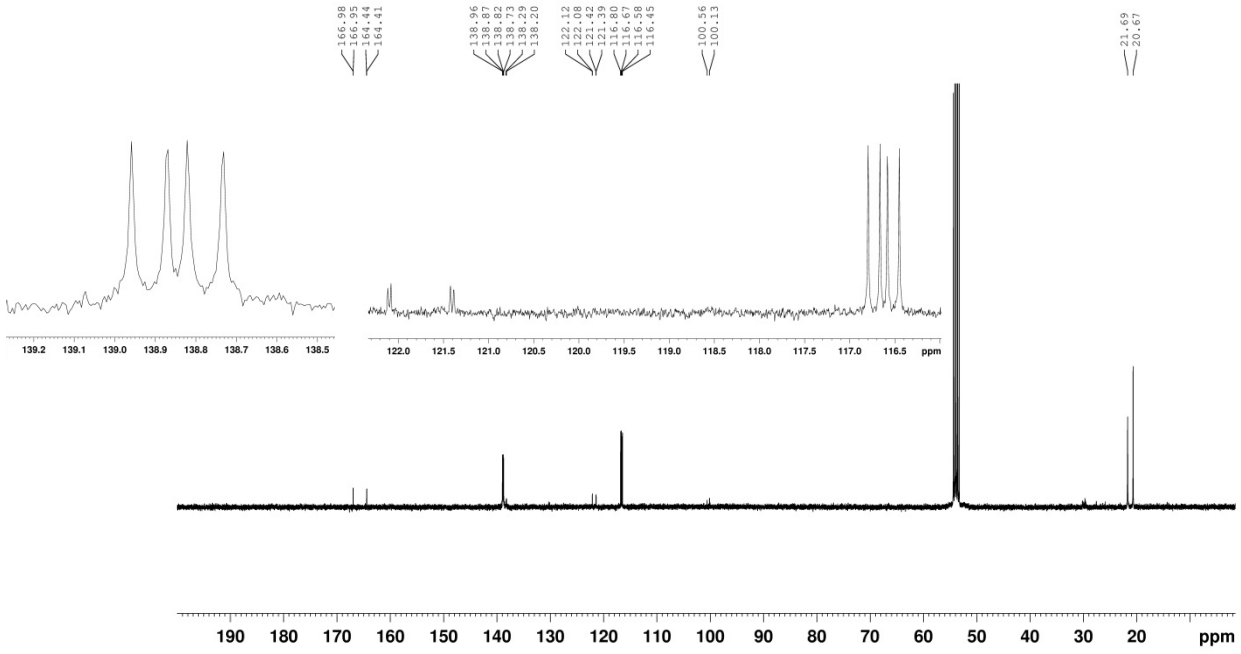

^{1}H NMR spectrum (400 MHz, CD_2Cl_2) **2.22**

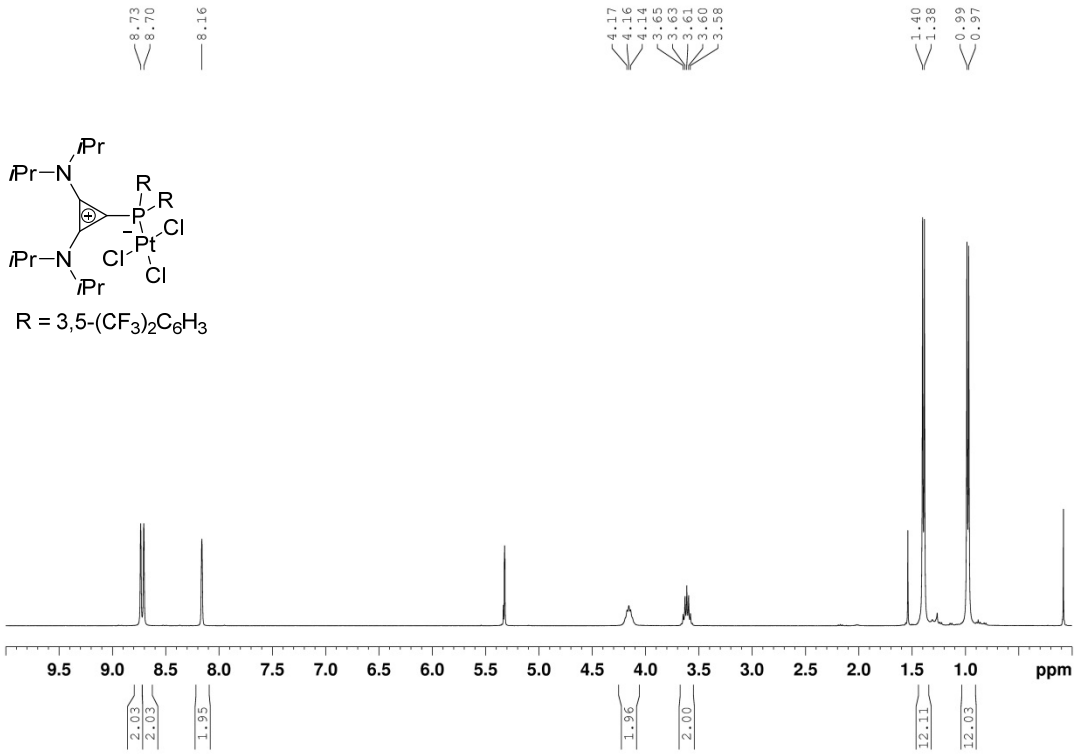

^{31}P NMR spectrum (121 MHz, CD_2Cl_2) **2.22**

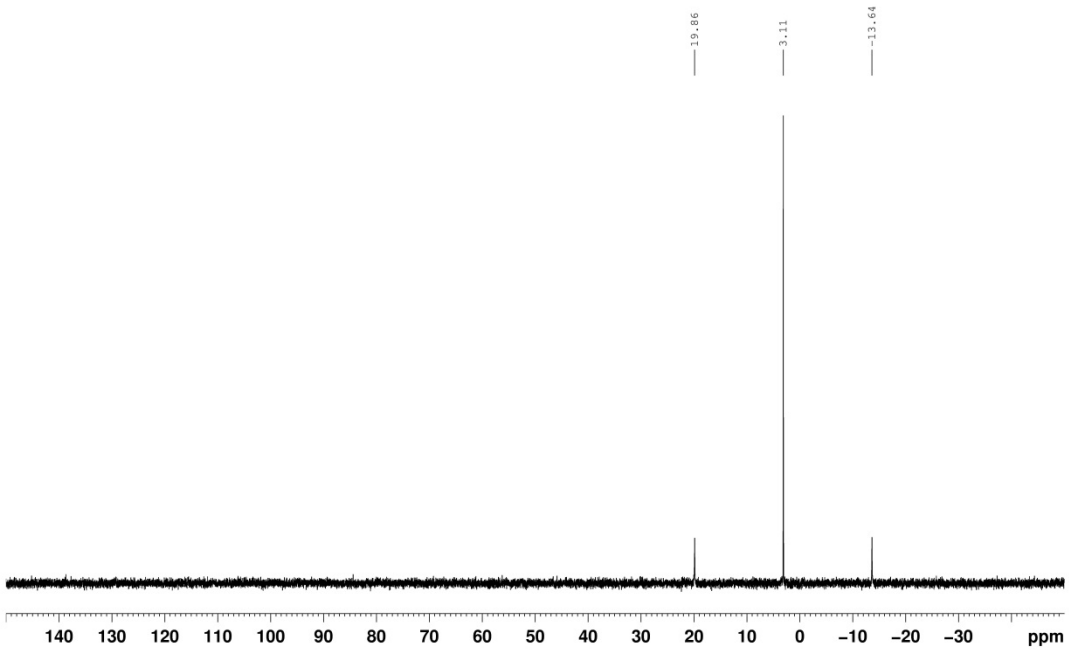

^{19}F NMR spectrum (282 MHz, CD_2Cl_2) **2.22**

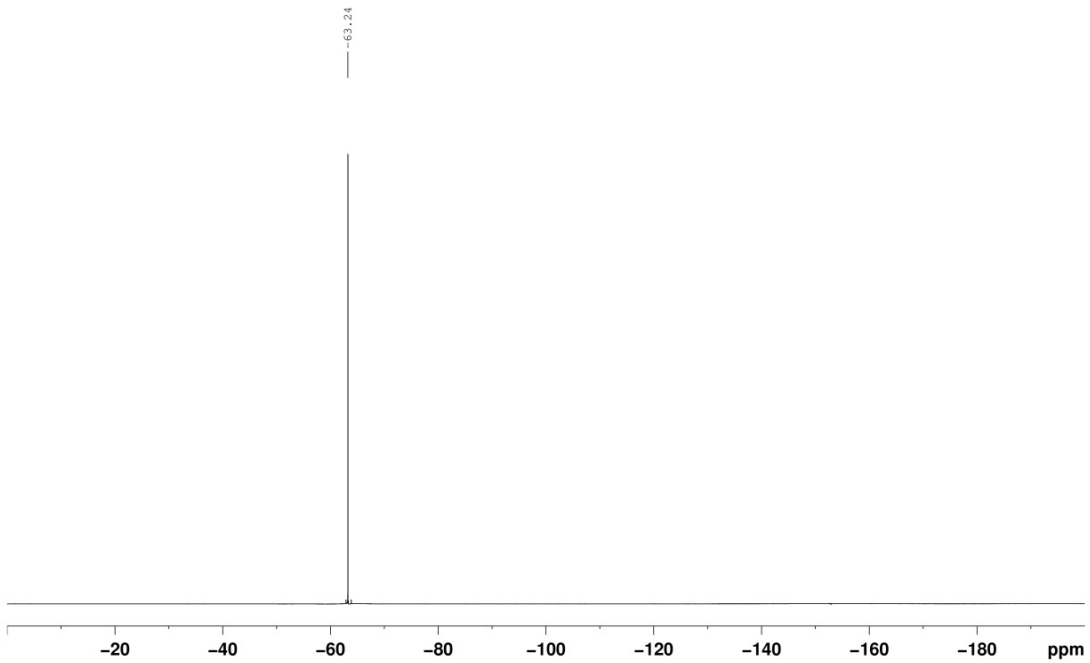

^{13}C NMR spectrum (101 MHz , CD_2Cl_2) **2.22**

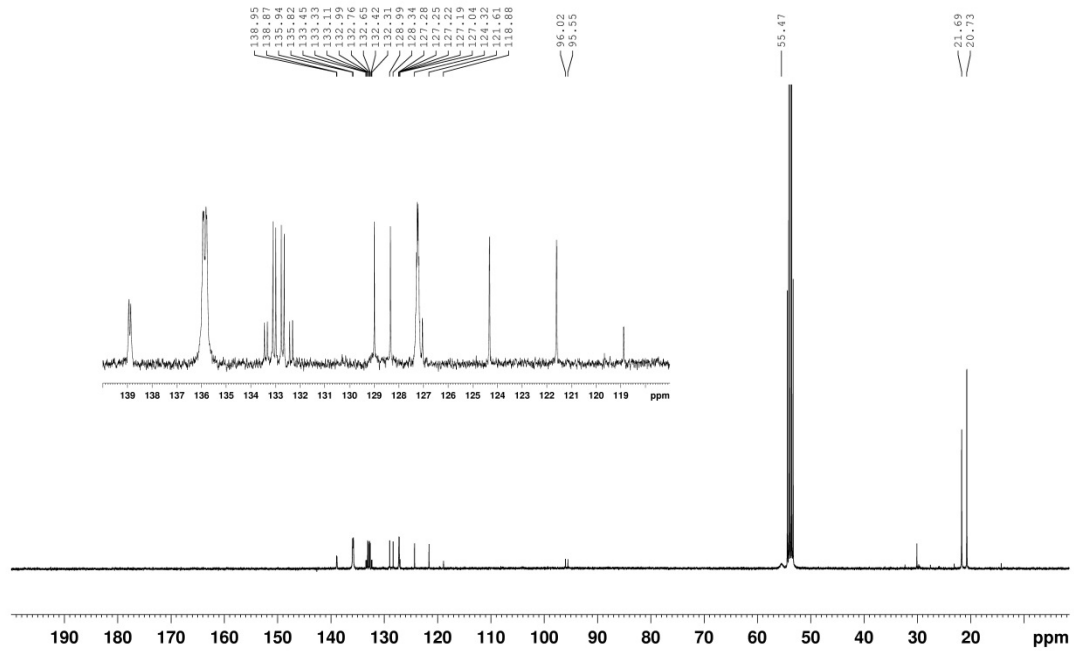

^{1}H NMR spectrum (400 MHz, CD_2Cl_2) **2.25**

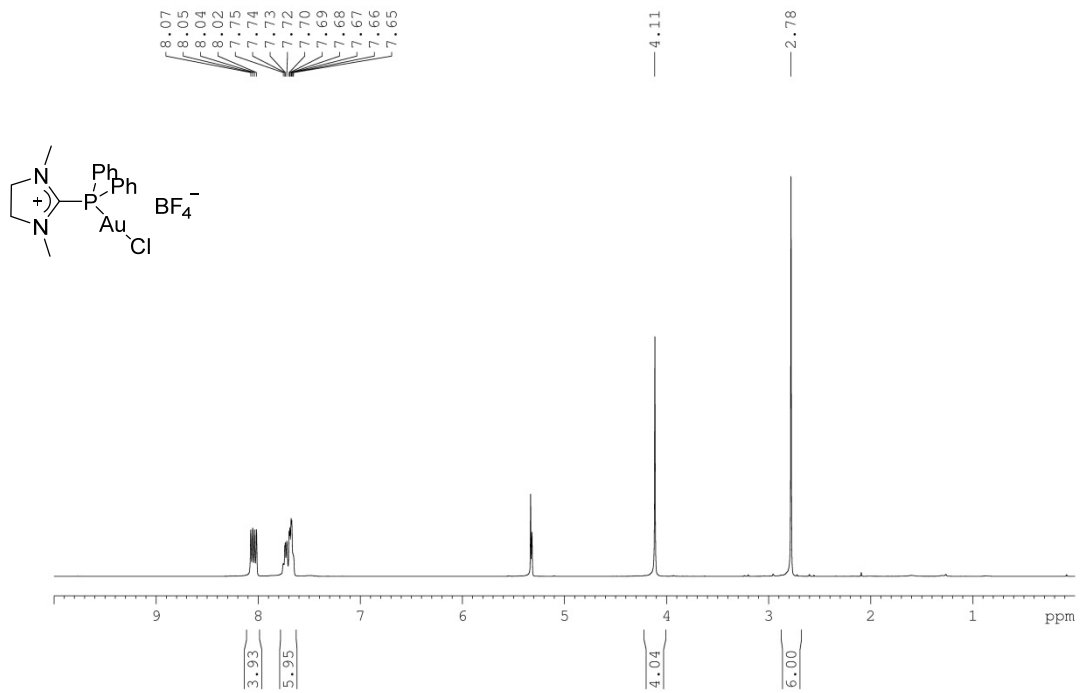

$^{31}P\{^{1}H\}$ NMR spectrum (162 MHz, CD_2Cl_2) **2.25**

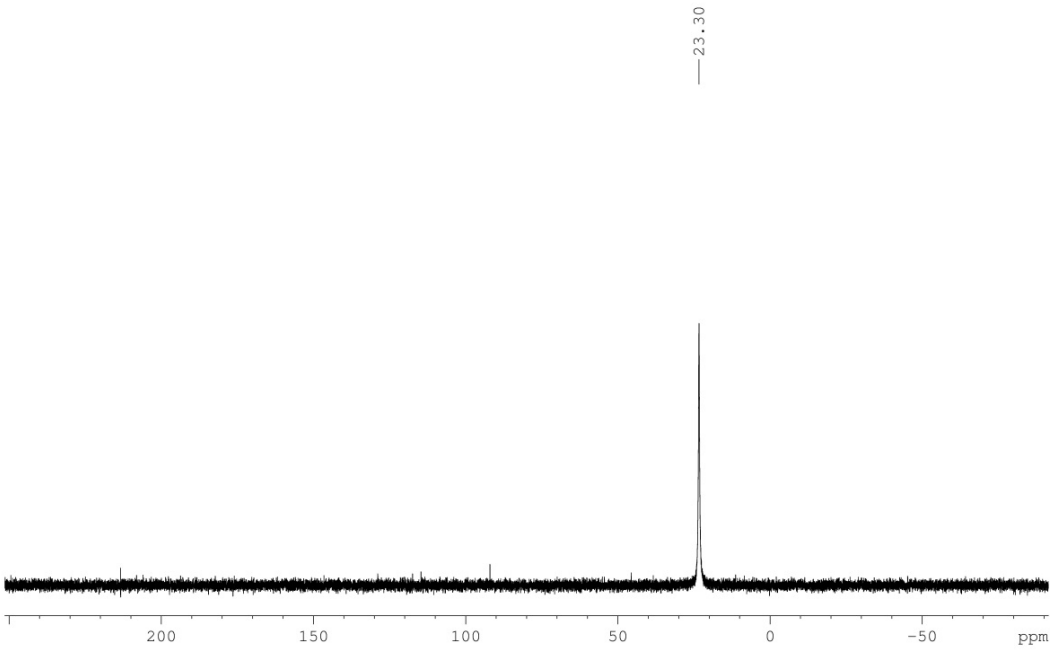

$^{13}C\{^{1}H\}$ NMR spectrum (101 MHz, CD_2Cl_2) **2.25**

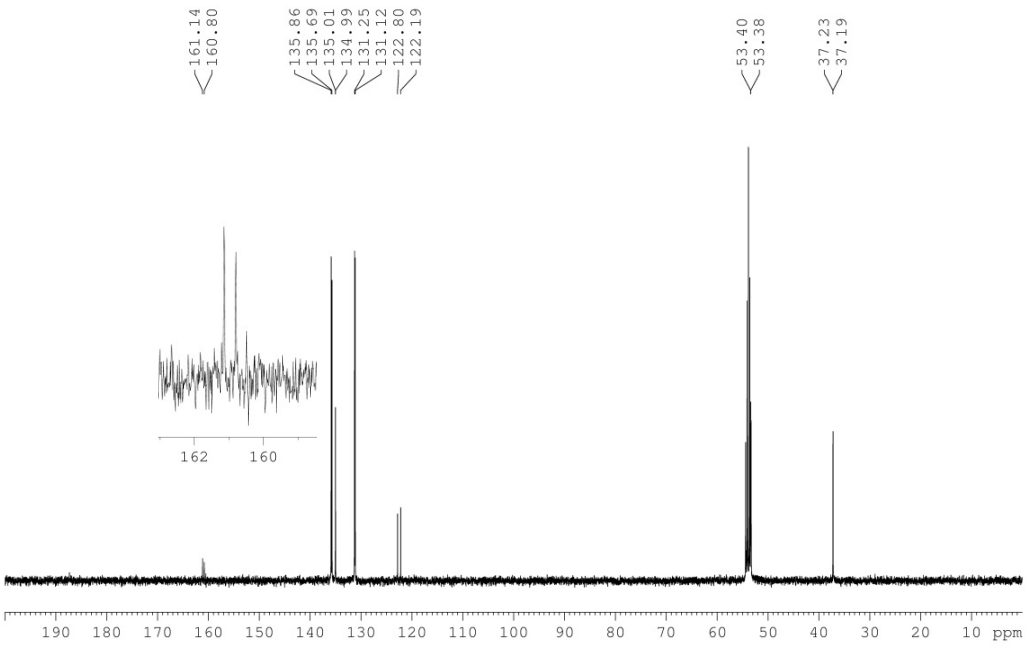

^{1}H NMR spectrum (400 MHz, CD_3CN) **2.26**

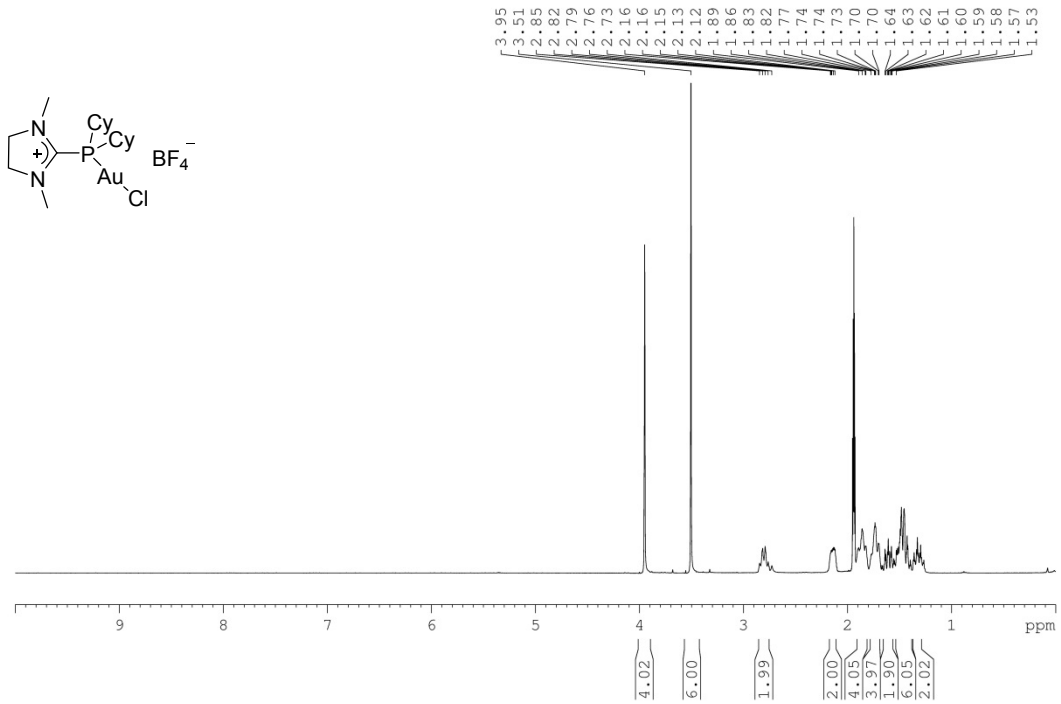

^{31}P{^{1}H} NMR spectrum (162 MHz, CD_3CN) **2.26**

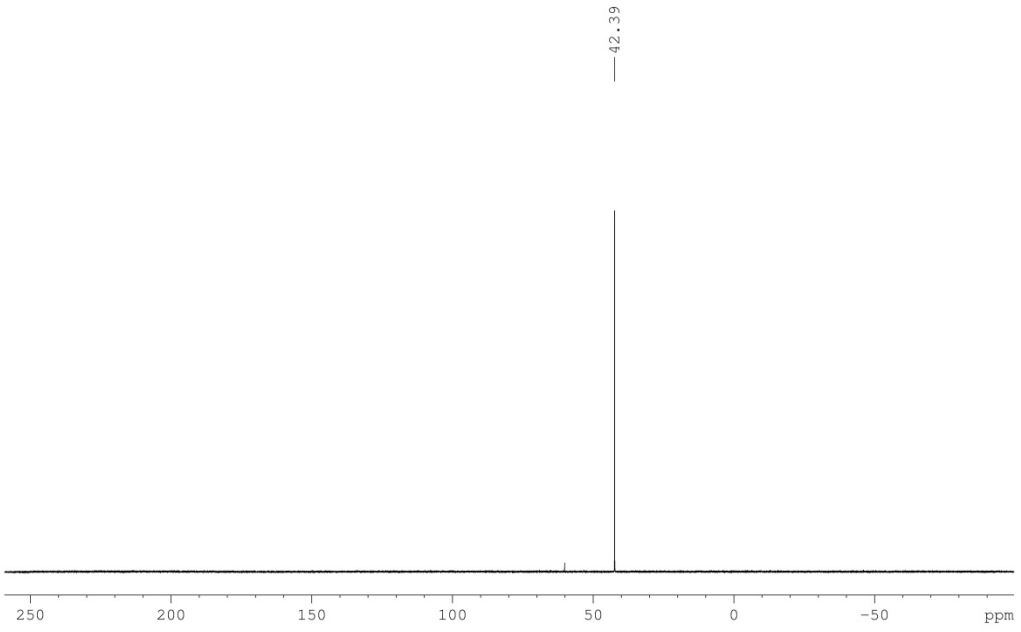

$^{13}C\{^{1}H\}$ NMR spectrum (101 MHz, CD_2Cl_2) **2.26**

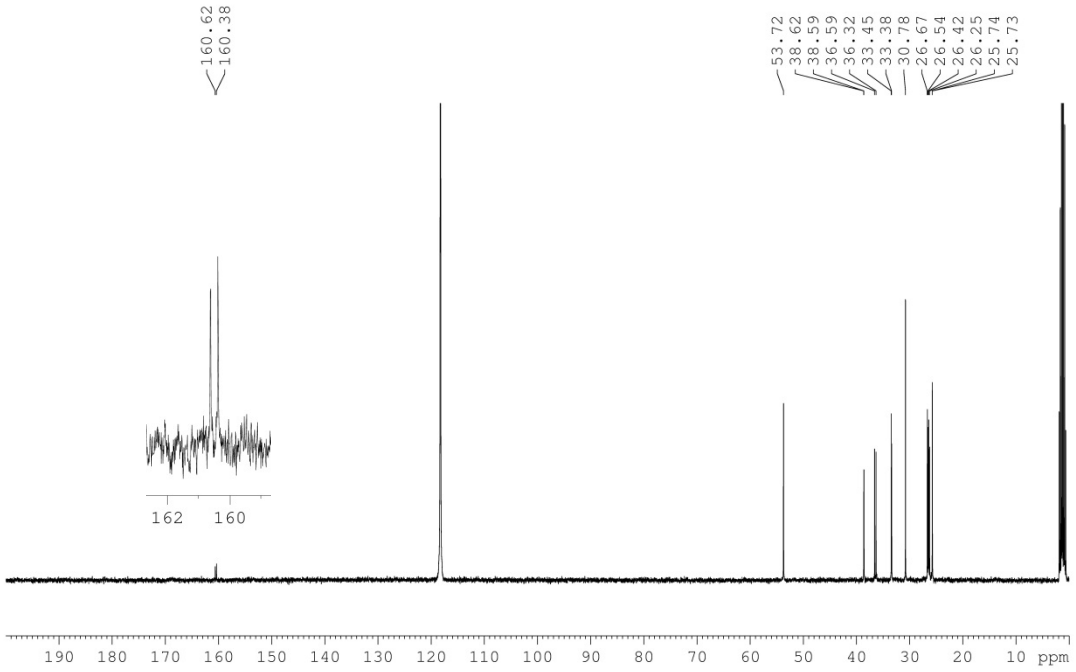

^{1}H NMR spectrum (300 MHz, CD_2Cl_2) **2.27**

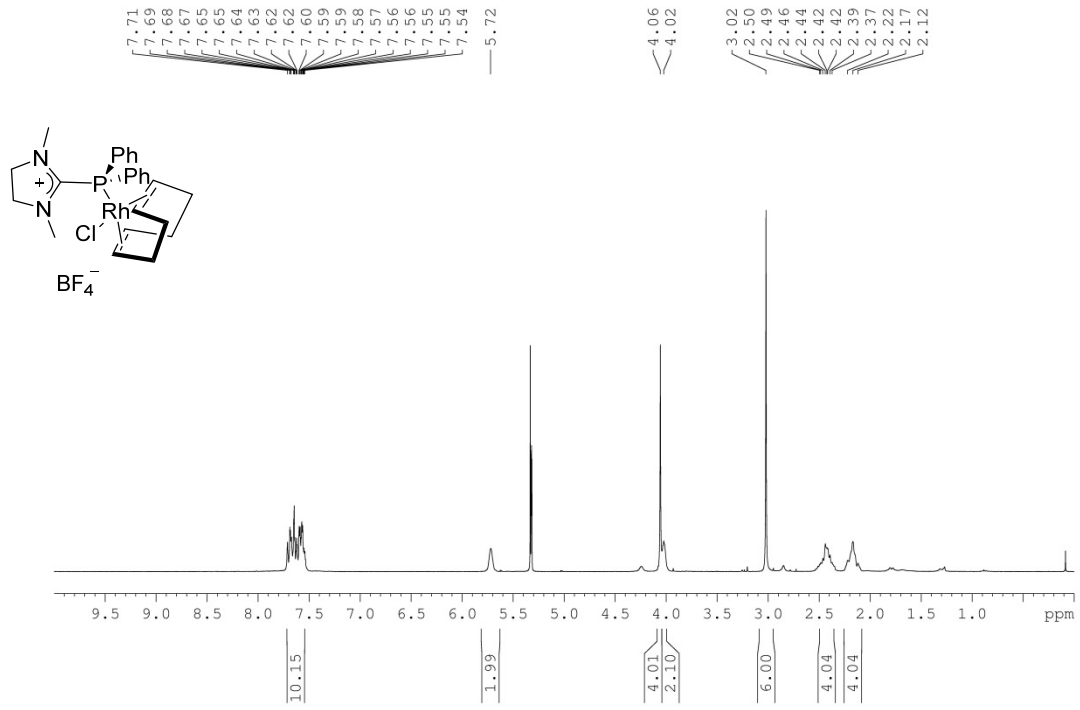

$^{31}P\{^{1}H\}$ NMR spectrum (121 MHz, CD_2Cl_2) **2.27**

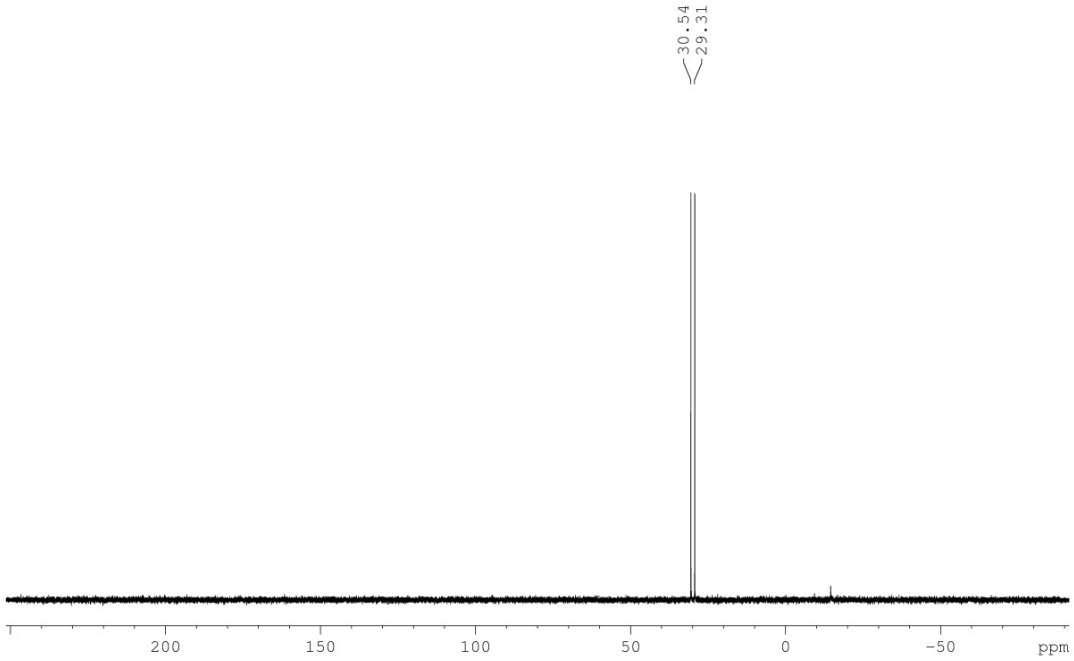

$^{13}C\{^{1}H\}$ NMR spectrum (101 MHz, CD_2Cl_2) **2.27**

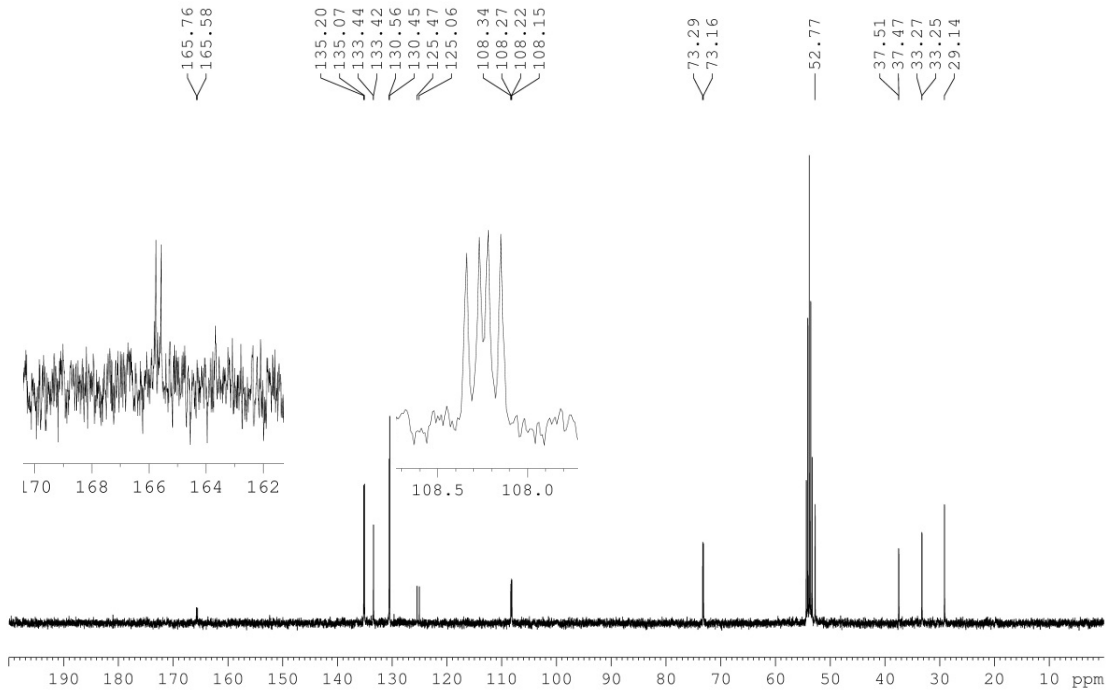

^{1}H NMR spectrum (400 MHz, CD_2Cl_2) **2.29**

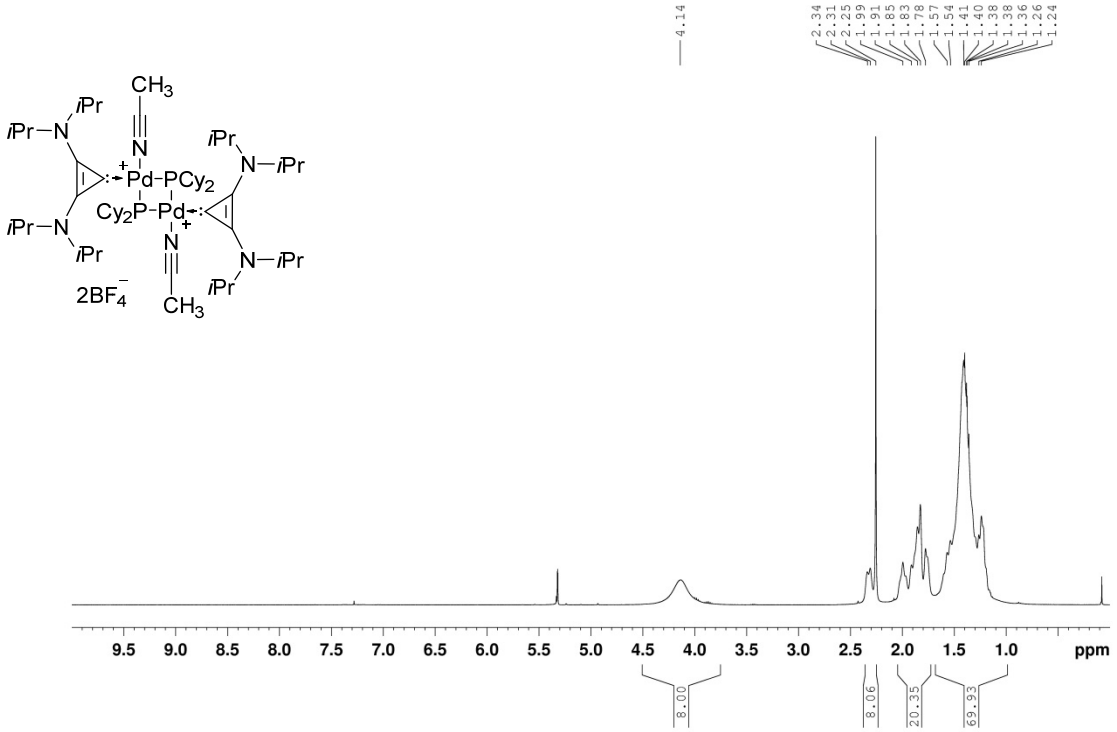

^{31}P{^{1}H} NMR spectrum (162 MHz, CD_2Cl_2) **2.29**

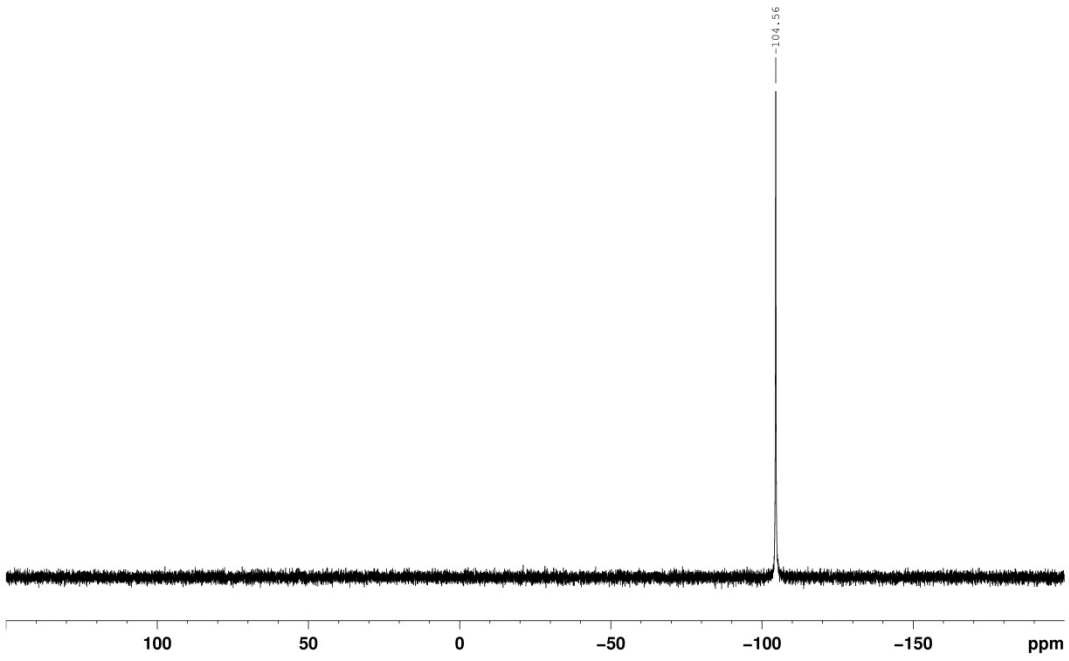

$^{13}C\{^{1}H\}$ NMR spectrum (101 MHz, CD_2Cl_2) **2.29**

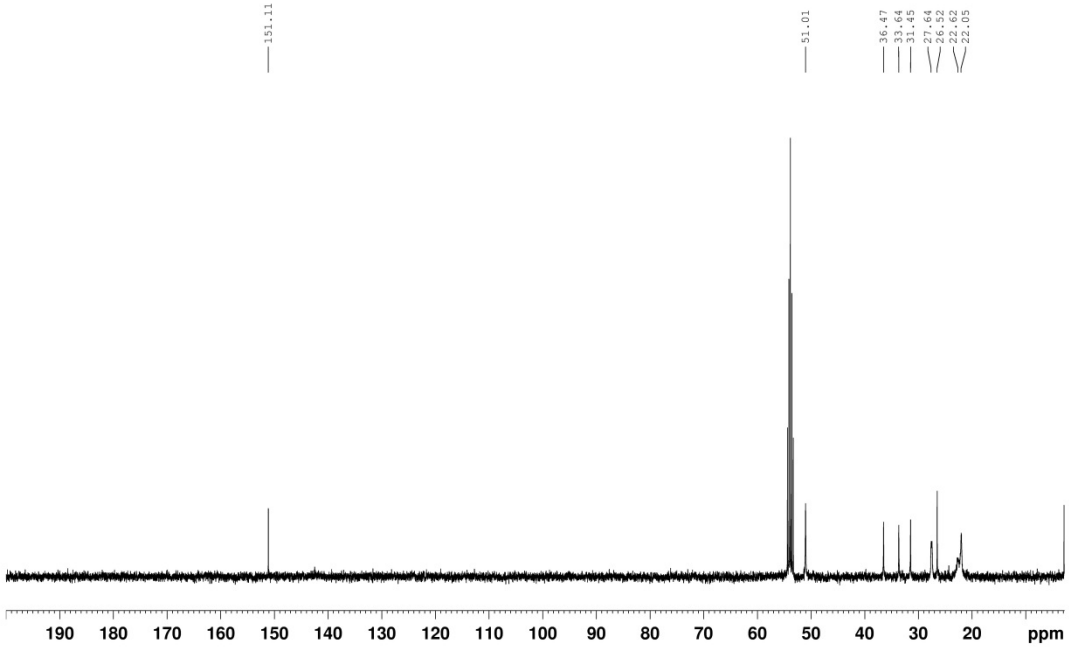

^{1}H NMR spectrum (400 MHz, CD_2Cl_2) **2.30**

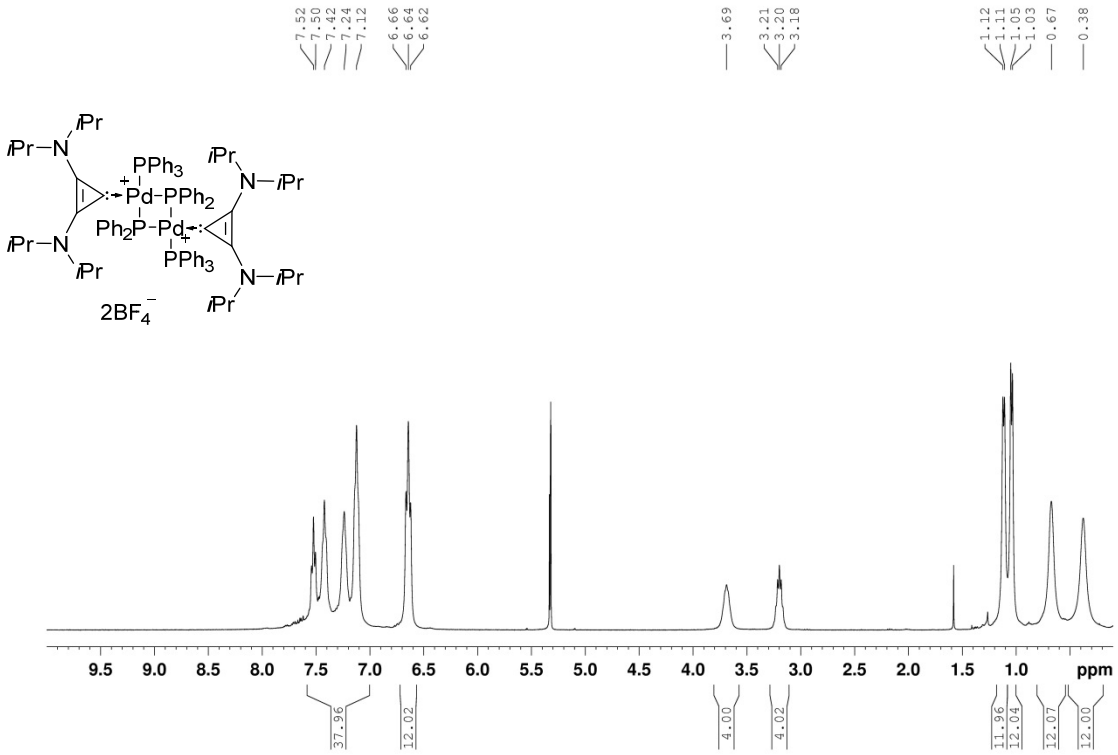

$^{31}P\{^{1}H\}$ NMR spectrum (162 MHz, CD_2Cl_2) **2.30**

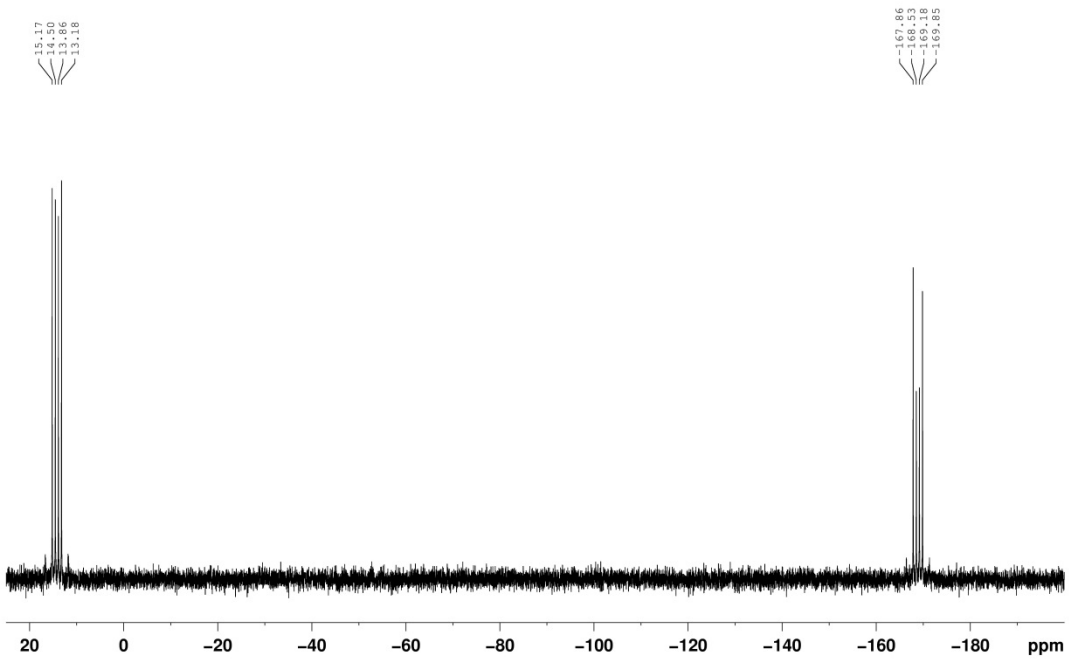

$^{13}C\{^{1}H\}$ NMR spectrum (101 MHz, CD_2Cl_2) **2.30**

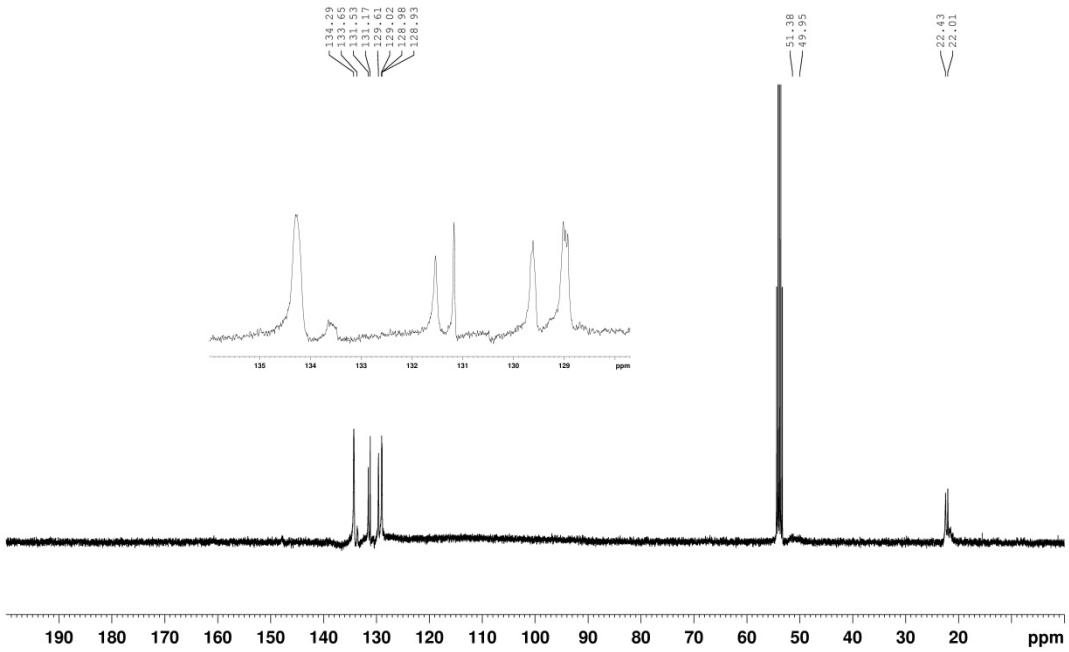

^{1}H NMR spectrum (400 MHz, $CDCl_3$) **2.33**

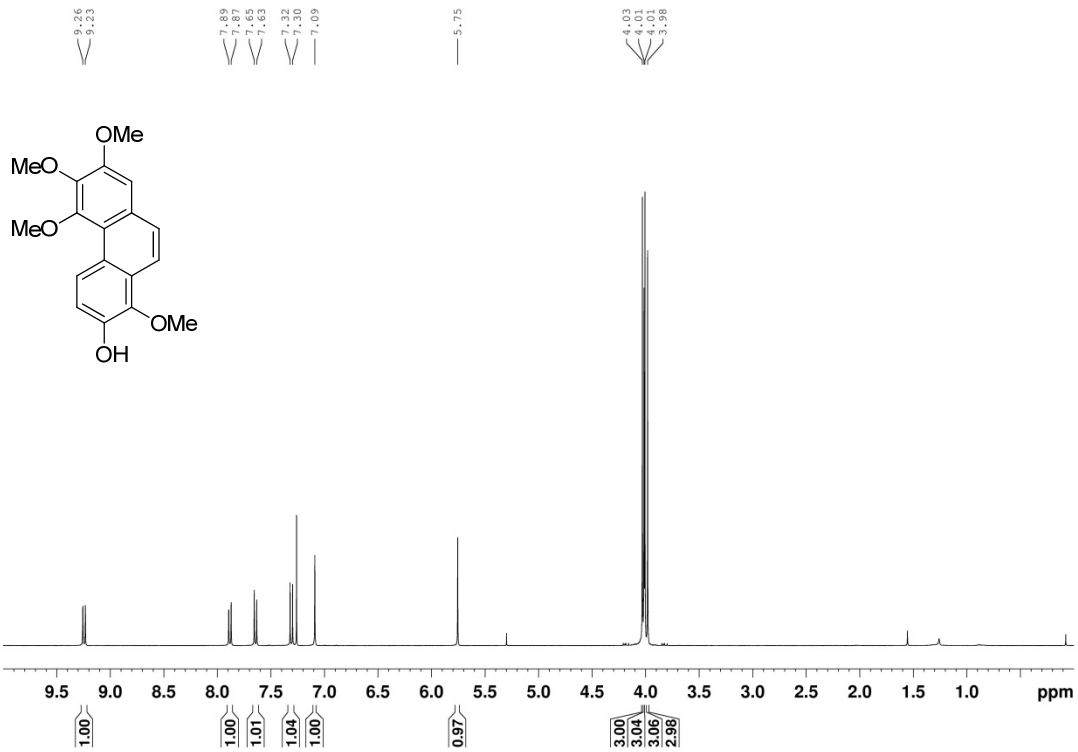

^{13}C{^{1}H} NMR spectrum (151 MHz, $CDCl_3$, LB = 0.8) **2.33**

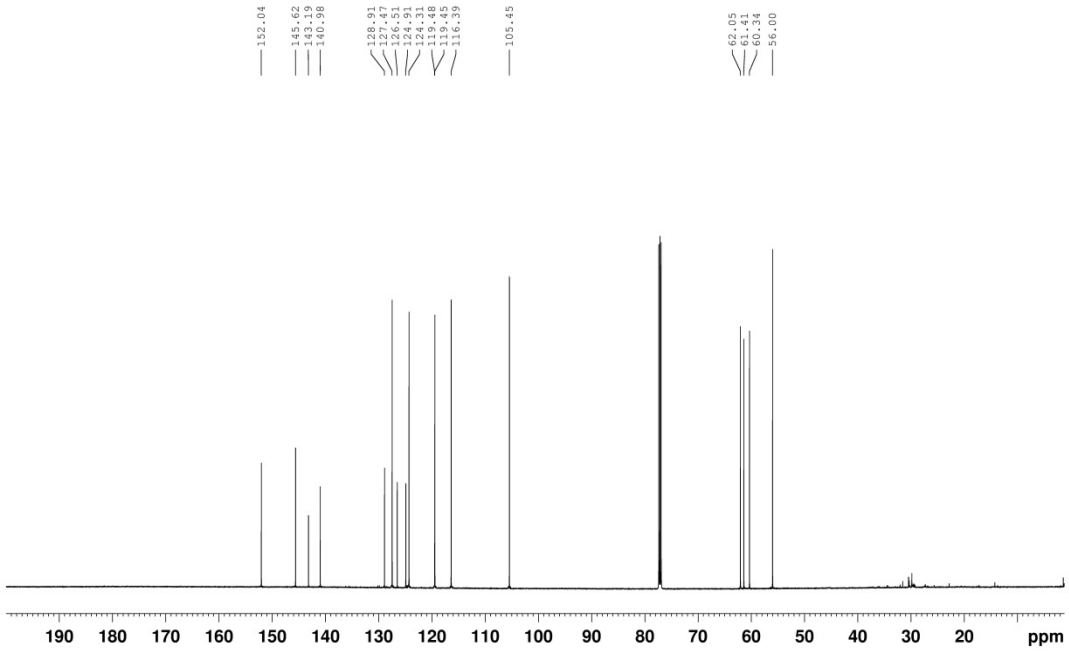

$^{13}C\{^{1}H\}$ NMR spectrum (151 MHz, $CDCl_3$, LB = 0.0) **2.33**

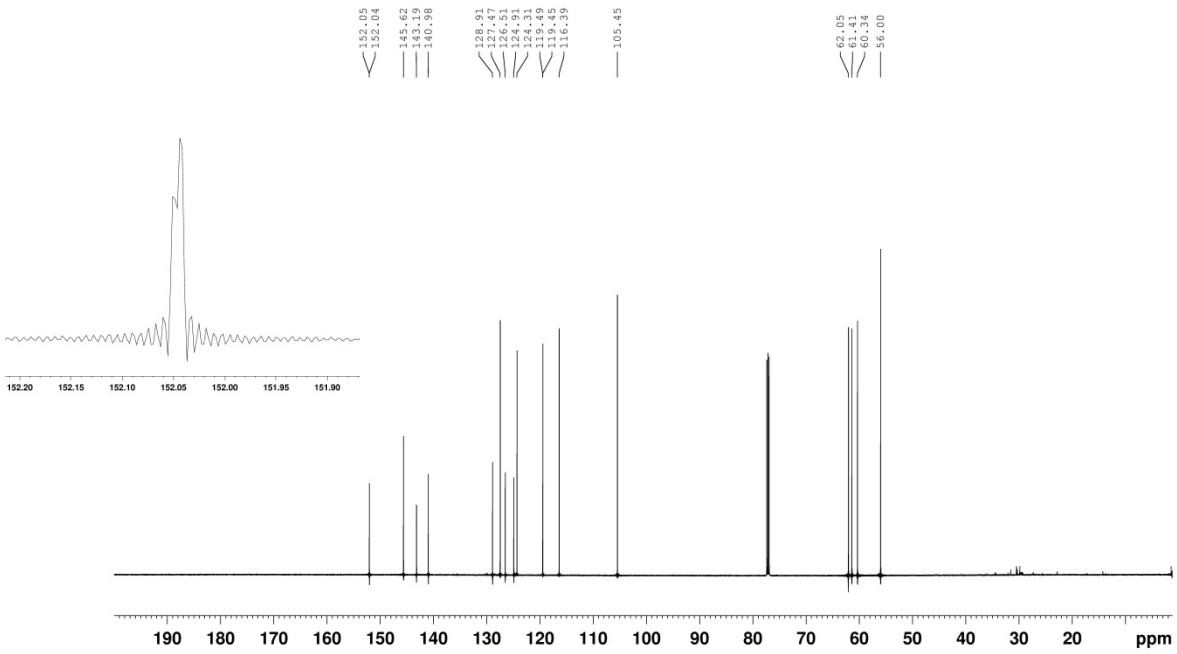

$^{13}C\{^{1}H\}$ NMR - DEPT (151 MHz, $CDCl_3$) **2.33**

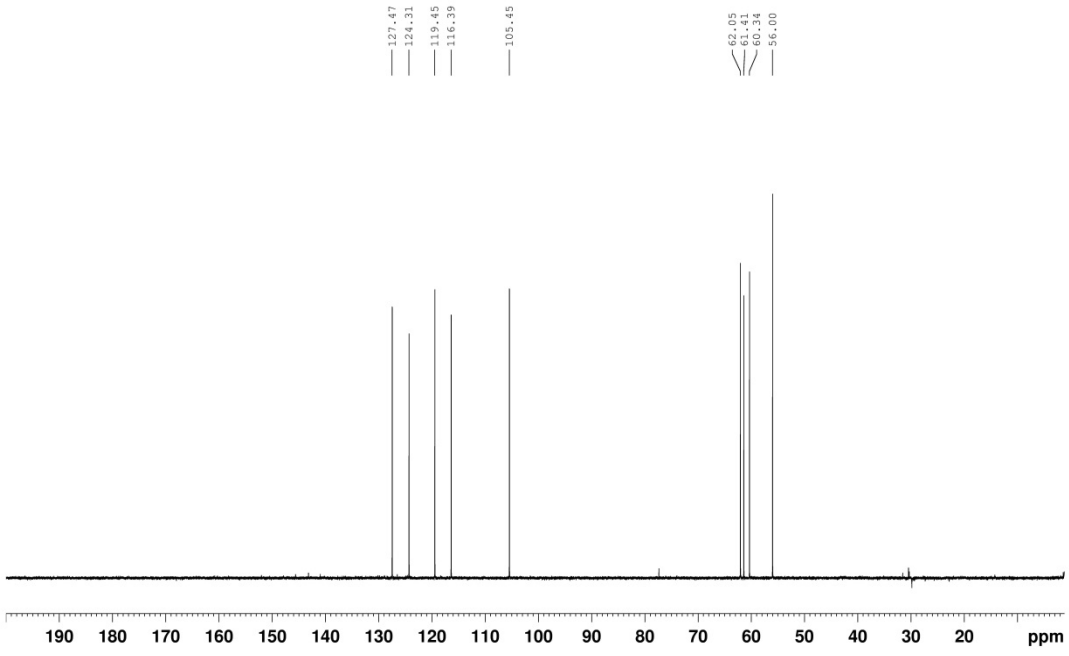

$^{13}C\{^{1}H\}$ NMR – GATED (151 MHz, $CDCl_3$) **2.33**

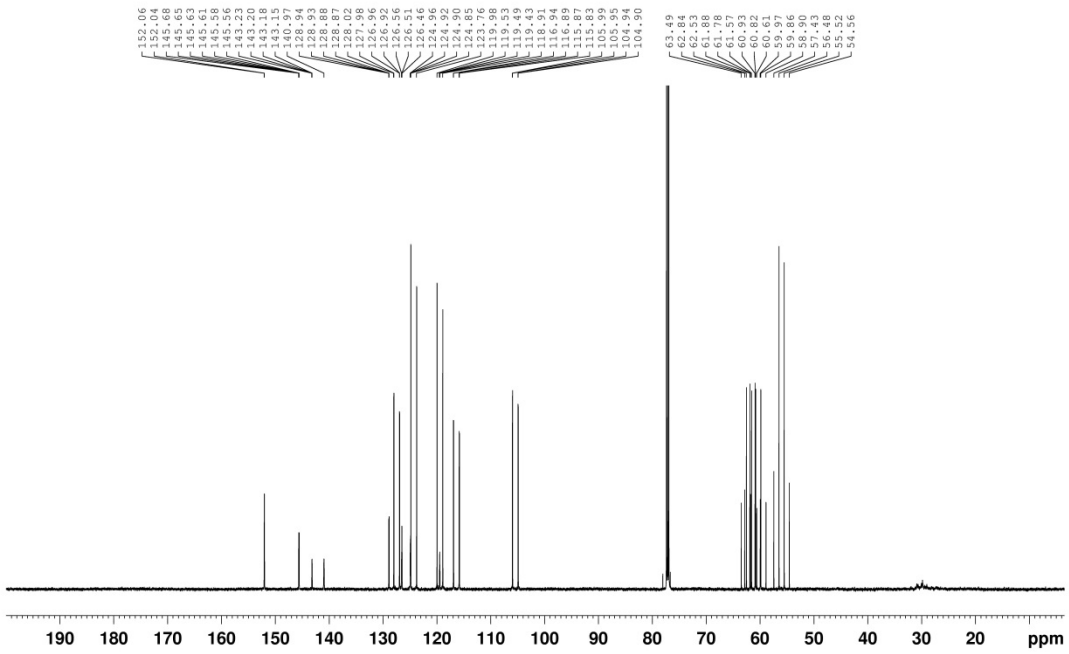

$^{13}C\{^{1}H\}$ NMR - COSY (151 MHz, $CDCl_3$) **2.33**

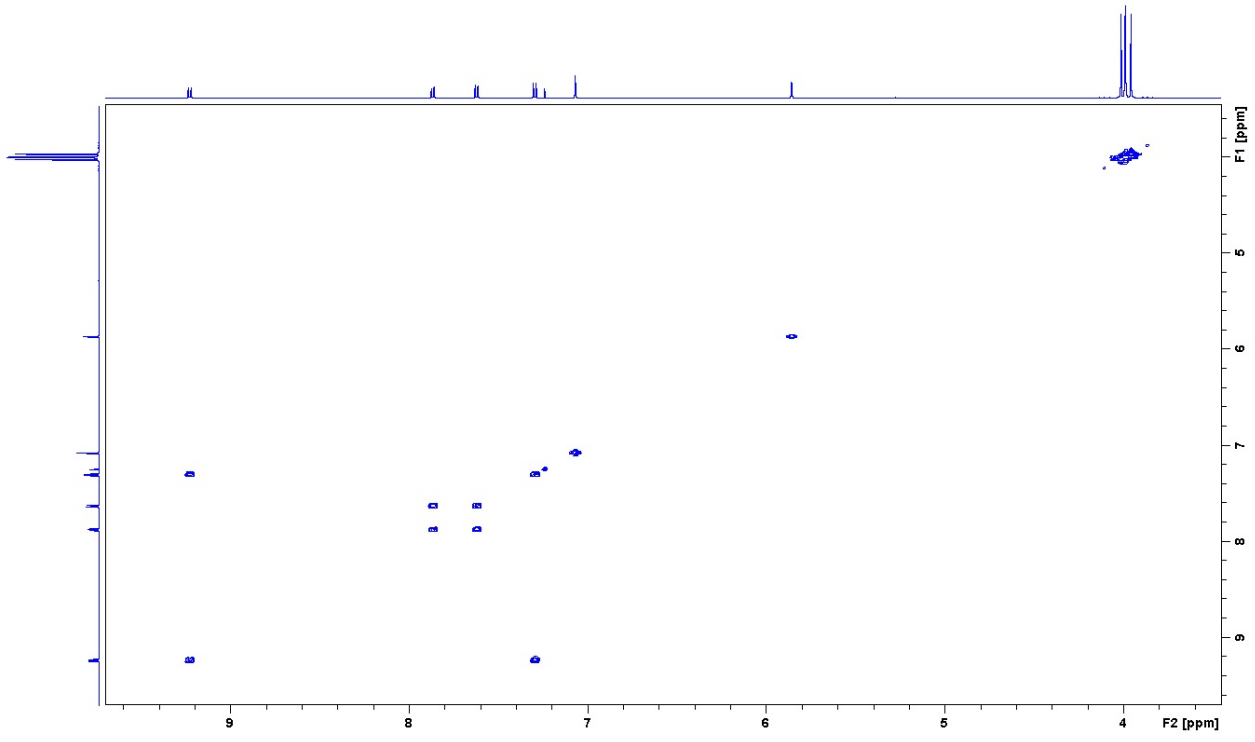

$^{13}C\{^{1}H\}$ NMR - NOESY (151 MHz, $CDCl_3$) **2.33**

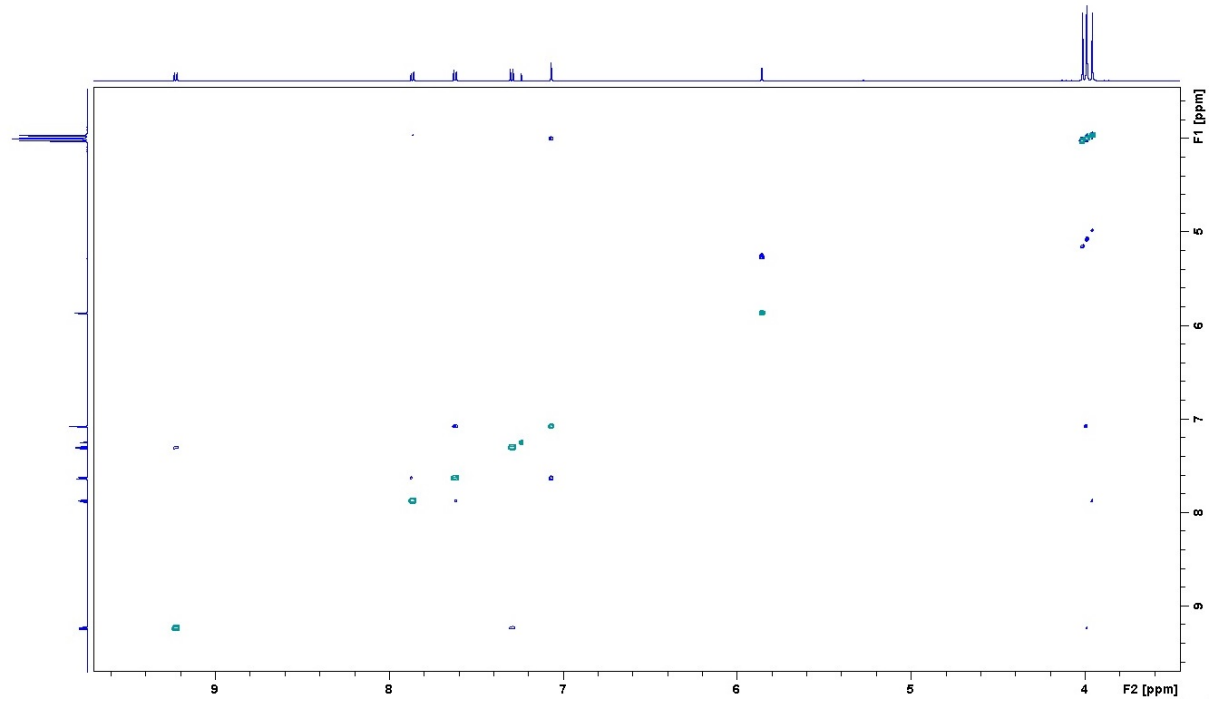

^{13}C NMR - HSQC (151 MHz, $CDCl_3$) **2.33**

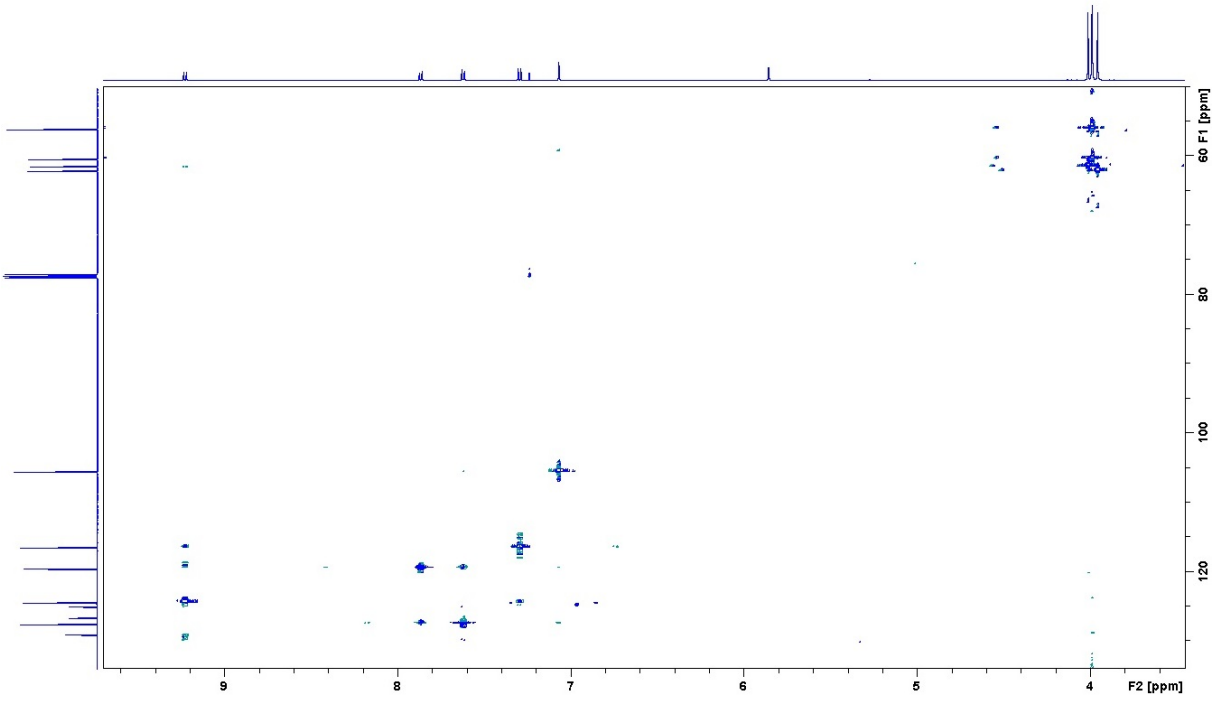

$^{13}C\{^{1}H\}$ NMR - HMQC (151 MHz, $CDCl_3$) **2.33**

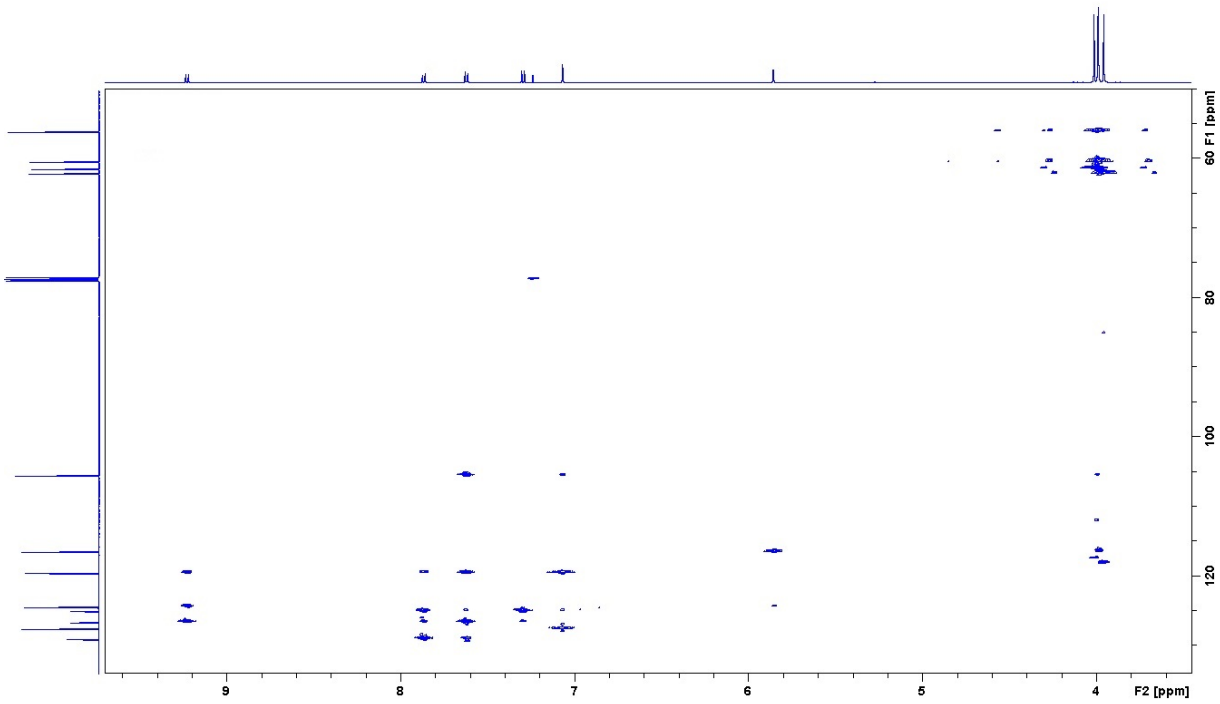

^{1}H NMR spectrum (400 MHz, $CDCl_3$) **2.36**

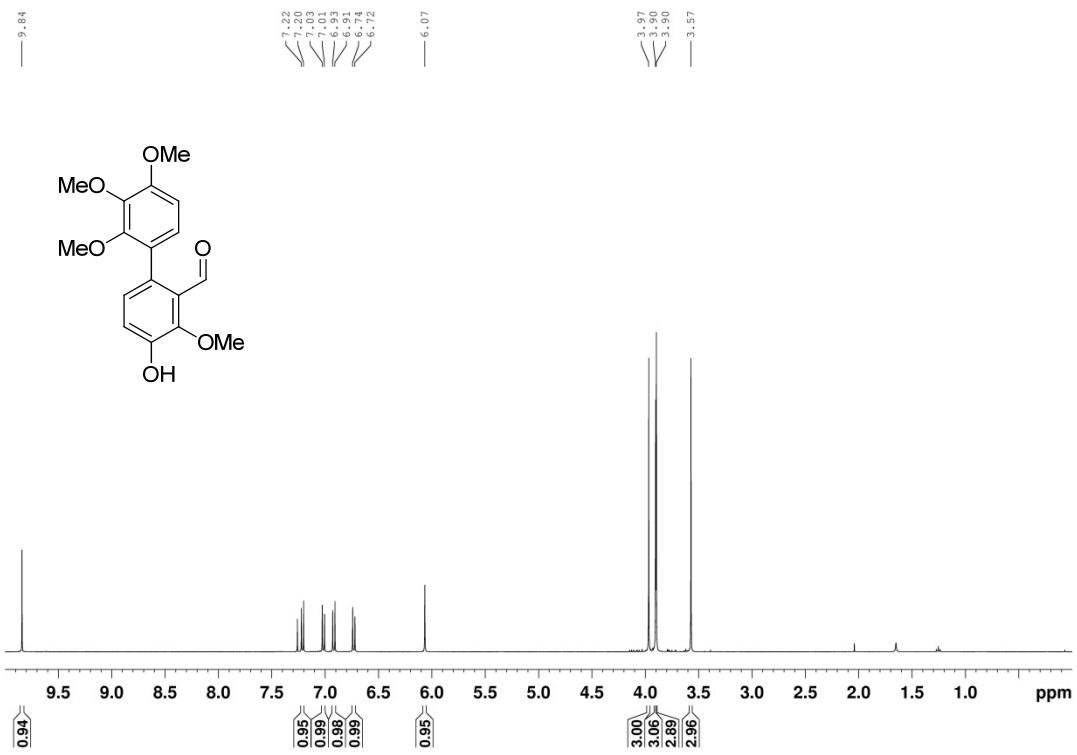

$^{13}C\{^{1}H\}$ NMR spectrum NMR (101 MHz, $CDCl_3$) **2.36**

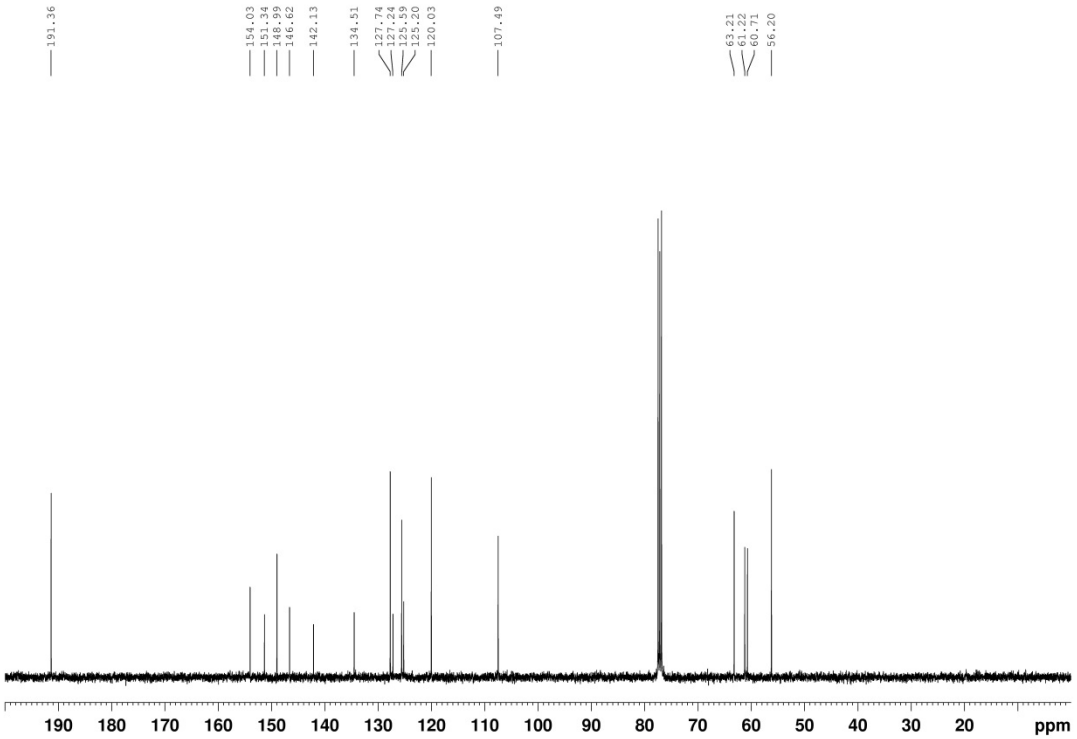

^{1}H NMR spectrum (400 MHz, $CDCl_3$) **2.37**

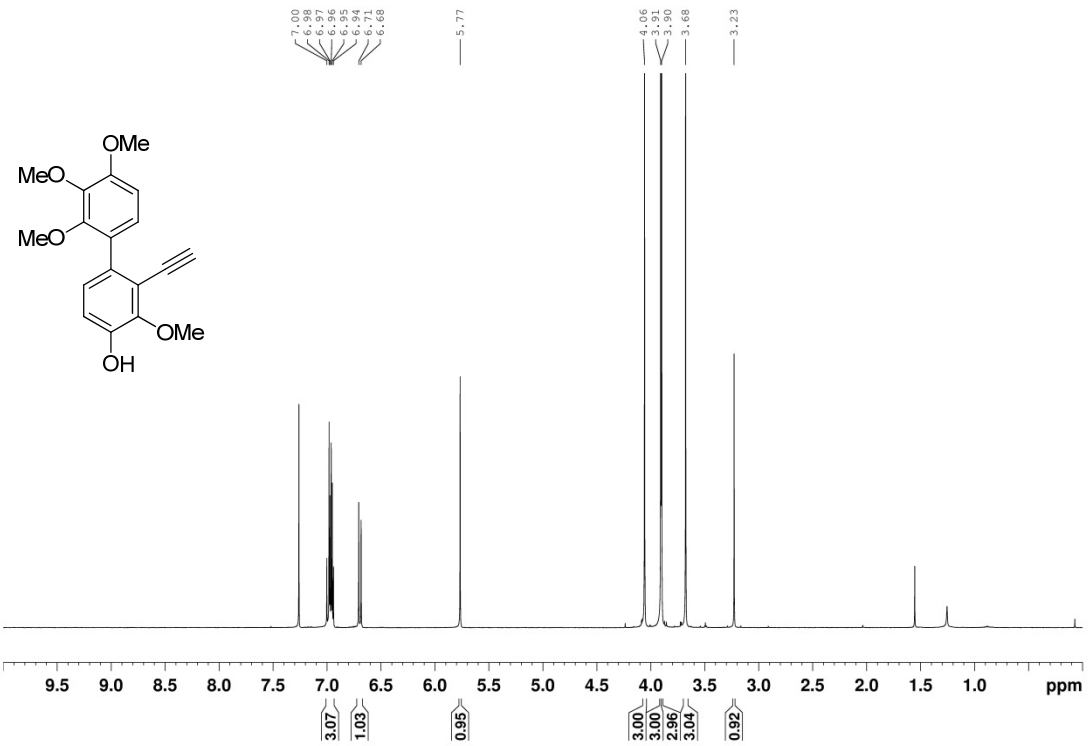

$^{13}C\{^{1}H\}$ NMR spectrum (101 MHz, $CDCl_3$) **2.37**

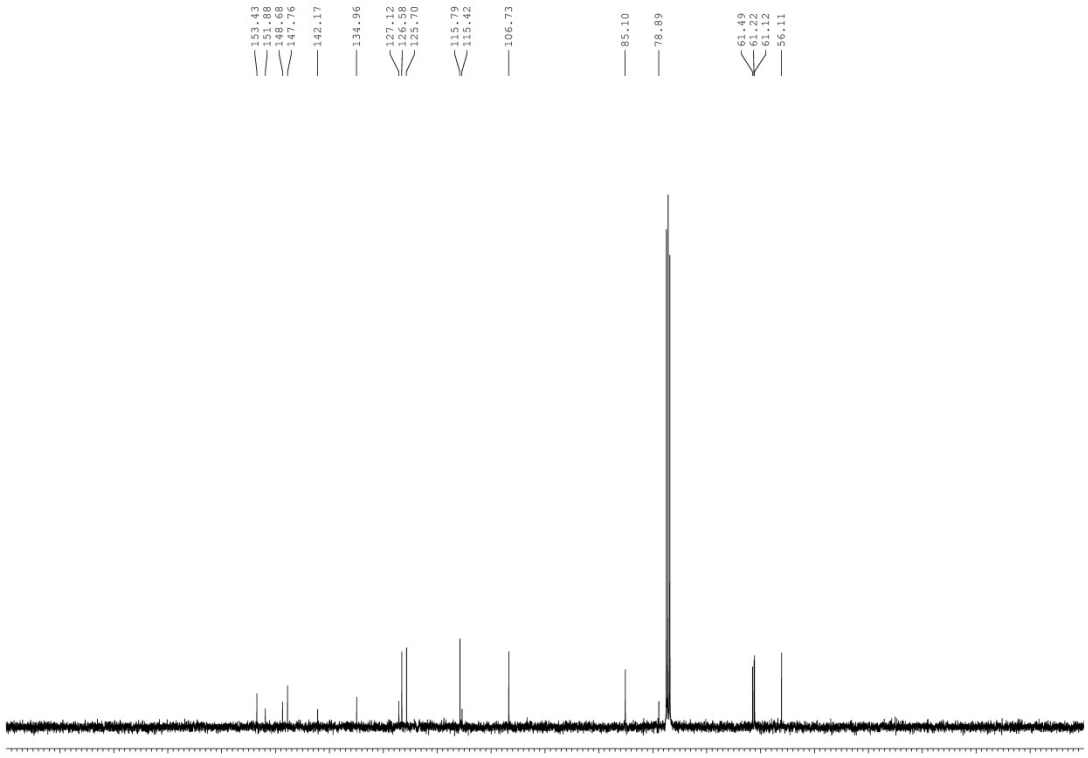

^{1}H NMR spectrum (400 MHz, $CDCl_3$) **2.38**

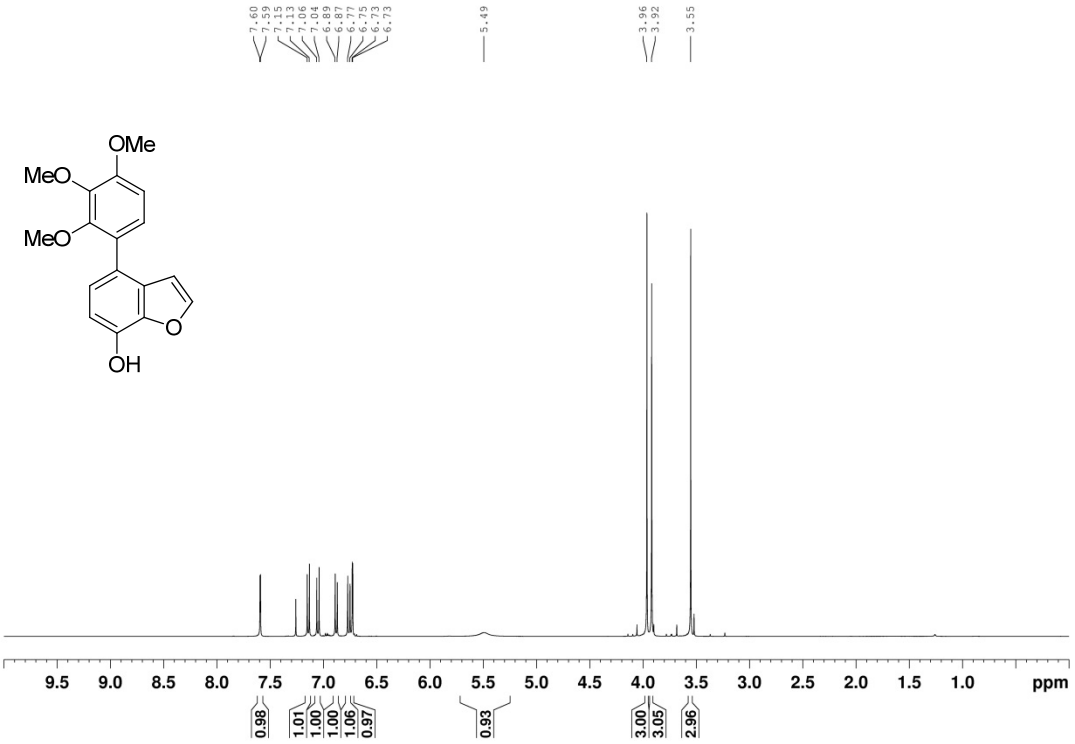

$^{13}C\{^{1}H\}$ NMR spectrum (101 MHz,$CDCl_3$) **2.38**

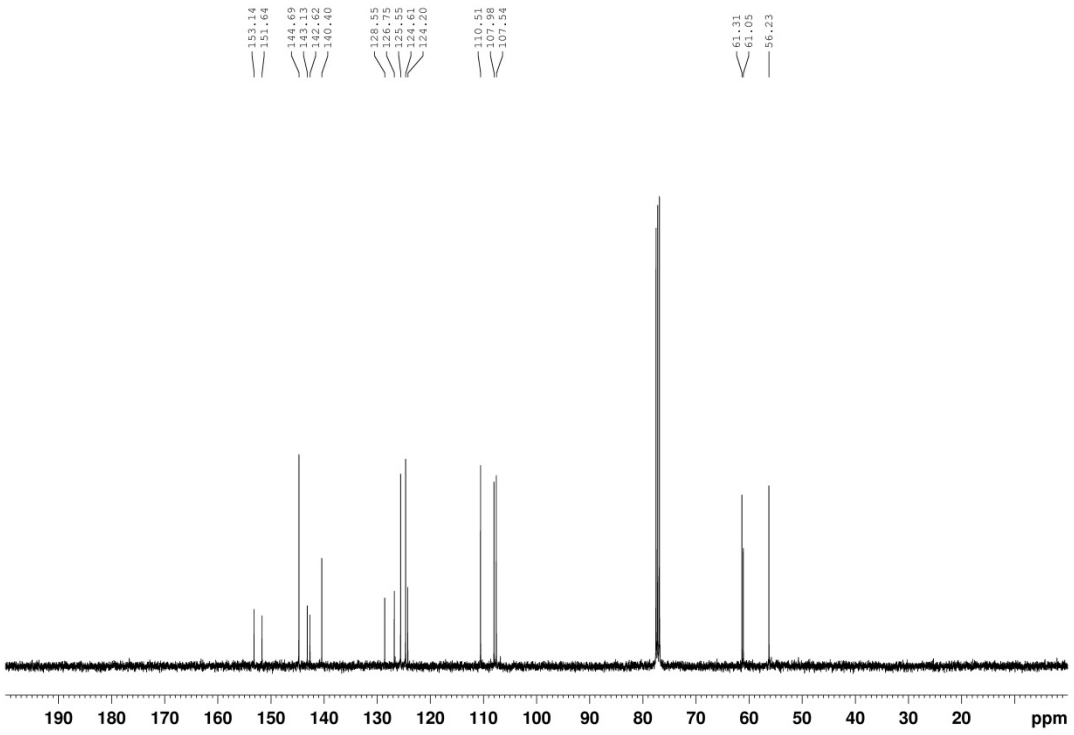

^{1}H NMR spectrum (400 MHz, CD_2Cl_2) **3.38**

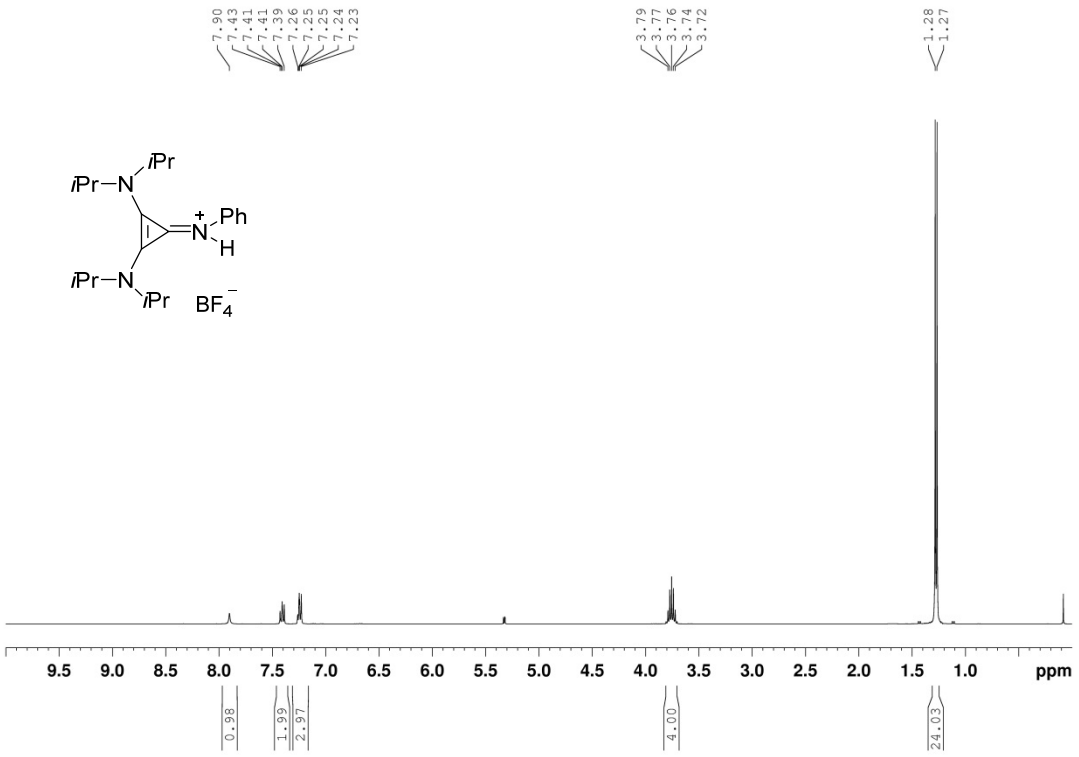

$^{13}C\{^{1}H\}$ NMR spectrum (101 MHz, CD_2Cl_2) **3.38**

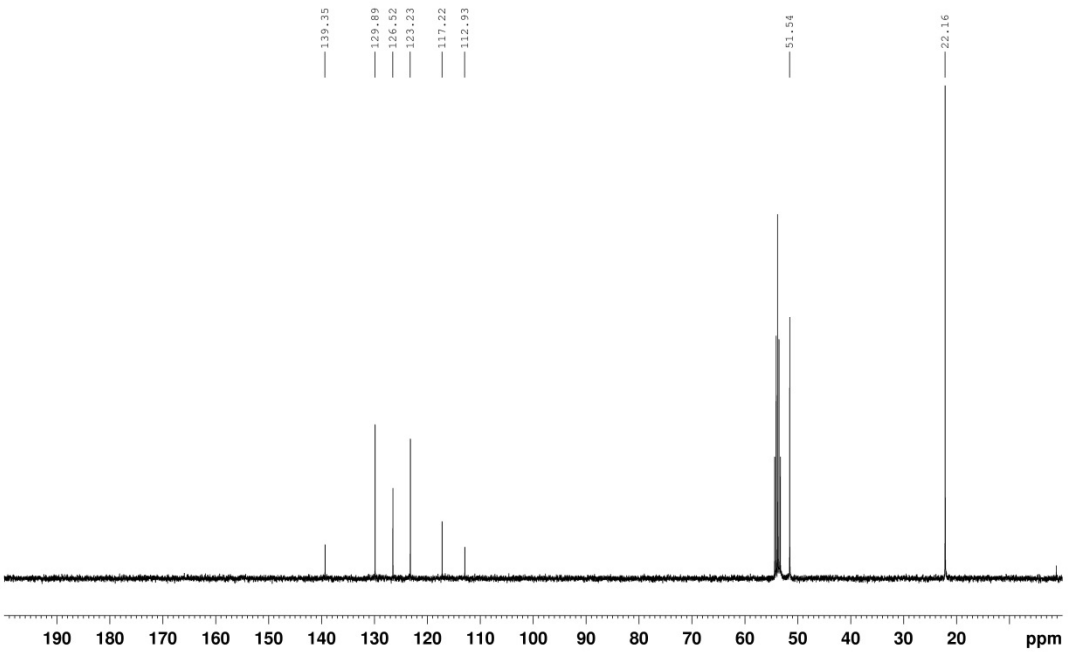

^{1}H NMR spectrum (400 MHz, CD_2Cl_2) **3.42**

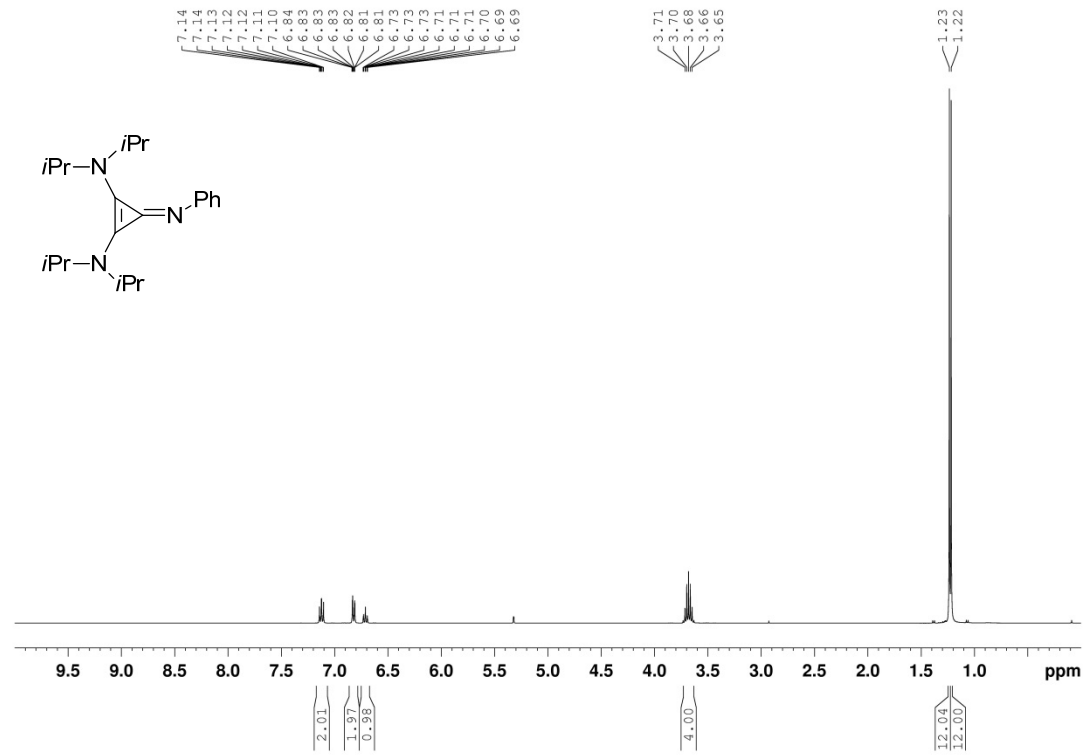

$^{13}C\{^{1}H\}$ NMR spectrum (101 MHz, CD_2Cl_2) **3.42**

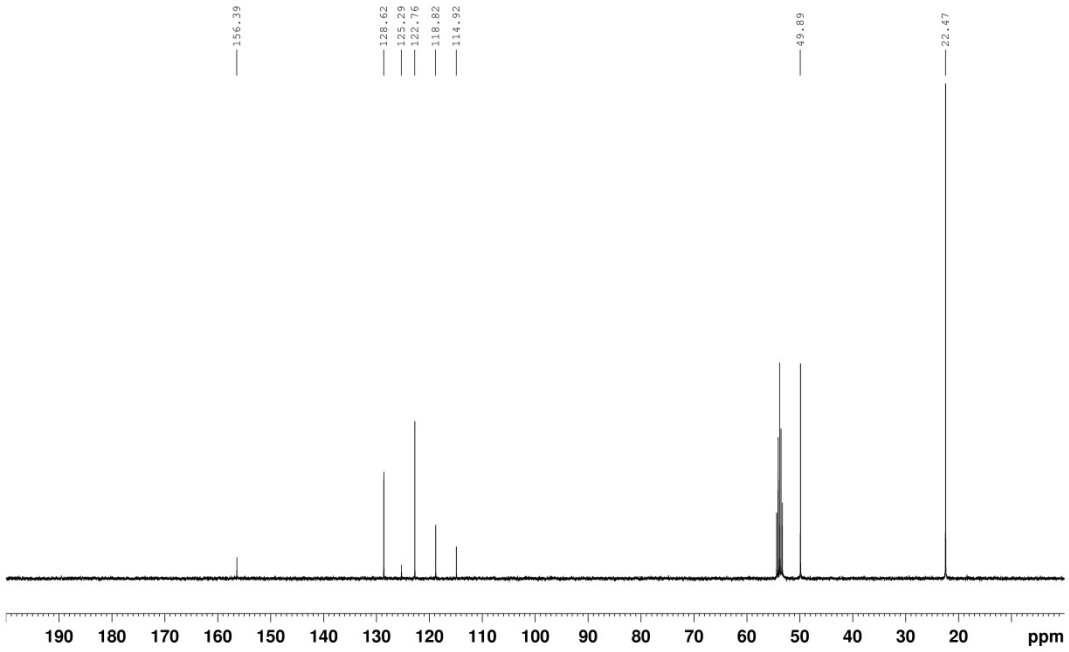

^{1}H NMR spectrum (400 MHz, CD_2Cl_2) **3.45**

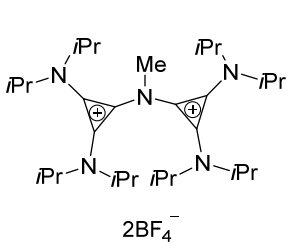

$^{13}C\{^{1}H\}$ NMR spectrum (101 MHz, CD_2Cl_2) **3.45**

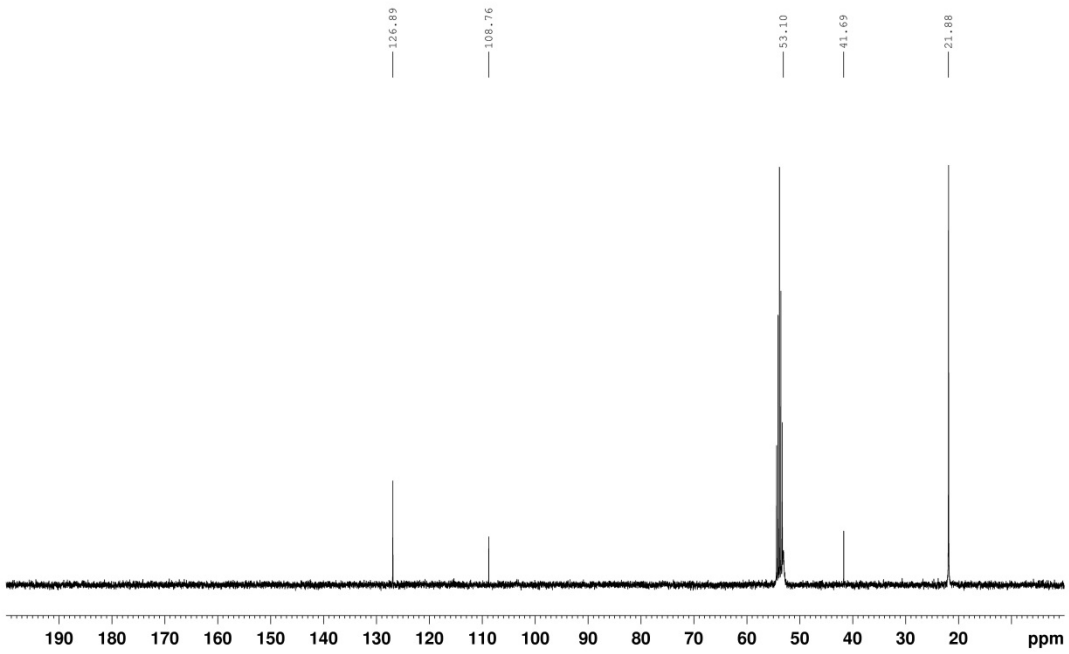

^{1}H NMR spectrum (400 MHz, CD_2Cl_2) **3.47**

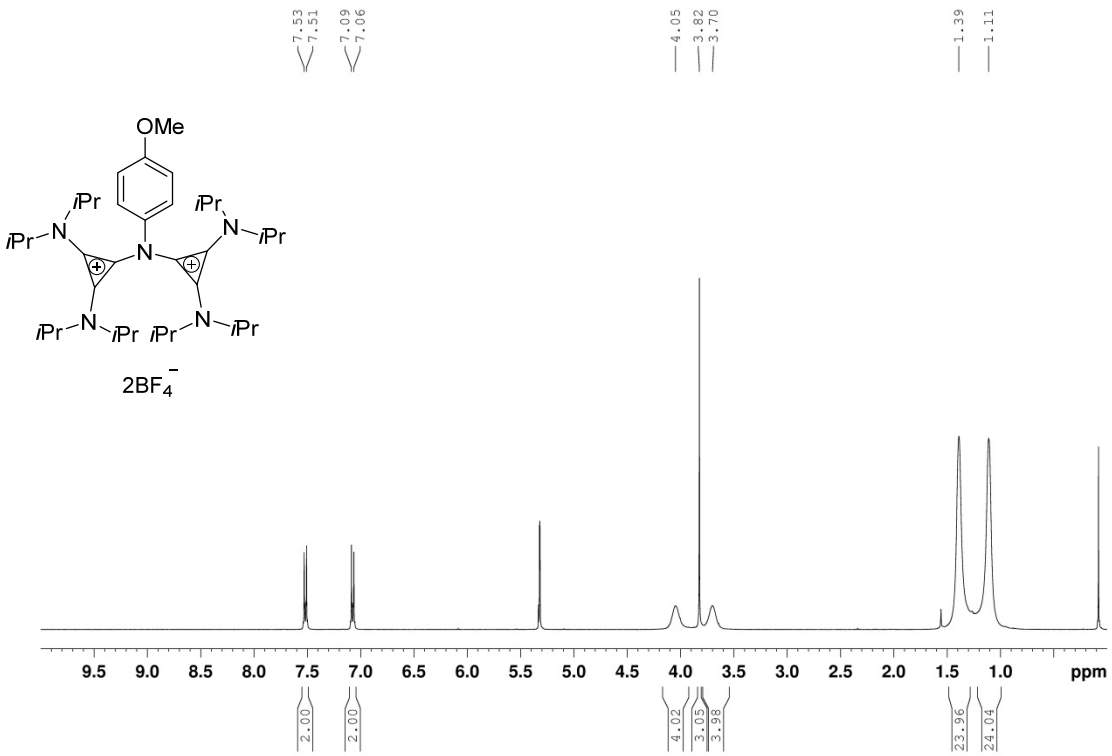

$^{13}C\{^{1}H\}$ NMR spectrum (101 MHz, CD_2Cl_2) **3.47**

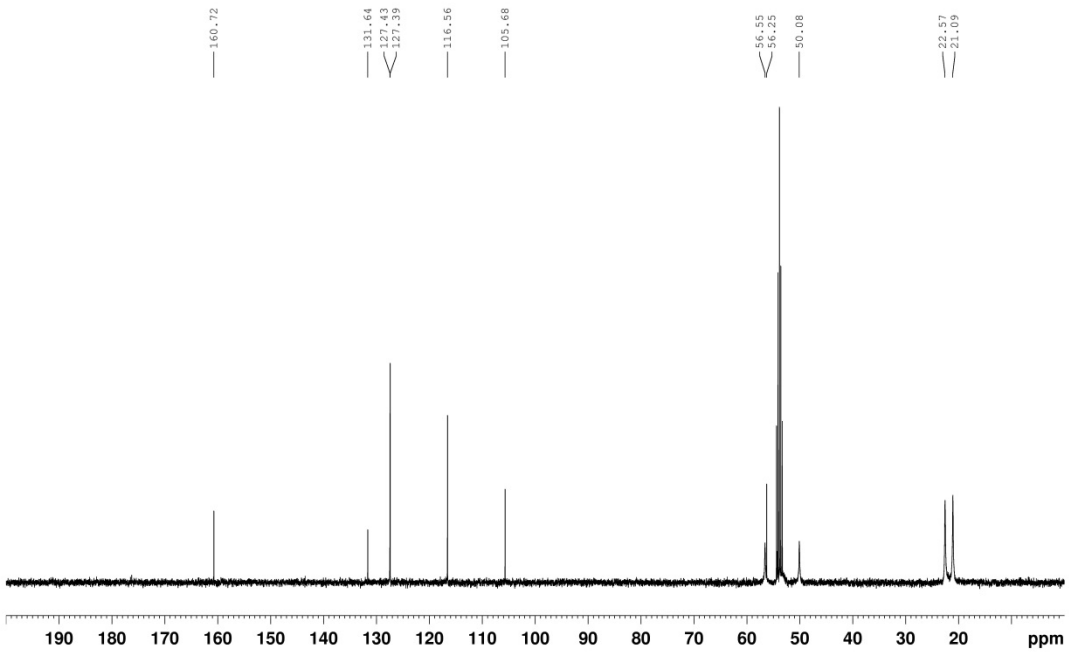

^{1}H NMR spectrum (400 MHz, CD_2Cl_2) **3.52**

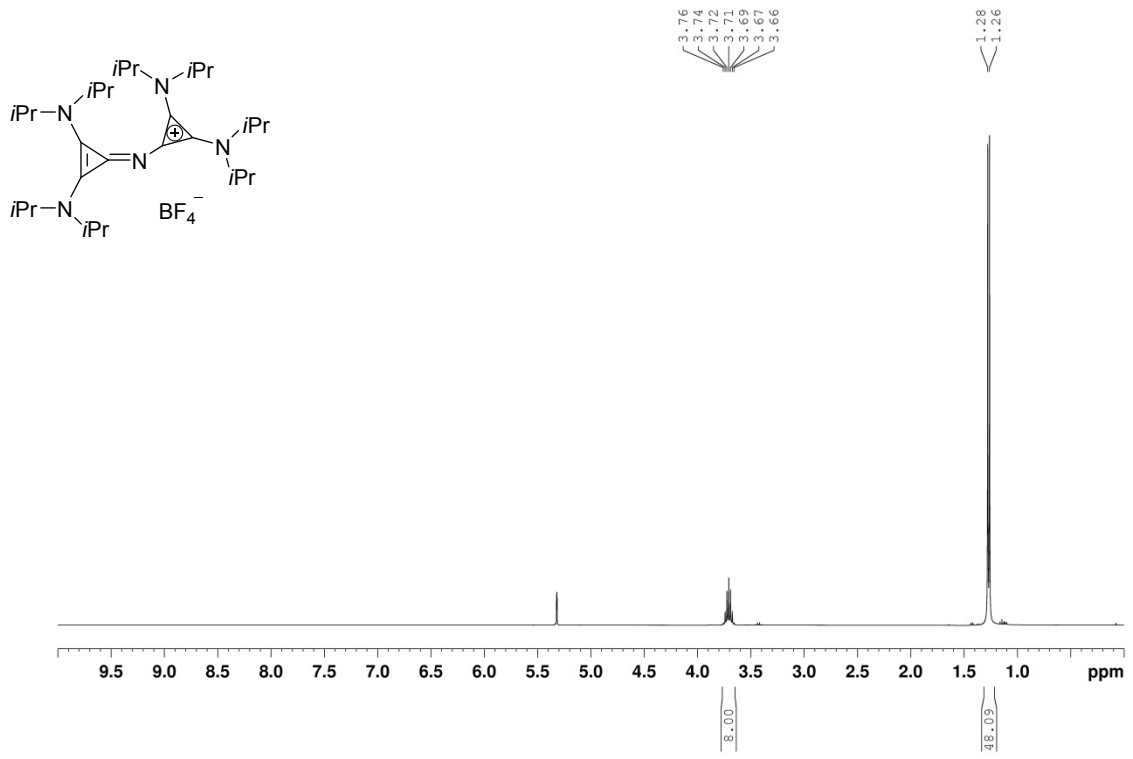

$^{13}C\{^{1}H\}$ NMR spectrum (101 MHz, CD_2Cl_2) **3.52**

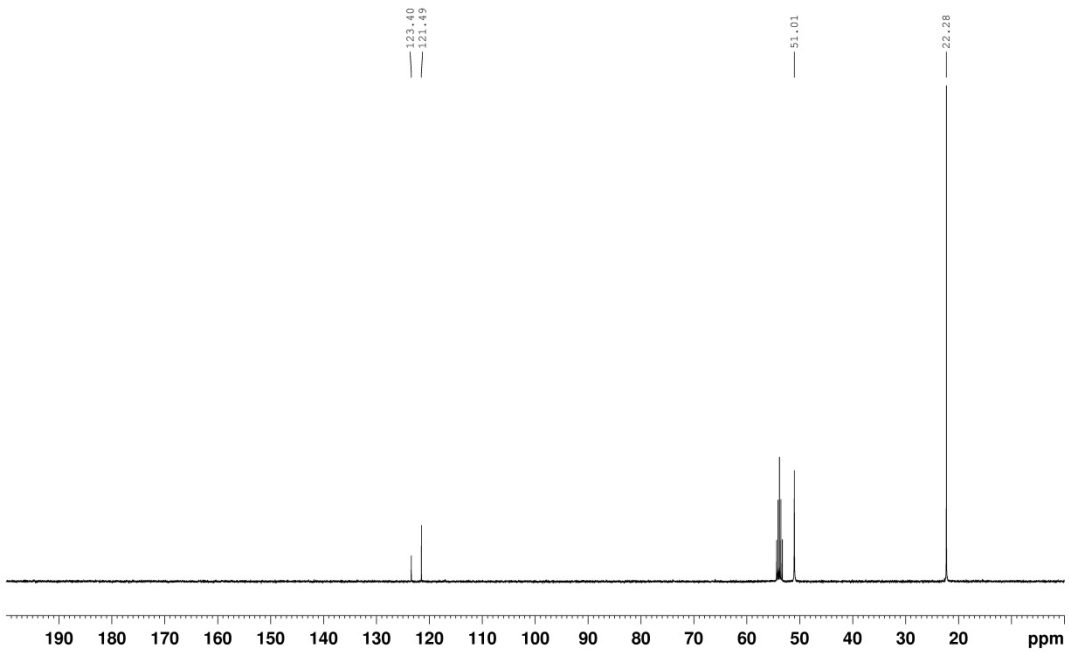

^{1}H NMR spectrum (400 MHz, CD_2Cl_2) **3.54**

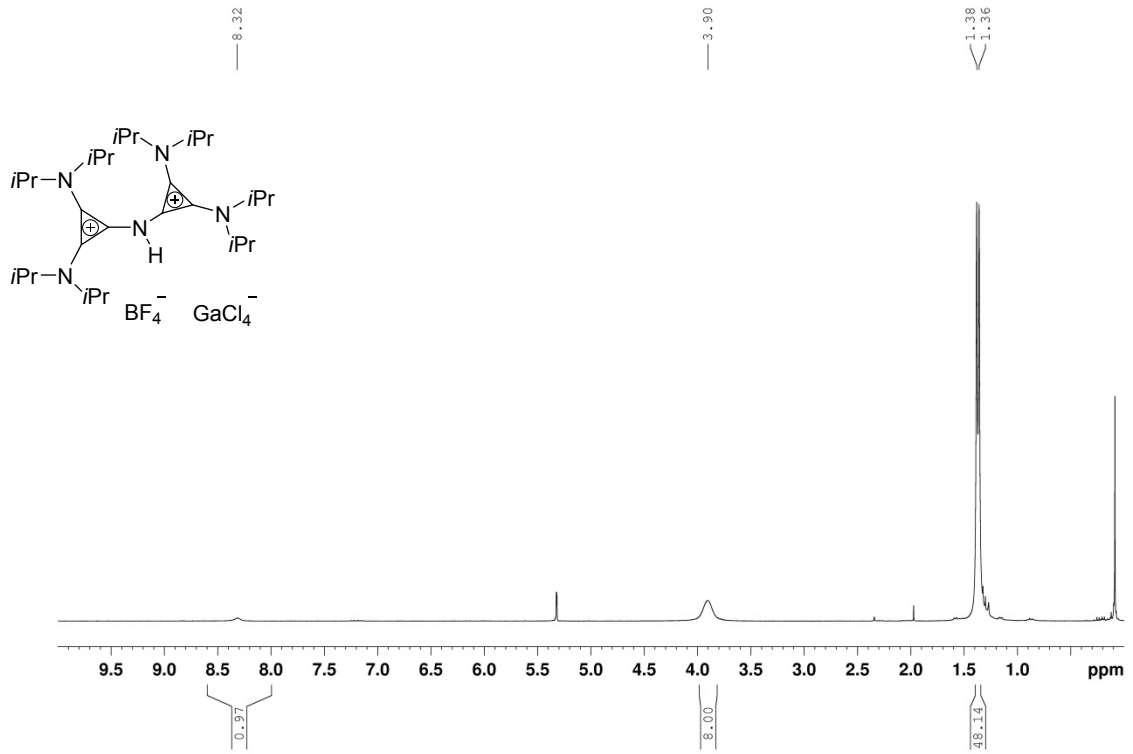

$^{13}C\{^{1}H\}$ NMR spectrum (101 MHz, CD_2Cl_2) **3.54**

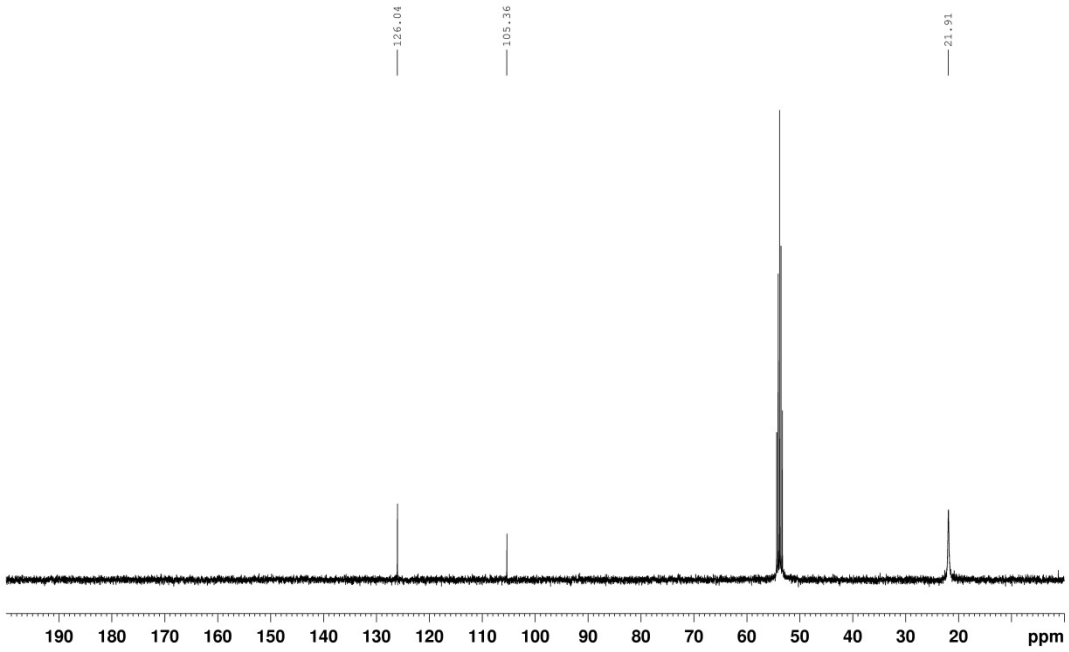

^{1}H NMR spectrum (400 MHz, CD_3CN) **3.56**

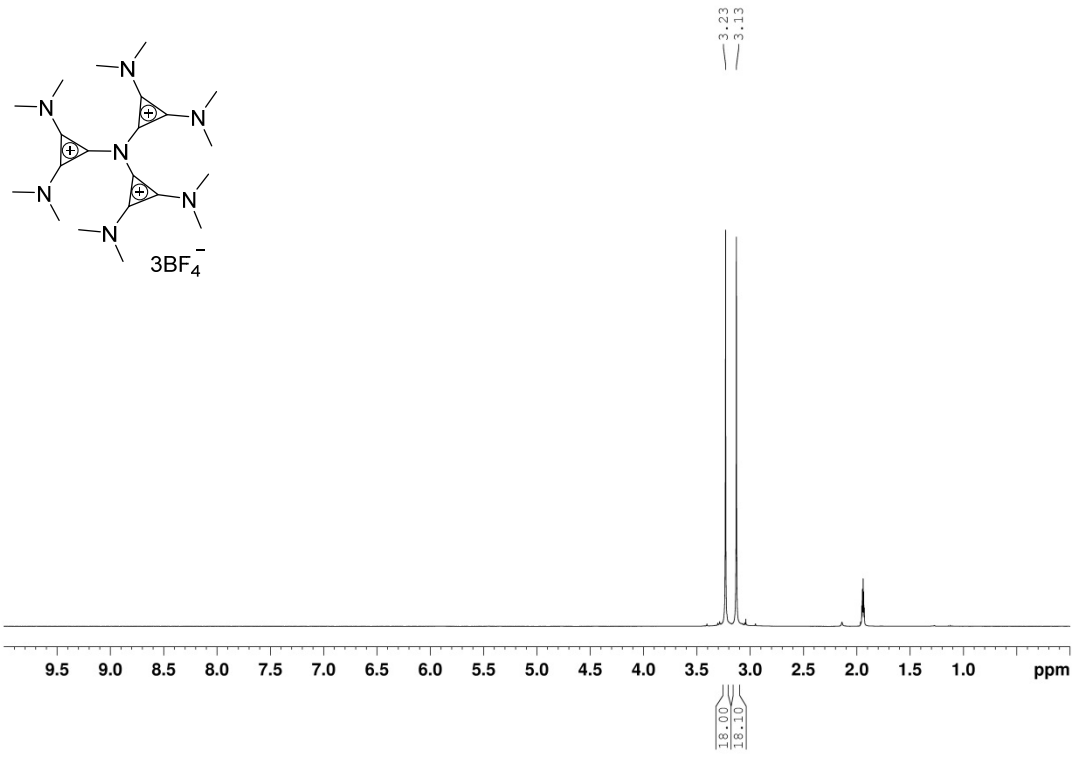

$^{13}C\{^{1}H\}$ NMR spectrum (101 MHz, CD_3CN) **3.56**

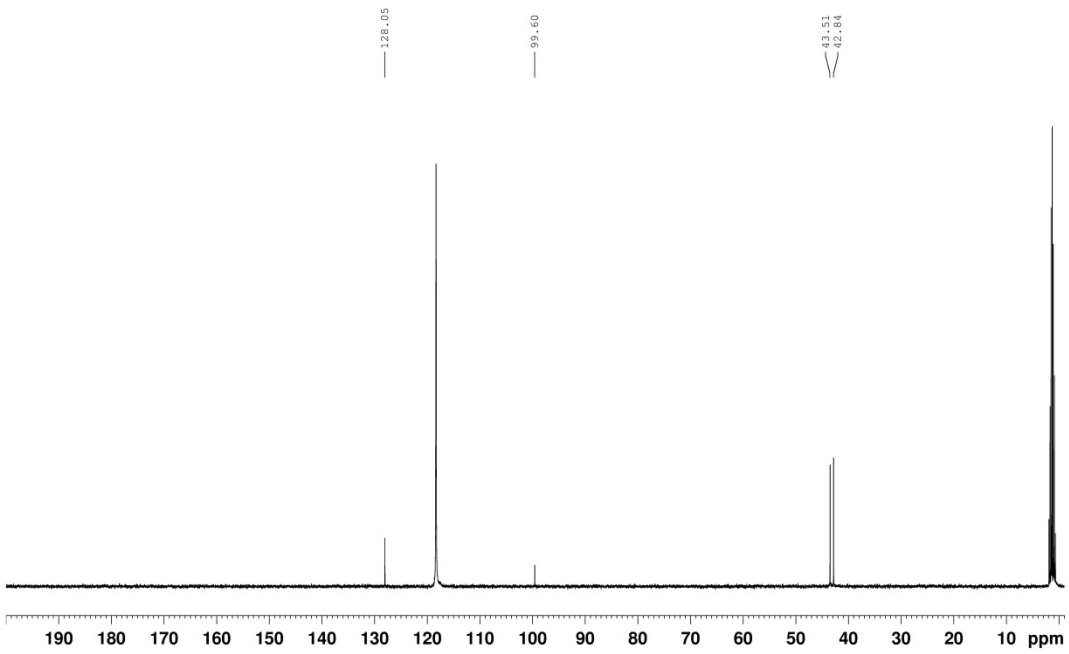

^{1}H NMR spectrum (400 MHz, CD_2Cl_2) **4.27**

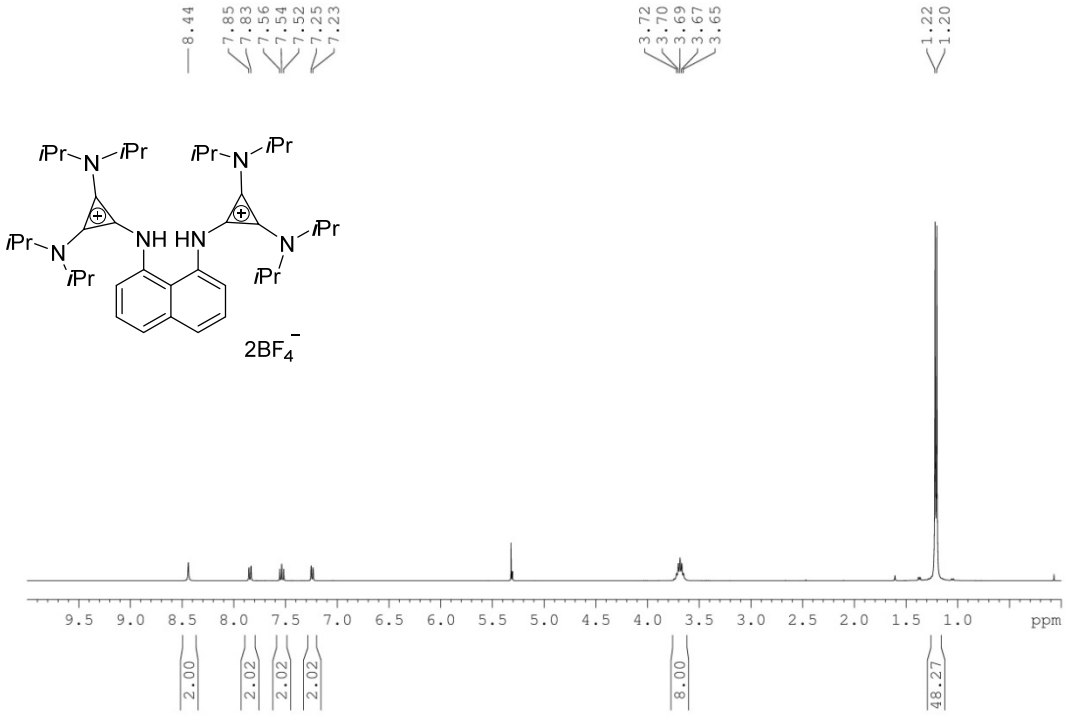

$^{13}C\{^{1}H\}$ NMR spectrum (101 MHz, CD_2Cl_2) **4.27**

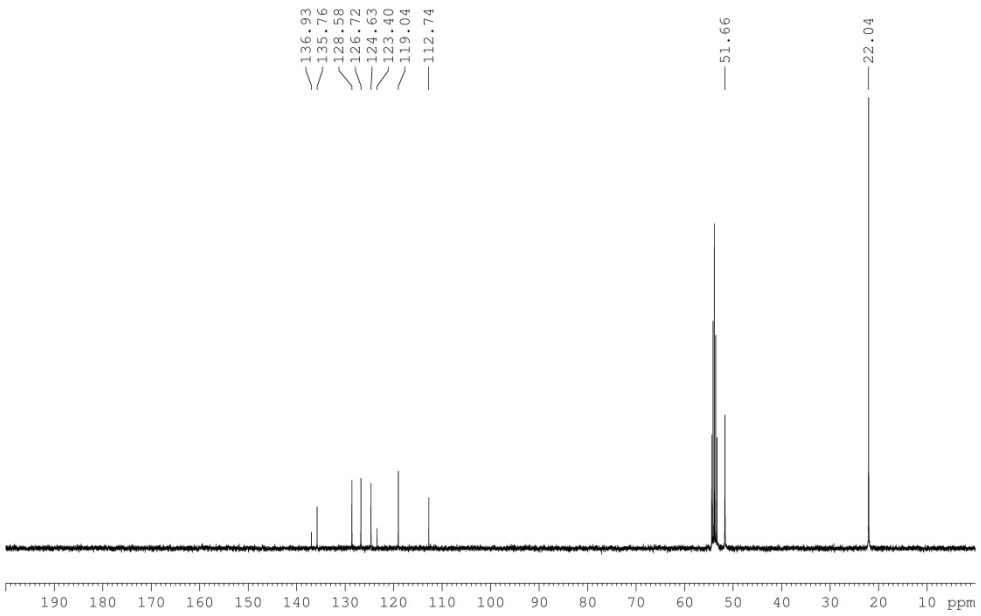

^{1}H NMR spectrum (400 MHz, CD_2Cl_2) **4.30**

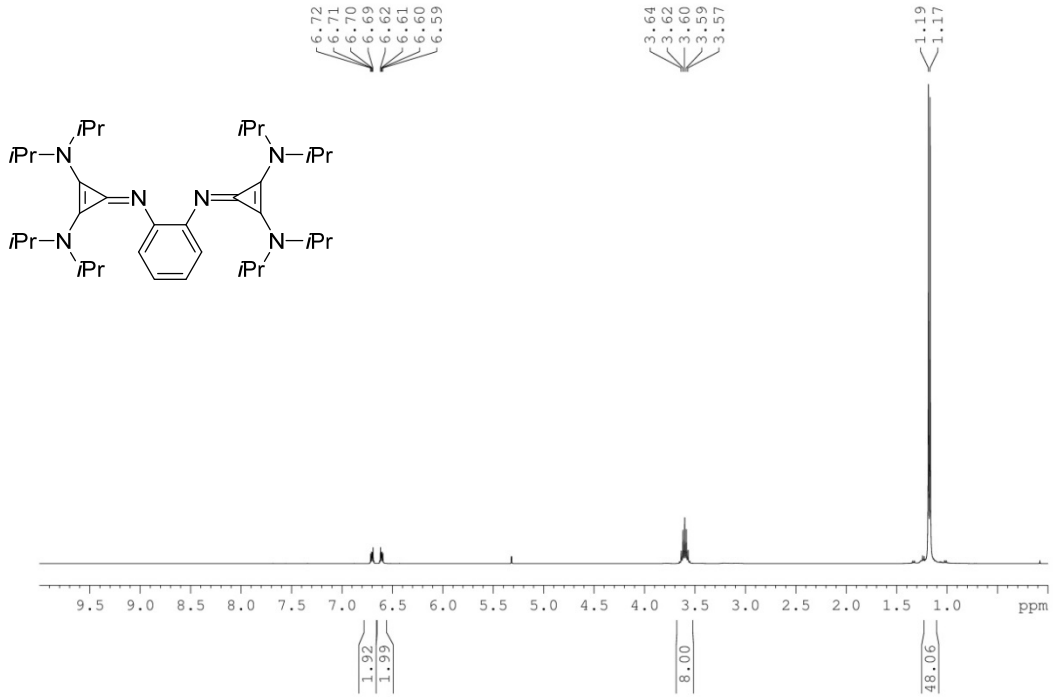

$^{13}C\{^{1}H\}$ NMR spectrum (101 MHz, CD_2Cl_2) **4.30**

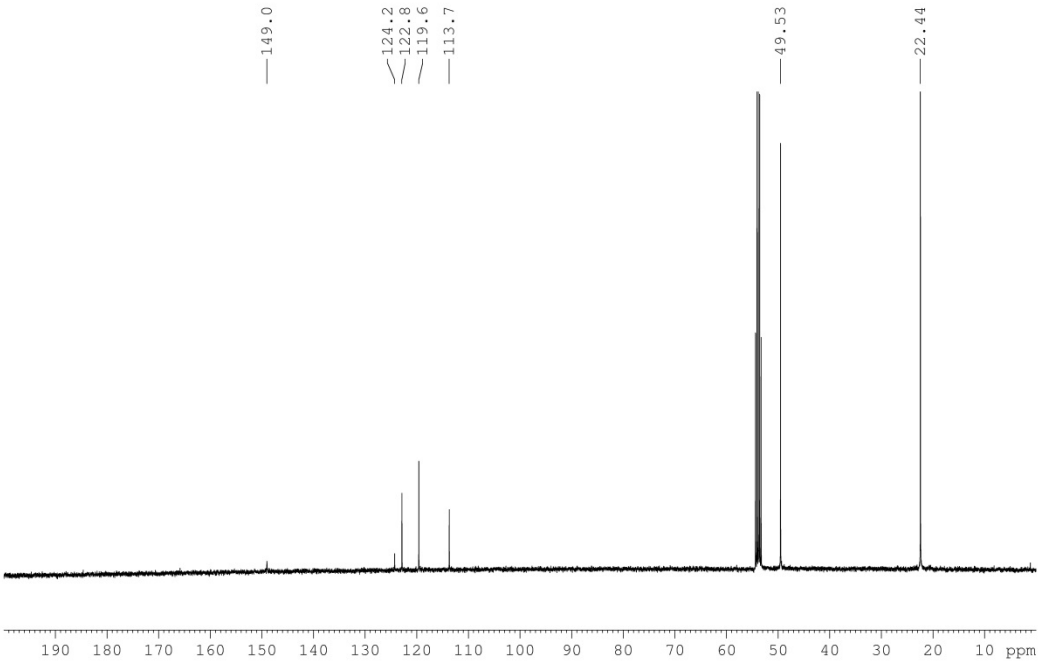

^{1}H NMR spectrum (400 MHz, CD_2Cl_2) **4.31**

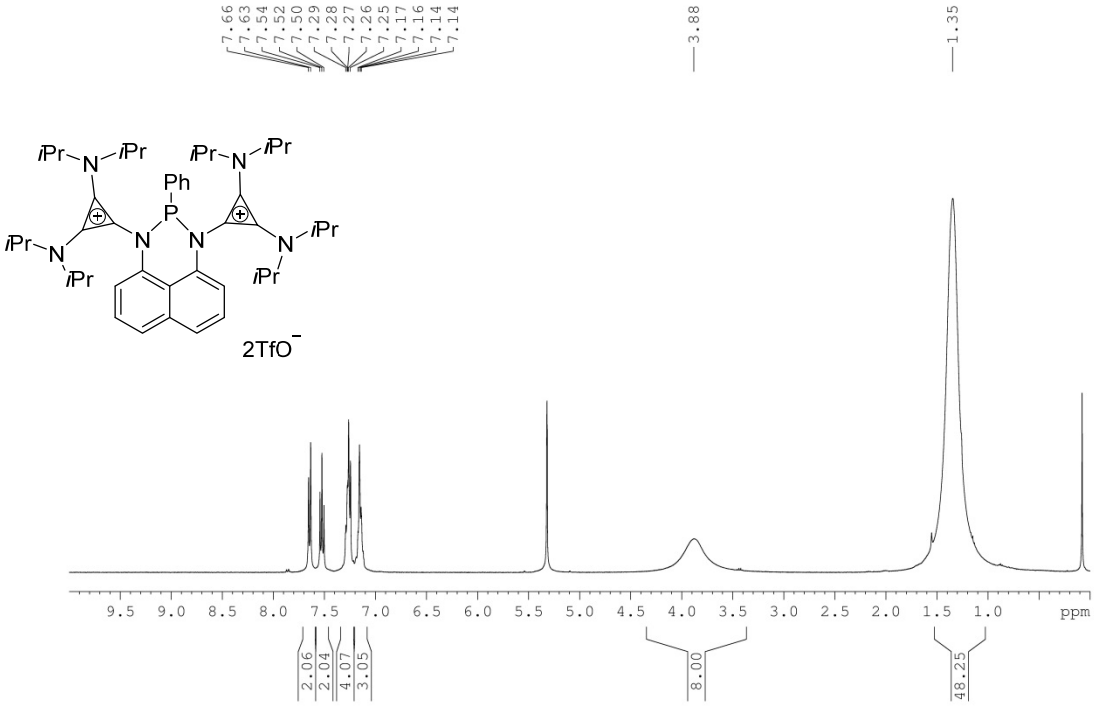

$^{31}P\{^{1}H\}$ NMR spectrum (162 MHz, CD_2Cl_2) **4.31**

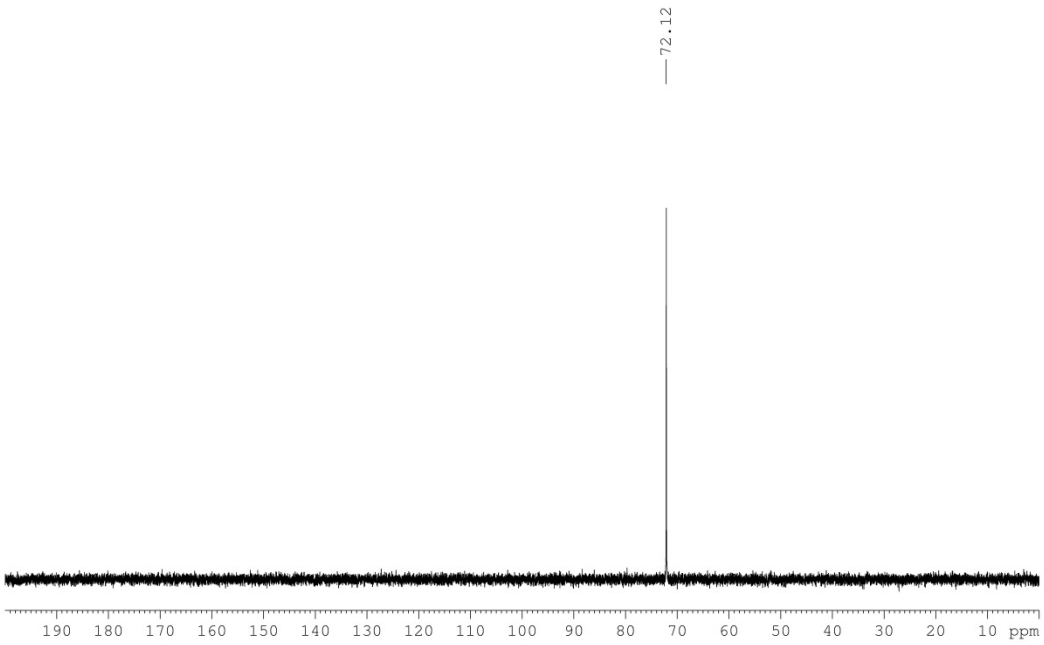

$^{13}C\{^{1}H\}$ NMR spectrum (101 MHz, CD_2Cl_2) **4.31**

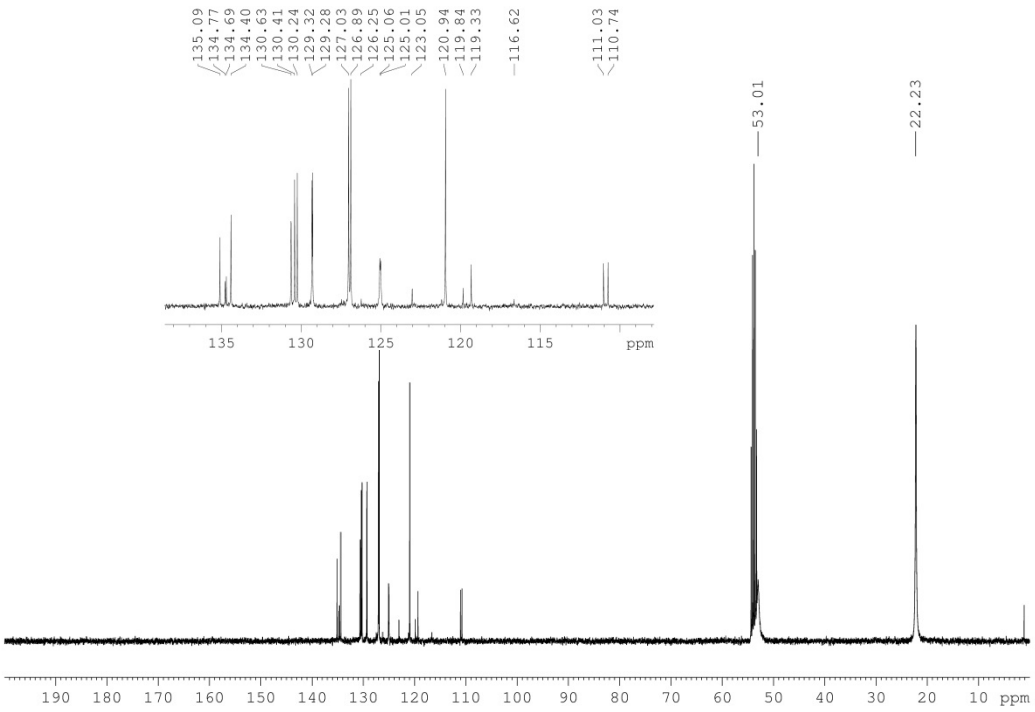

^{1}H NMR spectrum (400 MHz, CD_2Cl_2) **4.33**

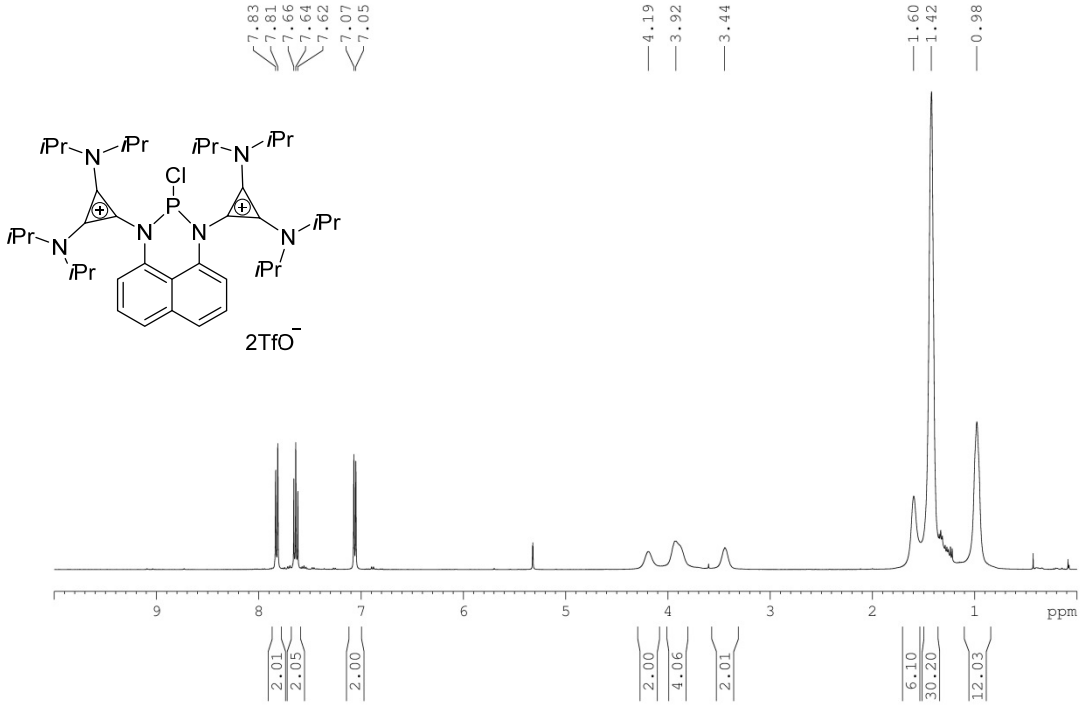

^{31}P{^{1}H} NMR spectrum (162 MHz, CD_2Cl_2) **4.33**

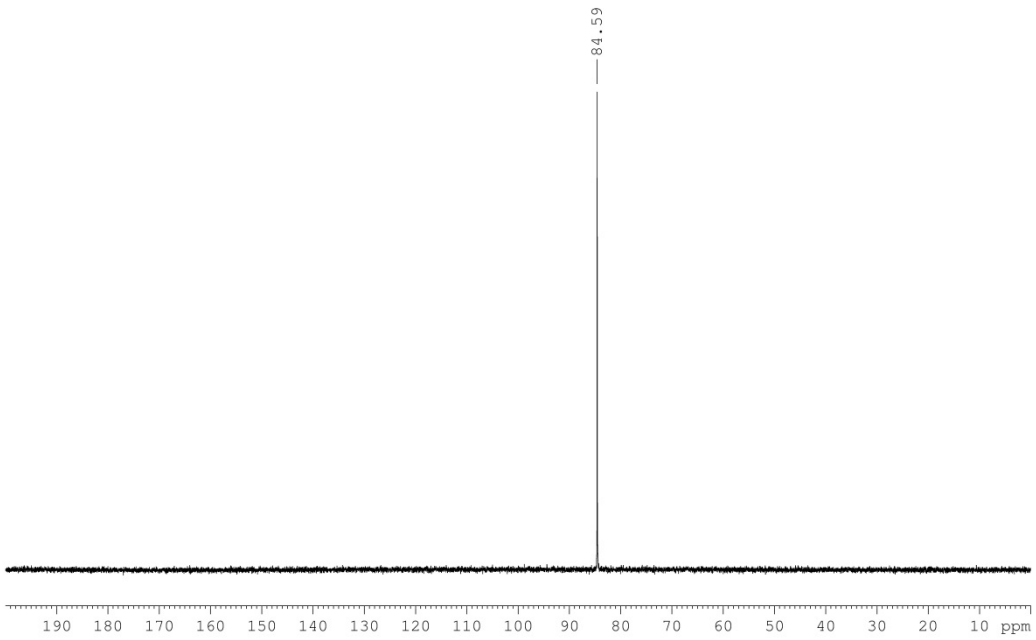

$^{13}C\{^{1}H\}$ NMR spectrum (101 MHz, CD_2Cl_2) **4.33**

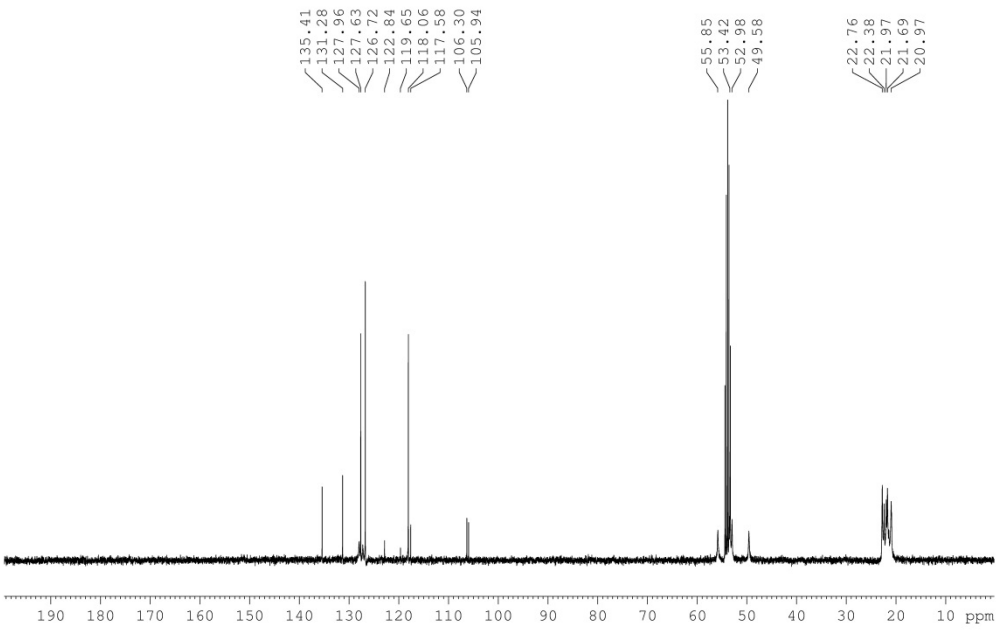

^{1}H NMR spectrum (400 MHz, CD_2Cl_2) **4.36**

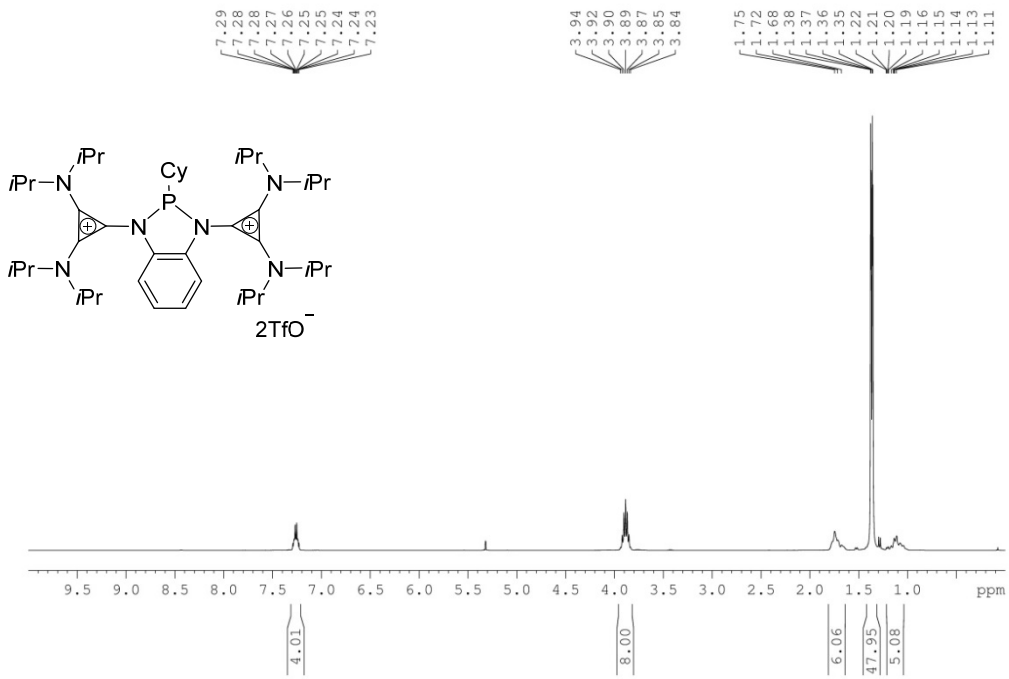

$^{31}P\{^{1}H\}$ NMR spectrum (162 MHz, CD_2Cl_2) **4.36**

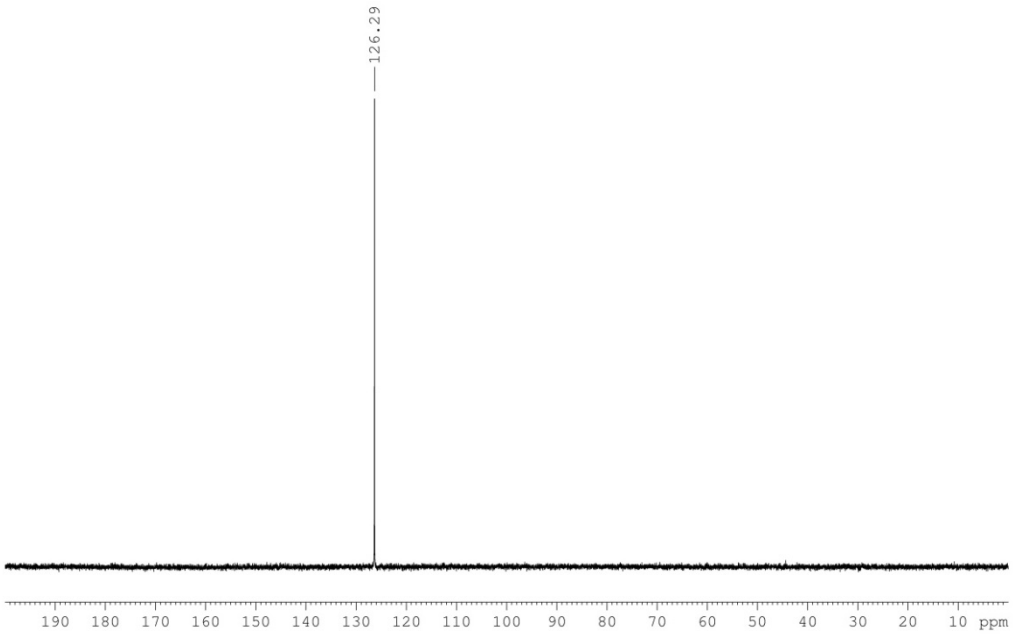

$^{13}C\{^{1}H\}$ NMR spectrum (101 MHz, CD_2Cl_2) **4.36**

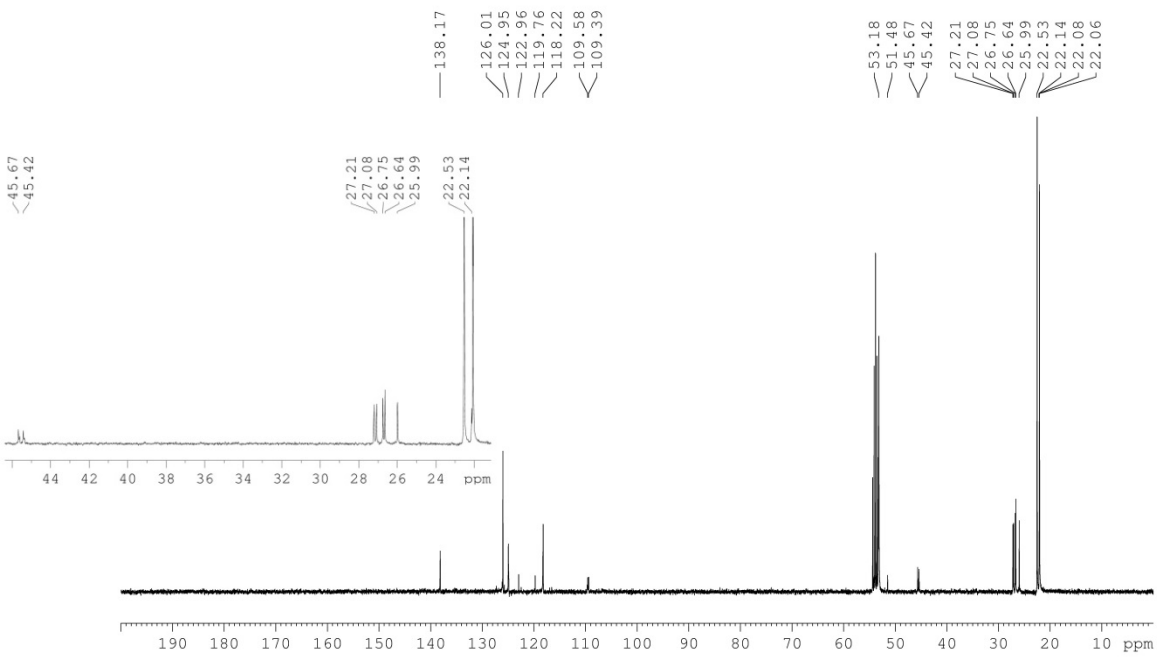

^{1}H NMR spectrum (400 MHz, CD_2Cl_2) **4.37**

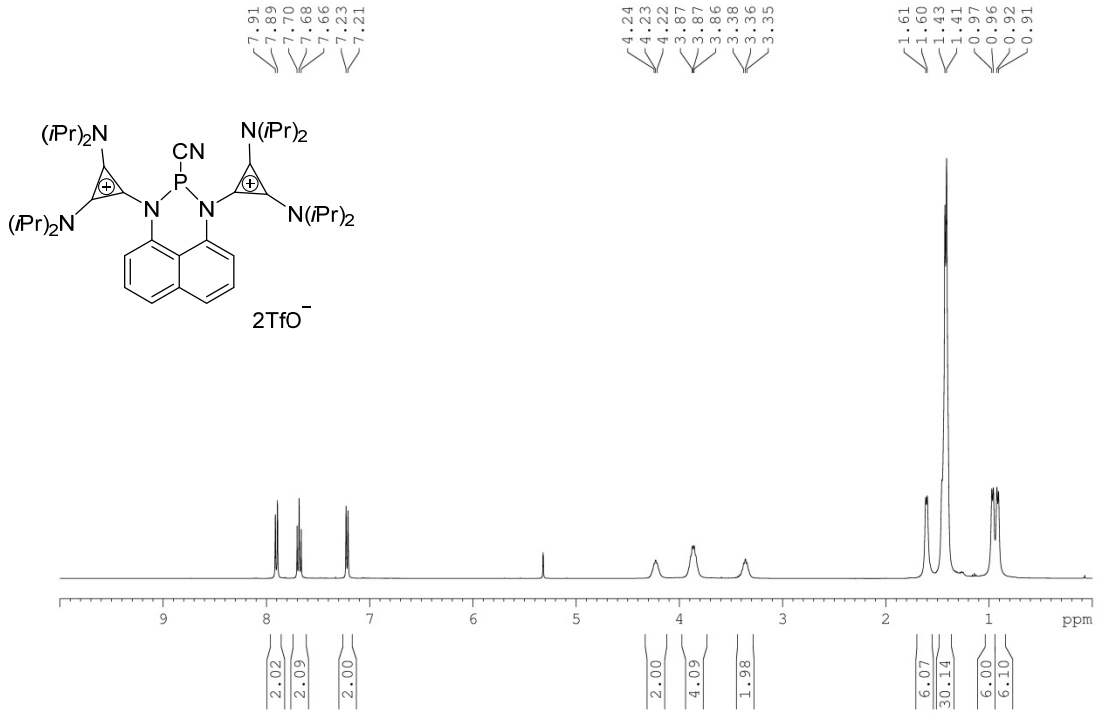

^{31}P{^{1}H} NMR spectrum (162 MHz, CD_2Cl_2) **4.37**

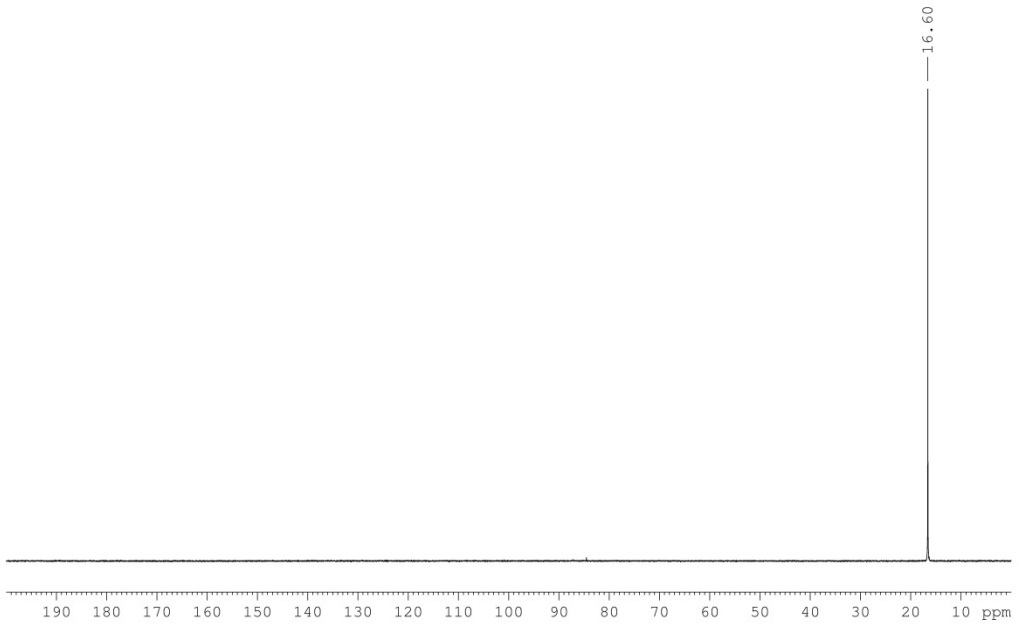

$^{13}C\{^{1}H\}$ NMR spectrum (101 MHz, CD_2Cl_2) **4.37**

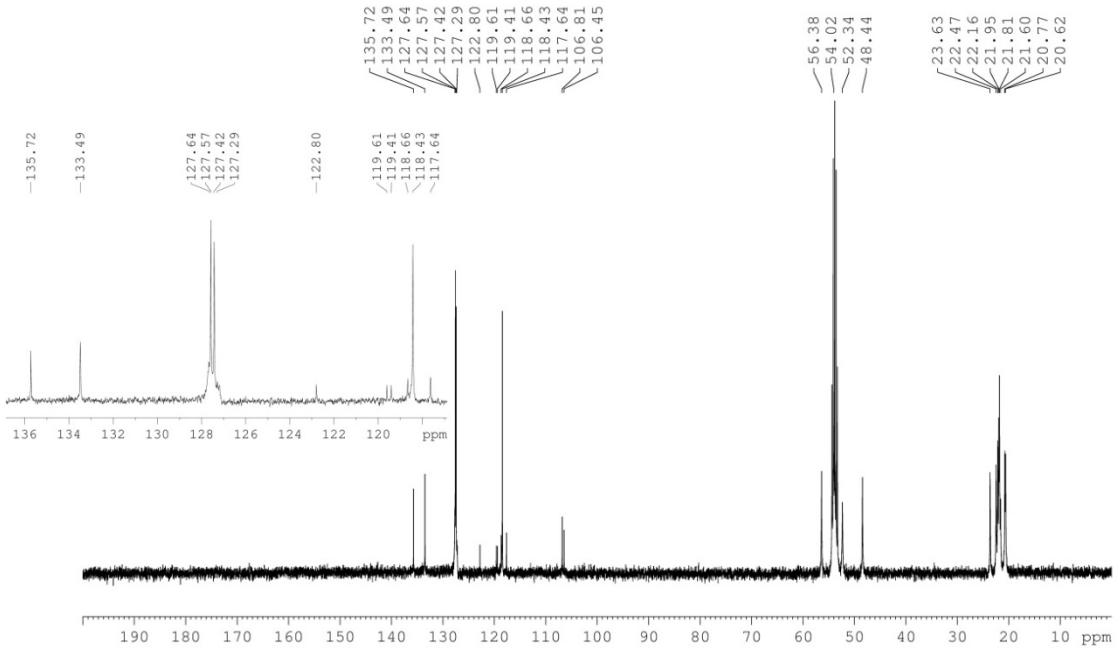

^{1}H NMR spectrum (400 MHz, CD_2Cl_2) **4.39**

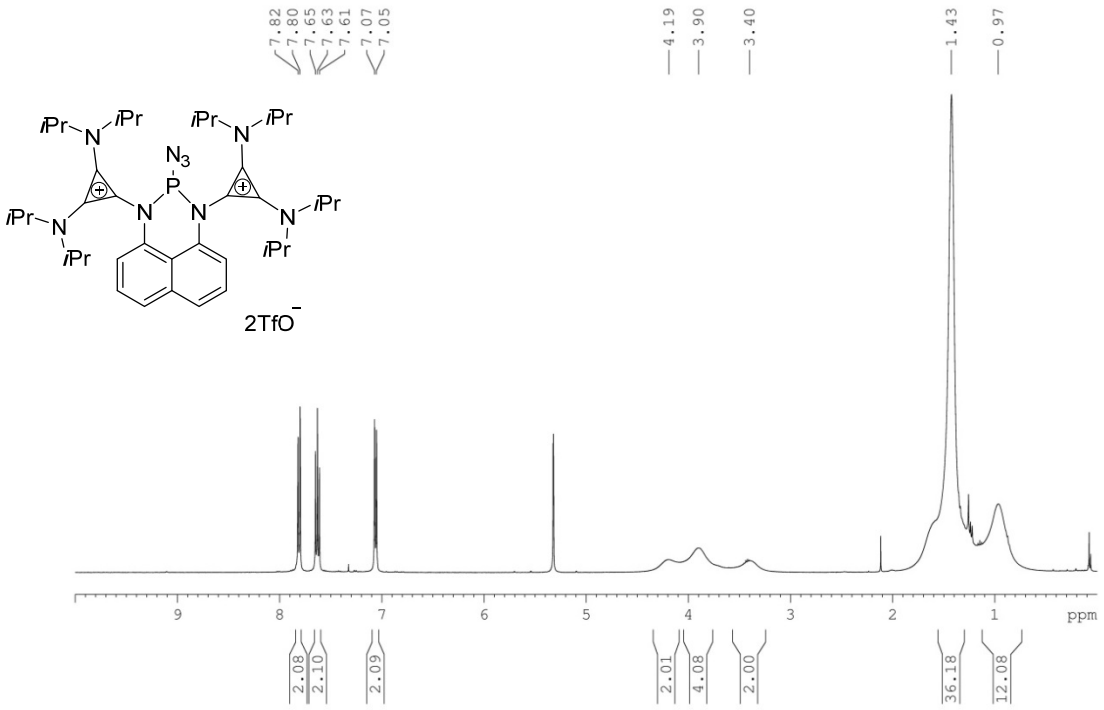

^{31}P NMR spectrum (162 MHz, CD_2Cl_2) **4.39**

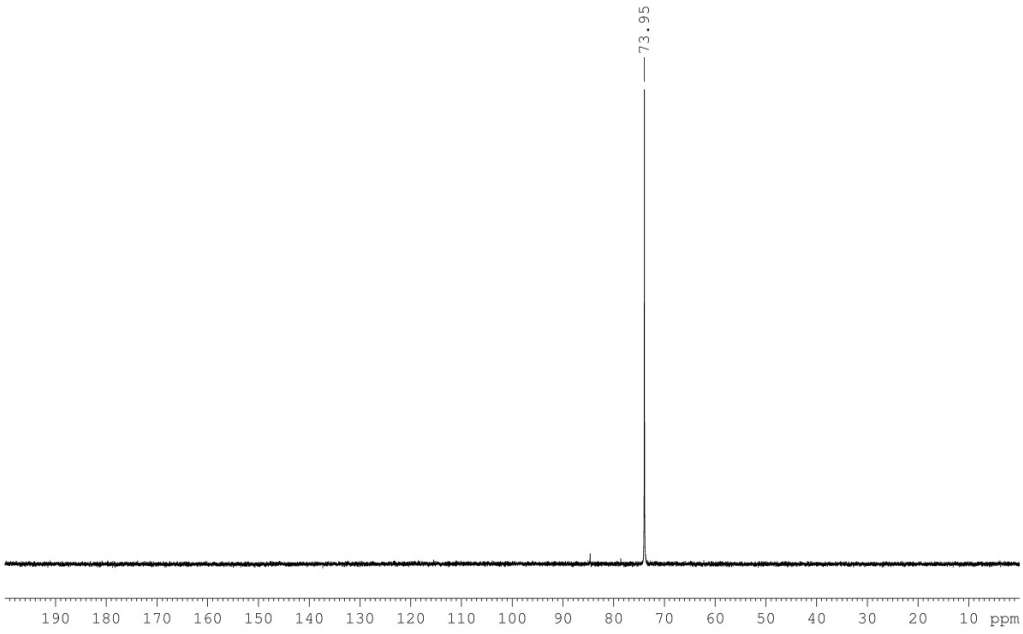

$^{13}C\{^1H\}$ NMR spectrum (101 MHz, CD_2Cl_2) **4.39**

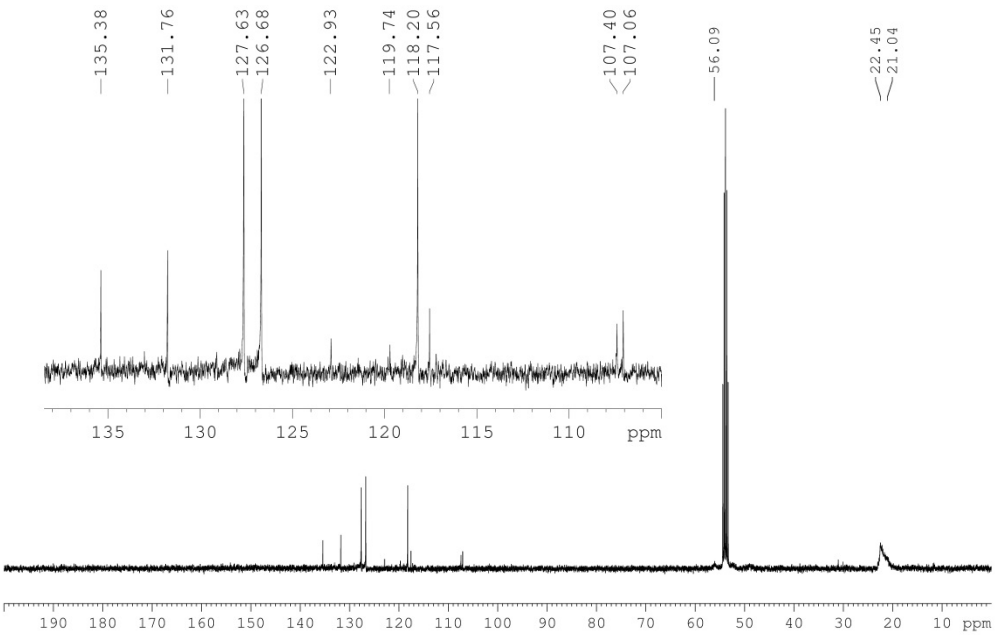

^{1}H NMR spectrum (400 MHz, CD_2Cl_2) **4.40**

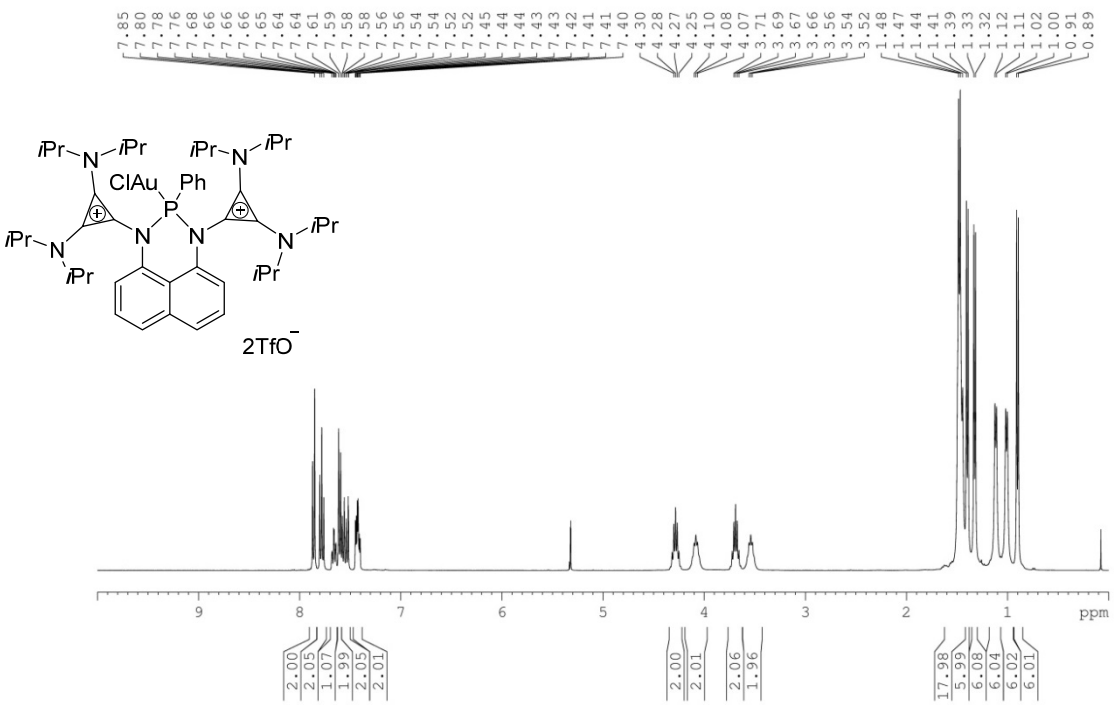

^{31}P{^{1}H} NMR spectrum (162 MHz, CD_2Cl_2) **4.40**

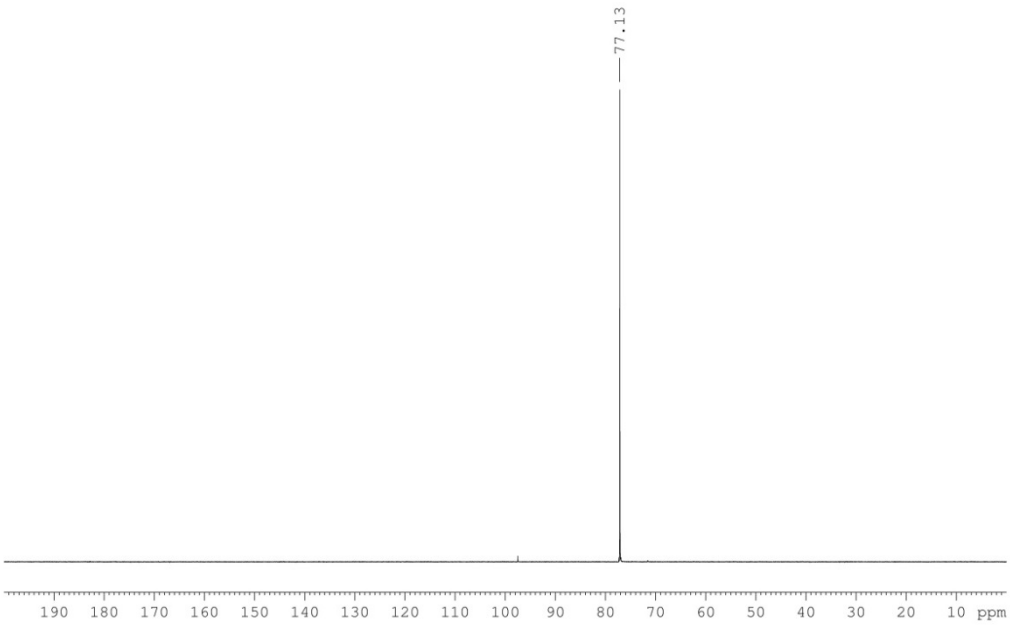

$^{13}C\{^{1}H\}$ NMR spectrum (101 MHz, CD_2Cl_2) **4.40**

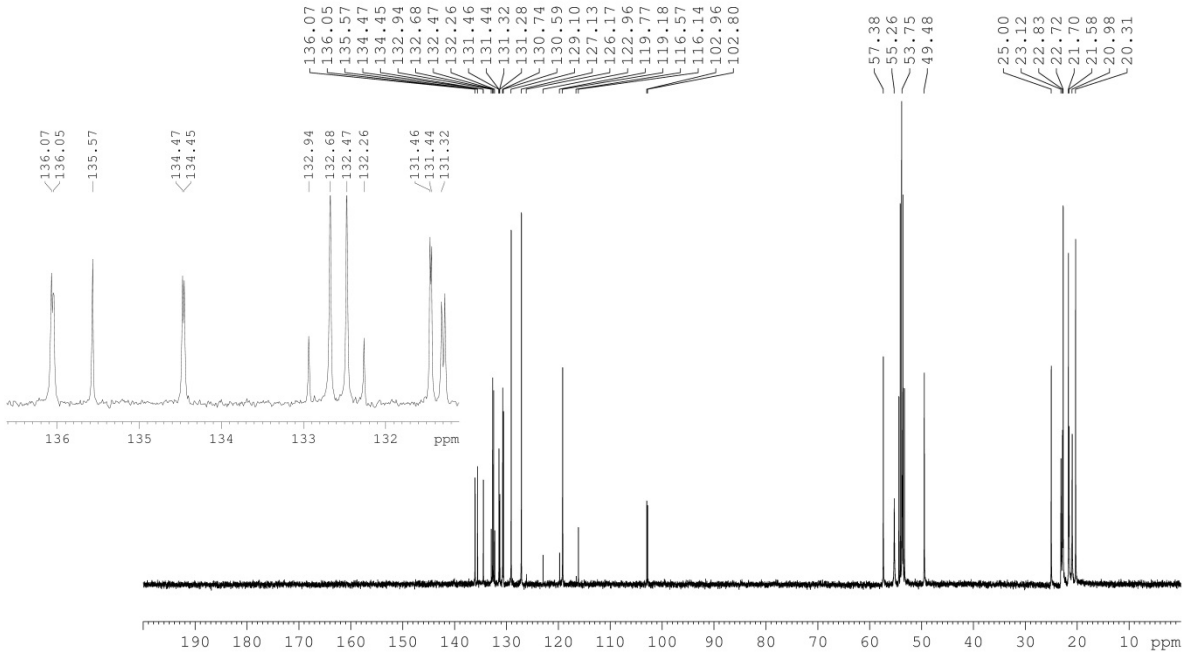

^{1}H NMR spectrum (400 MHz, CD_2Cl_2) **4.41**

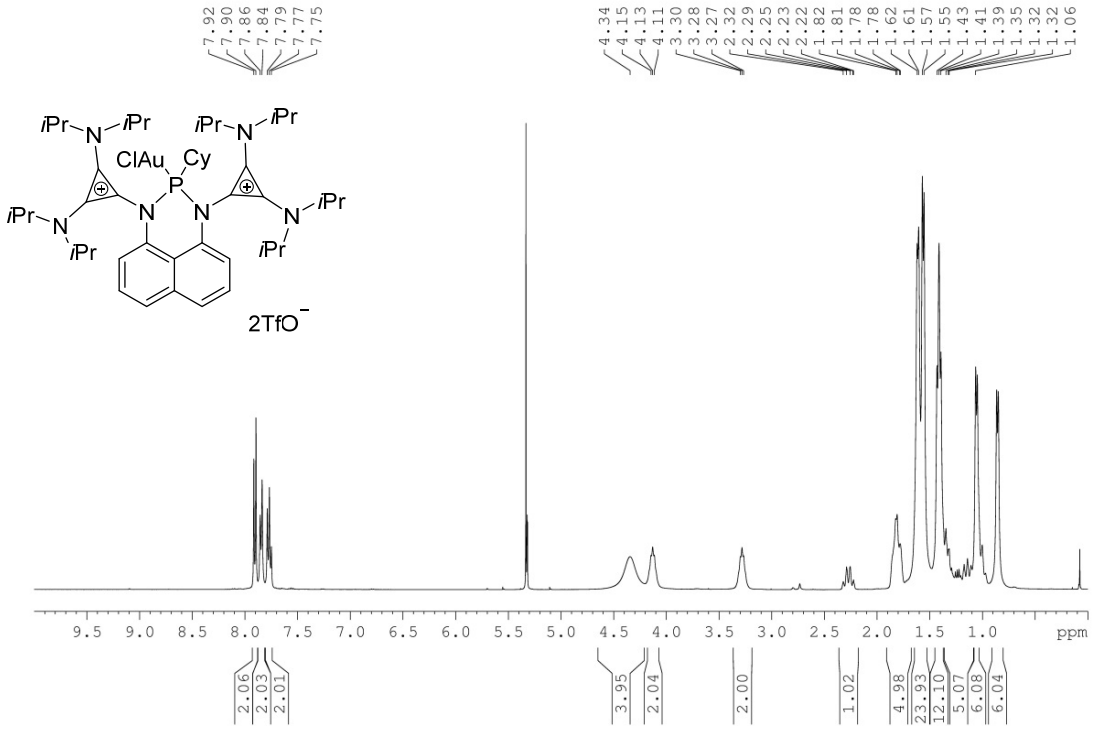

$^{31}P\{^{1}H\}$ NMR spectrum (162 MHz, CD_2Cl_2) **4.41**

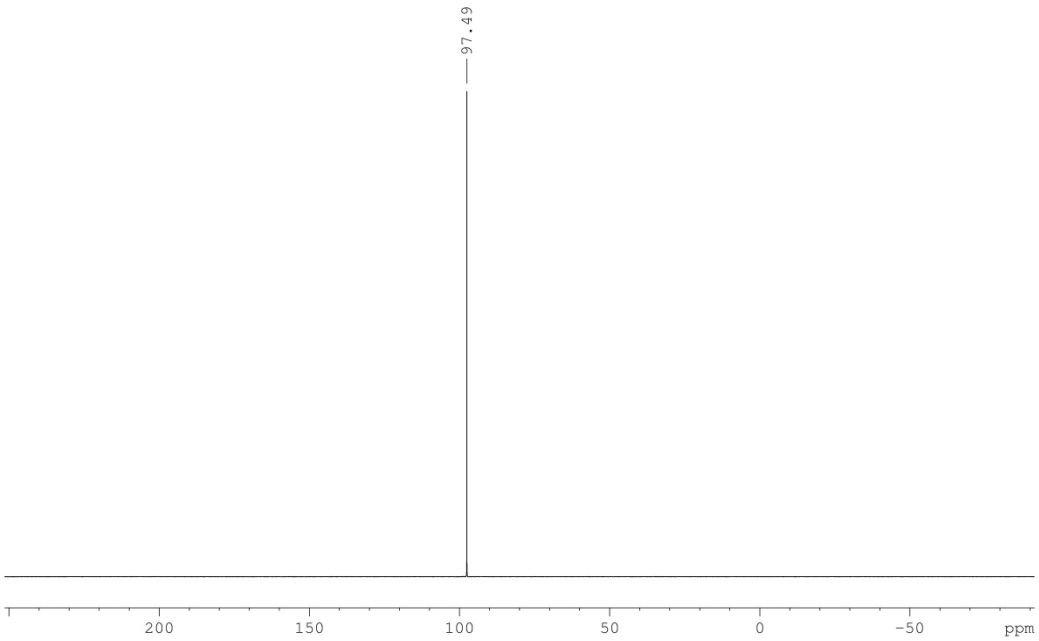

$^{13}C\{^{1}H\}$ NMR spectrum (101 MHz, CD_2Cl_2) **4.41**

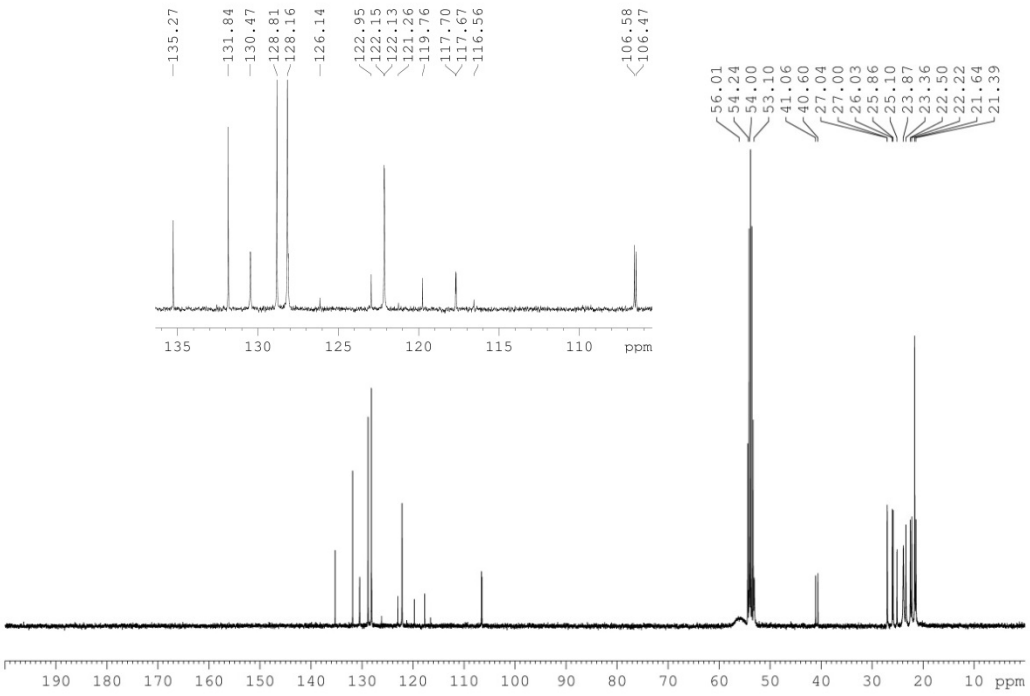

^{1}H NMR spectrum (400 MHz, CD_2Cl_2) **4.43**

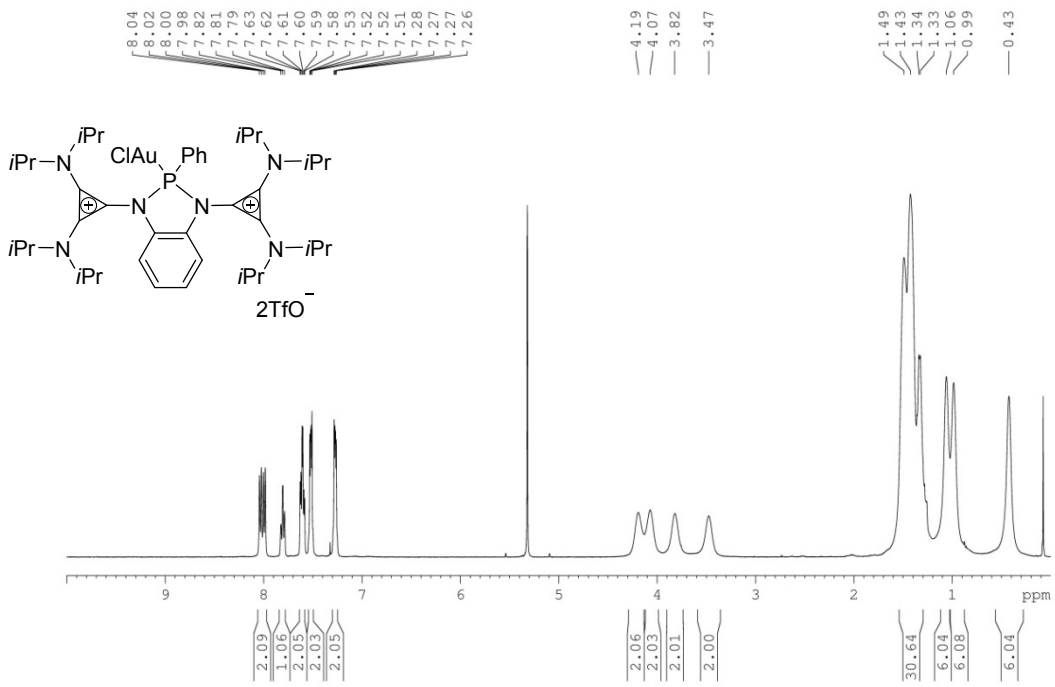

^{31}P{^{1}H} NMR spectrum (162 MHz, CD_2Cl_2) **4.43**

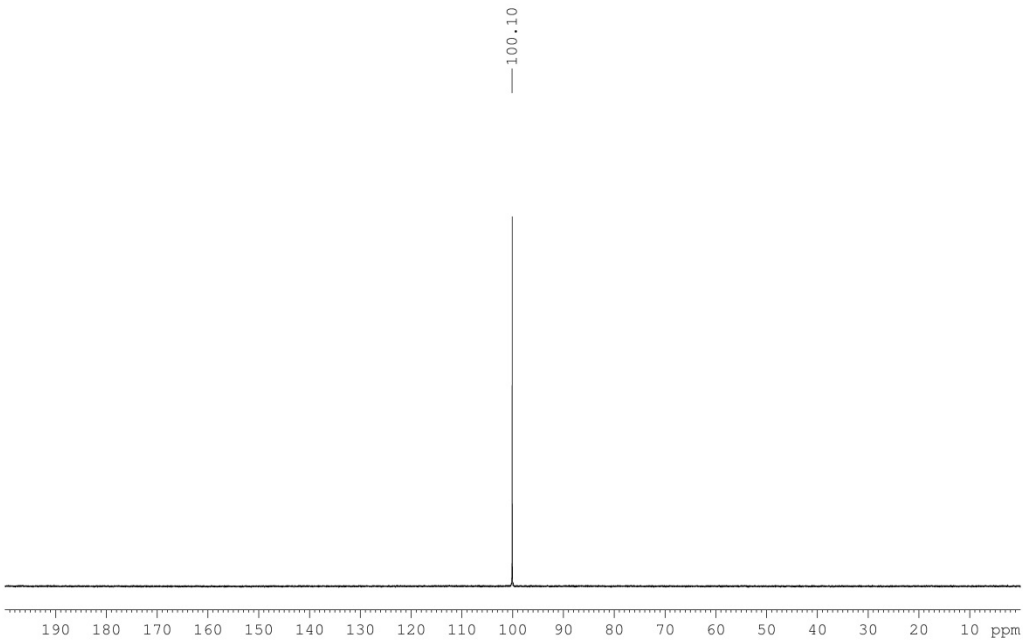

$^{13}C\{^{1}H\}$ NMR spectrum (101 MHz, CD_2Cl_2) **4.43**

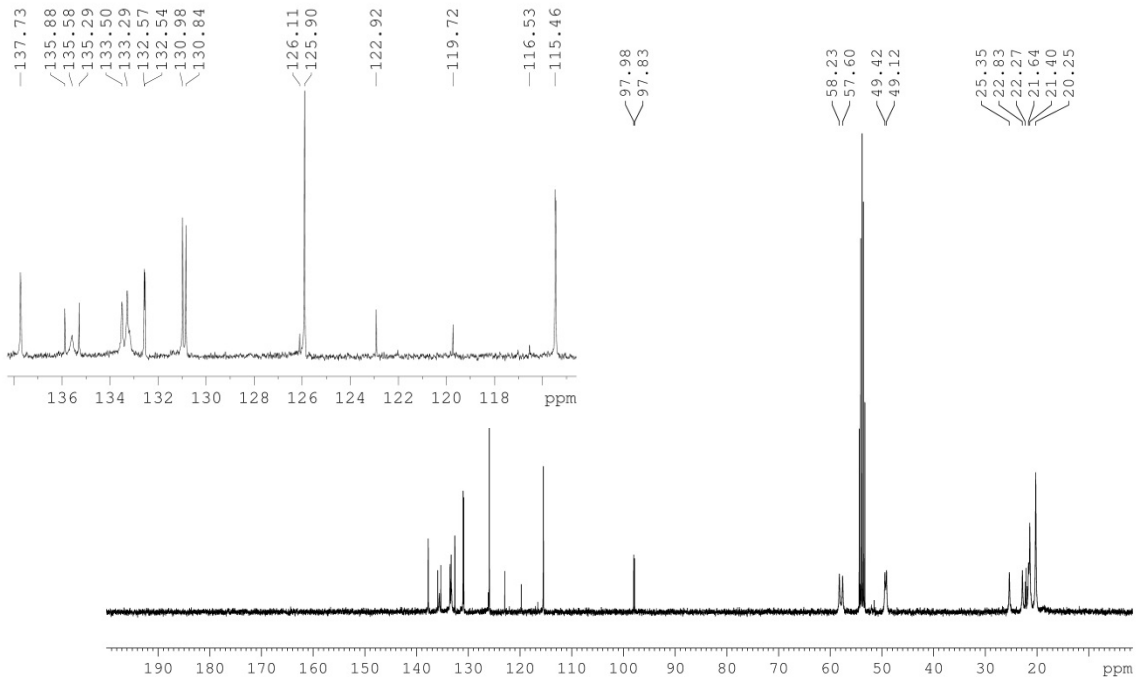

^{1}H NMR spectrum (400 MHz, CD_2Cl_2) **4.45**

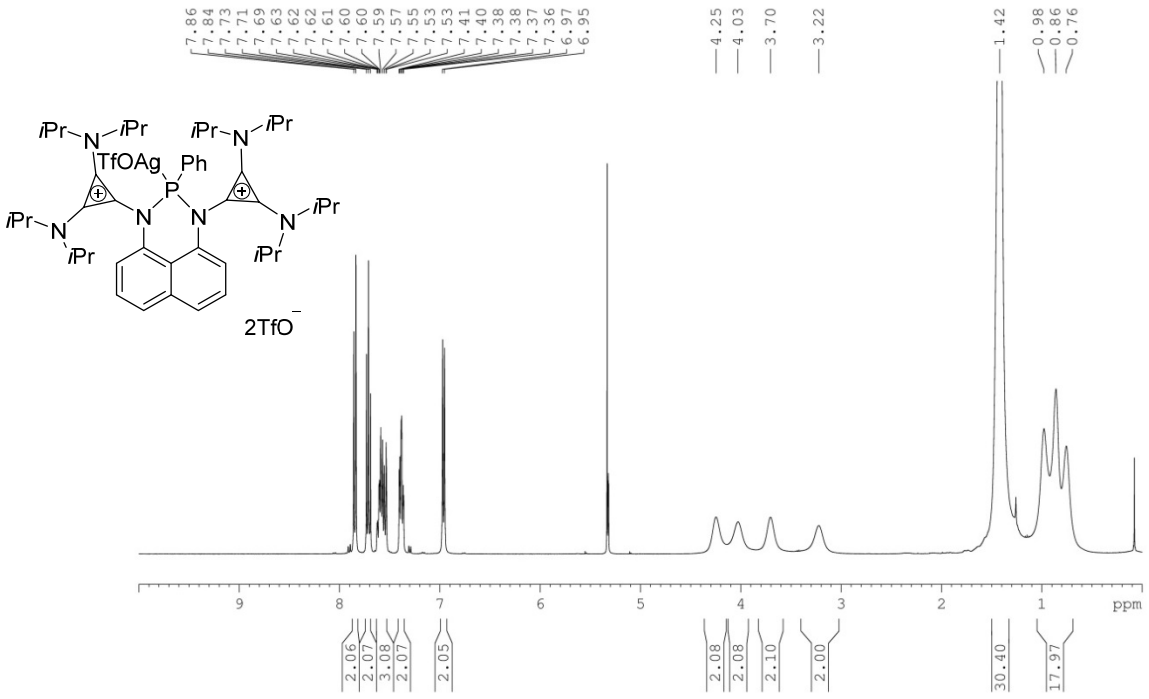

$^{31}P\{^{1}H\}$ NMR spectrum (162 MHz, CD_2Cl_2) **4.45**

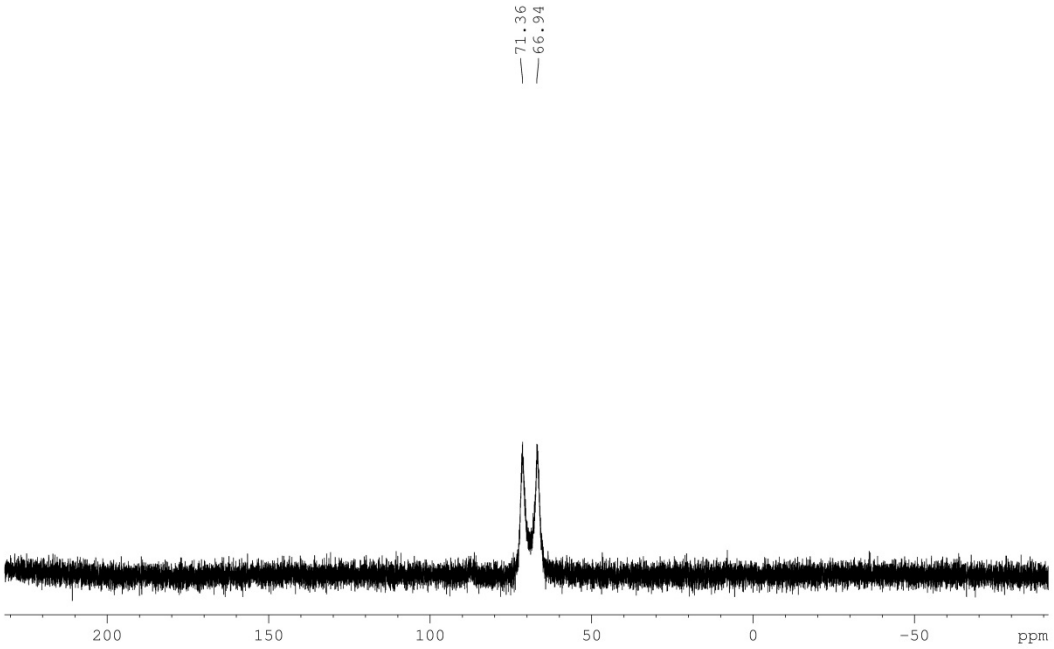

$^{13}C\{^{1}H\}$ NMR spectrum (101 MHz, CD_2Cl_2) **4.45**

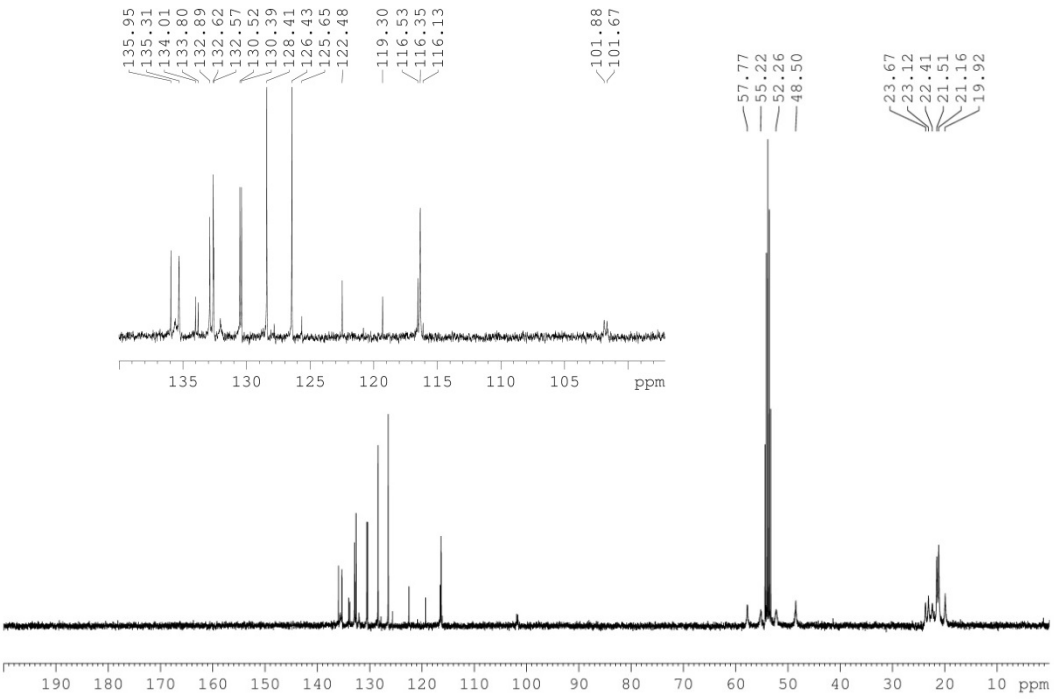

^{1}H NMR spectrum (400 MHz, CD_2Cl_2) **4.47**

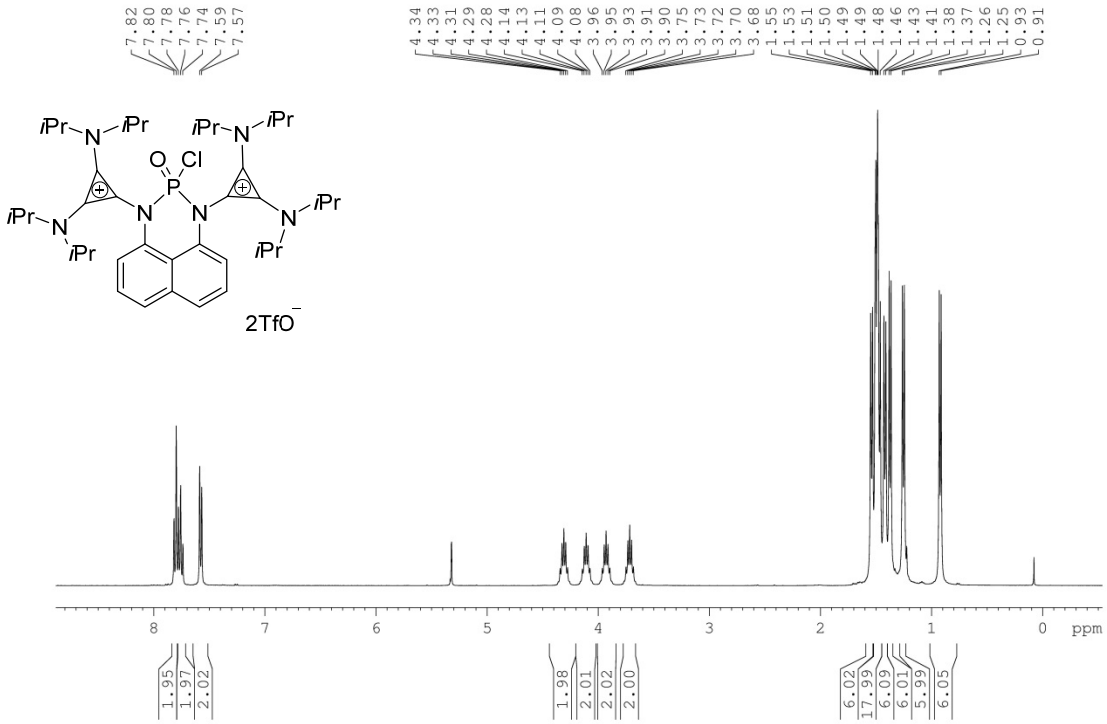

^{31}P{^{1}H} NMR spectrum (162 MHz, CD_2Cl_2) **4.47**

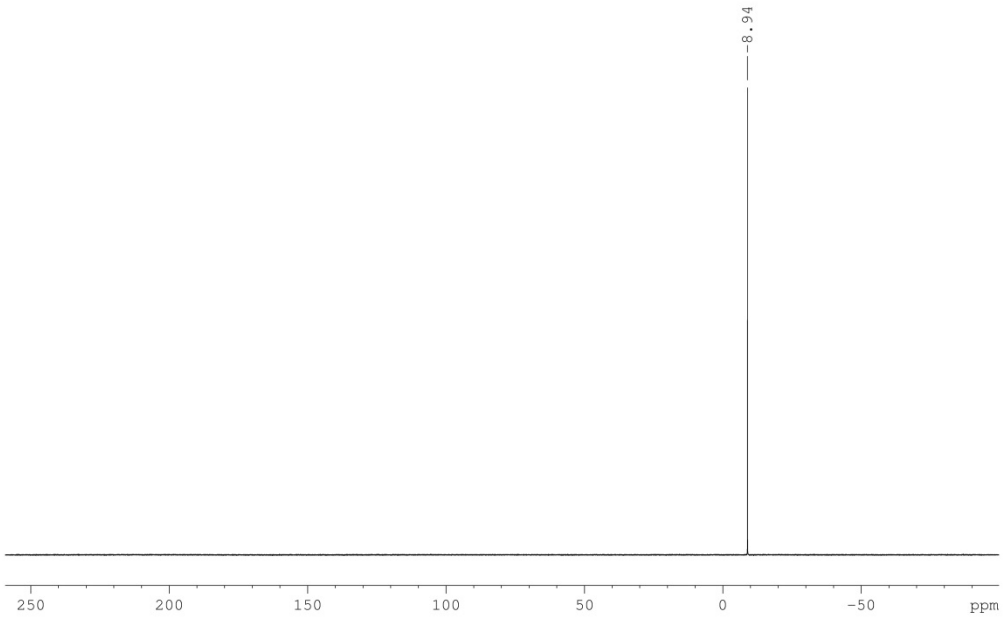

$^{13}C\{^{1}H\}$ NMR spectrum (101 MHz, CD_2Cl_2) **4.47**

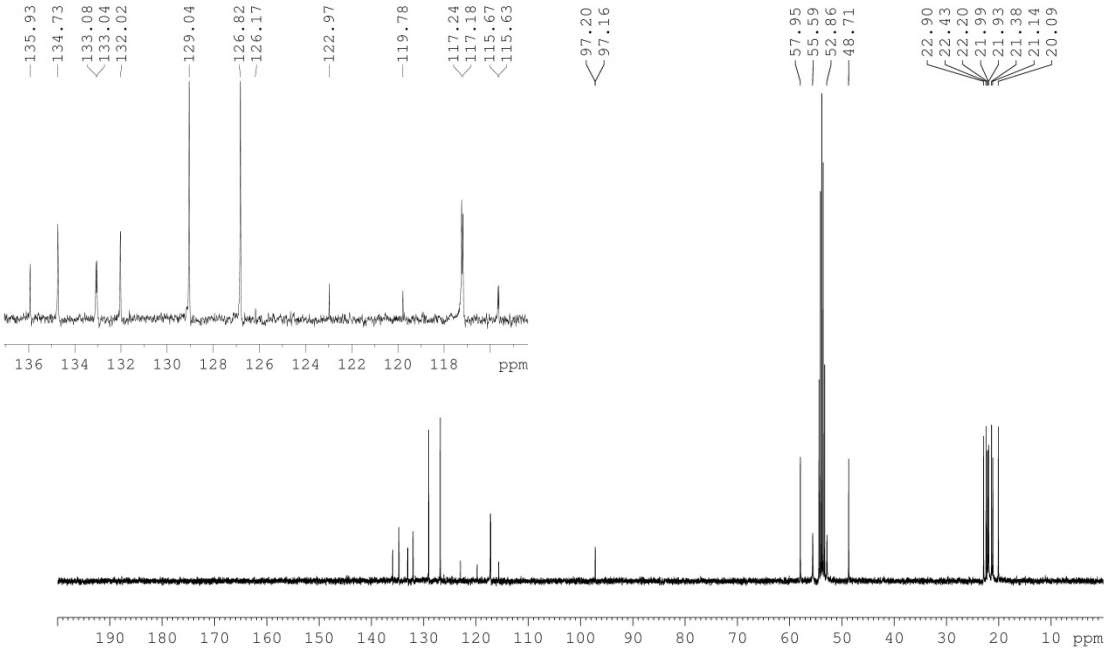

^{1}H NMR spectrum (400 MHz, CD_2Cl_2) **4.48**

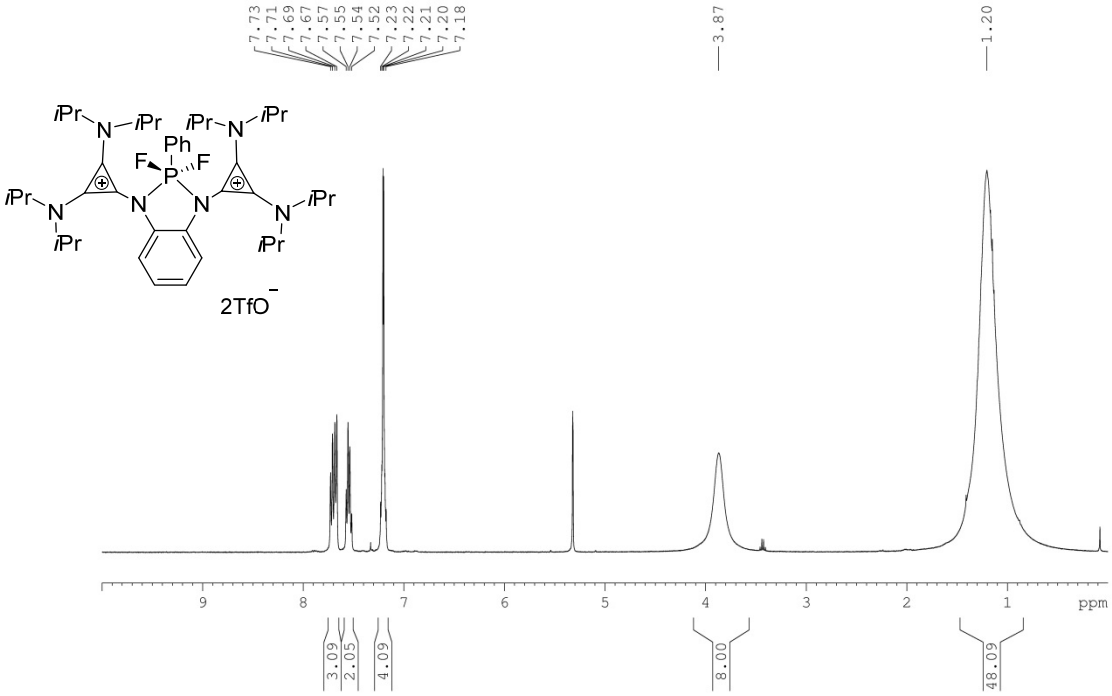

$^{31}P\{^{1}H\}$ NMR spectrum (162 MHz, CD_2Cl_2) **4.48**

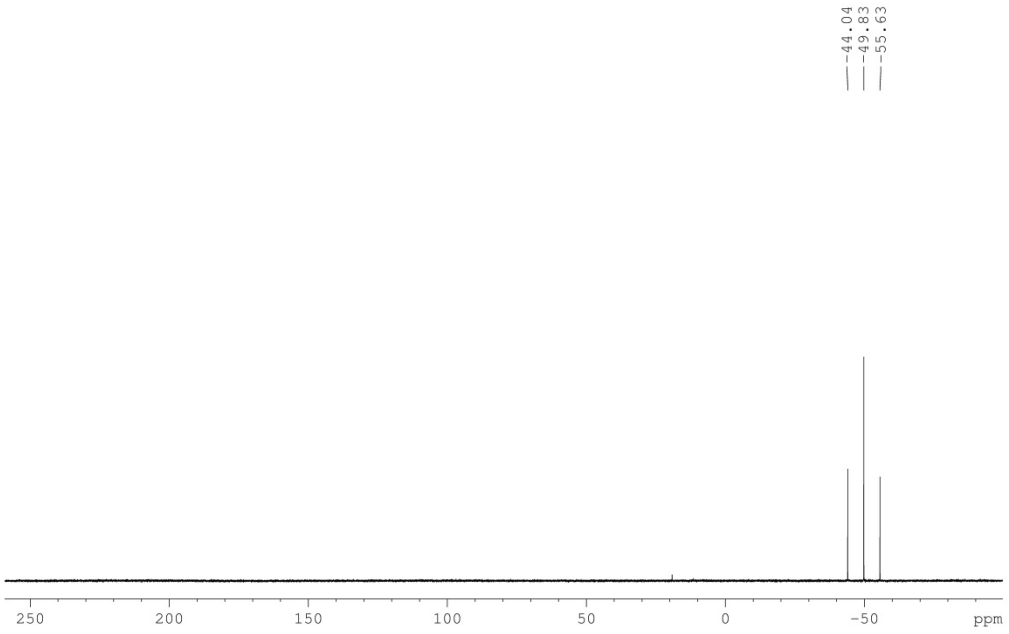

$^{13}C\{^{1}H\}$ NMR spectrum (101 MHz, CD_2Cl_2) **4.48**

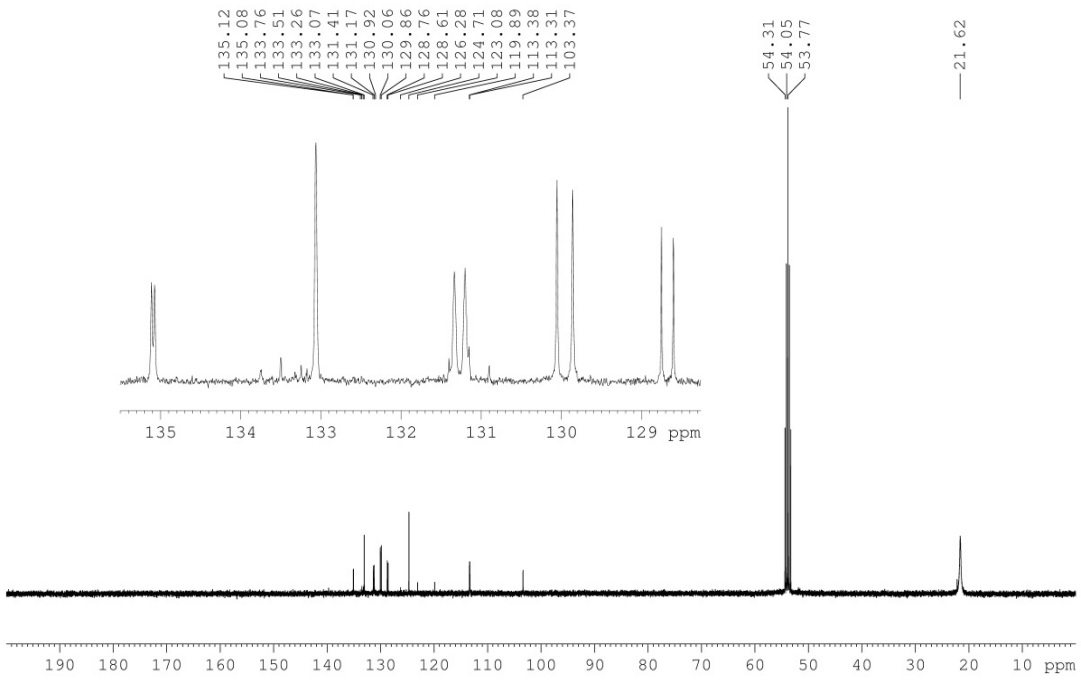

$^{19}F\{^{1}H\}$ NMR spectrum (282 MHz, CD_2Cl_2) **4.48**

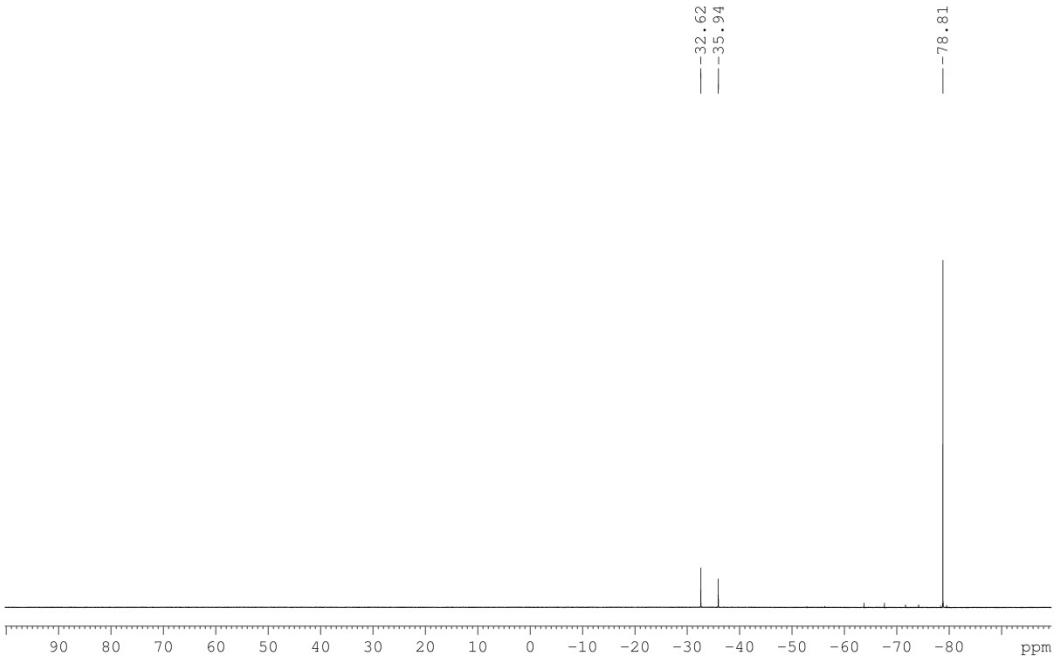

7.3. X-Ray Structure Analyses

Compound **2.15**

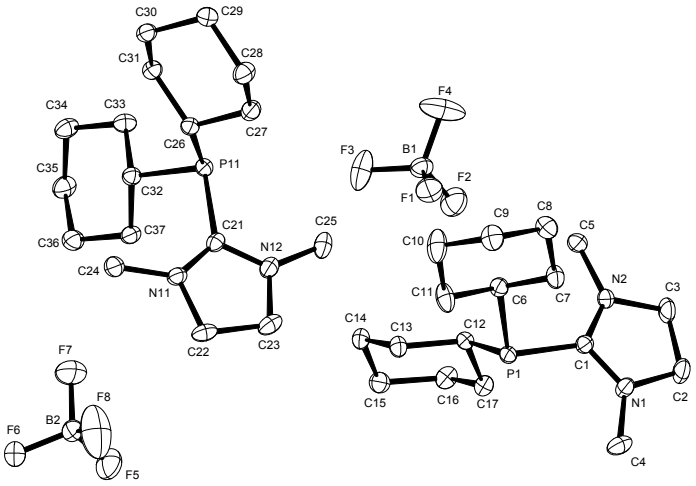

CCDC number	1407664	
Empirical formula	$C_{17}H_{32}BF_4N_2P$	
Color	colorless	
Formula weight	382.22 g · mol^{-1}	
Temperature	100 K	
Wavelength	1.54178 Å	
Crystal system	monoclinic	
Space group	$P2_1/n$, (no. 14)	
Unit cell dimensions	a = 12.3705(5) Å	α = 90°.
	b = 22.6919(9) Å	β = 113.6237(13)°.
	c = 15.1987(6) Å	γ = 90°.
Volume	3908.9(3) Å^3	
Z	8	
Density (calculated)	1.299 Mg · m^{-3}	
Absorption coefficient	1.598 mm^{-1}	
F(000)	1632 e	
Crystal size	0.33 x 0.13 x 0.10 mm^3	
θ range for data collection	3.724 to 67.698°.	
Index ranges	$-14 \le h \le 14$, $-27 \le k \le 27$, $-18 \le l \le 18$	
Reflections collected	92285	
Independent reflections	7040 [R_{int} = 0.0467]	
Reflections with I>2σ (I)	6294	
Completeness to θ = 67.679°	99.5 %	
Absorption correction	Gaussian	
Max. and min. transmission	0.89 and 0.65	
Refinement method	Full-matrix least-squares on F^2	
Data / restraints / parameters	7040 / 0 / 455	
Goodness-of-fit on F^2	1.055	
Final R indices [I>2σ (I)]	R_1 = 0.0409	wR^2 = 0.1005
R indices (all data)	R_1 = 0.0464	wR^2 = 0.1046
Largest diff. peak and hole	0.6 and -0.5 e · Å^{-3}	

Compound **2.19**

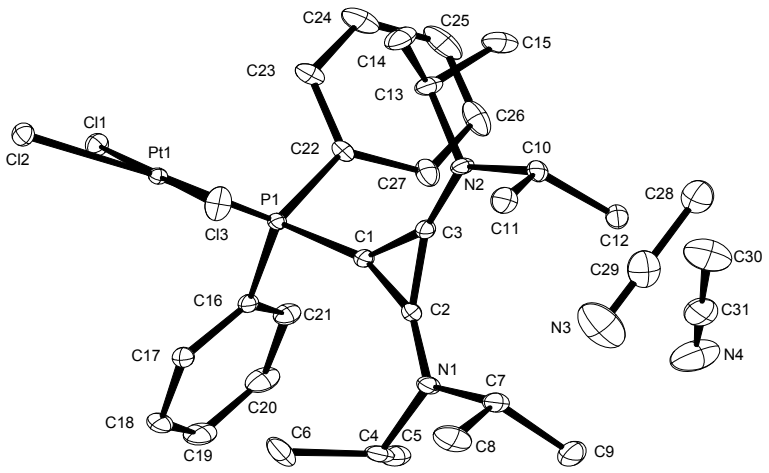

CCDC number	Φ	
Empirical formula	C_{31} H_{44} Cl_3 N_4 P Pt	
Color	yellow	
Formula weight	805.11 g·mol^{-1}	
Temperature	100 K	
Wavelength	0.71073 Å	
Crystal system	Monoclinic	
Space group	c c, (no. 9)	
Unit cell dimensions	a = 17.5137(19) Å	α = 90°.
	b = 11.2456(12) Å	β = 101.136(2)°.
	c = 18.225(2) Å	γ = 90°.
Volume	3521.9(7) Å^3	
Z	4	
Density (calculated)	1.518 Mg·m^{-3}	
Absorption coefficient	4.283 mm^{-1}	
F(000)	1608 e	
Crystal size	0.12 x 0.09 x 0.05 mm^3	
θ range for data collection	2.954 to 34.530°.	
Index ranges	$-27 \le h \le 27$, $-17 \le k \le 17$, $-29 \le l \le 29$	
Reflections collected	61228	
Independent reflections	14755 [R_{int} = 0.0467]	
Reflections with I>2σ(I)	13928	
Completeness to θ = 25.242°	99.8 %	
Absorption correction	Gaussian	
Max. and min. transmission	0.82511 and 0.57449	
Refinement method	Full-matrix least-squares on F^2	
Data / restraints / parameters	14755 / 2 / 371	
Goodness-of-fit on F^2	0.867	
Final R indices [I>2σ(I)]	R_1 = 0.0215	wR^2 = 0.0365
R indices (all data)	R_1 = 0.0237	wR^2 = 0.0368
Absolute structure parameter	0.006(3)	
Extinction coefficient	n/a	
Largest diff. peak and hole	1.095 and -0.982 e·Å^{-3}	

Compound **2.20**

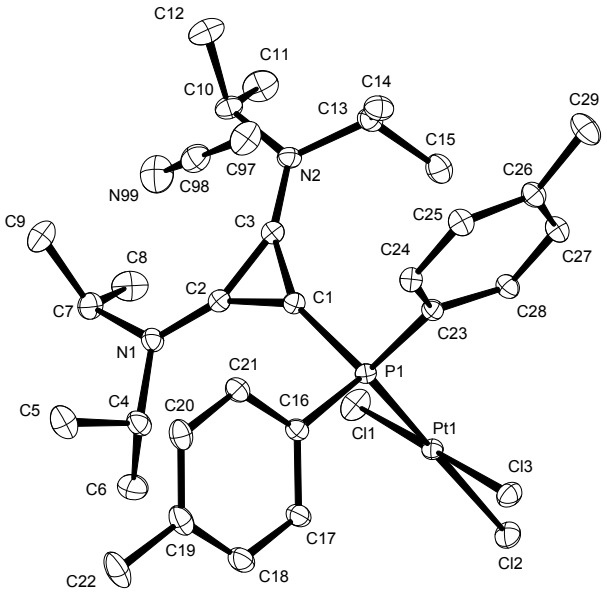

CCDC number	960681	
Empirical formula	$C_{29}H_{42}Cl_3N_2PPt \cdot CH_3CN$	
Color	yellow	
Formula weight	792.11 g · mol^{-1}	
Temperature	100 K	
Wavelength	0.71073 Å	
Crystal system	orthorhombic	
Space group	Pbca, (no. 61)	
Unit cell dimensions	a = 15.4474(15) Å	α = 90°.
	b = 17.4383(17) Å	β = 90°.
	c = 24.944(2) Å	γ = 90°.
Volume	6719.3(11) $Å^3$	
Z	8	
Density (calculated)	1.566 Mg · m^{-3}	
Absorption coefficient	4.487 mm^{-1}	
F(000)	3168 e	
Crystal size	0.30 x 0.12 x 0.11 mm^3	
θ range for data collection	1.63 to 33.76°.	
Index ranges	$-24 \le h \le 24$, $-27 \le k \le 27$, $-38 \le l \le 38$	
Reflections collected	407730	
Independent reflections	13448 [R_{int} = 0.0892]	
Reflections with I>2σ (I)	11540	
Completeness to θ = 27.50°	100.0 %	
Absorption correction	Gaussian	
Max. and min. transmission	0.71 and 0.19	
Refinement method	Full-matrix least-squares on F^2	
Data / restraints / parameters	13448 / 0 / 363	
Goodness-of-fit on F^2	1.188	
Final R indices [I>2σ (I)]	R_1 = 0.0274	wR^2 = 0.0617
R indices (all data)	R_1 = 0.0380	wR^2 = 0.0707
Largest diff. peak and hole	2.573 and -1.662 e · $Å^{-3}$	

Compound **2.21**

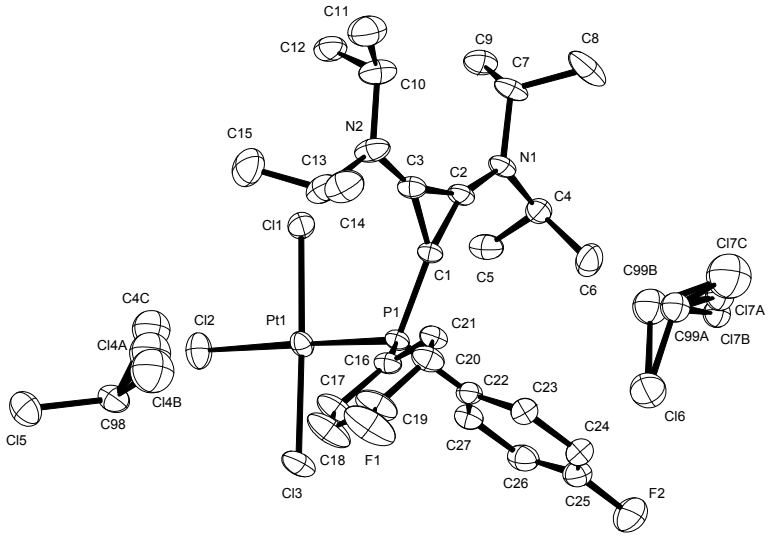

CCDC number	Φ	
Empirical formula	$C_{28.50}H_{40}Cl_{6.50}F_2N_2PPt$	
Color	yellow	
Formula weight	905.11 g · mol^{-1}	
Temperature	100 K	
Wavelength	0.71073 Å	
Crystal system	orthorhombic	
Space group	Pbca, (no. 61)	
Unit cell dimensions	a = 16.057(2) Å	α = 90°.
	b = 20.710(4) Å	β = 90°.
	c = 22.5009(19) Å	γ = 90°.
Volume	7482.3(19) $Å^3$	
Z	8	
Density (calculated)	1.607 Mg · m^{-3}	
Absorption coefficient	4.289 mm^{-1}	
F(000)	3572 e	
Crystal size	0.28 x 0.16 x 0.08 mm^3	
θ range for data collection	2.673 to 35.022°.	
Index ranges	$-25 \le h \le 24$, $-33 \le k \le 33$, $-36 \le l \le 36$	
Reflections collected	175652	
Independent reflections	16466 [R_{int} = 0.0465]	
Reflections with I>2σ(I)	13190	
Completeness to θ = 25.242°	99.8 %	
Absorption correction	Gaussian	
Max. and min. transmission	0.65 and 0.35	
Refinement method	Full-matrix least-squares on F^2	
Data / restraints / parameters	16466 / 0 / 392	
Goodness-of-fit on F^2	1.239	
Final R indices [I>2σ(I)]	R_1 = 0.0601	wR^2 = 0.1398
R indices (all data)	R_1 = 0.0776	wR^2 = 0.1475
Largest diff. peak and hole	2.7 and -2.1 e · $Å^{-3}$	

Compound **2.22**

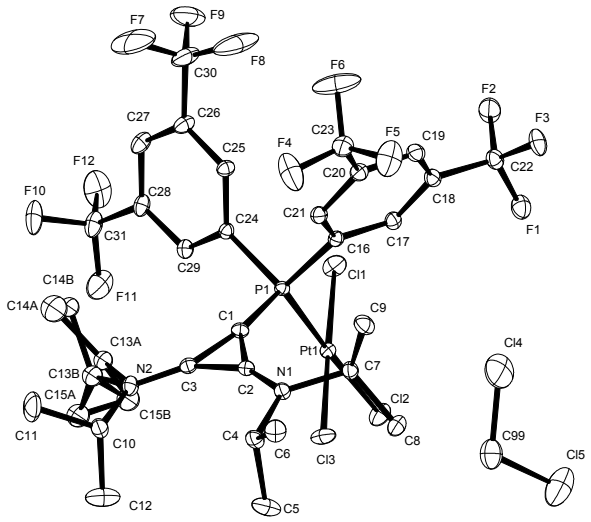

CCDC number	973072	
Empirical formula	$C_{32}H_{36}Cl_5F_{12}N_2PPt$	
Color	yellow	
Formula weight	1079.94 g · mol^{-1}	
Temperature	100 K	
Wavelength	0.71073 Å	
Crystal system	monoclinic	
Space group	$P2_1/n$, (no. 14)	
Unit cell dimensions	a = 13.8721(16) Å	α = 90°.
	b = 16.0809(18) Å	β = 96.461(2)°.
	c = 17.854(2) Å	γ = 90°.
Volume	3957.5(8) $Å^3$	
Z	4	
Density (calculated)	1.813 Mg · m^{-3}	
Absorption coefficient	4.007 mm^{-1}	
F(000)	2112 e	
Crystal size	0.27 x 0.20 x 0.13 mm^3	
θ range for data collection	1.709 to 35.121°.	
Index ranges	$-22 \le h \le 21$, $-25 \le k \le 26$, $-28 \le l \le 28$	
Reflections collected	145660	
Independent reflections	17544 [R_{int} = 0.0286]	
Reflections with I>2σ (I)	15704	
Completeness to θ = 25.242°	100.0 %	
Absorption correction	Gaussian	
Max. and min. transmission	0.67 and 0.43	
Refinement method	Full-matrix least-squares on F^2	
Data / restraints / parameters	17544 / 0 / 484	
Goodness-of-fit on F^2	1.018	
Final R indices [I>2σ (I)]	R_1 = 0.0198	wR^2 = 0.0457
R indices (all data)	R_1 = 0.0249	wR^2 = 0.0478
Largest diff. peak and hole	2.9 and -2.3 e · $Å^{-3}$	

Compound **2.23**

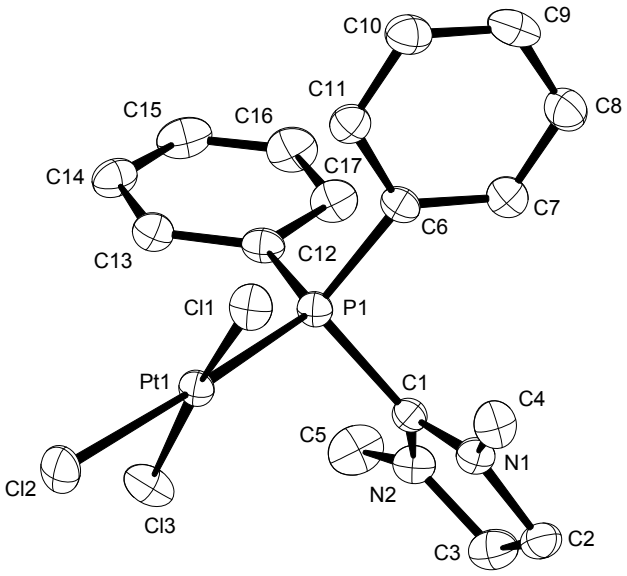

CCDC number	1407664	
Empirical formula	$C_{17}H_{20}Cl_3N_2PPt$	
Color	yellow	
Formula weight	584.76 g · mol^{-1}	
Temperature	150 K	
Wavelength	0.71073 Å	
Crystal system	monoclinic	
Space group	$P2_1/n$, (no. 14)	
Unit cell dimensions	a = 10.6985(8) Å	α = 90°.
	b = 17.0969(13) Å	β = 91.790(7)°.
	c = 10.7451(11) Å	γ = 90°.
Volume	1964.4(3) $Å^3$	
Z	4	
Density (calculated)	1.977 Mg · m^{-3}	
Absorption coefficient	7.634 mm^{-1}	
F(000)	1120 e	
Crystal size	0.07 x 0.07 x 0.06 mm^3	
θ range for data collection	2.646 to 33.166°.	
Index ranges	$-16 \le h \le 16$, $-25 \le k \le 26$, $-15 \le l \le 16$	
Reflections collected	22176	
Independent reflections	7474 [R_{int} = 0.0627]	
Reflections with I>2σ (I)	5707	
Completeness to θ = 25.242°	99.9 %	
Absorption correction	Gaussian	
Max. and min. transmission	0.69 and 0.60	
Refinement method	Full-matrix least-squares on F^2	
Data / restraints / parameters	7474 / 0 / 219	
Goodness-of-fit on F^2	1.033	
Final R indices [I>2σ (I)]	R_1 = 0.0563	wR^2 = 0.1374
R indices (all data)	R_1 = 0.0775	wR^2 = 0.1527
Largest diff. peak and hole	2.540 and -6.738 e · $Å^{-3}$	

Compound **2.27**

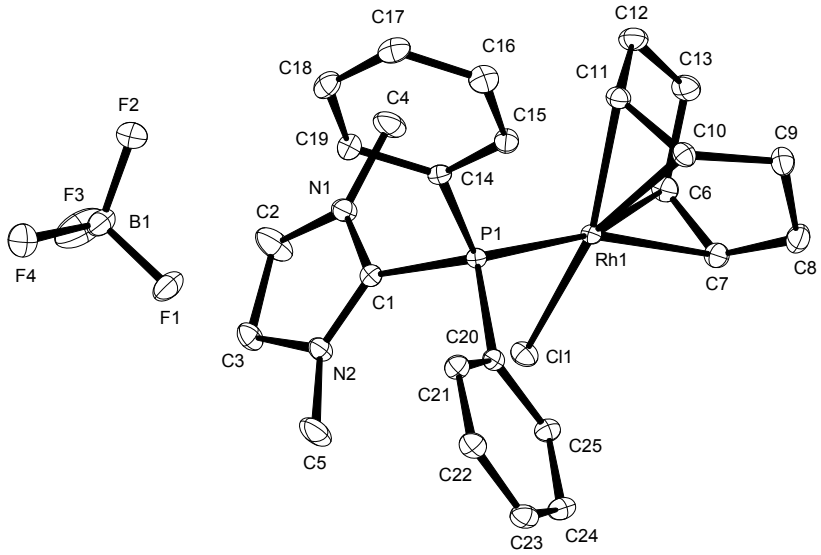

CCDC number	Φ	
Empirical formula	$C_{25}H_{32}BClF_4N_2PRh$	
Color	yellow	
Formula weight	616.67 g · mol^{-1}	
Temperature	100(2) K	
Wavelength	0.71073 Å	
Crystal system	monoclinic	
Space group	$P2_1/c$, (no. 14)	
Unit cell dimensions	a = 14.3945(16) Å	α = 90°.
	b = 12.8839(12) Å	β = 101.195(7)°.
	c = 13.9175(10) Å	γ = 90°.
Volume	2532.0(4) $Å^3$	
Z	4	
Density (calculated)	1.618 Mg · m^{-3}	
Absorption coefficient	0.891 mm^{-1}	
F(000)	1256 e	
Crystal size	0.32 x 0.08 x 0.06 mm^3	
θ range for data collection	2.76 to 33.13°.	
Index ranges	$-22 \le h \le 22$, $-19 \le k \le 19$, $-21 \le l \le 21$	
Reflections collected	71947	
Independent reflections	9636 [R_{int} = 0.0503]	
Reflections with I>2σ (I)	8079	
Completeness to θ = 33.13°	99.8 %	
Absorption correction	Gaussian	
Max. and min. transmission	0.96 and 0.78	
Refinement method	Full-matrix least-squares on F^2	
Data / restraints / parameters	9636 / 0 / 334	
Goodness-of-fit on F^2	1.039	
Final R indices [I>2σ (I)]	R_1 = 0.0308	wR^2 = 0.0681
R indices (all data)	R_1 = 0.0431	wR^2 = 0.0732
Largest diff. peak and hole	1.0 and -1.3 e·$Å^{-3}$	

Compound **2.29**

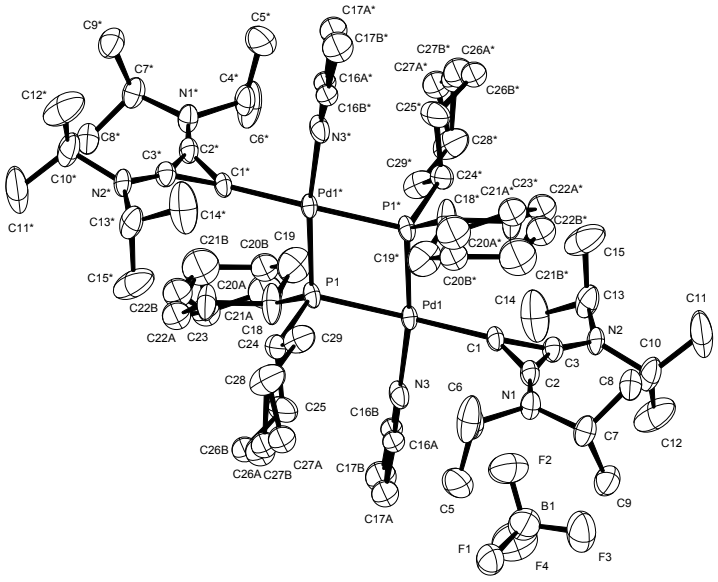

CCDC number	960688	
Empirical formula	$C_{29}H_{53}BF_4N_3PPd$	
Color	colorless	
Formula weight	667.92 g · mol^{-1}	
Temperature	100 K	
Wavelength	0.71073 Å	
Crystal system	triclinic	
Space group	$P\bar{1}$, (no. 2)	
Unit cell dimensions	a = 11.910(2) Å	α = 99.923(4)°.
	b = 12.072(2) Å	β = 105.144(5)°.
	c = 14.873(4) Å	γ = 109.581(3)°.
Volume	1863.6(7) $Å^3$	
Z	2	
Density (calculated)	1.190 Mg · m^{-3}	
Absorption coefficient	0.580 mm^{-1}	
F(000)	700 e	
Crystal size	0.140 x 0.120 x 0.070 mm^3	
θ range for data collection	1.48 to 29.13°.	
Index ranges	$-16 \le h \le 16$, $-16 \le k \le 16$, $-20 \le l \le 20$	
Reflections collected	41584	
Independent reflections	10043 [R_{int} = 0.1654]	
Reflections with I>2σ (I)	7830	
Completeness to θ = 27.50°	100.0 %	
Absorption correction	Gaussian	
Max. and min. transmission	0.96 and 0.92	
Refinement method	Full-matrix least-squares on F^2	
Data / restraints / parameters	10043 / 0 / 355	
Goodness-of-fit on F^2	1.010	
Final R indices [I>2σ (I)]	R_1 = 0.0735	wR^2 = 0.1938
R indices (all data)	R_1 = 0.0891	wR^2 = 0.2040
Largest diff. peak and hole	1.630 and -1.807 e · $Å^{-3}$	

Compound **2.30**

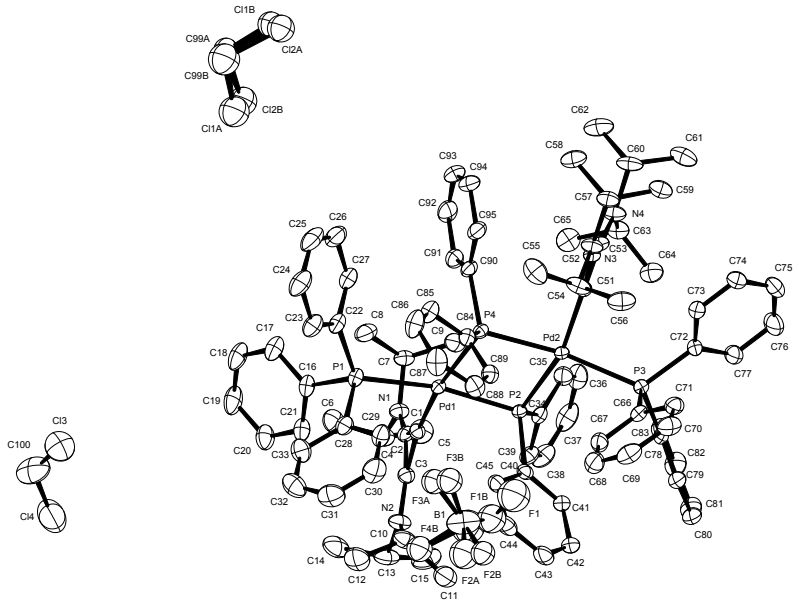

CCDC number	960682	
Empirical formula	2 ($C_{90}H_{106}N_4P_4Pd_2 \cdot BF_4^-$) · 3 CH_2Cl_2	
Color	orange	
Formula weight	3589.35 g · mol^{-1}	
Temperature	150 K	
Wavelength	0.71073 Å	
Crystal system	triclinic	
Space group	$P\bar{1}$, (no. 2)	
Unit cell dimensions	a = 14.9923(14) Å	α = 88.907(8)°.
	b = 15.0686(12) Å	β = 85.865(10)°.
	c = 24.293(3) Å	γ = 84.908(6)°.
Volume	5451.7(9) $Å^3$	
Z	1	
Density (calculated)	1.093 Mg · m^{-3}	
Absorption coefficient	0.506 mm^{-1}	
F(000)	1860 e	
Crystal size	0.26 x 0.22 x 0.21 mm^3	
θ range for data collection	2.73 to 27.50°.	
Index ranges	$-19 \le h \le 19$, $-19 \le k \le 19$, $-31 \le l \le 31$	
Reflections collected	108051	
Independent reflections	25020 [R_{int} = 0.0321]	
Reflections with I>2σ (I)	20928	
Completeness to θ = 27.50°	99.9 %	
Absorption correction	Gaussian	
Max. and min. transmission	0.87 and 0.80	
Refinement method	Full-matrix least-squares on F^2	
Data / restraints / parameters	25020 / 0 / 1011	
Goodness-of-fit on F^2	1.088	
Final R indices [I>2σ (I)]	R_1 = 0.0431	wR^2 = 0.1267
R indices (all data)	R_1 = 0.0523	wR^2 = 0.1333
Largest diff. peak and hole	1.870 and -1.576 e · $Å^{-3}$	

Compound **2.33**

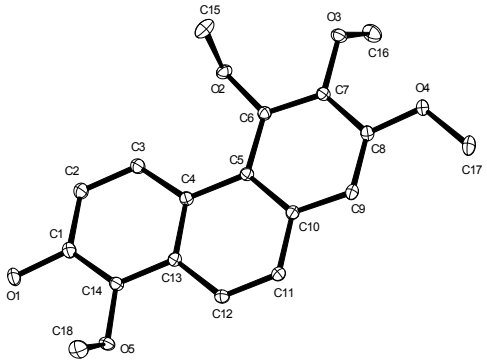

CCDC number	966990	
Empirical formula	$C_{18}H_{18}O_5$	
Color	yellow	
Formula weight	314.32 g · mol^{-1}	
Temperature	100 K	
Wavelength	0.71073 Å	
Crystal system	orthorhombic	
Space group	$P2_12_12_1$, (no. 19)	
Unit cell dimensions	a = 7.6876(5) Å	α = 90°.
	b = 11.3305(7) Å	β = 90°.
	c = 17.3270(8) Å	γ = 90°.
Volume	1509.26(15) $Å^3$	
Z	4	
Density (calculated)	1.383 Mg · m^{-3}	
Absorption coefficient	0.101 mm^{-1}	
F(000)	664 e	
Crystal size	0.42 x 0.37 x 0.20 mm^3	
θ range for data collection	2.90 to 33.06°.	
Index ranges	$-11 \le h \le 11$, $-17 \le k \le 17$, $-26 \le l \le 26$	
Reflections collected	40870	
Independent reflections	5698 [R_{int} = 0.0265]	
Reflections with I>2σ (I)	5125	
Completeness to θ = 27.50°	99.4 %	
Absorption correction	Gaussian	
Max. and min. transmission	0.98 and 0.97	
Refinement method	Full-matrix least-squares on F^2	
Data / restraints / parameters	5698 / 0 / 213	
Goodness-of-fit on F^2	1.211	
Final R indices [I>2σ (I)]	R_1 = 0.0375	wR^2 = 0.1009
R indices (all data)	R_1 = 0.0484	wR^2 = 0.1099
Largest diff. peak and hole	0.4 and -0.3 e·$Å^{-3}$	

Compound **2.38**

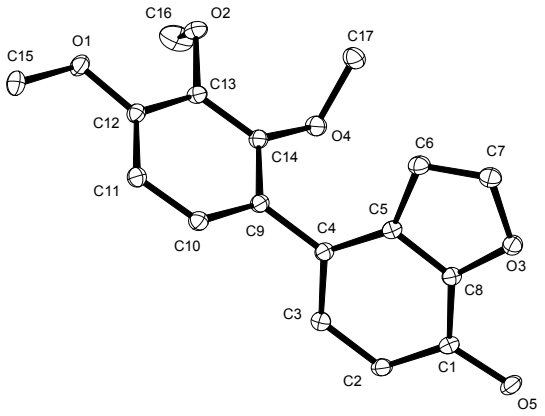

CCDC number	960689	
Empirical formula	$C_{17}H_{16}O_5$	
Color	colorless	
Formula weight	300.30 g · mol^{-1}	
Temperature	100 K	
Wavelength	0.71073 Å	
Crystal system	monoclinic	
Space group	$P2_1/c$, (no. 14)	
Unit cell dimensions	a = 11.1834(12) Å	α = 90°.
	b = 12.5326(13) Å	β = 106.040(3)°.
	c = 10.6579(11) Å	γ = 90°.
Volume	1435.6(3) $Å^3$	
Z	4	
Density (calculated)	1.389 $Mg·m^{-3}$	
Absorption coefficient	0.103 mm^{-1}	
F(000)	632 e	
Crystal size	0.24 x 0.08 x 0.07 mm^3	
θ range for data collection	2.50 to 35.46°.	
Index ranges	$-18 \le h \le 18$, $-20 \le k \le 20$, $-17 \le l \le 17$	
Reflections collected	126675	
Independent reflections	6504 [R_{int} = 0.0511]	
Reflections with I>2σ (I)	5349	
Completeness to θ = 27.50°	99.9 %	
Absorption correction	Gaussian	
Max. and min. transmission	0.99 and 0.98	
Refinement method	Full-matrix least-squares on F^2	
Data / restraints / parameters	6504 / 0 / 203	
Goodness-of-fit on F^2	1.071	
Final R indices [I>2σ (I)]	R_1 = 0.0367	wR^2 = 0.0997
R indices (all data)	R_1 = 0.0485	wR^2 = 0.1089
Largest diff. peak and hole	0.6 and -0.3 e·$Å^{-3}$	

Compound **3.38**

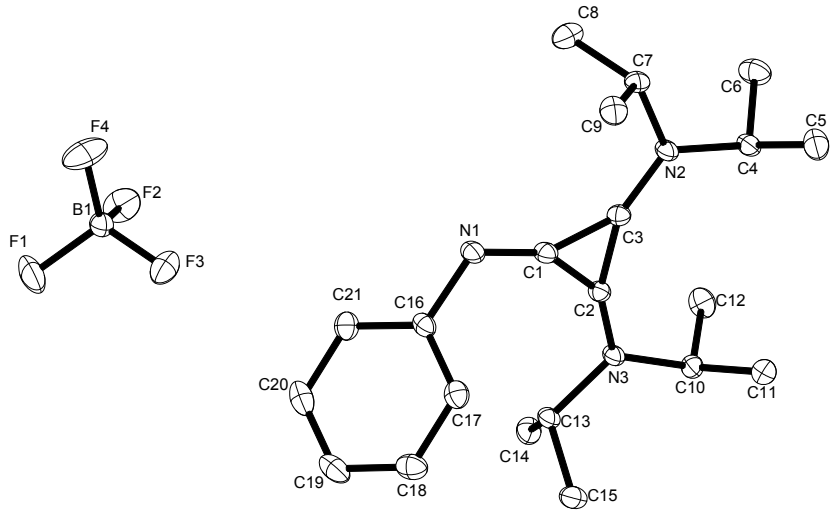

CCDC number	Φ	
Empirical formula	$C_{21}H_{34}BF_4N_3$	
Color	colorless	
Formula weight	415.32 g · mol^{-1}	
Temperature	100 K	
Wavelength	0.71073 Å	
Crystal system	monoclinic	
Space group	$P2_1/n$, (no. 14)	
Unit cell dimensions	a = 11.1709(17) Å	α = 90°.
	b = 10.7099(16) Å	β = 97.672(3)°.
	c = 18.497(3) Å	γ = 90°.
Volume	2193.1(6) $Å^3$	
Z	4	
Density (calculated)	1.258 Mg · m^{-3}	
Absorption coefficient	0.097 mm^{-1}	
F(000)	888 e	
Crystal size	0.13 x 0.12 x 0.08 mm^3	
θ range for data collection	2.20 to 28.45°.	
Index ranges	$-14 \le h \le 14$, $-14 \le k \le 14$, $-24 \le 1 \le 24$	
Reflections collected	52987	
Independent reflections	5502 [R_{int} = 0.0366]	
Reflections with I>2σ (I)	4590	
Completeness to θ = 27.50°	100.0 %	
Absorption correction	Gaussian	
Max. and min. transmission	0.99296 and 0.98682	
Refinement method	Full-matrix least-squares on F^2	
Data / restraints / parameters	5502 / 0 / 270	
Goodness-of-fit on F^2	1.029	
Final R indices [I>2σ (I)]	R_1 = 0.0352	w R^2 = 0.0812
R indices (all data)	R_1 = 0.0452	w R^2 = 0.0871
Largest diff. peak and hole	0.323 and -0.280 e · $Å^{-3}$	

Compound **3.45**

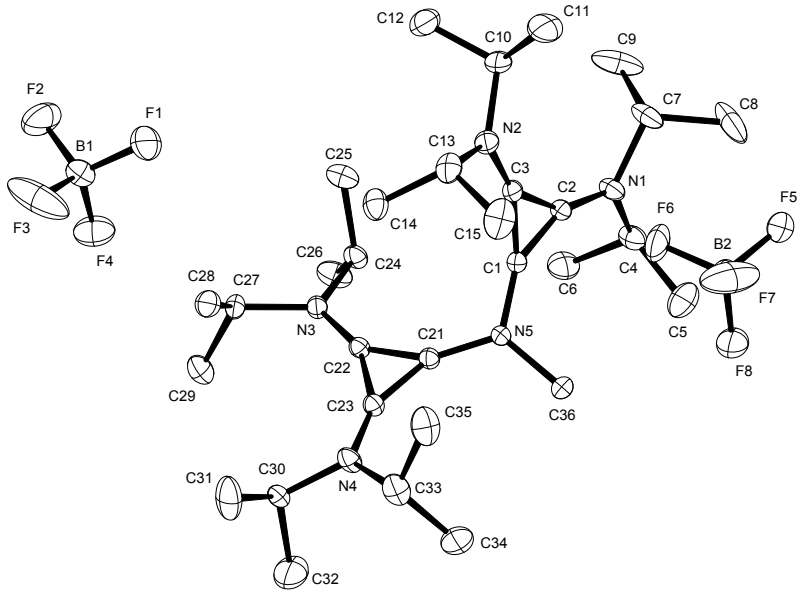

CCDC number	911776	
Empirical formula	$C_{31}H_{59}B_2F_8N_5$	
Color	colorless	
Formula weight	675.45 g · mol^{-1}	
Temperature	100 K	
Wavelength	0.71073 Å	
Crystal system	orthorhombic	
Space group	Pbca, (no. 61)	
Unit cell dimensions	a = 17.1328(15) Å	α = 90°.
	b = 13.996(2) Å	β= 90°.
	c = 31.391(7) Å	γ = 90°.
Volume	7527(2) $Å^3$	
Z	8	
Density (calculated)	1.192 Mg · m^{-3}	
Absorption coefficient	0.097 mm^{-1}	
F(000)	2896 e	
Crystal size	0.40 x 0.38 x 0.33 mm^3	
θ range for data collection	2.71 to 32.03°.	
Index ranges	$-25 \le h \le 25$, $-20 \le k \le 20$, $-46 \le 1 \le 46$	
Reflections collected	92524	
Independent reflections	13048 [R_{int} = 0.0464]	
Reflections with I>2σ(I)	9310	
Completeness to θ = 32.03°	99.6 %	
Absorption correction	Gaussian	
Max. and min. transmission	0.97 and 0.96	
Refinement method	Full-matrix least-squares on F^2	
Data / restraints / parameters	13048 / 0 / 432	
Goodness-of-fit on F^2	1.080	
Final R indices [I>2σ (I)]	R_1 = 0.0668	wR^2 = 0.1583
R indices (all data)	R_1 = 0.0995	wR^2 = 0.1838
Largest diff. peak and hole	0.984 and -0.994 e · $Å^{-3}$	

Compound **3.51**

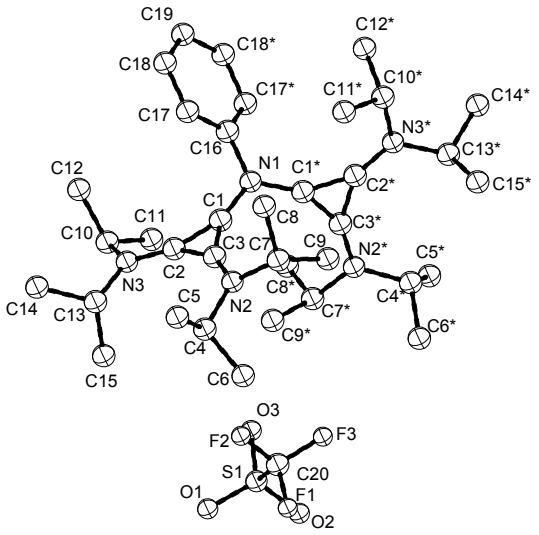

CCDC number	911774	
Empirical formula	$C_{38}H_{61}F_6N_5O_6S_2$	
Color	colorless	
Formula weight	862.04 g · mol^{-1}	
Temperature	100 K	
Wavelength	0.71073 Å	
Crystal system	tetragonal	
Space group	p 43 21 2, (no. 96)	
Unit cell dimensions	a = 10.7973 (6) Å	α = 90°.
	b = 10.7973 (6) Å	β = 90°.
	c = 39.0810(13) Å	γ = 90°.
Volume	4556.1(4) Å^3	
Z	4	
Density (calculated)	1.257 Mg · m^{-3}	
Absorption coefficient	0.188 mm^{-1}	
F(000)	1832 e	
Crystal size	0.18 x 0.17 x 0.16 mm^3	
θ range for data collection	2.86 to 31.82°.	
Index ranges	$-16 \le h \le 16$, $-16 \le k \le 15$, $-57 \le l \le 57$	
Reflections collected	66441	
Independent reflections	7772 [R_{int} = 0.0414]	
Reflections with I>2σ(I)	6764	
Completeness to θ = 27.50°	99.8 %	
Absorption correction	Gaussian	
Max. and min. transmission	0.97598 and 0.96843	
Refinement method	Full-matrix least-squares on F^2	
Data / restraints / parameters	7772 / 0 / 267	
Goodness-of-fit on F^2	1.116	
Final R indices [I>2σ(I)]	R_1 = 0.0434	w R^2 = 0.0967
R indices (all data)	R_1 = 0.0556	w R^2 = 0.1039
Absolute structure parameter	-0.04(7)	
Largest diff. peak and hole	0.390 and -0.568 e · Å^{-3}	

Compound **3.52**

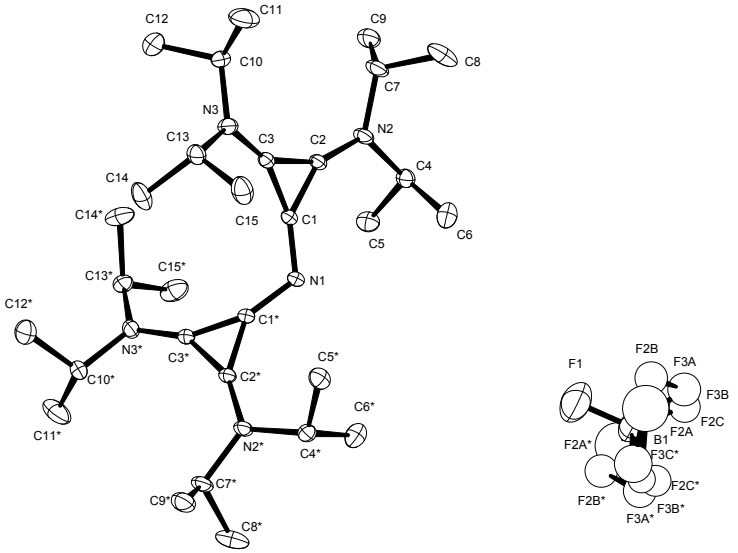

CCDC number	911773	
Empirical formula	$C_{30}H_{56}N_5^+ \cdot BF_4^-$	
Color	colorless	
Formula weight	573.61 g · mol^{-1}	
Temperature	100 K	
Wavelength	0.71073 Å	
Crystal system	monoclinic	
Space group	C2/c, (no. 15)	
Unit cell dimensions	a = 16.8763(17) Å	α = 90°.
	b = 19.577(2) Å	β = 120.553(2)°.
	c = 11.6565(12) Å	γ = 90°.
Volume	3316.5(6) Å^3	
Z	4	
Density (calculated)	1.149 Mg · m^{-3}	
Absorption coefficient	0.083 mm^{-1}	
F(000)	1248 e	
Crystal size	0.330 x 0.261 x 0.082 mm^3	
θ range for data collection	1.75 to 37.17°.	
Index ranges	$-28 \le h \le 28$, $-32 \le k \le 33$, $-19 \le l \le 19$	
Reflections collected	63706	
Independent reflections	8173 [R_{int} = 0.0285]	
Reflections with I>2σ(I)	6656	
Completeness to θ = 27.50°	100.0 %	
Absorption correction	Gaussian	
Max. and min. transmission	0.99 and 0.98	
Refinement method	Full-matrix least-squares on F^2	
Data / restraints / parameters	8173 / 0 / 201	
Goodness-of-fit on F^2	1.044	
Final R indices [I>2σ(I)]	R_1 = 0.0625	wR^2 = 0.1709
R indices (all data)	R_1 = 0.0764	wR^2 = 0.1835
Largest diff. peak and hole	1.110 and -1.004 e · Å^{-3}	

Compound **3.54**

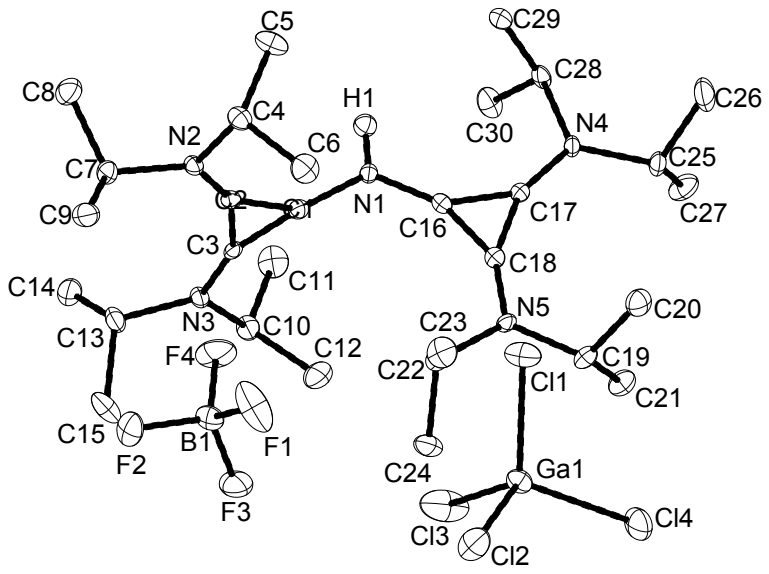

CCDC number	911777	
Empirical formula	$C_{30}H_{57}BCl_4F_4GaN_5$	
Color	colorless	
Formula weight	786.14 g·mol^{-1}	
Temperature	100 K	
Wavelength	0.71073 Å	
Crystal system	monoclinic	
Space group	p 2_1/n, (no. 14)	
Unit cell dimensions	a = 13.8508(9) Å	α = 90°.
	b = 15.2339(12) Å	β= 109.855(5)°.
	c = 20.1399(10) Å	γ = 90°.
Volume	3996.9(5) Å^3	
Z	4	
Density (calculated)	1.306 Mg·m^{-3}	
Absorption coefficient	1.001 mm^{-1}	
F(000)	1648 e	
Crystal size	0.16 x 0.06 x 0.02 mm^3	
θ range for data collection	3.07 to 29.00°.	
Index ranges	$-18 \le h \le 18$, $-20 \le k \le 20$, $-27 \le l \le 27$	
Reflections collected	57956	
Independent reflections	10595 [R_{int} = 0.0921]	
Reflections with I>2σ (I)	7048	
Completeness to θ = 27.50°	99.8 %	
Absorption correction	Gaussian	
Max. and min. transmission	0.98258 and 0.89743	
Refinement method	Full-matrix least-squares on F^2	
Data / restraints / parameters	10595 / 0 / 422	
Goodness-of-fit on F^2	1.106	
Final R indices [I>2σ (I)]	R_1 = 0.0559	wR^2 = 0.0937
R indices (all data)	R_1 = 0.1068	wR^2 = 0.1086
Largest diff. peak and hole	0.450 and -0.504 e·Å^{-3}	

Compound **3.56**

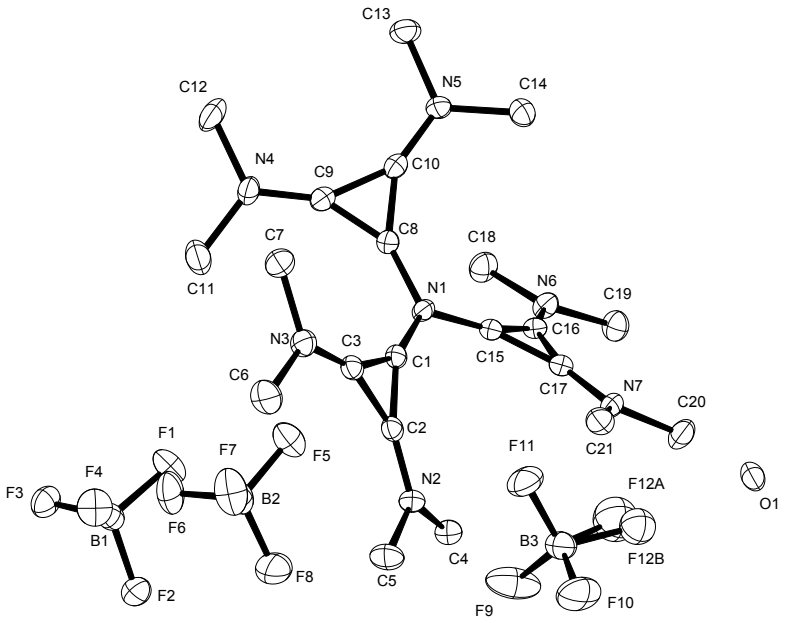

CCDC number	911775	
Empirical formula	$C_{21}H_{36}B_3F_{12}N_7O_{0.25}$	
Color	colorless	
Formula weight	651.00 g · mol^{-1}	
Temperature	100 K	
Wavelength	0.71073 Å	
Crystal system	monoclinic	
Space group	P 21/n, (no. 14)	
Unit cell dimensions	a = 12.149(2) Å	α = 90°.
	b = 12.495(2) Å	β= 92.304(3)°.
	c = 19.670(4) Å	γ = 90°.
Volume	2983.7(10) Å^3	
Z	4	
Density (calculated)	1.449 Mg · m^{-3}	
Absorption coefficient	0.140 mm^{-1}	
F(000)	1344 e	
Crystal size	0.08 x 0.07 x 0.05 mm^3	
θ range for data collection	1.93 to 23.51°.	
Index ranges	$-13 \le h \le 13$, $-13 \le k \le 13$, $-22 \le 1 \le 22$	
Reflections collected	45846	
Independent reflections	4405 [R_{int} = 0.0516]	
Reflections with I>2σ(I)	3619	
Completeness to θ = 23.51°	99.7 %	
Absorption correction	Gaussian	
Max. and min. transmission	0.75 and 0.67	
Refinement method	Full-matrix least-squares on F^2	
Data / restraints / parameters	4405 / 0 / 408	
Goodness-of-fit on F^2	1.094	
Final R indices [I>2σ(I)]	R_1 = 0.0441	wR^2 = 0.1041
R indices (all data)	R_1 = 0.0571	wR^2 = 0.1122
Largest diff. peak and hole	0.492 and -0.554 e · Å^{-3}	

Compound **4.28**

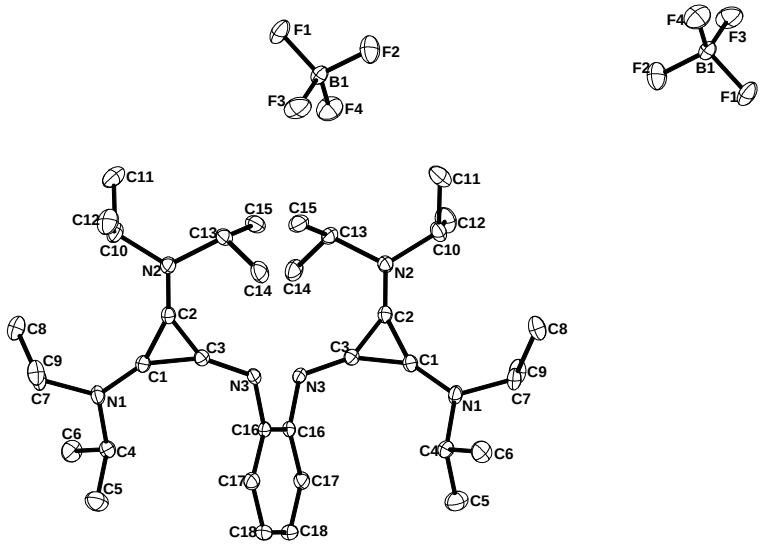

CCDC number	1048797	
Empirical formula	$C_{36}H_{62}B_2F_8N_6$	
Color	colorless	
Formula weight	752.53 g·mol^{-1}	
Temperature	100 K	
Wavelength	0.71073 Å	
Crystal system	monoclinic	
Space group	c 2/c, (no. 15)	
Unit cell dimensions	a = 28.091(4) Å	α = 90°.
	b = 11.2966(17) Å	β = 91.416(3)°.
	c = 12.9833(19) Å	γ = 90°.
Volume	4118.8(11) Å^3	
Z	4	
Density (calculated)	1.214 Mg·m^{-3}	
Absorption coefficient	0.097 mm^{-1}	
F(000)	1608 e	
Crystal size	0.29 x 0.21 x 0.04 mm^3	
θ range for data collection	1.450 to 30.672°.	
Index ranges	$-40 \le h \le 40$, $-16 \le k \le 16$, $-18 \le l \le 18$	
Reflections collected	56414	
Independent reflections	6362 [R_{int} = 0.0581]	
Reflections with I>2σ (I)	5002	
Completeness to θ = 25.242°	99.9 %	
Absorption correction	Gaussian	
Max. and min. transmission	0.99621 and 0.97173	
Refinement method	Full-matrix least-squares on F^2	
Data / restraints / parameters	6362 / 0 / 247	
Goodness-of-fit on F^2	1.131	
Final R indices [I>2σ(I)]	R_1 = 0.0431	wR^2 = 0.1176
R indices (all data)	R_1 = 0.0633	wR^2 = 0.1376
Extinction coefficient	n/a	
Largest diff. peak and hole	0.426 and -0.357 e·Å^{-3}	

Compound **4.29**

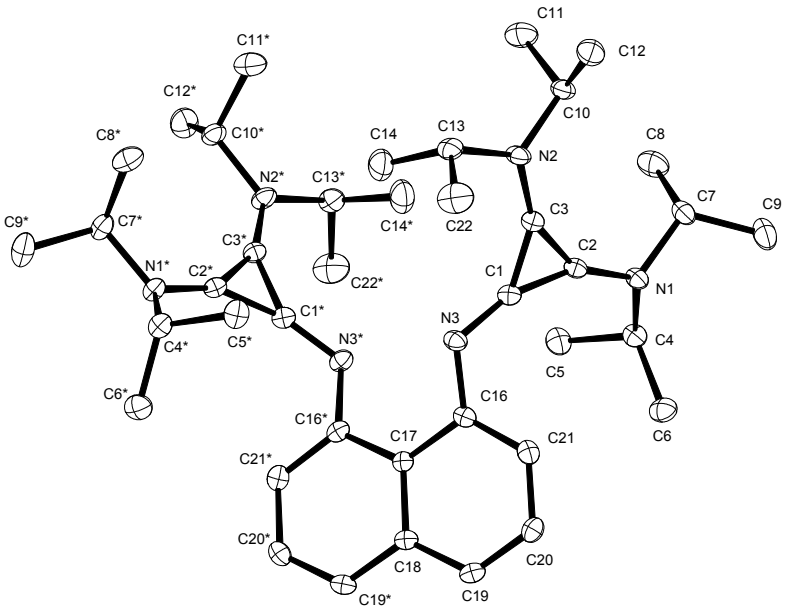

CCDC number	1048792	
Empirical formula	$C_{40}H_{62}N_6$	
Color	colorless	
Formula weight	626.95 g · mol^{-1}	
Temperature	100 K	
Wavelength	0.71073 Å	
Crystal system	monoclinic	
Space group	C2/c, (no. 15)	
Unit cell dimensions	a = 25.030(4) Å	α = 90°.
	b = 13.133(2) Å	β = 124.579(3)°.
	c = 14.480(2) Å	γ = 90°.
Volume	3919.1(11) $Å^3$	
Z	4	
Density (calculated)	1.063 Mg · m^{-3}	
Absorption coefficient	0.063 mm^{-1}	
F(000)	1376 e	
Crystal size	0.23 x 0.05 x 0.03 mm^3	
θ range for data collection	1.839 to 28.636°.	
Index ranges	$-33 \le h \le 33$, $-17 \le k \le 17$, $-19 \le l \le 19$	
Reflections collected	48213	
Independent reflections	5015 [R_{int} = 0.0835]	
Reflections with I>2σ (I)	3596	
Completeness to θ = 25.242°	100.0 %	
Absorption correction	Gaussian	
Max. and min. transmission	1.00 and 0.99	
Refinement method	Full-matrix least-squares on F^2	
Data / restraints / parameters	5015 / 0 / 217	
Goodness-of-fit on F^2	1.120	
Final R indices [I>2σ (I)]	R_1 = 0.0432	wR^2 = 0.1129
R indices (all data)	R_1 = 0.0751	wR^2 = 0.1396
Largest diff. peak and hole	0.3 and -0.4 e · $Å^{-3}$	

Compound **4.31**

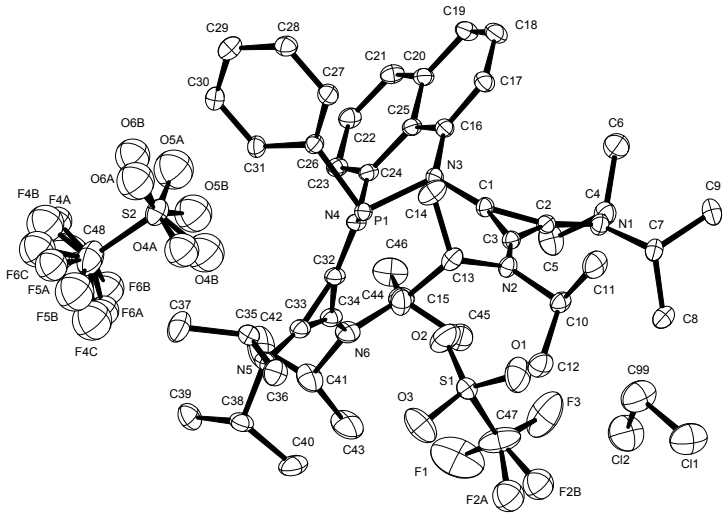

CCDC number	1048790	
Empirical formula	$C_{49}H_{69}Cl_2F_6N_6O_6PS_2$	
Color	orange yellow	
Formula weight	1118.09 g · mol^{-1}	
Temperature	100 K	
Wavelength	0.71073 Å	
Crystal system	orthorhombic	
Space group	$Pna2_1$, (no. 33)	
Unit cell dimensions	a = 22.0269(19) Å	α = 90°.
	b = 17.1879(13) Å	β = 90°.
	c = 14.9672(9) Å	γ = 90°.
Volume	5666.5(7) Å^3	
Z	4	
Density (calculated)	1.311 Mg · m^{-3}	
Absorption coefficient	0.286 mm^{-1}	
F(000)	2352 e	
Crystal size	0.22 x 0.12 x 0.05 mm^3	
θ range for data collection	2.885 to 33.126°.	
Index ranges	$-33 \le h \le 33$, $-26 \le k \le 26$, $-23 \le l \le 22$	
Reflections collected	99155	
Independent reflections	21460 [R_{int} = 0.0324]	
Reflections with I>2σ (I)	19101	
Completeness to θ = 25.242°	99.6 %	
Absorption correction	Gaussian	
Max. and min. transmission	1.00 and 0.99	
Refinement method	Full-matrix least-squares on F^2	
Data / restraints / parameters	21460 / 1 / 670	
Goodness-of-fit on F^2	1.034	
Final R indices [I>2σ (I)]	R_1 = 0.0561	wR^2 = 0.1441
R indices (all data)	R_1 = 0.0655	wR^2 = 0.1519
Absolute structure parameter	0.029(9)	
Largest diff. peak and hole	1.362 and -0.527 e · Å^{-3}	

Compound **4.32**

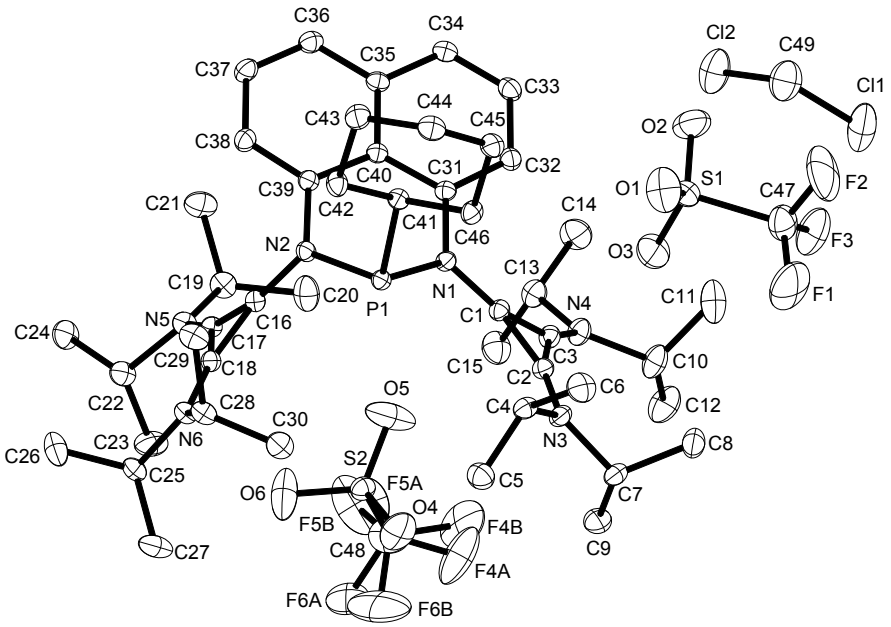

CCDC number	1048795	
Empirical formula	$C_{49}\ H_{75}\ Cl_2\ F_6\ N_6\ O_6\ P\ S_2$	
Color	yellow	
Formula weight	1124.14 $g \cdot mol^{-1}$	
Temperature	100 K	
Wavelength	0.71073 Å	
Crystal system	orthorhombic	
Space group	P n a 2_1, (no. 33)	
Unit cell dimensions	a = 22.245(4) Å	α = 90°.
	b = 17.313(3) Å	β = 90°.
	c = 14.918(3) Å	γ = 90°.
Volume	5745.1(17) $Å^3$	
Z	4	
Density (calculated)	1.300 $Mg \cdot m^{-3}$	
Absorption coefficient	0.283 mm^{-1}	
F(000)	2376 e	
Crystal size	0.16 x 0.09 x 0.09 mm^3	
θ range for data collection	2.871 to 33.173°.	
Index ranges	$-34 \le h \le 34$, $-26 \le k \le 26$, $-22 \le l \le 22$	
Reflections collected	121390	
Independent reflections	21863 [R_{int} = 0.0384]	
Reflections with I>2σ (I)	19679	
Completeness to θ = 25.242°	99.6 %	
Absorption correction	Gaussian	
Max. and min. transmission	0.98498 and 0.97216	
Refinement method	Full-matrix least-squares on F^2	
Data / restraints / parameters	21863 / 67 / 694	
Goodness-of-fit on F^2	1.049	
Final R indices [I>2σ (I)]	R_1 = 0.0354	wR^2 = 0.0848
R indices (all data)	R_1 = 0.0435	wR^2 = 0.0899
Absolute structure parameter	0.16(3)	
Extinction coefficient	0	
Largest diff. peak and hole	0.524 and -0.568 $e \cdot Å^{-3}$	

Compound **4.33**

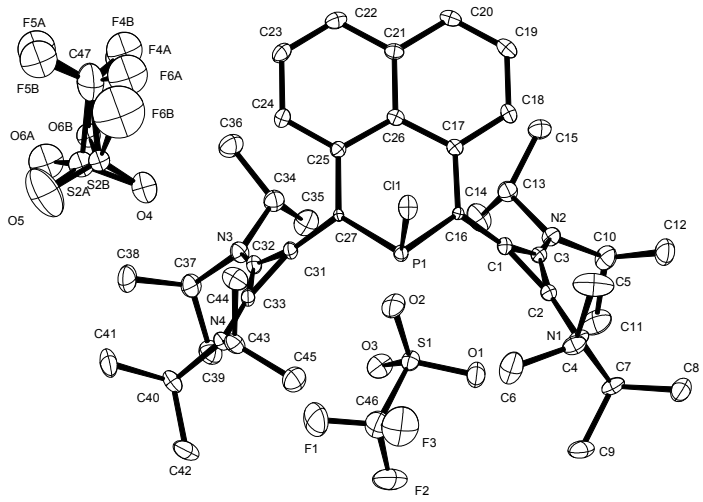

CCDC number	1048791	
Empirical formula	$C_{44}H_{62}ClF_6N_4O_6PS_2$	
Color	colorless	
Formula weight	987.51 g · mol^{-1}	
Temperature	100 K	
Wavelength	0.71073 Å	
Crystal system	monoclinic	
Space group	$P2_1$, (no. 4)	
Unit cell dimensions	a = 13.201(3) Å	α = 90°.
	b = 14.234(3) Å	β = 91.635(4)°.
	c = 13.385(3) Å	γ = 90°.
Volume	2514.2(9) Å^3	
Z	2	
Density (calculated)	1.304 Mg · m^{-3}	
Absorption coefficient	0.261 mm^{-1}	
F(000)	1040 e	
Crystal size	0.30 x 0.09 x 0.08 mm^3	
θ range for data collection	2.104 to 33.025°.	
Index ranges	$-20 \le h \le 20$, $-21 \le k \le 21$, $-20 \le l \le 20$	
Reflections collected	83744	
Independent reflections	18889 [R_{int} = 0.0370]	
Reflections with I>2σ (I)	17115	
Completeness to θ = 25.242°	99.6 %	
Absorption correction	Gaussian	
Max. and min. transmission	0.98 and 0.91	
Refinement method	Full-matrix least-squares on F^2	
Data / restraints / parameters	18889 / 1 / 588	
Goodness-of-fit on F^2	1.033	
Final R indices [I>2σ (I)]	R_1 = 0.0549	wR^2 = 0.1448
R indices (all data)	R_1 = 0.0620	wR^2 = 0.1513
Absolute structure parameter	0.007(14)	
Largest diff. peak and hole	1.4 and -1.4 e · Å^{-3}	

Compound **4.35**

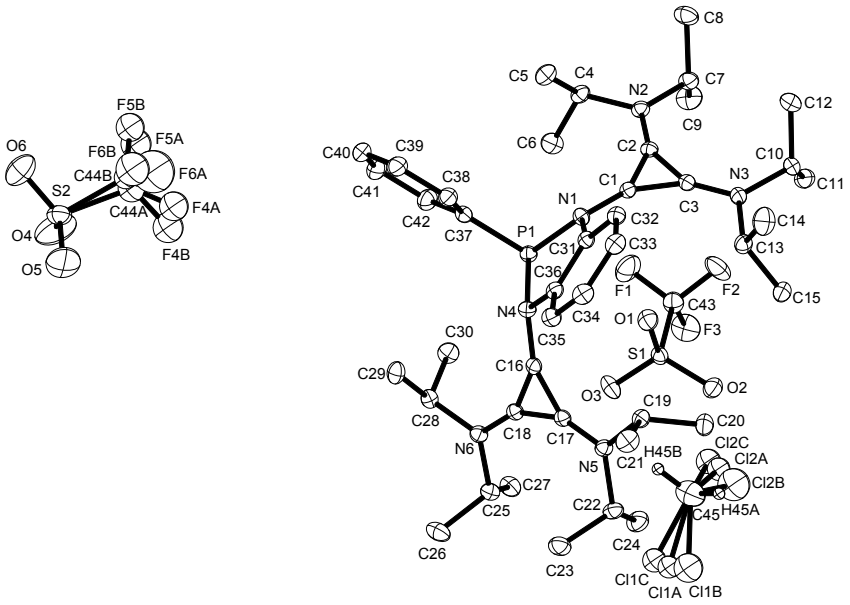

CCDC number	1048798	
Empirical formula	$C_{45}H_{67}Cl_2F_6N_6O_6PS_2$	
Color	colorless	
Formula weight	1068.03 g·mol^{-1}	
Temperature	100 K	
Wavelength	0.71073 Å	
Crystal system	triclinic	
Space group	P -1, (no. 2)	
Unit cell dimensions	a = 11.5789(8) Å	α = 112.456(6)°.
	b = 15.7217(13) Å	β = 92.869(5)°.
	c = 16.3126(15) Å	γ = 103.419(7)°.
Volume	2637.5(4) Å^3	
Z	2	
Density (calculated)	1.345 Mg·m^{-3}	
Absorption coefficient	0.304 mm^{-1}	
F(000)	1124 e	
Crystal size	0.12 x 0.10 x 0.02 mm^3	
θ range for data collection	2.631 to 33.167°.	
Index ranges	$-17 \le h \le 17$, $-24 \le k \le 24$, $-25 \le l \le 24$	
Reflections collected	58156	
Independent reflections	19971 [R_{int} = 0.0591]	
Reflections with I>2σ (I)	13565	
Completeness to θ = 25.242°	99.7 %	
Absorption correction	Gaussian	
Max. and min. transmission	0.99609 and 0.97904	
Refinement method	Full-matrix least-squares on F^2	
Data / restraints / parameters	19971 / 0 / 639	
Goodness-of-fit on F^2	1.029	
Final R indices [I>2σ (I)]	R_1 = 0.0680	wR^2 = 0.1586
R indices (all data)	R_1 = 0.1086	wR^2 = 0.1831
Extinction coefficient	0	
Largest diff. peak and hole	1.478 and -1.126 e·Å^{-3}	

Compound **4.36**

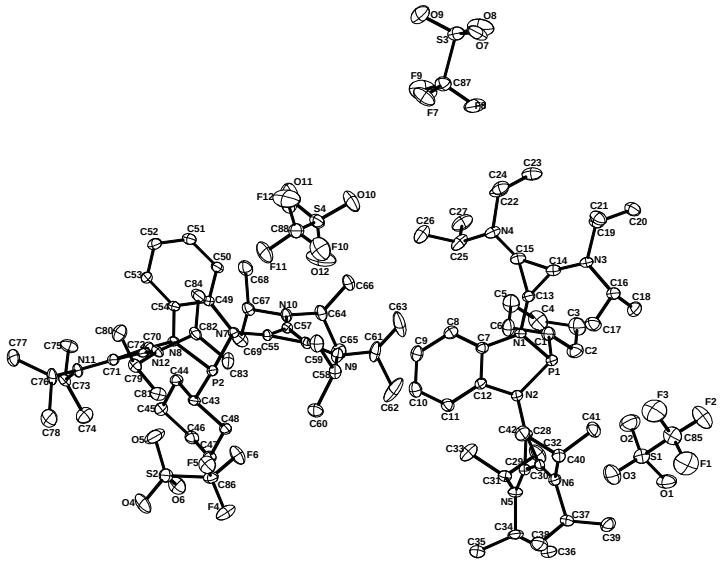

CCDC number	1048799	
Empirical formula	C_{44} H_{71} F_6 N_6 O_6 P S_2	
Color	yellow	
Formula weight	989.15 g·mol^{-1}	
Temperature	100 K	
Wavelength	0.71073 Å	
Crystal system	orthorhombic	
Space group	p 2_1 2_1 2_1, (no. 19)	
Unit cell dimensions	a = 16.216(5) Å	α = 90°.
	b = 16.530(5) Å	β = 90°.
	c = 37.757(10) Å	γ = 90°.
Volume	10121(5) Å^3	
Z	8	
Density (calculated)	1.298 Mg·m^{-3}	
Absorption coefficient	0.209 mm^{-1}	
F(000)	4208 e	
Crystal size	0.15 x 0.12 x 0.10 mm^3	
θ range for data collection	2.949 to 28.698°.	
Index ranges	$-21 \le h \le 21$, $-22 \le k \le 22$, $-51 \le l \le 51$	
Reflections collected	223730	
Independent reflections	26115 [R_{int} = 0.1354]	
Reflections with I>2σ (I)	20003	
Completeness to θ = 25.242°	99.7 %	
Absorption correction	Gaussian	
Max. and min. transmission	0.98300 and 0.97161	
Refinement method	Full-matrix least-squares on F^2	
Data / restraints / parameters	26115 / 0 / 1203	
Goodness-of-fit on F^2	1.022	
Final R indices [I>2σ (I)]	R_1 = 0.0665	wR^2 = 0.1492
R indices (all data)	R_1 = 0.0943	wR^2 = 0.1648
Absolute structure parameter	0.02(3)	
Extinction coefficient	n/a	
Largest diff. peak and hole	0.819 and -0.521 e·Å^{-3}	

Compound **4.40**

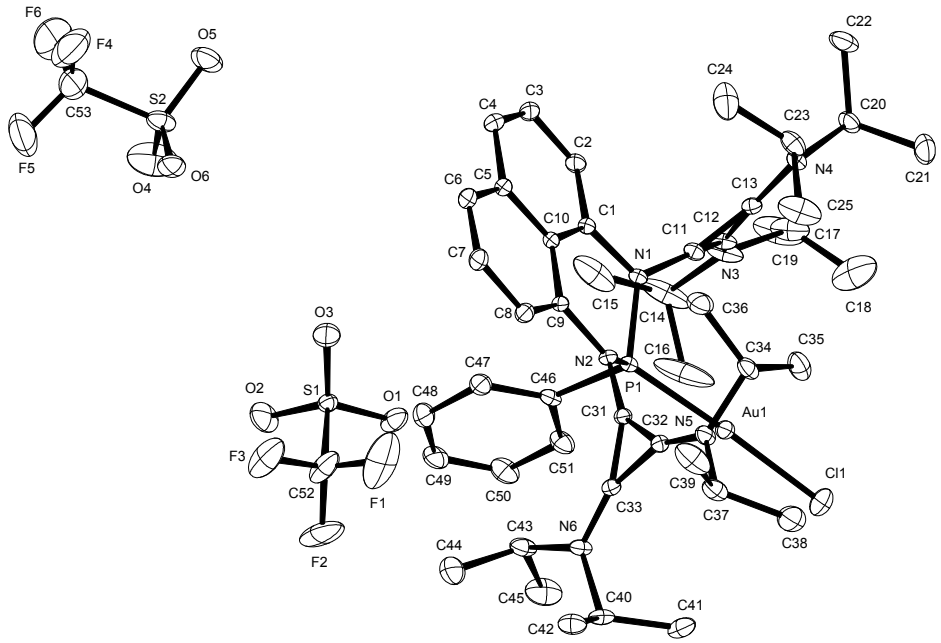

CCDC number	1048793	
Empirical formula	$C_{48}H_{67}AuClF_6N_6O_6PS_2$	
Color	colorless	
Formula weight	1265.58 g · mol^{-1}	
Temperature	100 K	
Wavelength	0.71073 Å	
Crystal system	triclinic	
Space group	$P\bar{1}$, (no. 2)	
Unit cell dimensions	a = 9.8026(10) Å	α = 74.1395(17)°.
	b = 15.8275(16) Å	β = 88.8135(18)°.
	c = 19.1970(19) Å	γ = 74.8983(18)°.
Volume	2762.0(5) Å^3	
Z	2	
Density (calculated)	1.522 Mg · m^{-3}	
Absorption coefficient	2.887 mm^{-1}	
F(000)	1284 e	
Crystal size	0.18 x 0.08 x 0.05 mm^3	
θ range for data collection	1.104 to 33.142°.	
Index ranges	$-15 \le h \le 15$, $-24 \le k \le 24$, $-29 \le l \le 29$	
Reflections collected	93569	
Independent reflections	21043 [R_{int} = 0.0326]	
Reflections with I>2σ (I)	18959	
Completeness to θ = 25.242°	100.0 %	
Absorption correction	Gaussian	
Max. and min. transmission	0.88 and 0.70	
Refinement method	Full-matrix least-squares on F^2	
Data / restraints / parameters	21043 / 0 / 656	
Goodness-of-fit on F^2	1.155	
Final R indices [I>2σ (I)]	R_1 = 0.0231	wR^2 = 0.0613
R indices (all data)	R_1 = 0.0297	wR^2 = 0.0731
Largest diff. peak and hole	0.8 and -1.1 e · Å^{-3}	

Compound **4.41**

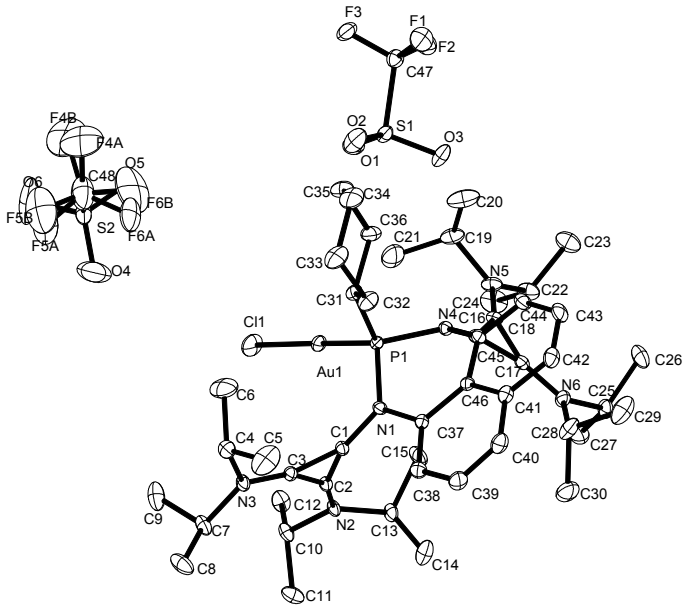

CCDC number	1048796	
Empirical formula	C_{48} H_{73} Au Cl F_6 N_6 O_6 P S_2	
Color	orange	
Formula weight	1271.63 g·mol^{-1}	
Temperature	100 K	
Wavelength	0.71073 Å	
Crystal system	monoclinic	
Space group	p 21/n, (no. 14)	
Unit cell dimensions	a = 13.766(2) Å	α = 90°.
	b = 29.691(5) Å	β = 105.121(3)°.
	c = 14.118(2) Å	γ = 90°.
Volume	5570.6(16) Å^3	
Z	4	
Density (calculated)	1.516 Mg·m^{-3}	
Absorption coefficient	2.863 mm^{-1}	
F(000)	2592 e	
Crystal size	0.20 x 0.12 x 0.09 mm^3	
θ range for data collection	2.989 to 33.182°.	
Index ranges	$-21 \le h \le 21$, $-45 \le k \le 45$, $-21 \le l \le 21$	
Reflections collected	187161	
Independent reflections	21272 [R_{int} = 0.0384]	
Reflections with I>2σ (I)	18511	
Completeness to θ = 25.242°	99.8 %	
Absorption correction	Gaussian	
Max. and min. transmission	0.80384 and 0.58211	
Refinement method	Full-matrix least-squares on F^2	
Data / restraints / parameters	21272 / 66 / 683	
Goodness-of-fit on F^2	1.044	
Final R indices [I>2σ (I)]	R_1 = 0.0286	wR^2 = 0.0629
R indices (all data)	R_1 = 0.0367	wR^2 = 0.0658
Extinction coefficient	0	
Largest diff. peak and hole	4.610 and -1.644 e·Å^{-3}	

Compound **4.46**

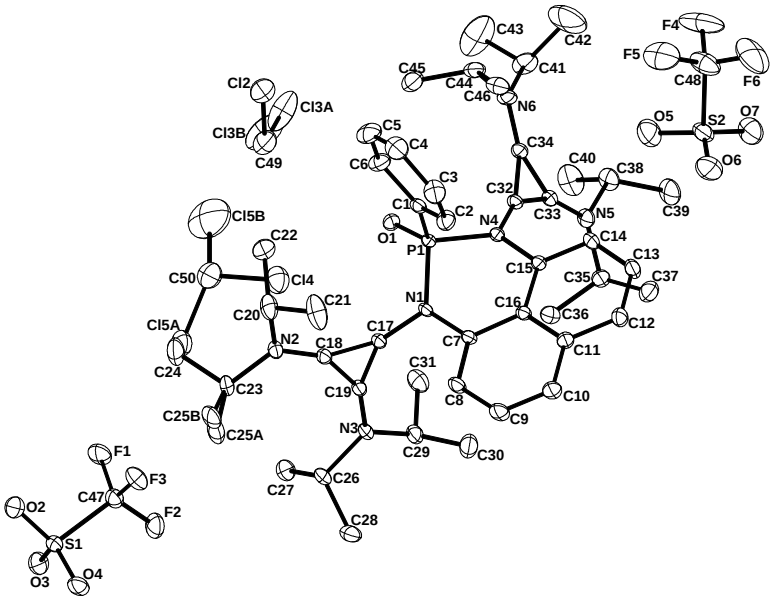

CCDC number	1048794	
Empirical formula	C_{50} H_{71} Cl_4 F_6 N_6 O_7 P S_2	
Color	colorless	
Formula weight	1219.01 g·mol^{-1}	
Temperature	100 K	
Wavelength	0.71073 Å	
Crystal system	triclinic	
Space group	p -1, (no. 2)	
Unit cell dimensions	a = 8.8243(15) Å	α = 72.431(3)°.
	b = 14.834(3) Å	β = 80.395(3)°.
	c = 23.823(4) Å	γ = 89.145(3)°.
Volume	2929.1(9) Å^3	
Z	2	
Density (calculated)	1.382 Mg·m^{-3}	
Absorption coefficient	0.373 mm^{-1}	
F(000)	1276 e	
Crystal size	0.18 x 0.17 x 0.10 mm^3	
θ range for data collection	1.441 to 31.274°.	
Index ranges	$-12 \le h \le 12$, $-21 \le k \le 21$, $-34 \le l \le 34$	
Reflections collected	72657	
Independent reflections	18676 [R_{int} = 0.0440]	
Reflections with I>2σ (I)	13287	
Completeness to θ = 25.242°	98.3 %	
Absorption correction	Gaussian	
Max. and min. transmission	0.96878 and 0.92914	
Refinement method	Full-matrix least-squares on F^2	
Data / restraints / parameters	18676 / 24 / 736	
Goodness-of-fit on F^2	1.030	
Final R indices [I>2σ (I)]	R_1 = 0.0555	wR^2 = 0.1524
R indices (all data)	R_1 = 0.0857	wR^2 = 0.1763
Extinction coefficient	n/a	
Largest diff. peak and hole	1.390 and -1.028 e·Å^{-3}	